

Université de Montréal

Utilisation des interactions stériques de la *5-tert-butylproline* pour  
mimer la structure secondaire peptidique.

par

Liliane Halab

Département de chimie  
Faculté des arts et des sciences

Thèse présentée à la Faculté des études supérieures

En vue de l'obtention du grade de

Philosophiae Doctor (Ph.D.)

En chimie

Août, 2001

©Liliane Halab, 2001



QD

3

054

2002

V.015

Université de Montréal  
Faculté des études supérieures

Cette thèse intitulée:

Utilisation des interactions stériques de la 5-*tert*-butylproline pour  
mimer la structure secondaire peptidique.

Présentée par:

Liliane Halab

a été évaluée par un jury composé des personnes suivantes:

Stephen Hanessian	président rapporteur
William D. Lubell	directeur de recherche
James D. Wuest	membre du jury
Gilles Guichard	examinateur externe
Stephen Hanessian	représentant du Doyen

Thèse acceptée le:

23 avril 2002

## SOMMAIRE

Cette thèse présente nos études sur l'utilisation des interactions stériques pour contraindre la conformation des peptides. Nos travaux ont porté sur la synthèse de prolines substituées énantiopures et l'incorporation dans des peptides afin de mimer des structures secondaires définies.

L'incorporation d'un groupement *tert*-butyle à la position 5 de la proline peut influencer l'équilibre conformationnel ainsi que la population d'isomère *cis* dans les peptides. Nous avons développé alors une synthèse efficace de la *N*-BOC-(2*S*,5*S*)-5-*tert*-butylproline via une addition stéréosélective d'hydrure à l'imine du 5-*tert*-butylprolinol.

Les interactions stériques de la (2*S*,5*R*)-5-*tert*-butylproline ont été employées pour étudier la stabilisation de repliement  $\beta$  de type VI. Nous avons introduit la (2*S*,5*R*)-5-*tert*-butylproline dans une série de dipeptides *N*-acétyles *N'*-méthylamides. L'analyse conformationnelle par spectroscopie RMN, DC et diffraction de rayon-X ont démontré que les dipeptides incorporant la 5-*tert*-butylproline adoptent un lien amide en isomère *cis* dans un repliement  $\beta$  de type VI. De plus, la conformation de ces dipeptides dépend de la stéréochimie de l'acide aminé *N*-terminal. Des repliements  $\beta$  de type VIa et VIb sont obtenus respectivement lorsque l'acide aminé *N*-terminal possède une stéréochimie de configuration L et D. Ainsi, nous sommes capables de mimer les deux classes de repliements  $\beta$  de type VI.

Une étude fondamentale des effets de la séquence sur les mimétiques de repliement  $\beta$  de type VI est présentée. Nous avons étudié la séquence des acides aminés *N*-terminaux de la proline et 5-*tert*-butylproline dans des dipeptides *N*-acétyles *N'*-méthylamides. Une augmentation de la population d'isomère *cis* a été observée pour les résidus aromatiques. En utilisant la spectroscopie RMN, DC et la diffraction de rayon-X, nous avons étudié les facteurs qui influencent le repliement des peptides.

Une série de tétrapeptides incorporant la *5-tert*-butylproline a été synthétisée sur support solide afin de comprendre les effets de la séquence sur l’isomérisation *cis-trans* du lien prolyl amide. De plus, nous avons exploré la possibilité d’induire une conformation en épingle  $\beta$  avec un repliement  $\beta$  de type VIa. La conformation des tétrapeptides a été analysée par la spéctroscopie RMN et DC.

Finalement, nous avons étudié la relation entre la conformation d’un peptide et l’activité biologique. Des acides aminés azabicycloalkanes possèdent différentes tailles de cycles et un mimétique de repliement  $\beta$  de type VIa ont été introduits dans des peptides pour explorer le récepteur opiacé ORL1.

## NOTE

Je désire énoncer ma contribution à cette thèse de Ph.D. dans le but d'éviter un questionnement et une confusion de la part du lecteur.

L'article du chapitre 1, qui décrit la synthèse de la (2S,5S)-*N*-BOC-5-*tert*-butylproline a été rédigé par moi-même en collaboration avec mon collègue Laurent Bélec et le professeur William D. Lubell. J'ai effectué la majorité des travaux de laboratoire décrits dans ce chapitre.

Les articles des chapitres 2 et 3, décrivant l'utilisation de la (2S,5R)-5-*tert*-butylproline dans des peptides pour mimer la conformation de repliement  $\beta$  de type VI, ont été rédigés par moi-même, sous la supervision du professeur William D. Lubell.

L'article du chapitre 4, décrivant l'utilisation de contraintes structurales et stériques pour étudier le récepteur ORL1, a été rédigé par moi-même en collaboration avec les professeurs William D. Lubell, Dirk Tourwé et Frédéric Simonin. J'ai effectué l'ensemble des travaux de laboratoire décrits dans ce chapitre, sauf la synthèse du peptide incorporant le I<sup>9</sup>aa et les expériences pour l'évaluation biologique des peptides.

J'ai rédigé, bien sûr, la conclusion de la thèse.

Finalement, l'article de l'annexe est une revue de la chimie effectuée dans le laboratoire du professeur William D. Lubell. L'article a été rédigé par l'ensemble des auteurs.

## TABLE DES MATIÈRES

<b>SOMMAIRE</b>	<b>I</b>
<b>NOTE</b>	<b>III</b>
<b>TABLE DES MATIÈRES</b>	<b>XIV</b>
<b>LISTE DES FIGURES</b>	<b>XIV</b>
<b>LISTE DES SCHÉMAS</b>	<b>XIV</b>
<b>LISTE DES TABLEAUX</b>	<b>XIV</b>
<b>LISTE DES ABRÉVIATIONS</b>	<b>XV</b>
<b>REMERCIEMENTS</b>	<b>XIX</b>
<b>CHAPITRE 1</b>	
<b>Introduction</b>	<b>1</b>
1.1. Les peptides	2
1.2. Le lien amide et l'équilibre conformationnel de la proline	2
1.3. Les structures secondaires des peptides	4
1.4. Utilisation des interactions stériques pour stabiliser une conformation.	6
1.5. Références	7
<b>Article 1</b>	
1.6. Abstract	11
1.7. Introduction	11
1.8. Results and Discussion	17
1.9. Experimental Section	25
1.10. References	31
<b>CHAPITRE 2</b>	
<b>Synthèse et étude conformationnelle de dipeptides <i>N</i>-acétyles <i>N</i>-méthylamides incorporant la proline et la 5-<i>tert</i>-butylproline, mimétique de repliement <math>\beta</math> de type VIa et VIb.</b>	<b>36</b>
2.1. Les repliements $\beta$ de type VI	37
2.2. Outil pour stabiliser l'isomère <i>cis</i> <i>N</i> -terminal de la proline	39

2.2.1. Utilisation des prolines rigidifiées	39
2.2.2. Utilisation des analogues de prolines	42
2.3. Références	43
<b>Article 2</b>	
2.4. Introduction	48
2.5. Results and Discussion	48
2.6. References	50
<b>Article 3</b>	
2.7. Abstract	52
2.8. Introduction	53
2.9. Results	56
2.9.1. Synthesis of Ac-Xaa-Pro-NHMe dipeptides <b>1</b> and <b>2</b>	56
2.9.2. Conformational analysis of prolyl dipeptides <b>1</b> and <b>2</b> by NMR spectroscopy	58
2.9.3. X-Ray crystallographic analysis of <i>N</i> -acetyl-L-leucyl-5- <i>tert</i> -butylproline <i>N</i> -methylamide ( <b>1d</b> )	62
2.9.4. Conformational analysis of dipeptides <b>1</b> and <b>2</b> by circular dichroism spectroscopy	64
2.10. Discussion	65
2.11. Experimental Section	68
2.12. References	78
<b>Article 4</b>	
2.13. Introduction	86
2.14. Results and Discussion	86
2.15. References	88
<b>Article 5</b>	
2.16. Abstract	90
2.17. Introduction	91
2.18. Results and Discussion	95
2.18.1. Synthesis of dipeptides <b>1</b> and <b>2</b>	95
2.18.2. Conformational analysis of dipeptides <b>1</b> and <b>2</b> by NMR spectroscopy	96

2.18.3. Conformational analysis of dipeptides <b>1</b> and <b>2</b> by circular dichroism spectroscopy	99
2.18.4. X-ray crystallographic analysis of dipeptide ( <i>R</i> )- <b>1b</b>	102
2.19. Conclusions	104
2.20. Experimental Section	106
2.21. References	112

## CHAPITRE 3

<b>Repliement <math>\beta</math> de type VI: Effet de séquence et formation d'épingle <math>\beta</math>.</b>	<b>118</b>
3.1. Séquence et conformation	119
3.2. L'Épingle $\beta$	120
3.2.1. Épingle $\beta$ induit par la séquence du peptide	120
3.2.2. Mimétique d'épingle $\beta$	121
3.3. Références	124

## Article 6

3.4. Introduction	127
3.5. Results and Discussion	127
3.6. References	129

## Article 7

3.7. Abstract	131
3.8. Introduction	132
3.9. Results and Discussion	135
3.9.1. Synthesis of dipeptides <b>1</b> and <b>2</b>	135
3.9.2. Synthesis of tetrapeptides	136
3.9.3. Conformational analysis of the dipeptides	138
3.9.4. Circular dichroism spectroscopy	141
3.9.5. X-ray crystallographic analysis	144
3.9.6. Conformational analysis of the tetrapeptides	146
3.10. Discussion	151
3.11. Experimental Section	155
3.12. References	173

**CHAPITRE 4****Incorporation des acides aminés azacycloalcanes dans des ligands peptidiques pour étudier le récepteur ORL1.** **179**4.1. ORL1 et ses ligands **180**4.2. Références **182****Article 8**4.3. Abstract **186**4.4 Introduction **186**4.5. Experimental Section **190**4.6. Results **197**    4.6.1. Synthesis **197**    4.6.2. Conformational analysis by NMR spectroscopy **198**    4.6.3. Conformational analysis by circular dichroism spectroscopy **201**    4.6.4. Biological activity **203**4.7. Discussion **207**4.8. References **211****CHAPITRE 5****Conclusion** **216****ANNEXE** **XXI****Article 9**

## LISTE DES FIGURES

### CHAPITRE 1

<b>Figure 1.</b> Formes de résonance du lien amide.	2
<b>Figure 2.</b> Isomérisation du lien amide.	3
<b>Figure 3.</b> Isomérisation du lien amide de la proline.	3
<b>Figure 4.</b> Pyramidalisation du lien amide de la proline.	4
<b>Figure 5.</b> Géométrie du cycle pyrrolidine de la proline.	4
<b>Figure 6.</b> Angles de torsion d'une chaîne peptidique.	5
<b>Figure 7.</b> Structure générale des repliements $\beta$ et $\gamma$ .	5
<b>Figure 8.</b> Exemples représentatives d'acides aminés substitués.	7

### Article 1

<b>Figure 1.</b> Representative examples of $\alpha$ -, $\beta$ - and $\gamma$ -alkyl substituted acyclic $\alpha$ -amino acids.	12
<b>Figure 2.</b> Representative examples of $\alpha$ -, $\beta$ - $\gamma$ - and $\delta$ -alkyl substituted cyclic $\alpha$ -amino acids.	14
<b>Figure 3.</b> Iminium ion intermediates used in the synthesis of <i>trans</i> -5- <i>tert</i> -butylproline.	16
<b>Figure 4.</b> Prolyl lactam 3.	17
<b>Figure 5.</b> Proposed transition state for hydride addition to imine 19.	23

### CHAPITRE 2

<b>Figure 1.</b> Structures des repliements $\beta$ de type VI.	37
<b>Figure 2.</b> Structures des substrats 1 et 2 qui adoptent une conformation de repliement $\beta$ de type VI.	38
<b>Figure 3.</b> Structure générale d'une proline contrainte en isomère <i>cis</i> .	39
<b>Figure 4.</b> Exemples représentatifs des lactames bicycliques.	40
<b>Figure 5.</b> Structures de la bradykinine, d'un analogue de somatostatin et de leurs dérivés avec des prolines rigidifiées.	41

<b>Figure 6.</b> Mimétique de l'isomère <i>cis</i> du lien prolylamide.	41
<b>Figure 7.</b> Exemples d'analogues de proline où l'équilibre conformationnel est possible.	42

### Article 3

<b>Figure 1.</b> Central, $i + 1$ and $i + 2$ residues of type VIa and VIb turn conformations found respectively in ribonuclease S and Bence-Jones protein. Only amide protons shown (C, black; N, dark gray; O, light gray; H, white).	53
<b>Figure 2.</b> ORTEP view of Ac-Leu-5- <i>t</i> BuPro-NHMe <b>1d</b> . Ellipsoids drawn at 40% probability level. Hydrogens represented by spheres of arbitrary size.	62
<b>Figure 3.</b> Circular dichroism spectra of <i>N</i> -(acetyl)alanyl- and <i>N</i> -(acetyl)leucyl-5- <i>tert</i> -butylproline <i>N'</i> -methylamides ( <b>1b</b> and <b>1d</b> ) in water and acetonitrile.	64
<b>Figure 4:</b> Circular dichroism spectra of <i>N</i> -(acetyl)alanyl- and <i>N</i> -(acetyl)leucyl-proline <i>N'</i> -methylamides ( <b>2b</b> and <b>2d</b> ) in water and acetonitrile.	65

### Article 5

<b>Figure 1.</b> Type VIa and VIb turn conformation found respectively in the central $i + 1$ and $i + 2$ residues of Ribonuclease S and Bence-Jones protein (C, black; N, dark gray; O, light gray; H, white).	94
<b>Figure 2.</b> Synthesis of <i>N</i> -(acetyl)dipeptide <i>N'</i> -methylamides <b>1</b> and <b>2</b> .	95
<b>Figure 3.</b> Circular dichroism spectra of <i>N</i> -(acetyl)dipeptide <i>N'</i> -methylamides ( <i>S</i> )- <b>1b</b> (A), ( <i>R</i> )- <b>1b</b> (B), ( <i>S</i> )- <b>2b</b> (C) and ( <i>R</i> )- <b>2b</b> (D) in water (—) and acetonitrile (---).	100
<b>Figure 4.</b> Circular dichroism spectra of <i>N</i> -(acetyl)dipeptide <i>N'</i> -methylamides ( <i>S</i> )- <b>1a</b> (A), ( <i>R</i> )- <b>1a</b> (B), ( <i>S</i> )- <b>2a</b> (C) and ( <i>R</i> )- <b>2a</b> (D) in water (—) and acetonitrile (---).	101

<b>Figure 5.</b> Two dipeptide turn structures ( <i>R</i> )- <b>1b</b> and ( <i>R</i> )- <b>1b'</b> engaged in intermolecular hydrogen bonds between their leucyl residues in the crystal structure. Ellipsoids drawn at 40% probability level. Hydrogens represented by spheres of arbitrary size.	102
---	-----

### CHAPITRE 3

<b>Figure 1.</b> Représentation des différentes classes de structures épingle β.	121
--	-----

<b>Figure 2.</b> Représentation de mimétiques d'épingles $\beta$ basés sur des systèmes aromatiques.	122
<b>Figure 3.</b> Représentations de mimétiques d'épingles $\beta$ .	123
<b>Figure 4.</b> Représentation de mimétiques d'épingles $\beta$ basés sur des prolines.	123
<b>Article 7</b>	
<b>Figure 1.</b> Amide equilibrium of <i>N</i> -acetyl dipeptide <i>N'</i> -methylamides.	139
<b>Figure 2.</b> Circular dichroism spectra of dipeptides <b>1c-e</b> (A, in water and B, in acetonitrile) and <b>2c-e</b> (C, in water and D, in acetonitrile) at 0.1 mM.	142
<b>Figure 3.</b> Circular dichroism spectra of dipeptides <b>1a</b> , <b>1b</b> and <b>1f</b> (A, in water and B, in acetonitrile) and <b>2a</b> , <b>2b</b> and <b>2f</b> (C, in water and D, in acetonitrile) at 0.1 mM..	143
<b>Figure 4.</b> A) Ball and stick representation of the X-ray structure of Ac-L-Tyr-5- <i>t</i> BuPro-NHMe <b>1c</b> . B) Side-view of the X-ray structure of <b>1c</b> .	144
<b>Figure 5.</b> Rotamers around the C $\alpha$ -C $\beta$ axis in amino acids	145
<b>Figure 6.</b> Influence of sequence in 5- <i>t</i> BuPro-tetrapeptides.	148
<b>Figure 7.</b> Circular dichroism spectra of tetrapeptides <b>14d</b> and <b>14f</b> in water at 0.1 mM.	150
<b>CHAPITRE 4</b>	
<b>Figure 1.</b> Structures de NC et de ses dérivés.	180
<b>Figure 2.</b> Structures de ligands peptidiques du récepteur ORL1.	181
<b>Figure 3.</b> Structures de ligands non peptidiques du récepteur ORL1.	181
<b>Article 8</b>	
<b>Figure 1.</b> Structure of nociceptin/orphanin FQ.	186
<b>Figure 2.</b> Structures of peptide III-BTD ( <b>1</b> ) and JTC-801.	187
<b>Figure 3.</b> Structures of alternative turn mimics incorporated at residues 3 and 4 of hexapeptide ligands.	188
<b>Figure 4.</b> Structures of dipeptide mimics used in the present study of the ORL1 receptor.	189
<b>Figure 5.</b> Dihedral angle values from X-ray data of turn mimics and ideal peptide turns. <sup>20-25</sup>	190

<b>Figure 6.</b> Circular dichroism spectra of Ac-Arg-D-Cha-Xaa-D-Arg-D- <i>p</i> -ClPhe-NH <sub>2</sub> in water at 0.1mM.	202
<b>Figure 7.</b> Stimulation of [ <sup>35</sup> S]GTP $\gamma$ S binding to hORL1 by orphanin FQ/nociceptin and peptides <b>15</b> and <b>17</b> .	204
<b>Figure 8.</b> Stimulation of [ <sup>35</sup> S]GTP $\gamma$ S binding by nociceptin/orphanin FQ on hORL1 in presence of putative antagonist peptides.	205
<b>Figure 9.</b> Stimulation of [ <sup>35</sup> S]GTP $\gamma$ S binding to hKOR by CI-977 and peptides <b>15</b> and <b>17</b> .	206
<b>Figure 10.</b> Stimulation of [ <sup>35</sup> S]GTP $\gamma$ S binding to hMOR by DAMGO and peptides <b>15</b> and <b>17</b> .	207

## LISTE DES SCHÉMAS

### CHAPITRE 1

#### Article 1

<b>Scheme 1.</b> Synthesis of 2-cyano-5- <i>tert</i> -butylpyrrolidines <b>7</b> and <b>8</b> .	18
<b>Scheme 2.</b> Synthesis of <i>N</i> -BOC-5- <i>tert</i> -butylproline via addition of <i>tert</i> -butylcopper reagent.	19
<b>Scheme 3.</b> Synthesis of ketone <b>16</b> .	20
<b>Scheme 4.</b> Synthesis of prolinol <b>21</b> .	22
<b>Scheme 5.</b> Oxidation of <b>21</b> to (2 <i>S</i> ,5 <i>S</i> )- <i>N</i> -BOC-5- <i>tert</i> -butylproline.	24

### CHAPITRE 2

#### Article 3

<b>Scheme 1.</b> Synthesis of <i>N</i> -(acetyl)dipeptide <i>N</i> <sup>1</sup> -methylamides <b>1</b> .	57
--	----

### CHAPITRE 3

#### Article 7

<b>Scheme 1.</b> Synthesis of <i>N</i> -(acetyl)dipeptide <i>N</i> <sup>1</sup> -methylamides <b>1a-f</b> and <b>2a-f</b> .	136
<b>Scheme 2.</b> Solid-phase synthesis of 5- <i>tert</i> -butylprolyl tetrapeptides <b>13</b> and <b>14</b>	137

### CHAPITRE 4

#### Article 8

<b>Scheme 1.</b> Synthesis of peptides <b>15-18</b> .	197
---	-----

## LISTE DES TABLEAUX

### CHAPITRE 2

#### Article 2

<b>Table 1.</b> Acylation of (2 <i>S</i> ,5 <i>R</i> )-5- <i>t</i> BuPro-R with <i>N</i> -(BOC)-amino acids (Xaa).	49
<b>Table 2.</b> Solvent effects on Ac-Xaa-(2 <i>S</i> , 5 <i>R</i> )-5- <i>t</i> BuPro-NHMe conformation.	50

#### Article 3

<b>Table 1.</b> Influence of solvent on the chemical shifts and amide isomer equilibrium of <b>1</b> and <b>2</b> .	59
<b>Table 2.</b> Influence of temperature on the NH chemical shifts of <i>N</i> -(acetyl)dipeptide <i>N</i> <sup>l</sup> -methylamides <b>1</b> and <b>2</b> in DMSO.	60
<b>Table 3.</b> Comparison of the dihedral angles of ideal type VIa β-turn and X-ray structure of <i>N</i> -(acetyl)leucyl-5- <i>tert</i> -butylproline <i>N</i> <sup>l</sup> -methylamide <b>1d</b> .	62

#### Article 4

<b>Table 1.</b> Solvent effect on amide isomer equilibrium of Ac-Xaa-(2 <i>S</i> ,5 <i>R</i> )-5- <i>t</i> BuPro-NHMe.	87
<b>Table 2.</b> Solvent effects on NH chemical shifts of Ac-Xaa-(2 <i>S</i> ,5 <i>R</i> )-5- <i>t</i> BuPro-NHMe.	88

#### Article 5

<b>Table 1.</b> Influence of solvent on the chemical shifts and amide isomer equilibrium of <b>1</b> and <b>2</b> .	96
<b>Table 2.</b> Comparison of the dihedral angles of ideal type VI β-turn and X-ray structure of <i>N</i> -(acetyl)-D-leucyl-5- <i>tert</i> -butylproline <i>N</i> <sup>l</sup> -methylamide ( <i>R</i> )- <b>1b</b> .	103

### CHAPITRE 3

#### Article 6

<b>Table 1.</b> Amide isomer equilibrium of 5- <i>tert</i> -butylprolyl tetrapeptides in 10% D <sub>2</sub> O/H <sub>2</sub> O.	129
---	-----

<b>Table 2.</b> Influence of temperature on amide NH chemical shifts in the major tetrapeptide conformer in 10% D <sub>2</sub> O/H <sub>2</sub> O.	129
--	-----

#### Article 7

<b>Table 1.</b> Comparison of the dihedral angles of ideal type VIa β-turn and X-ray structure of <i>N</i> -(acetyl)tyrosyl-5- <i>tert</i> -butylproline <i>N</i> <sup>1</sup> -methylamide <b>1c</b> .	144
<b>Table 2.</b> Amide isomer equilibrium of tetrapeptides Ac-Xaa-Yaa-5- <i>t</i> BuPro-Zaa-XMe and Ac-Xaa-Yaa-Pro-Zaa-XMe in 10% D <sub>2</sub> O/H <sub>2</sub> O.	147
<b>Table 3.</b> Influence of temperature on the NH chemical shifts of the major isomer of the tetrapeptides <b>13i</b> , <b>14d</b> , <b>14f</b> , <b>15</b> and <b>16</b> in water and in DMSO.	149

### CHAPITRE 4

#### Article 8

<b>Table 1.</b> Chemical shift (ppm) assignments of selected proton resonances and coupling constant values ( <sup>3</sup> J <sub>NH</sub> ) for amide protons within peptides <b>15-18</b> in 10% D <sub>2</sub> O/H <sub>2</sub> O.	200
<b>Table 2.</b> Temperature coefficient Δδ/ΔT (–ppb/K) values of peptides <b>15-18</b> in 10% D <sub>2</sub> O/H <sub>2</sub> O and DMSO.	201
<b>Table 3.</b> Binding affinities for hKOR, hMOR, hDOR and hORL1 of peptides <b>15-18</b> .	203

## LISTE DES ABRÉVIATIONS

$[\alpha]$	rotation spécifique [en (deg mL) / (g dm)]
$\text{\AA}$	angstrom
IAA	acide aminé indolizidinone
Ac	acétyle
$\text{Ac}_2\text{O}$	anhydride acétique
AcOH	acide acétique
Ar	aryle
atm	atmosphere
Bn	benzyle
BOC	<i>tert</i> -butyloxycarbonyle
$(\text{BOC})_2\text{O}$	dicarbonate de di- <i>tert</i> -butyle
BOP-Cl	<i>N,N</i> -bis(2-oxo-3-oxazolidinyl)phosphonic chloride
br	<i>broad</i>
BTD	<i>beta-turn dipeptide</i>
<i>t</i> -Bu	<i>tert</i> -butyle
5- <i>t</i> BuPro	(2 <i>S</i> ,5 <i>R</i> )-5- <i>tert</i> -butylproline
BZA	3-amino-1-carboxymethyl-2,3,4,5-tetrahydro-1 <i>H</i> -[1]-benzazepine-2-one
BZD	3-amino- <i>N</i> -1-carboxymethyl-2-oxo-5-phenyl-1,4-benzodiazepine
<i>c</i>	concentration
°C	degré Celsius
calcd	<i>calculated</i>
CBz	benzyloxycarbonyle
CD	<i>circular dichroism</i>
CI-977	[5 <i>R</i> -(5 $\alpha$ ,7 $\alpha$ ,8 $\beta$ )- <i>N</i> -methyl- <i>N</i> -(7-(1-pyrrolidinyl)oxaspiro[4.5]dec-8-yl]benzo[ <i>b</i> ]furan-4-acetamide
COSY	<i>correlated spectroscopy</i>
$\delta$	déplacement chimique en parties par million
d	doublet

DAMGO	[D-Ala <sup>2</sup> ,N-Me-Phe <sup>4</sup> ,Gly-ol <sup>5</sup> ]enkephalin
dd	doublet de doublet
DC	dichroisme circulaire
DCC	<i>N,N</i> -dicyclohexylcarbodiimide
deg	degré
DIEA	<i>N,N</i> -diisopropyléthylamine
DMAP	4-diméthylaminopyridine
DMF	<i>N,N</i> -diméthylformamide
DMSO	diméthylsulfoxyde
ee	excès énantiomérique
Et	éthyle
Et <sub>2</sub> O	éther diéthylique
EtOAc	acétate d'éthyle
EtOH	éthanol
FAB	<i>fast-atom bombardment</i>
g	gramme
h	heure
Haic	5-amino-1,2,4,5,6,7-tetrahydroazepino[3,2,1-hi]indole-4-one-2-carboxylate
hDOR	human $\delta$ -opioid receptor
hKOR	human $\kappa$ -opioid receptor
hMOR	human $\mu$ -opioid receptor
hORL1	human opioid receptor like
HPLC	<i>high performance liquid chromatography</i>
HRMS	<i>high resolution mass spectrometry</i>
I <sup>2</sup> aa	(3S,6R,10S)-3-amino indolizidin-2-one-9-carboxylate
I <sup>9</sup> aa	(2S,6R,8S)-8-amino indolizidin-9-one-2-carboxylate
J	constante de couplage
K	degré Kelvin
Kcal	kilocalorie
$\lambda$	longueur d'onde

LRMS	<i>low resolution mass spectrometry</i>
$\mu$	micro
M	mole par litre
mM	millimole par litre
MBHA	méthylbenzyhydrylamine
Me	méthyle
MHz	mégahertz
Min	minute
Mol	mole
mmol	millimole
m	multiplet
mp	<i>melting point</i>
NMR	<i>nuclear magnetic resonance</i>
NOE	<i>nuclear Overhauser effect</i>
NOESY	<i>nuclear Overhauser effect spectroscopy</i>
ORL1	<i>Opioid receptor like</i>
ORTEP	<i>Oak Ridge Thermal Ellipsoid Program</i>
Ph	phényle
PhF	phénylfluorényle
ppm	parties par million
Pr	propyle
q	quartet
QAA	(3S,6R,10S)-3-amino quinolizidin-2-one-10-carboxylate
RMN	résonance magnétique nucléaire
ROESY	<i>rotating nuclear Overhauser effect spectroscopy</i>
rt	<i>room temperature</i>
s	singulet
t	triplet
TBTU	<i>benzotriazol-1-yl-1,1,3,3-tetramethyluronium tetrafluoroborate</i>
TEMPO	<i>2,2,6,6-tetramethyl-1-piperidinyloxy, free radical</i>

TFA	acide trifluoroacétique
THF	tétrahydrofurane
TLC	<i>thin layer chromatography</i>
TOCSY	Spectroscopie de corrélation totale
<i>p</i> -TsOH	acide <i>para</i> -toluènesulfonique
Xaa	acide aminé de configuration L

## REMERCIEMENTS

En premier lieu, je tiens à remercier le professeur William D. Lubell pour m'avoir donné l'opportunité d'effectuer ces recherches doctorales au sein de son groupe, pour ses conseils et pour son enthousiasme.

Je désire également remercier les membres du groupe Lubell, Éric Beausoleil, Laurent Bélec, Jérôme Cluzeau, Kenza Dairi, Evelyne Dietrich, James Dettwiler, Zhe Feng, Patrice Gill, Francis Gosselin, Mostafa Hatam, Henry-Georges Lombart, Rosa Melendez, Felix Polyak, Dany Rondeau, Simon Roy, Martin E. Swarbrick, Eryk Thouin, Jo Van Betsbrugge et Lan Wei pour l'esprit d'équipe formidable.

Je voudrais remercier le Dr. Minh Tan Phan Viet, Sylvie Bilodeau et Robert Mayer du Laboratoire de résonance magnétique nucléaire, Francine Bélanger-Gariépy du Laboratoire de diffraction des rayons-X, Mike Evans et Mustapha Harraj du Centre régional de spectrométrie de masse pour leur service.

Je voudrais aussi remercier nos collaborateurs en Belgique, Dirk Tourwé et Zsuzsanna Darula, et en France, Frédéric Simonin, Jérôme A.J. Becker et Brigitte L. Keiffer.

J'aimerais exprimer toute ma reconnaissance à ma famille, Simon, Aida, Viviane, Suzane, Vera, George et mon cher François pour votre support, votre enthousiasme et votre amour. Merci de tout mon cœur!

Finalement, je dois remercier le Conseil de recherches en sciences naturelles et en génie du Canada pour le support financier.

*A Simon et Aida*

# **CHAPITRE 1**

## **Introduction**

### 1.1. Les peptides

Les peptides sont une classe importante de molécules en biochimie, physiologie et chimie médicinale. Plusieurs peptides fonctionnent comme des hormones, des neurotransmetteurs, des antibiotiques, des toxines et immunosuppresseurs.<sup>1</sup> Toutefois, le développement de médicaments basés sur une structure peptidique demeure limité dû à leur dégradation rapide, leur instabilité métabolique et leur flexibilité conformationnelle.<sup>1</sup> Des analogues de peptides naturels possèdant des contraintes conformationnelles sont utiles pour étudier l'interaction entre leur conformation et leur activité biologique. Ainsi, plusieurs chercheurs ont rapporté le design de structures rigides capable d'induire ou de stabiliser des structures secondaires.<sup>2-3</sup>

### 1.2. Le lien amide et l'équilibre conformationnel de la proline

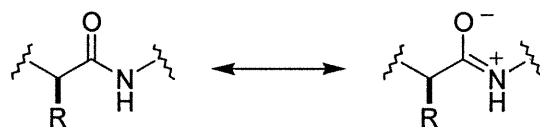


**Figure 1.** Formes de résonance du lien amide.

Un peptide est un polymère d'acide  $\alpha$ -aminé qui est constitué de lien amide. Le lien amide est caractérisé par une forme de résonance où un lien double est obtenu entre le carbone et l'azote du lien peptidique (Figure 1). Ainsi, le carbone du carbonyle, l'oxygène, l'azote et l'hydrogène de l'azote sont tous dans le même plan. L'angle de torsion de ce lien,  $\omega$ , est défini par les atomes du squelette peptidique  $C_{\alpha}$ -C(O)-N-C $_{\alpha}$  (Figure 2). Il existe deux isomères du lien amide: l'isomère *trans* ( $\omega = 180^\circ$ ) et l'isomère *cis* ( $\omega = 0^\circ$ ). L'énergie de rotation du *N,N*-diméthylacétamide est 19.3 kcal/mole (*cis*  $\rightarrow$  *trans*).<sup>4</sup> L'isomère avec le lien amide *trans* possède la plus basse énergie et il est généralement retrouvé pour tous les liens peptidiques sauf pour les amides *N,N*-disubstitués.

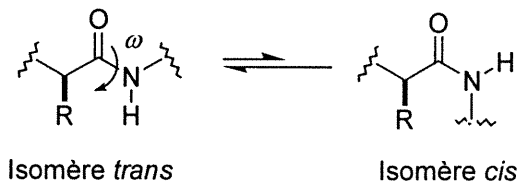


**Figure 2. Isomérisation du lien amide.**

La forme de résonance du lien amide donne à la structure peptidique une autre caractéristique importante, la polarité. Le lien amide est polaire et il possède un moment dipolaire significatif qui rend l'oxygène du carbonyle du lien amide un bon accepteur de pont hydrogène et l'hydrogène de l'amide un bon donneur de lien d'hydrogène. Les ponts hydrogène dans les chaînes peptidiques sont un facteur stabilisant important dans les structures secondaires.<sup>5</sup>

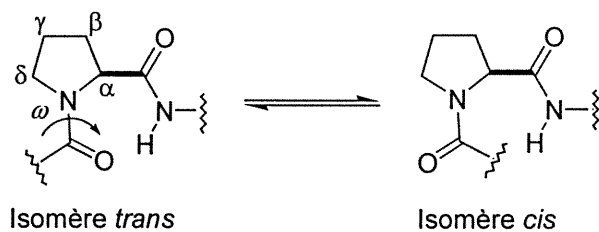


**Figure 3. Isomérisation du lien amide de la proline.**

Pour les liens amides de la proline, l'énergie de l'isomère *trans* du lien Xaa-Pro est élevée, et la différence d'énergie entre les isomères *cis* et *trans* ainsi que la barrière de rotation sont diminuées. La déstabilisation de l'isomère *trans* peut être causée par la répulsion stérique entre le carbone  $\delta$  du cycle pyrrolidine et le carbone  $\alpha$  de l'acide aminé N-terminale de la proline. Les peptides qui contiennent une proline peuvent montrer une isomérisation *cis-trans* du lien Xaa-Pro (Figure 3).<sup>4</sup> Cette isomérisation *cis-trans* des peptides est un processus lent avec une énergie d'activation ( $\Delta G^\ddagger$ ) de 20-22 kcal/mole dans l'eau.<sup>4,6</sup> Ceci peut être observé par des études RMN, car les déplacements chimiques de certains hydrogènes et certains carbones du cycle pyrrolidine sont différents.<sup>7</sup>

La pyramidalisation de l'amide de la proline et la présence d'une interaction de cet amide avec l'hydrogène de l'amide C-terminale de la proline peuvent diminuer l'énergie d'activation et ainsi augmenter la vitesse d'isomérisation (Figure 4).<sup>8</sup>

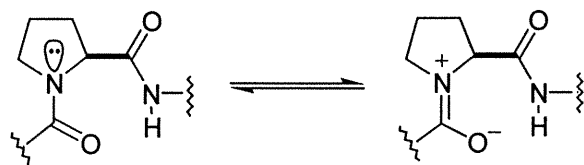


**Figure 4. Pyramidalisation du lien amide de la proline.**

Par ailleurs, le cycle pyrrolidine possède deux géométries, les enveloppes *endo* et *exo* (Figure 5). Lorsque l'amine de la proline est libre, les deux géométries sont d'énergies similaires. Par contre, l'amine acylée de la proline stabilise l'enveloppe *endo* par 1.1 kcal/mole.<sup>9</sup>

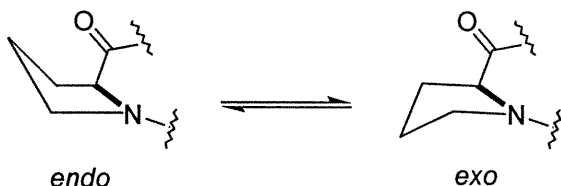


**Figure 5. Géométrie du cycle pyrrolidine de la proline.**

### 1.3. Les structures secondaires des peptides

L'étude des structures secondaires des peptides est importante pour comprendre la relation entre la structure secondaire du peptide et l'activité biologique. La structure des peptides est organisée dans plusieurs niveaux hiérarchiques croissants en complexité structurale. L'évolution structurale d'un peptide débute par sa structure primaire qui est la séquence de résidus d'acides aminés. C'est le premier échelon d'organisation structurale et à certains points de vue, le plus important, car la conformation et la fonction d'un peptide en dépendent. La structure secondaire d'un peptide définit la conformation du squelette polypeptidique. Les types de structure secondaire dans les peptides incluent les hélices  $\alpha$ , les feuillets plissés  $\beta$  ( $\beta$ -sheets),

les épingles  $\beta$  ( $\beta$ -hairpins) et les repliements  $\beta$ . La conformation d'un peptide est décrite selon quatre angles de torsion: l'angle  $\phi$  qui est défini par C(O)-N-C $\alpha$ -C(O), l'angle  $\psi$  qui est défini par N-C $\alpha$ -C(O)-N, l'angle  $\chi$  qui définit les chaînes latérales et l'angle de torsion du lien amide  $\omega$  (Figure 6).<sup>10</sup>

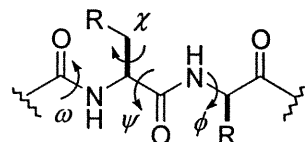


**Figure 6. Angles de torsion d'une chaîne peptidique.**

Parmi les structures secondaires, les repliements jouent un rôle important dans la structure, la fonction et la biologie des peptides.<sup>11</sup> Les repliements sont classés par le nombre de résidus qui sont impliqués dans le tour; les repliements  $\beta$  contiennent quatre résidus d'acides aminés<sup>11,12</sup> et les repliements  $\gamma$  en ont trois<sup>13</sup> (Figure 7). Parmi les tours inversés retrouvés dans les protéines, le repliement  $\beta$  est le plus dominant. En général, dans les repliements  $\beta$ , la structure est stabilisée par un lien d'hydrogène intramoléculaire entre le carbonyle du premier résidu  $i$  et l'hydrogène du lien amide du résidu  $i + 3$  pour former un cycle de 10 membres. Plusieurs types de repliements  $\beta$  existent et sont définis selon les angles de torsion des résidus  $i + 1$  et  $i + 2$ .<sup>14</sup>

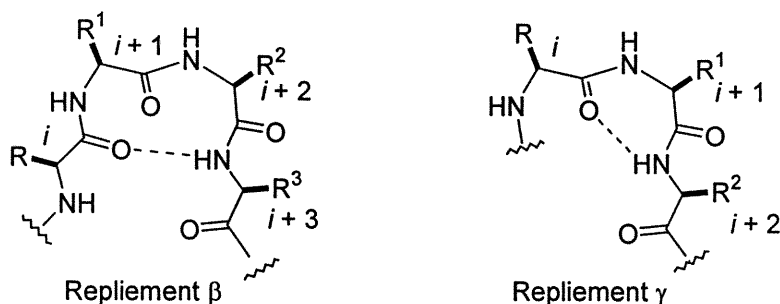


**Figure 7. Structure générale des repliements  $\beta$  et  $\gamma$ .**

#### **1.4. Utilisation des interactions stériques pour stabiliser une conformation.**

En général, les peptides linéaires courts sont des molécules flexibles en milieu aqueux et n'adoptent pas une conformation définie. Ceci peut être détourné par le développement de méthodes pour contraindre les chaînes peptidiques dans des conformations stabilisées. La contrainte conformationnelle peut être divisée conceptuellement dans trois catégories: les contraintes locales qui restreignent la mobilité conformationnelle d'un seul résidu du peptide, les contraintes régionales qui impliquent un groupe de résidus qui forment une unité de structure secondaire comme les repliements  $\beta$  et les contraintes globales qui affectent la structure peptidique complètement.<sup>5</sup>

Les peptides courts requièrent des modifications covalentes pour adopter des conformations stables qui introduisent des contraintes conformationnelles locales ou régionales. Ces contraintes impliquent l'addition de substituent stériquement encombré adjacent à un lien flexible et l'incorporation de mimétique de tour tels que le lactame de Freidinger<sup>15</sup> ou les acides aminés azabicycloalcanes.<sup>2</sup>

Une simple contrainte locale peut être la substitution d'un hydrogène par un groupement méthyle. Par exemple, le remplacement de l'hydrogène  $\alpha$  de l'acide aminé alanine par un groupement méthyle donne l'acide aminoisobutyrique (Aib) 1 (Figure 8). L'encombrement stérique du groupement méthyle diminue la liberté rotationnelle des deux angles adjacents du squelette peptidique  $\phi$  et  $\psi$ . Plusieurs résidus Aib se retrouvent dans les peptides antibiotiques naturels peptaibols qui adoptent une conformation d'hélices.<sup>16</sup> Les substituents en position  $\beta$  d'un acide aminé peuvent influencer l'angle de torsion  $\chi$  et ainsi la géométrie du squelette peptidique. Par exemple, l'acide aminé  $\beta$ -méthyle phénylalanine (3) a été synthétisé et incorporé dans des peptides biologiquement actifs tels que la somatostatine et l'enkephalin pour contraindre l'angle dièdre de la chaîne latérale  $\chi$  (Figure 8).<sup>17</sup>

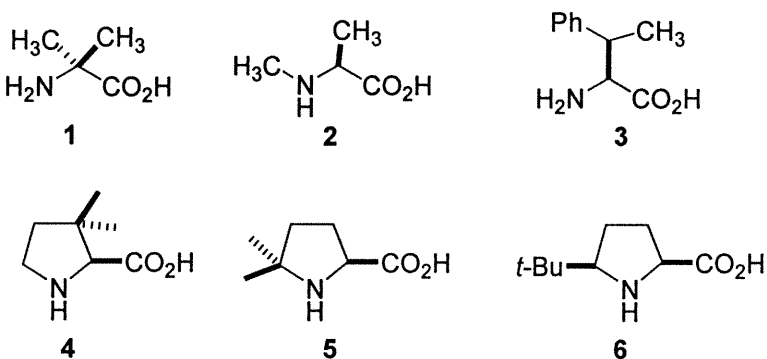


**Figure 8. Exemples représentatifs d'acides aminés substitués.**

Un autre exemple de contrainte locale est la substitution de l'hydrogène du groupement amine d'alanine par un méthyle pour donner l'alanine *N*-méthylé (2) qui joue un effet sur le rapport d'isomérisation *cis-trans* du lien amide en diminuant l'énergie de l'isomère *cis*.<sup>5</sup> La proline est un autre exemple d'acide aminé *N*-méthylé où son angle  $\phi$  est contraint à  $-80^\circ$  à cause du cycle pyrrolidine. Des analogues de la proline avec des groupements substitués en position  $\alpha$ ,  $\beta$ ,  $\gamma$  et  $\delta$  ont été synthétisés et incorporés dans des peptides (4-6).<sup>18</sup> Ces groupements influencent la géométrie du cycle pyrrolidine, l'angle dièdre  $\psi$  de la proline et l'équilibre d'isomérisation de l'amide *N*-terminal de la proline.<sup>18</sup>

L'article qui suit présente une revue détaillée de l'utilisation des interactions stériques pour contraindre certaines conformations. Les effets stériques de substituents sur la géométrie des acides aminés acycliques et cycliques ont été étudiés dans une variété de peptides. Une synthèse améliorée de la *N*-BOC-(2*S*,5*S*)-5-*tert*-butylproline est présentée avec une pureté énantiomérique de >96%. Cet acide aminé pourra ainsi être incorporé dans des peptides pour étudier l'effet de l'encombrement stérique du groupement *tert*-butyle et de sa stéréochimie sur la conformation des peptides.

### 1.5. Références

1. Schmidt, G. *Top. Curr. Chem.* **1986**, *136*, 109.
2. (a) Hanessian, S.; McNaughton-Smith, G.; Lombart, H.-G.; Lubell, W. D. *Tetrahedron* **1997**, *53*, 12789. (b) Gillespie, P.; Cicariello, J.; Olson, G. L.

- Biopolymers, Peptide Science* **1997**, *43*, 191. (c) Etzkorn, F.A.; Travins, J.M.; Hart, S.A. *Adv. Amino Acid Peptidomim.* **1999**, *2*, 125.
3. (a) Giannis, A.; Kolter, T. *Angew. Chem. Int. Ed. Engl.* **1993**, *32*, 1244. (b) Liskamp, R. M.J. *Recl. Trav. Chim. Pays-Bas* **1994**, *113*, 1. (c) Adang, A. E. P.; Hermkens, P. H. H.; Linders, J. T. M.; Ottenheijm, H. C. J.; van Staveren, C. J *Recl. Trav. Chim. Pays-Bas* **1994**, *113*, 63. (d) Gante, J. *Angew. Chem. Int. Ed. Engl.* **1994**, *33*, 1699.
  4. Stein R.L. *Adv. Protein Chem.* **1993**, *44*, 1.
  5. Moore, M. L. "Peptide Design Consideration" in "Synthetic Peptides: A Users's Guide"; Grant, G., Freeman, W.H. and Company Eds, New York, 1993, p.22.
  6. (a) Revue dans: Schmid, F.X.; Mayr, L.M.; Mücke, M.; Schönbrunner, E.R. *Adv. Protein Chem.* **1993**, *44*, 25. (b) Brandts, J.F.; Halvorson, H.R.; Brennan, M. *Biochemistry* **1975**, *14*, 4953.
  7. Deslauriers, R.; Smith, I.C.P. In "Biological Magnetic Resonance"; Berliner, L.J.; Reuben, J., Eds.; Plenum Press: New York, 1980; Vol. 2, pp 275.
  8. (a) Cox, C.; Lectka, T. *J. Am. Chem. Soc.* **1998**, *120*, 10660. (b) Ostergaard, S.; Holm, A. *Molecular Diversity* **1997**, *3*, 17.
  9. Haasnoot, C.A.G.; De Leeuw, F.A.A.M.; Leeuw, H.P.M.; Attona, C. *Biopolymers* **1981**, *20*, 1211.
  10. (a)"IUPAC-IUB Commission on Biochemical Nomenclature" *Biochemistry* **1970**, *9*, 3471. (b) "Principles of Protein Structure"; Schultz, G.E.; Schirmer, R.H.; Cantor, C.R. Eds, Springer, New York, 1979.
  11. Revue dans: Rose, G.D.; Giersch, L.M.; Smith, J.A. *Adv. Protein Chem.* **1985**, *37*, 1.
  12. Venkatachalam, C.M. *Biopolymers* **1968**, *6*, 1425.
  13. Milner-White, E.J.; Ross, B.M.; Ismail, R.; Belhadj-Mostefa, K.; Poet, R. *J. Mol. Biol.* **1988**, *204*, 777.
  14. (a) Ball, J.B.; Alewood, P.F. *J. Mol. Recognit.* **1990**, *3*, 55. (b) Ball, J.B.; Andrews, P.F.; Alewood, P.F.; Hughes, R.A. *FEBS, Lett.* **1990**, *273*, 15.

15. Freidinger, R.M.; Veber, D.F.; Perlow, D.S.; Brooks, J.R.; Saperstein, R. *Science* **1980**, *210*, 656.
16. (a) Chandrasekhar, K.; Das, M.K.; Kumar, A.; Balaram, P. *Int. J. Peptide Protein Res.* **1988**, *32*, 167. (b) Fox, R.O., Jr.; Richards, F.M. *Nature* **1992**, *300*, 325.
17. (a) Huang, Z.; He, Y.-B.; Raynor, K.; Tallent, M.; Reisine, T.; Goodman, M. *J. Am. Chem. Soc.* **1992**, *114*, 9390. (b) Hruby, V.J.; Toth, G.; Gehrig, C.A.; Kao, L.F.; Knapp, R.; Lui, G.K.; Yamamura, H.I.; Kramer, T.H.; Davies, P.; Burks, T.F. *J. Med. Chem.* **1991**, *34*, 1823.
18. (a) Sharma, R.; Lubell, W.D. *J. Org. Chem.* **1996**, *61*, 202. (b) Magaard, V.W.; Sanchez, R.M.; Bean, J.W.; Moore, M.L. *Tetrahedron Lett.* **1993**, *34*, 381. (c) Beausoleil, E.; L'Archevêque, B.; Bélec, L.; Atfani, M.; Lubell, W. D. *J. Org. Chem.* **1996**, *61*, 9447.

**Article 1**

**Halab, L.; Bélec, L.; Lubell, W. D.** "Improved synthesis  
of (2S,5S)-5-*tert*-butylproline." Publié dans  
*Tetrahedron* 2001, 57, 6439-6446.

## Improved Synthesis of (2S,5S)-5-*tert*-Butylproline.

Liliane Halab, Laurent Bélec and William D. Lubell\*

Département de chimie, Université de Montréal

C. P. 6128, Succursale Centre Ville, Montréal, Québec, Canada H3C 3J7

### 1.6. Abstract

(2S,5S)-*N*-BOC-5-*tert*-Butylproline (**1**) was synthesized by an improved procedure featuring the conversion of (2S)-1-*tert*-butyldimethylsiloxy-2-*N*-(PhF)amino-5-oxo-6,6-dimethylheptane (**16**) into its corresponding imino alcohol followed by directed hydride delivery to reduce the imine functionality with a 95:5 diastereoselectivity. Ketone **16** was obtained from methyl 2-*N*-(PhF)amino-5-oxo-6,6-dimethylheptanoate (**13**), a previously reported precursor for the synthesis of (2S,5*R*)-5-*tert*-butylproline, by reduction to its corresponding diol, selective protection of the primary alcohol and oxidation of the secondary alcohol. This route provided (2S,5S)-*N*-BOC-5-*tert*-butylproline (**1**) of >96% enantiomeric purity suitable for peptide chemistry in 39% overall yield from ketone **13**.

**Keywords** : steric effects, 5-*tert*-butylproline, *trans*-diastereomer, directed hydride addition, prolinol, imine, prolinal

**Dedication** We dedicate this work to our colleague Professor Stephen Hanessian on the occasion of his entering into his golden years.

### 1.7. Introduction

Amino acids possessing alkyl substituents have emerged as important tools for controlling peptide conformation. Because their steric interactions can restrict the motion about the backbone and side-chain dihedral angles within a peptide, alkyl-substituted amino acids may promote particular peptide secondary structures.<sup>1-34</sup> Although the steric bulk of the alkyl-substituted amino acid may interfere with

binding and alter biological activity of a peptide analog, the structure-activity relationships of peptides possessing such alkyl-substituted amino acids have in some cases provided a better understanding of the biologically active conformation responsible for receptor recognition and signal transduction. Furthermore, the hydrophobic nature of the alkyl substituent may enhance affinity of conformations that favor antagonist activity at the receptor.<sup>2,3</sup>

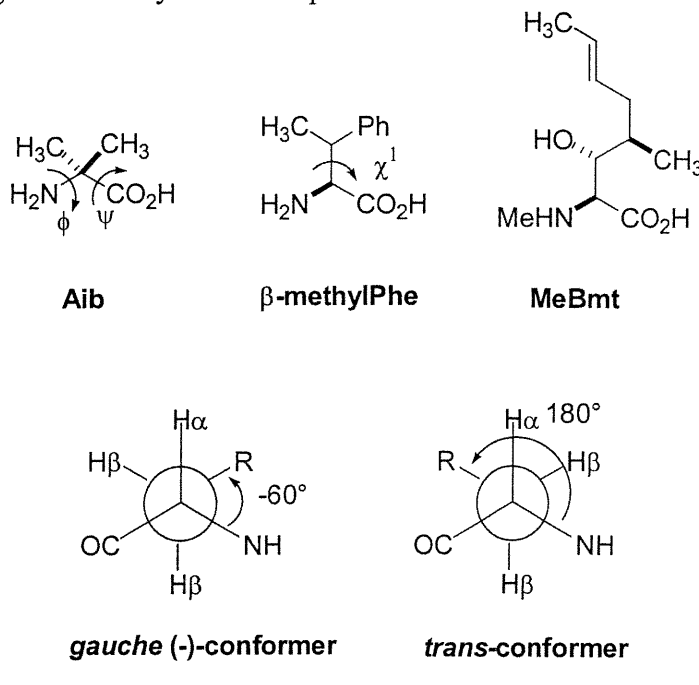


**Figure 1. Representative examples of  $\alpha$ -,  $\beta$ - and  $\gamma$ -alkyl substituted acyclic  $\alpha$ -amino acids.**

Among the acyclic amino acids,  $\alpha,\alpha$ -dialkylglycines, such as  $\alpha$ -aminoisobutyric acid (Aib), exert significant constraints on the backbone dihedral angles in a peptide<sup>4</sup> (Figure 1) and many approaches for their stereoselective synthesis have been reported.<sup>5</sup> Replacement of the  $\alpha$ -proton in an alanine residue with a methyl substituent restricts the  $\phi$  and  $\psi$ -torsion angles to regions that correspond to right- and left-handed  $\alpha$ -helices and  $3_{10}$ -helix geometry as demonstrated by computational analysis.<sup>6</sup> Naturally-occurring Aib-rich peptide antibiotics, peptaibols which produce voltage-gated ion channels in lipid membranes,

have been shown to adopt helical conformations by X-ray analysis and NMR spectroscopy.<sup>7</sup> Related long synthetic peptides containing at least one Aib residue among 5 to 20 residues have been shown by X-ray analysis to adopt predominantly helical geometry.<sup>8</sup> Type III  $\beta$ -turn conformations have been observed by X-ray crystallography to be stabilized when Aib residues were introduced into shorter peptides composed of 2-4 amino acids.<sup>4</sup>  $\alpha,\alpha$ -Dialkylglycines containing larger  $\alpha$ -alkyl substituents, such as  $\alpha,\alpha$ -diethylglycine (Deg),  $\alpha,\alpha$ -di-*n*-propylglycine (Dpg),  $\alpha,\alpha$ -di-*n*-butylglycine (Dbg),  $\alpha,\alpha$ -diphenylglycine (D $\Phi$ g) and  $\alpha,\alpha$ -dibenzylglycine (Db<sub>z</sub>g), have favored fully extended C<sub>5</sub> structures in peptides characterized by 180°  $\phi$  and  $\psi$ -dihedral angles and intramolecular H-bonds between the amide hydrogen and carbonyl oxygen groups within the same residue.<sup>9,10</sup> 1-Aminocycloalkane-1-carboxylic acids of 3-, and 5- to 7-carbon ring-sizes have induced helical,  $\beta$ -turn and  $\gamma$ -turn conformations in peptides of 3 to 10 residues as observed in solution and in the solid state.<sup>10,11</sup>  $\beta$ -Alkyl substituents can influence significantly the side-chain dihedral angle and to some extent the backbone geometry of amino acid residues in peptides. Several  $\beta$ -methyl analogs of the naturally occurring amino acids (Asp, Glu, His, Phe, Trp and Tyr) have been stereoselectively synthesized for application in peptide mimics.<sup>12-14</sup> For example,  $\beta$ -methylphenylalanine has been employed to constrain the side-chain  $\chi^1$  dihedral angles in enkephalin and somatostatin analogs.<sup>3,15</sup> The steric effects of the  $\beta$ -methyl group are contingent on stereochemistry.<sup>12,16</sup> In (2*S*,3*R*)- $\beta$ -MePhe, the side-chain  $\chi^1$  dihedral angle adopted the *trans*-conformer and in (2*S*,3*S*)- $\beta$ -MePhe the *gauche* (-) conformer was preferred (Figure 1).<sup>15,16</sup>  $\gamma$ -Alkyl substituents may also influence side-chain geometry of an amino acid residue in a peptide. Although several  $\gamma$ -alkyl analogs of the naturally occurring amino acids have been synthesized,<sup>17-19,26,56a</sup> their influence on peptide conformation and biology has been less thoroughly studied. Their significance to peptide biology has been illustrated in an analog of the natural cyclic peptide cyclosporine, where removal of

the  $\gamma$ -alkyl substituents from the MeBmt residue caused a dramatic reduction in immunosuppressive activity (Figure 1).<sup>20</sup>

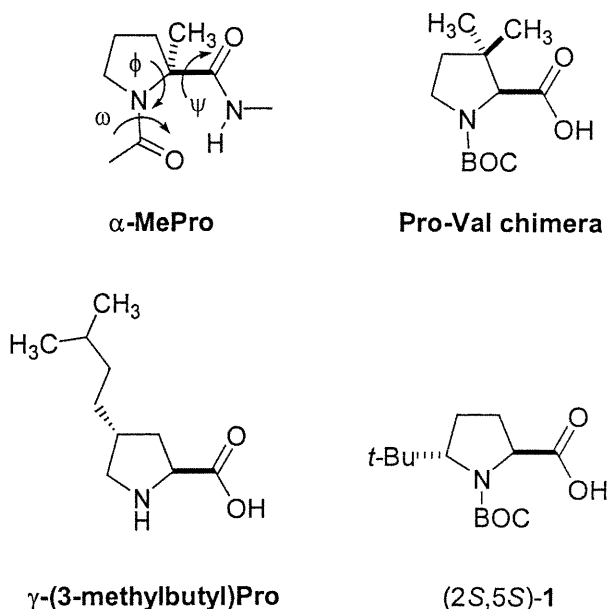


**Figure 2. Representative examples  $\alpha$ -,  $\beta$ -  $\gamma$ - and  $\delta$ -alkyl substituted acyclic  $\alpha$ -amino acids.**

Among cyclic amino acids, azetidine-2-carboxylic acids, prolines and pipecolates possessing alkyl substituents have been synthesized and introduced into peptides.<sup>1,2,21-38</sup> In prolyl peptides, alkyl substituents can influence the ring puckering, the  $\psi$ -dihedral angle and the *N*-terminal amide equilibrium of the proline residue. For example, in *N*-acetyl  $\alpha$ -methylproline *N'*-methylamide, only the *trans*-amide isomer was observed by NMR spectroscopy in CDCl<sub>3</sub> and in water.<sup>23</sup> Several  $\beta$ -substituted azetidine-2-carboxylates, prolines and pipecolates have been synthesized to serve as amino acid chimeras in which the functional groups of the amino acid side-chain are combined with the conformational restrictions characteristic of the cyclic amino acid residue.<sup>22a,24,35-37</sup> Chimeras with proline bodies have been used to study the relationship of side-chain geometry to bioactivity in biologically active peptides such as angiotensin II, bradykinin, morphiceptin, and

cholecystokinin.<sup>24</sup> Although  $\beta$ -substituents exhibited little effect on the populations of the prolyl amide isomers, they have influenced the proline  $\psi$ -dihedral angle as well as the energy barrier for amide isomerization. In the case of *N*-acetyl  $\beta$ -methylproline *N*-methylamides, the *cis*- $\beta$ -methyl substituent imposed steric interactions that restricted the  $\psi$  dihedral angle and prevented formation of a  $\gamma$ -turn conformation ( $\psi \approx 80^\circ$ ) as observed by IR spectroscopy.<sup>23a</sup> A similar effect was observed in *N*-acetyl  $\beta,\beta$ -dimethylproline *N*-methylamide; moreover, the presence of the two methyl substituents in this proline-valine chimera was shown to cause a nearly seven-fold reduction in the rate of prolyl amide isomerization as demonstrated by magnetization transfer experiments (Figure 2).<sup>25</sup>  $\gamma$ -Alkylprolines have been stereoselectively synthesized and used to prepare proline oligomers because their ring substituents interact minimally with the prolyl residue conformation.<sup>26-28</sup> For example, natural poly-proline type II geometry was adopted by short oligomers composed of *trans*-4-(3-methylbutyl)prolines as observed by NMR spectroscopy.<sup>28</sup> On the other hand,  $\delta$ -alkyl substituents can exhibit significant steric interactions that may disturb the preferred conformation about the prolyl residue.<sup>1,2,29-34,38</sup> For example, replacement of proline by (2*S*,5*R*)-5-*tert*-butylproline in peptides has increased the prolyl amide *cis*-isomer population, diminished the barrier for prolyl amide isomerization and favored the formation of type VI  $\beta$ -turns.<sup>2,30-33</sup> In *N*-acetylproline *N*-methylamides, (2*S*,5*S*)-5-*tert*-butylproline caused a greater increase in *cis*-isomer population relative to its *cis*-diastereomer counterpart without influencing the barrier for amide isomerization relative to proline.<sup>30</sup> In addition, *N*-acetyl-*trans*-5-*tert*-butylproline *N*-methylamide was shown by IR spectroscopy not to adopt a seven member  $\gamma$ -turn conformation, which was a favored conformer for its natural proline and *cis*-diastereomer counterparts in CHCl<sub>3</sub>.<sup>30</sup>

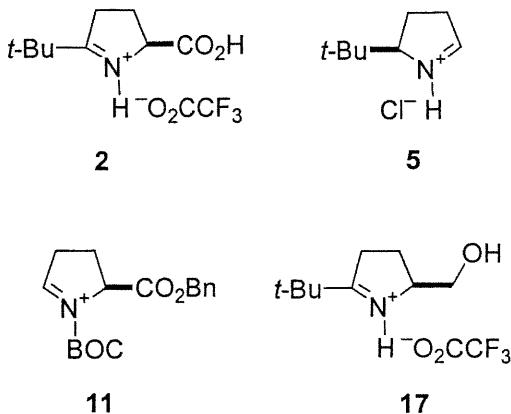


**Figure 3. Iminium ion intermediates used in the synthesis of *trans*-5-*tert*-butylproline.**

These examples demonstrate the ability of alkyl substituted amino acids to reinforce and to disturb natural peptide secondary structures. Improved methods for synthesizing alkyl substituted amino acids advance their use by making them more readily accessible for peptide science. In our own work with 5-*tert*-butylproline, we have until now focused primarily on the (2*S*,5*R*)-diastereomer, because it can be synthesized effectively via our high-yielding stereoselective sequence featuring acylation of  $\gamma$ -methyl *N*-(PhF)-L-glutamate followed by ester hydrolysis, decarboxylation and reductive amination.<sup>21</sup> Less attention has been given to the (2*S*,5*S*)-diastereomer because of drawbacks in its stereoselective synthesis. For example, although good diastereoselectivity was achieved in the hydride reduction of (2*S*)-5-*tert*-butyl- $\Delta^5$ -dehydroproline trifluoroacetate (**2**) to furnish the *trans*-diastereomer, the iminium ion intermediate **2** proved to be configurationally labile and racemized product was obtained (Figure 3).<sup>21</sup> Although epimerization of the (2*S*,5*R*)-diastereomer of *N*-benzyl-5-*tert*-butylproline methyl ester could be used to provide enantiopure (2*R*,5*R*)-diasereomer, only a 1:1 ratio of (2*S*)-:(2*R*)-isomers was achieved under our best conditions: *t*-BuOK in *t*-BuOH at 50°C.<sup>21</sup> Encouraged by our success in the use of (2*S*,5*R*)-5-*tert*-butylproline in the synthesis of type VI  $\beta$ -turn mimics,<sup>31,32</sup> polyproline analogs<sup>33</sup> and biologically active derivatives of natural prolyl

peptides such as oxytocin,<sup>2</sup> we chose to explore the attributes of its (2*S*,5*S*)-diastereomer for peptide mimicry. We present now an improved synthesis of (2*S*,5*S*)-5-*tert*-butylproline that provides enantiopure material (>96% ee) suitably protected for peptide synthesis.

### 1.8. Results and Discussion

Several approaches were considered for the synthesis of enantiopure *trans*-5-*tert*-butylproline. Because of limited success in the epimerization of (2*S*,5*R*)- to (2*R*,5*R*)-*N*-benzyl-5-*tert*-butylproline methyl ester, we examined epimerization of its bicyclic lactam counterpart, proline **3** (Figure 4). Although protonation with inversion of configuration was considered for producing the *trans*-5-*tert*-butylproline, computational analysis of the *cis*- and *trans*-lactam diastereomers **3** indicated that the energy minimum for the *cis*-isomer was 0.9 kcal/mol lower than that of its *trans*-counterpart.<sup>39</sup>

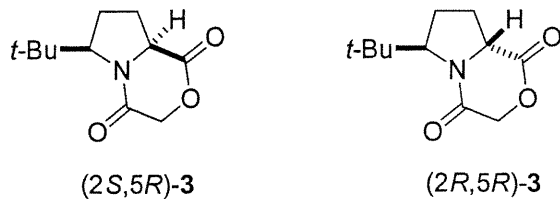
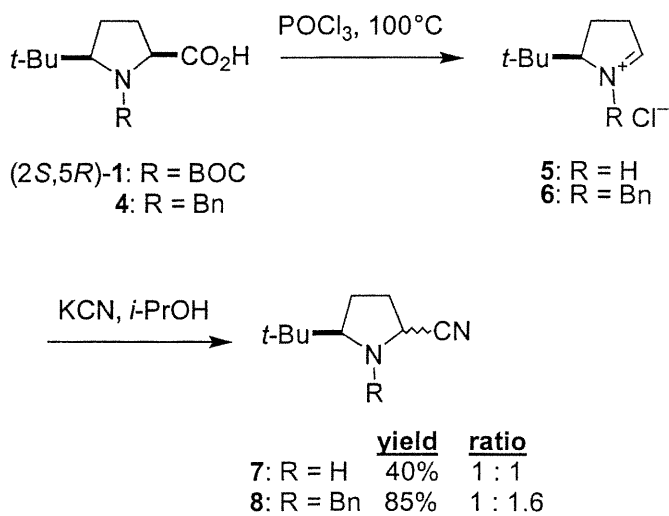


**Figure 4. Prolyl lactam **3**.**

Opting for a new strategy for synthesizing *trans*-5-*tert*-butylproline, we examined the addition of cyanide ion to iminium salt **5** obtained from decarboxylation of the (2*S*,5*R*)-diastereomer. A similar approach had been used previously for the synthesis of *N*-benzyl-2-cyano-5-heptylpyrrolidine to afford a 3:1 mixture of *trans:cis* diastereomers for the preparation of 2,5-dialkylpyrrolidines found in ant venum.<sup>40</sup> We prepared both iminium salt **5** and its *N*-benzyl analog **6** by heating their respective *N*-protected-(2*S*,5*R*)-5-*tert*-butylproline (**1** and **4**) with POCl<sub>3</sub> at 100°C (Scheme 1). Although the bulky *tert*-butyl substituent was envisioned to

direct attack towards the less hindered face of the iminium salt to provide the *trans*-isomer, the 2-cyano-5-*tert*-butylpyrrolidines (**7** and **8**) were obtained with low diastereoselectivity. For example, treatment of iminium salt **5** with KCN in isopropanol gave a 1:1 mixture of (2*S*,5*R*)- and (2*R*,5*R*)-2-cyano-5-*tert*-butylpyrrolidines in 40% yield.

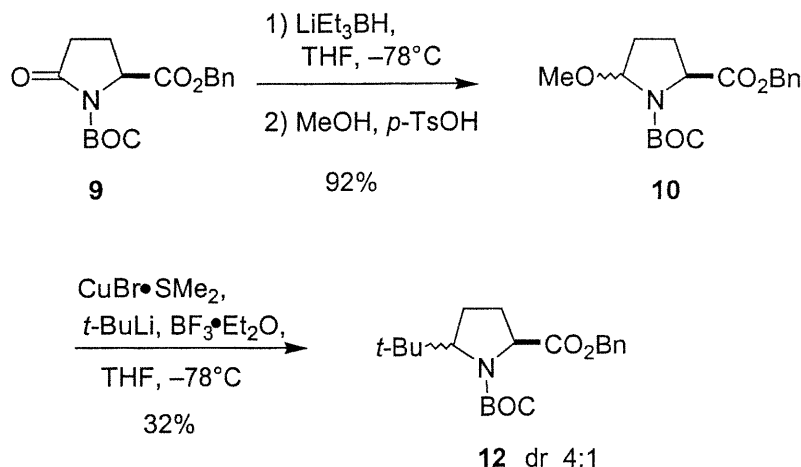


**Scheme 1. Synthesis of 2-cyano-5-*tert*-butylpyrrolidines **7** and **8**.**

This ratio remained unchanged after attempts to equilibrate the mixture with silica gel in an isoctane:EtOAc solution.<sup>40</sup> Although the overall yield was increased to 58% when TMSCN in THF was used in the second step of the two step sequence, diastereomeric 2-cyano-5-*tert*-butylpyrrolidines **7** were obtained again as a 1:1 mixture. The yield of the sequence could be improved to 85% by employing *N*-(benzyl)proline **4**,<sup>21</sup> however, *N*-benzyl-2-cyano-5-*tert*-butylpyrrolidines (**8**) were produced as a 1:1.6 mixture of diastereomers.

To improve diastereoselectivity, we investigated next the addition of a *tert*-butylcopper reagent to prolyl iminium ion **11** (Figure 3). Less sterically bulky alkylcopper reagents, possessing *n*-propyl, *n*-butyl, *n*-heptyl, phenyl, benzyl and *iso*-

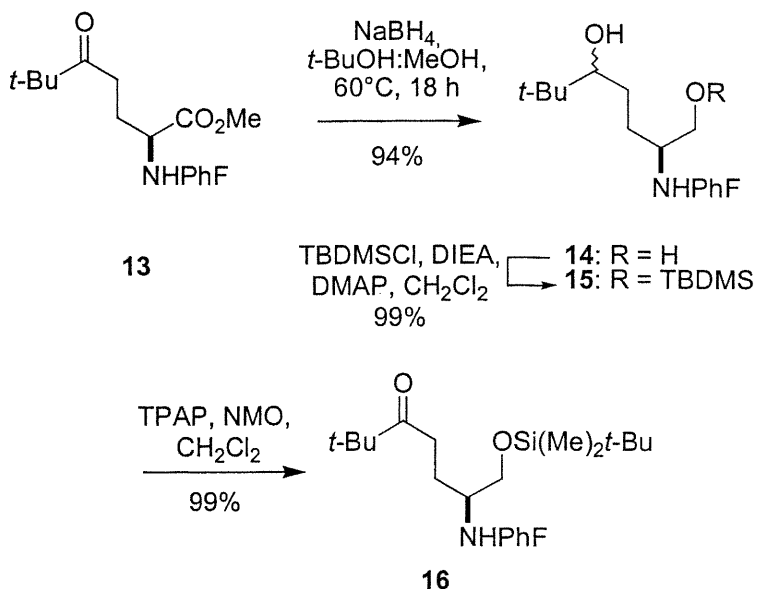
propenyl substituents, have been reported to add diastereoselectively to iminium ions to afford 5-alkylprolines with the *trans* configuration.<sup>41,42</sup>



**Scheme 2. Synthesis of *N*-BOC-5-*tert*-butylproline via addition of *tert*-butylcopper reagent.**

Furthermore, the *tert*-butylcopper reagent prepared from CuI and *t*-BuLi had been reported to react quantitatively with benzoyl chloride in dimethylsulfide at  $-78^\circ\text{C}$  to afford phenyl *tert*-butylketone.<sup>43</sup> Initially, *N*-BOC-5-methoxyproline benzyl ester (**10**) was synthesized as a 2:3 mixture of diastereomers in 92% yield by reduction of *N*-BOC-pyroglutamate benzyl ester<sup>44</sup> (**9**) with LiEt<sub>3</sub>BH in THF followed by etherification of the aminal in MeOH with a catalytic amount of *p*-toluenesulfonic acid (Scheme 3).<sup>45</sup> Although several attempts to add a *tert*-butylcopper reagent to **11** failed, in one experiment, addition of a diastereomeric mixture of *N*-BOC-5-methoxyproline benzyl ester (**10**) to a suspension of *t*-BuLi, CuBr•SMe<sub>2</sub> and BF<sub>3</sub>•OEt<sub>2</sub> in THF at  $-78^\circ\text{C}$  provided protected 5-*tert*-butylproline **12** as a 1:4 mixture of diastereomers in 32% yield.<sup>46</sup> Because we could not later reproduce this result, we abandoned this approach involving *tert*-butylcopper reagents which were known to be sensitive to variations in reaction solvent and temperature.<sup>43</sup>

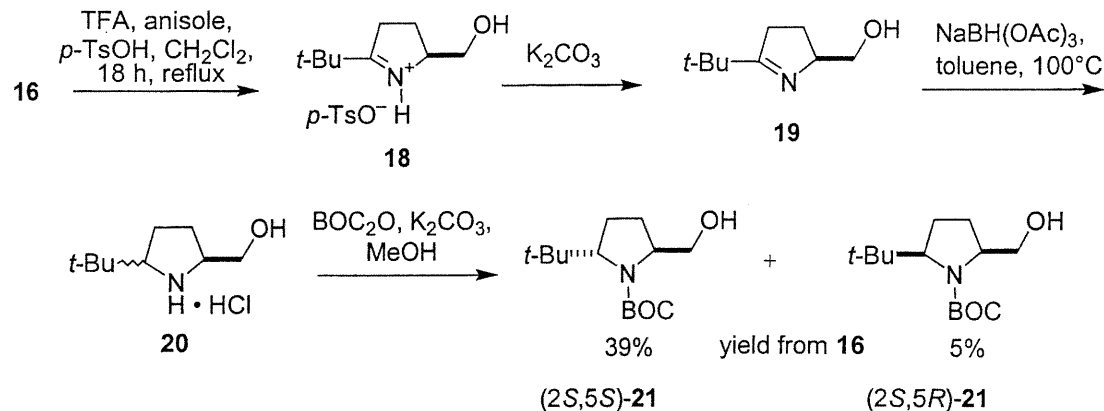
The less than satisfactory results we obtained in nucleophilic additions of cyanide ion and *tert*-butylcopper reagents respectively to iminium salts **5** and **11** (Figure 3) made us reconsider our published strategy for synthesizing (2*S*,5*S*)-5-*tert*-butylproline with a significant modification. As mentioned, we found previously that hydride reduction of iminium acid **2** provided *trans*-5-*tert*-butylproline diastereoselectively with significant racemization due to the configurational lability of this intermediate under the acidic conditions for its production.<sup>21</sup> Attempts to circumvent racemization by using its more configurationally stable amide counterpart resulted in lower diastereoselectivity.<sup>21</sup> Reduction of the carboxylate to its respective alcohol has now been investigated as a means to alleviate the problem of racemization and to install an effective site for metal hydride coordination in order to direct iminium ion reduction to afford the *trans*-diastereomer.  $\beta$ -Hydroxy ketones have been reported to reduce diastereoselectively using tetramethylammonium triacetoxyborohydride to provide *anti* diols by directed intramolecular hydride delivery.<sup>47</sup> Furthermore, reduction of imino alcohols under similar conditions have been reported to produce predominantly *trans*-2-hydroxymethyl-5-alkylpyrrolidines possessing 5-methyl and 5-*n*-nonyl substituents in 83:17 and 70:30 respective ratios.<sup>48</sup> We pursued thus the synthesis and reduction of (2*S*)-5-*tert*-butyl- $\Delta^5$ -dehydroprolinol **19** in order to prepare (2*S*, 5*S*)-5-*tert*-butylproline.



**Scheme 3. Synthesis of ketone 16.**

The synthesis of *(2S)*-5-*tert*-butyl- $\Delta^5$ -dehydroprolinol (**19**) started with methyl 2-*N*-(PhF)amino-5-oxo-6,6-dimethylheptanoate (**13**), an intermediate in the synthesis of *(2S,5R)*-5-*tert*-butylproline derived from acylation of  $\gamma$ -methyl *N*-PhF-L-glutamate with pivaloyl chloride, ester hydrolysis, decarboxylation and esterification.<sup>21</sup> Sodium borohydride reduction of ketone **13** in a mixture of methanol:*tert*-butanol at 60°C gave 2-*N*-(PhF)amino-5-hydroxy-6,6-dimethylheptanol **14** in 94% yield as a 1:1 mixture of diastereomers (Scheme 3).<sup>49</sup> 1-*tert*-Butyldimethylsiloxy-2-*N*-(PhF)amino-5-oxo-6,6-dimethylheptane **16** was then synthesized in quantitative yield by selective protection of the primary alcohol of diol **14** with *tert*-butyldimethylsilyl chloride, DIEA and DMAP in  $\text{CH}_2\text{Cl}_2$  heated at a reflux,<sup>49</sup> followed by oxidation of neopentyl alcohol **15** with tetrapropylammonium perruthenate (TPAP) and *N*-methylmorpholine oxide in  $\text{CH}_2\text{Cl}_2$ .<sup>50</sup> Earlier attempts failed to oxidize the secondary alcohol of **15** to its corresponding ketone **16** using DMSO and oxalyl chloride in dichloromethane,<sup>51</sup> as well as using methylsulfide and *N*-chlorosuccinamide in toluene,<sup>52</sup> and only starting material was isolated after each reaction.

Concurrent deprotection of the silyl ether and PhF groups with formation of the iminium salt **17** was achieved on heating ketone **16** with anisole in a 1:3 TFA:CH<sub>2</sub>Cl<sub>2</sub> solution at a reflux for 70 h (Scheme 4). Because trifluoroacetate **17** (Figure 3) was volatile, the acidic counter ion was exchanged with *p*-toluenesulfonic acid as monitored by comparison of the integrations for the *tert*-butyl and methyl singlets respectively at 1.35 and 2.36 ppm in the proton NMR spectrum in CDCl<sub>3</sub>. On larger scale, *p*-TsOH (100 mol%) was added at the start of the reaction to ketone **16** and anisole in 25% TFA:CH<sub>2</sub>Cl<sub>2</sub> and the conversion to **18** was complete after 18 h. The configurational stability of iminium salt **18** was demonstrated by measuring the specific rotation of **18** after treatments with 25% TFA:CH<sub>2</sub>Cl<sub>2</sub> at reflux for 18, 24, 48 and 72 h. Because the specific rotation value of **18** remained unchanged after these treatments, iminium salt **18** was concluded to be configurationally stable under these acidic conditions.



Scheme 4. Synthesis of prolinol **21**.

(*2S,5S*)-*N*-BOC-5-*tert*-Butylprolinol (**21**) was obtained from *p*-toluenesulfonate **18** by a sequence commencing with liberation of imine **19** on washing with aqueous potassium carbonate, imine reduction with sodium triacetoxyborohydride in toluene at 100°C and *N*-acylation with di-*tert*-butyldicarbonate in acetonitrile (Scheme 4). Alcohol **21** was obtained in 68% overall

yield from ketone **16** as a >95:5 diastereomeric mixture on small scale. Lower diastereoselectivity (87:13 *trans:cis*) was obtained when *p*-toluenesulfonate **18** was reduced under the same conditions. On larger scale, the diastereomeric *N*-(BOC)amino alcohols were separated by chromatography and (2*S*,5*S*)- and (2*S*,5*R*)-**21** were isolated in 39% and 5% respective overall yield from ketone **16**. The predominant *trans*-isomer is proposed to result from a transition state involving coordination of the borohydride by the alcohol and intramolecular hydride delivery to the *si* face of the iminium ion (Figure 5).<sup>47,48</sup> For comparison, an authentic sample of the minor alcohol isomer (2*S*,5*R*)-**21** was synthesized by reduction of acid (2*S*,5*R*)-**1** using borane in THF.<sup>53</sup>

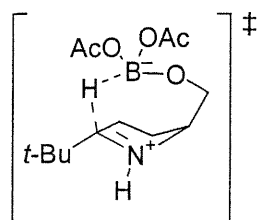
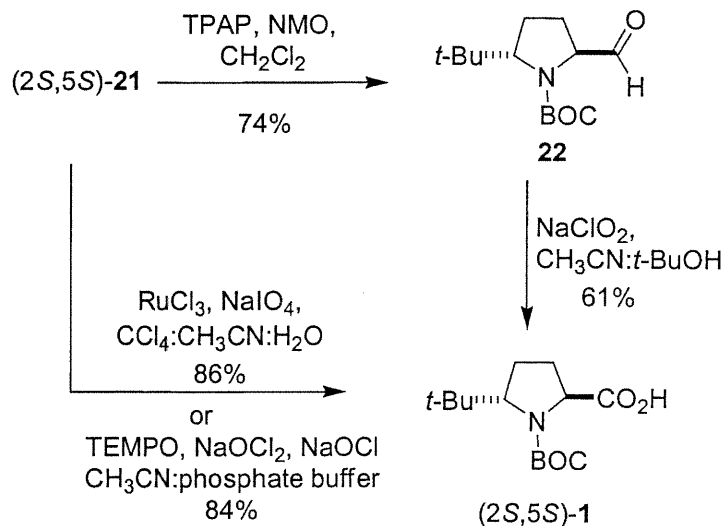


**Figure 5.** Proposed transition state for hydride addition to imine **19**.

(2*S*,5*S*)-*N*-BOC-5-*tert*-Butylproline was produced by two different oxidation procedures. Direct oxidation of alcohol **21** to acid (2*S*,5*S*)-**1** was accomplished in 86% yield using ruthenium trichloride and sodium periodate in a solvent mixture of 2:2:3 CCl<sub>4</sub>:CH<sub>3</sub>CN:H<sub>2</sub>O (Scheme 5).<sup>54</sup> On larger scale, alcohol **21** was oxidized to the corresponding acid in 84% yield using 2,2,6,6-tetramethyl-1-piperidinyloxy (TEMPO), sodium chlorite and sodium hypochlorite in a sodium phosphate buffered acetonitrile solution.<sup>55</sup>



**Scheme 5. Oxidation of 21 to (2*S,5S*)-*N*-BOC-5-*tert*-butylproline.**

Alternatively, oxidation of **21** to the prolinal **22** was achieved using TPAP and *N*-methylmorpholine oxide in CH<sub>2</sub>Cl<sub>2</sub>.<sup>50</sup> Subsequent oxidation to the corresponding acid was then performed using NaClO<sub>2</sub> in 1:1 CH<sub>3</sub>CN:*t*-BuOH to provide (2*S,5S*)-**1** in 45% overall yield from the two step process.<sup>56</sup> Because no epimerization was observed after purification of aldehyde **22** on silica gel nor during conversion to acid **1**, prolinal **22** is an attractive intermediate for synthesizing analogs of prolyl residues having *C*-terminal modifications, such as those found in the dolastatins,<sup>57</sup> to study relationships between their amide isomer geometry and bioactivity.

The enantiomeric purity of (2*S,5S*)-5-*tert*-butylproline (**1**) was determined as described previously.<sup>21</sup> Formation of diastereomeric  $\alpha$ -methylbenzylamides was first performed on coupling (*R*)- and (*S*)-methylbenzylamine to (2*S,5S*)-**1** using TBTU in acetonitrile, then the BOC group was removed with TFA in CH<sub>2</sub>Cl<sub>2</sub>.<sup>21</sup> Integration of the *tert*-butyl singlets (1.055 and 1.065 ppm) in the proton 600 MHz NMR spectra in CD<sub>3</sub>OD revealed the amides to be of a >98:2 diastereomeric ratio. Hence, (2*S,5S*)-5-*tert*-butylproline is presumed to be of >96% enantiomeric purity.

In conclusion, we have developed an efficient synthesis of *(2S,5S)-5-tert-butylproline*. Starting from methyl 2-*N*-(PhF)amino-5-oxo-6,6-dimethylheptanoate (**13**), a precursor of *(2S,5R)-5-tert-butylproline*, *(2S,5S)-N*-BOC-5-*tert*-butylproline was obtained in 39% overall yield and >96% enantiomeric purity via directed hydride addition to imine **19**. With an effective means for producing *(2S,5S)-5-tert-butylproline* in hand, we are now exploring its introduction into peptides in order to study the influence of this stereoisomer on peptide conformation and biology.

### 1.9. Experimental Section

**General.** Unless otherwise noted, all reactions were run under a nitrogen atmosphere and distilled solvents were transferred by syringe. Dichloromethane was distilled over P<sub>2</sub>O<sub>5</sub>, THF was distilled over sodium/benzophenone, toluene was distilled over sodium and DIEA was distilled over ninhydrin and CaH<sub>2</sub>. Final reaction mixture solutions were dried over Na<sub>2</sub>SO<sub>4</sub>. Chromatography was on 230-400 mesh silica gel, and TLC was on aluminium-backed silica plates. Mass spectral data, HRMS (EI and FAB), were obtained by the Université de Montréal Mass Spectroscopy facility. <sup>1</sup>H and <sup>13</sup>C NMR experiments were performed on Brucker ARX400 and av400 spectrometers. The chemical shifts are reported in ppm ( $\delta$  units) downfield of internal tetramethylsilane ((CH<sub>3</sub>)<sub>4</sub>Si). Coupling constants are in hertz. Aromatic carbon resonances for PhF groups are not reported.

**(2*S*,5*RS*)-2-*N*-(PhF)Amino-5-hydroxy-6,6-dimethylheptanol (14).** A solution of ketone **13** (3.16 g, 7.16 mmol) in a mixture of *tert*-butanol (200 mL) and MeOH (12 mL) was treated with NaBH<sub>4</sub> (0.812 g, 300 mol%), stirred at 60°C for 4 h, cooled to room temperature and diluted with water (150 mL). The mixture was extracted with EtOAc (3 x 150 mL) and the organic phase was washed with brine, dried and evaporated to a residue that was purified by chromatography on silica gel using 25% EtOAc in hexane as eluant. Evaporation of the collected fractions furnished a 1:1

mixture of diastereomers **14** (2.80 g, 94% yield) as a white foam:  $^1\text{H}$  NMR ( $\text{CDCl}_3$ )  $\delta$  0.79 (s, 9 H), 0.83 (s, 9 H), 0.98 (m, 2 H), 1.18-1.28 (m, 4 H), 1.48 (m, 2 H), 2.13-2.20 (m, 2 H), 2.27 (br s, 2 H), 2.77-3.12 (m, 6 H), 7.19-7.43 (m, 22 H), 7.67-7.74 (m, 4 H);  $^{13}\text{C}$  NMR ( $\text{CDCl}_3$ )  $\delta$  25.5, 25.6, 27.5 (2 C), 30.8, 31.4, 34.7, 34.8, 53.5, 54.0, 63.7, 64.0, 72.5, 72.6, 79.3, 79.9; HRMS calcd for  $\text{C}_{28}\text{H}_{34}\text{O}_2\text{N} (\text{MH}^+)$  416.2589, found 416.2602.

**(2S,5RS)-1-*tert*-Butyldimethylsiloxy-2-N-(PhF)amino-5-hydroxy-6,6-dimethylheptane (15).** A solution of diol **14** (2.74 g, 6.6 mmol) in  $\text{CH}_2\text{Cl}_2$  (70 mL) was treated with DIEA (4.6 mL, 26.4 mmol), DMAP (0.08 g, 0.66 mmol) and TBDMSCl (1.99 g, 13.2 mmol). The mixture was heated at a reflux for 6 h when complete consumption of the starting alcohol ( $R_f = 0.18$ , 30% EtOAc in hexane) was observed by TLC. The solution was evaporated to a residue that was dissolved in EtOAc (100 mL) and washed with 0.1 M HCl (100 mL) and brine, dried and evaporated to a residue that was purified by chromatography on silica gel using 5% EtOAc in hexane as eluant. The alcohol **15**, an oil (3.50 g, 99% yield) was obtained as a 1:1 mixture of diastereomers:  $^1\text{H}$  NMR ( $\text{CDCl}_3$ )  $\delta$  -0.09 (t, 12 H,  $J = 7.9$ ), 0.84 (s, 18 H), 0.85 (s, 9 H), 0.89 (s, 9 H), 1.03-1.10 (m, 2 H), 1.25 (m, 4 H), 1.42-1.52 (m, 2 H), 2.12 (m, 1 H), 2.20 (m, 1 H), 2.70 (br s, 2 H), 2.88 (dd, 3 H,  $J = 4.9, 9.6$ ), 3.00 (m, 4 H), 3.22 (dd, 1 H,  $J = 5.2, 9.9$ ), 7.18-7.47 (m, 22 H), 7.67-7.71 (m, 4 H);  $^{13}\text{C}$  NMR ( $\text{CDCl}_3$ )  $\delta$  -5.7, -5.6, -5.5, -5.4, 18.2 (2 C), 25.7, 25.8, 27.3, 27.8, 30.7, 32.1, 34.7, 34.8, 53.8, 54.6, 65.4 (2 C), 72.5, 72.7, 79.6, 80.2; HRMS calcd for  $\text{C}_{34}\text{H}_{47}\text{O}_2\text{NSi} (\text{MH}^+)$  530.3455, found 530.3445.

**(2S)-1-*tert*-Butyldimethylsiloxy-2-N-(PhF)amino-5-oxo-6,6-Dimethylheptane (16).** A solution of diol **15** (3.50 g, 6.6 mmol) and *N*-methylmorpholine oxide (1.54 g, 13.2 mmol) in  $\text{CH}_2\text{Cl}_2$  (66 mL) over powdered 4 Å molecular sieves (4.0 g) was

treated with tetrapropylammonium perruthenate (0.23 g, 10 mol%) at room temperature, stirred for 3 h and filtered through a pad of silica gel using 5% EtOAc in hexanes as eluant. Evaporation of the filtrate gave ketone **16** (3.44 g, 99% yield) as an oil:  $[\alpha]^{20}_D -115.3^\circ$  (*c* 0.36, CHCl<sub>3</sub>); <sup>1</sup>H NMR (CDCl<sub>3</sub>)  $\delta$  –0.07 (d, 6 H, *J* = 8.8), 0.87 (s, 9 H), 1.16 (s, 9 H), 1.41–1.48 (m, 1 H), 1.53–1.62 (m, 1 H), 2.16 (m, 1 H), 2.40 (m, 1 H), 2.42 (m, 2 H), 2.98 (dd, 1 H, *J* = 5.3, 9.8), 3.11 (dd, 1 H, *J* = 3.7, 9.9), 7.21–7.48 (m, 11 H), 7.70–7.74 (m, 2 H); <sup>13</sup>C NMR (CDCl<sub>3</sub>)  $\delta$  –5.6, –5.5, 18.2, 25.8, 26.5, 28.5, 33.6, 43.9, 53.5, 65.5, 72.5, 216.3; HRMS calcd for C<sub>34</sub>H<sub>45</sub>O<sub>2</sub>NSi (MH<sup>+</sup>) 528.3298, found 528.3288.

**(2*S*)-5-*tert*-Butyl-Δ<sup>5</sup>-dehydroprolinol *p*-Toluenesulfonate (18).** Ketone **16** (2.15 g, 4.08 mmol) was treated with 25% TFA in CH<sub>2</sub>Cl<sub>2</sub> (41 mL), anisole (2.2 mL, 20.4 mmol) and *p*-TsOH (0.776 g, 4.08 mmol), heated at a reflux for 18 h, cooled to room temperature and evaporated. The residue was digested with MeOH (5 mL) and then triturated with hexane (3 x 5 mL) to furnish the iminium salt **18** as an oil that was used without further purification:  $[\alpha]^{20}_D +34.7^\circ$  (*c* 0.6, MeOH); <sup>1</sup>H NMR (CD<sub>3</sub>OD)  $\delta$  1.35 (s, 9 H), 2.28 (m, 2 H), 2.36 (s, 3 H), 3.00 (m, 1 H), 3.16 (m, 1 H), 3.66 (d, 1 H, *J* = 11.9), 4.30 (d, 1 H, *J* = 12.4), 4.60 (m, 1 H), 7.18 (d, 2 H, *J* = 7.98), 7.38 (br s, 1 H), 7.73 (d, 2 H, *J* = 7.99); <sup>13</sup>C NMR (CD<sub>3</sub>OD)  $\delta$  20.3, 22.2, 26.4, 35.0, 37.3, 61.6, 69.1, 125.9, 128.9, 140.8, 142.7, 205.0; HRMS calcd for C<sub>9</sub>H<sub>18</sub>ON (MH<sup>+</sup>) 156.1388, found 156.1381.

**(2*S,5S*)-*N*-BOC-5-*tert*-Butylprolinol (21).** *p*-Toluenesulfonate **18** (4.08 mmol) was dissolved in CHCl<sub>3</sub> (40 mL), washed with a saturated aqueous solution of K<sub>2</sub>CO<sub>3</sub> (30 mL), dried and evaporated to imine **19**:  $[\alpha]^{20}_D +45.9^\circ$  (*c* 0.4, MeOH); <sup>1</sup>H NMR (CD<sub>3</sub>OD)  $\delta$  1.18 (s, 9 H), 1.78 (m, 1 H), 2.00 (m, 1 H), 2.62 (m, 1 H), 2.71 (m, 1 H), 3.54 (dd, 1 H, *J* = 5.6, 11.1), 3.69 (dd, 1 H, *J* = 4.3, 11.1), 4.06 (m, 1 H); <sup>13</sup>C NMR

(CD<sub>3</sub>OD) δ 26.0, 28.7, 34.7, 37.1, 65.7, 74.8, 189.3. Imine **19** (4.08 mmol) was dissolved in toluene (40 mL), treated with NaHB(OAc)<sub>3</sub> (1.30 g, 6.12 mmol) and heated at a reflux for 18 h. The solution was cooled, treated with HCl (4 mL, 2 M) and evaporated to a residue that was dissolved in MeOH, filtered and evaporated to furnish (2*S*,5*S*)-5-*tert*-butylproline hydrochloride (**20**): <sup>1</sup>H NMR (CD<sub>3</sub>OD) δ 1.18 (s, 9 H), 1.75 (m, 1 H), 2.00 (m, 1 H), 2.64 (m, 2 H), 3.16 (m, 1 H), 3.55 (dd, 1 H, *J* = 5.6, 11.1), 3.70 (dd, 1 H, *J* = 4.4, 11.1), 4.06 (m, 1 H). The hydrochloride **20** was dissolved in CH<sub>3</sub>CN (30 mL), treated with K<sub>2</sub>CO<sub>3</sub> (1.60 g, 11.3 mmol) and di-*tert*-butyldicarbonate (2.40 g, 11.3 mmol). After 18 h, the mixture was treated with K<sub>2</sub>CO<sub>3</sub> (0.538 g, 3.8 mmol) and di-*tert*-butyldicarbonate (0.799 g, 3.8 mmol) and stirred for 2 h when complete consumption of the amine was observed by TLC (*R*<sub>f</sub> = 0.17, 10% MeOH in CHCl<sub>3</sub>). Evaporation of the volatiles gave a residue that was purified by chromatography on silica gel using a gradient of 0-20% EtOAc in hexane as eluant. First to elute was (2*S*,5*R*)-**21** (45.9 mg, 5% yield) which exhibited the same spectral and physical characteristics as material synthesized as described below. Last to elute was (2*S*,5*S*)-**21** (375 mg, 39% yield): [α]<sup>20</sup><sub>D</sub> -4.9° (*c* 1.05, CHCl<sub>3</sub>); <sup>1</sup>H NMR (CDCl<sub>3</sub>) δ 0.90 (s, 9 H), 1.48 (s, 9 H), 1.53 (m, 1 H), 1.74 (m, 1 H), 1.85 (m, 1 H), 2.10 (m, 1 H), 3.68 (m, 1 H), 3.75 (m, 1 H), 3.85 (m, 1 H), 3.89 (dd, 1 H, *J* = 1.5, 8.8), 5.00 (br s, 1 H); <sup>13</sup>C NMR (CDCl<sub>3</sub>) δ 25.2, 28.1, 28.2, 28.8, 29.9, 63.2, 67.5, 80.7, 211.0; HRMS calcd for C<sub>14</sub>H<sub>28</sub>O<sub>3</sub>N (MH<sup>+</sup>) 258.2069, found 258.2075.

**(2*S*,5*R*)-*N*-BOC-5-*tert*-Butylprolinol (21).** A solution of (2*S*,5*R*)-**1** (50.8 mg, 0.19 mmol) in THF (0.4 mL) was added to a solution of BH<sub>3</sub>•SMe<sub>2</sub> (46mL, 0.46 mmol) in THF (0.4 mL). The mixture was stirred and heated at a reflux for 18 h. The excess BH<sub>3</sub> was destroyed by addition of MeOH (0.2 mL) and the solvent was removed by evaporation. The residue was purified by chromatography on silica gel using a gradient of 0-20% EtOAc in hexane as eluant. Evaporation of the collected fractions

provided (2*S*,5*R*)-**21** (40 mg, 83% yield) as an oil:  $[\alpha]^{20}_D -8.2^\circ$  (*c* 0.16, CHCl<sub>3</sub>); <sup>1</sup>H NMR (CDCl<sub>3</sub>) δ 0.89 (s, 9 H), 1.48 (s, 9 H), 1.81 (m, 3 H), 2.01 (m, 1 H), 3.67 (m, 2 H), 3.81 (m, 1 H), 3.98 (m, 1 H), 5.50 (br s, 1 H); <sup>13</sup>C NMR (CDCl<sub>3</sub>) δ 26.4, 28.1, 28.7, 35.9, 63.3, 68.2, 81.4, 159.8.

**(2*S*,5*S*)-*N*-BOC-5-*tert*-Butylproline (2*S*,5*S*)-1 from direct oxidation of (2*S*,5*S*)-21 with RuCl<sub>3</sub>.** A solution of prolinol (2*S*,5*S*)-**21** (15.7 mg, 65 μmoL) in 2:2:3 CCl<sub>4</sub>:CH<sub>3</sub>CN:H<sub>2</sub>O (1 mL) was treated with NaIO<sub>4</sub> (57 mg, 267 μmol) and RuCl<sub>3</sub> (0.8 mg, 2 μmol) at room temperature and stirred for 90 min. The mixture was partitioned between water (1 mL) and CH<sub>2</sub>Cl<sub>2</sub> (10 mL) and the aqueous phase was extracted with CH<sub>2</sub>Cl<sub>2</sub> (3 x 2 mL). The combined organic layers were washed with brine, dried and evaporated to a residue that was purified by chromatography on silica gel using an initial gradient of 0-75% EtOAc in hexane followed by 80-90% EtOAc in hexane containing 0.5% AcOH as eluant to furnish (2*S*,5*S*)-**1** (15.2 mg, 86% yield) as an oil:  $[\alpha]^{20}_D -38.1^\circ$  (*c* 0.7, MeOH).

**(2*S*,5*S*)-*N*-BOC-5-*tert*-Butylproline (2*S*,5*S*)-1 from direct oxidation of (2*S*,5*S*)-21 with TEMPO.** A solution of (2*S*,5*S*)-**21** (0.172 g, 0.67 mmol) in a mixture of CH<sub>3</sub>CN (3.3 mL) and sodium phosphate buffer (0.67 M, pH = 6-7, 2.7 mL) was treated with TEMPO (10 mol%, 10.4 mg), a solution of NaClO<sub>2</sub> (0.121 g, 1.3 mmol) in H<sub>2</sub>O (0.66 mL) and a solution of NaOCl (0.1 mL, 2 mol%) in H<sub>2</sub>O (0.33 mL). After stirring at 35°C for 18 h, the mixture was cooled, partitionned between 0.1 M HCl (10 mL) and EtOAc (10 mL) and the aqueous phase was extracted with EtOAc (3 x 10 mL). The organic layers were combined, washed with brine, dried and evaporated to a residue that was purified by chromatography on silica gel using a gradient of 5-90% EtOAc in hexane as eluant. Evaporation of the collected fractions gave (2*S*,5*S*)-**1** (152 mg, 84%) as an oil:  $[\alpha]^{20}_D -38.5^\circ$  (*c* 0.7, MeOH). lit.<sup>21</sup>  $[\alpha]^{20}_D$

$-16.3^\circ$  (*c* 0.7, MeOH); spectroscopic values for (2*S*,5*S*)-1 were identical with those reported in Ref. 21.

**(2*S*,5*S*)-*N*-BOC-5-*tert*-Butylproline (2*S*,5*S*)-1 via prolinal 22.** Prolinol (2*S*,5*S*)-21 (12 mg, 50  $\mu$ moL) was oxidized to aldehyde 22 in 74% yield using the same conditions described for the oxidation of alcohol 15 to ketone 16: minor carbamate isomers are reported in brackets,  $^1\text{H}$  NMR ( $\text{CDCl}_3$ )  $\delta$  [0.90 (s, 2.2 H)] 0.92 (s, 6.8 H), 1.41 (s, 5.6 H) [1.47 (s, 3.2 H)], 1.86 (m, 3 H), 2.26 (m, 1 H), [3.88 (br s, 0.39 H)] 4.03 (br s, 0.60 H), 4.17 (d, 0.64 H, *J* = 8.1) [4.25 (br s, 0.28 H), 9.43 (d, 0.55 H, *J* = 2.7). Aldehyde 22 (9.5 mg, 37  $\mu$ moL) was dissolved in 1:1  $\text{CH}_3\text{CN}$ :*t*-BuOH (1 mL) and treated with a solution of  $\text{NaClO}_2$  (45 mg, 500  $\mu$ moL) and  $\text{NaH}_2\text{PO}_4$  (54 mg, 450  $\mu$ moL) in  $\text{H}_2\text{O}$  (0.25 mL). After 2 h, more  $\text{NaClO}_2$  (50 mg) was added, the reaction was stirred for 30 min and another portion of  $\text{NaClO}_2$  (50 mg) was added. After stirring for 30 min, the mixture was partitioned between ether (3 mL) and  $\text{H}_3\text{PO}_4$  (2 mL, 1M). The aqueous phase was extracted with  $\text{Et}_2\text{O}$  (3 x 3 mL). The combined organic layers were washed with brine, dried and evaporated to a residue that was purified by chromatography on silica gel using the same conditions reported above. Evaporation of the collected fractions gave (2*S*,5*S*)-1 (6.1 mg, 61% yield) as an oil:  $[\alpha]^{20}\text{D} -37.1^\circ$  (*c* 0.5, MeOH), lit.<sup>21</sup>  $[\alpha]^{20}\text{D} -16.3^\circ$  (*c* 0.7, MeOH); spectroscopic values for (2*S*,5*S*)-1 were identical with those reported in Ref. 21.

**Acknowledgment:** This research was supported in part by the Natural Sciences and Engineering Research Council of Canada and the Ministère de l'Éducation du Québec. We are grateful for a gift of  $\gamma$ -methylglutamate from NSC Technologies. We thank Christian Tornøe for providing useful lead references.

### 1.10. References

1. Halab, L.; Gosselin, F.; Lubell, W.D. *Biopolymers* **2000**, *55*, 101-122.
2. Bélec, L.; Slaninová, J.; Lubell, W. D. *J. Med. Chem.* **2000**, *43*, 1448-1455.
3. Huang, Z.; He, Y.-B.; Raynor, K.; Tallent, M.; Reisine, T.; Goodman, M. *J. Am. Chem. Soc.* **1992**, *114*, 9390-9401.
4. Prasad, B.V.; Balaram, P. *CRC. Crit. Rev. Biochem.* **1984**, *16*, 307-347.
5. (a) Reviewed in: Seebach, D.; Sting, A.R.; Hoffman, M. *Angew. Chem. Int. Ed. Engl.* **1996**, *35*, 2708-2748. (b) Berkowitz, D.B.; McFadden, J.M.; Sloss, M.K. *J. Org. Chem.* **2000**, *65*, 2907-2918 and Refs 10-11.
6. Marshall, G.R.; Hodgkin, E.E.; Langs, D.A.; Smith, G.D.; Zabrocki, J.; Leplawy, M.T. *Proc. Natl. Acad. Sci. USA* **1990**, *87*, 487-491.
7. (a) Chandrasekhar, K.; Das, M.K.; Kumar, A.; Balaram, P. *Int. J. Peptide Protein Res.* **1988**, *32*, 167-174. (b) Fox, R.O., Jr.; Richards, F.M. *Nature* **1992**, *300*, 325-330.
8. Karle, I.L.; Balaram, P. *Biochemistry* **1990**, *29*, 6747-6756.
9. (a) Benedetti, E.; Barone, V.; Bavoso, A.; Di Blasio, B.; Lelj, F.; Pavone, V.; Pedone, C.; Bonora, G. M.; Toniolo, C.; Leplawy, M.T.; Kaczmarek, K.; Redlinski, A. *Biopolymers* **1988**, *27*, 357-371. (b) Di Blasio, B.; Pavone, C.; Lombardi, A.; Pedone, C.; Benedetti, E. *Biopolymers* **1993**, *33*, 1037-1049.
10. Toniolo, C.; Benedetti, E. *Macromolecules* **1991**, *24*, 4004-4009.
11. (a) Burgess, K.; Ho, K.-K.; Pettitt, B.M. *J. Am. Chem. Soc.* **1995**, *117*, 54-65. (b) Paradisi, M.P.; Torrini, I.; Zecchini, G.P.; Lucente, G.; Gavuzzo, E.; Mazza, F.; Pochetti, G. *Tetrahedron* **1995**, *51*, 2379-2386. (c) Prasad, S.; Roa, R. B.; Balaram, P. *Biopolymers* **1995**, *35*, 11-20. (d) Toniolo, C.; Crisma, M.; Formaggio, F.; Benedetti, E.; Santini, A.; Iacovino, R.; Saviano, M.; Di Blasio, B.; Pedone, C.; Kamphuis, J. *Biopolymers* **1997**, *40*, 519-522.

12. Reviewed in: Hruby, V.J.; Li, G.; Haskell-Luevano, C.; Shenderovich, M. *Biopolymers* **1997**, *43*, 219-266.
13. Wang, S.; Tang, X.; Hruby, V.J. *Tetrahedron Lett.* **2000**, *41*, 1307-1310.
14. Hanessian, S.; Margarita, R.; Hall, A.; Luo, X. *Tetrahedron Lett.* **1998**, *39*, 5883-5886.
15. Hruby, V.J.; Toth, G.; Gehrig, C.A.; Kao, L.F.; Knapp, R.; Lui, G.K.; Yamamura, H.I.; Kramer, T.H.; Davies, P.; Burks, T.F. *J. Med. Chem.* **1991**, *34*, 1823-1830.
16. Gomez-Catalan, J.; Perez, J.J.; Jimenez, A.I.; Cativiela, C. *J. Peptide Sci.* **1999**, *5*, 251-262.
17. Hanessian, S.; Margarita, R. *Tetrahedron Lett.* **1998**, *39*, 5887-5890.
18. Baldwin, J. E.; North, M.; Flinn, A.; Moloney, M. G. *Tetrahedron* **1989**, *45*, 1453-1464 and 1465-1474.
19. Del Bosco, M.; Johnstone, A.N.C.; Bazza, G.; Lopatriello, S.; North, M. *Tetrahedron* **1995**, *51*, 8545-8554.
20. Wenger, R. M. *Angew. Chem. Int. Ed. Engl.* **1985**, *24*, 77-85.
21. Beausoleil, E.; L'Archevêque, B.; Bélec, L.; Atfani, M.; Lubell, W. D. *J. Org. Chem.* **1996**, *61*, 9447-9454 and Refs 15-16 therein.
22. (a) Swarbrick, M. E.; Gosselin, F.; Lubell, W. D. *J. Org. Chem.* **1999**, *64*, 1993-2002 and Refs 17-22 therein. (b) Swarbrick, M. E.; Lubell, W. D. *Chirality* **2000**, *12*, 366-373.
23. (a) Delaney, N.G.; Madison, V. *J. Am. Chem. Soc.* **1982**, *104*, 6635-6641. (b) Overberger, C. G.; Jon, Y.S. *J. Polym. Sci. Polym. Chem. Ed.* **1977**, *15*, 1413-1421.
24. Sharma, R.; Lubell, W.D. *J. Org. Chem.* **1996**, *61*, 202-209 and Refs 1-9 therein.
25. Beausoleil, E.; Sharma, R.; Michnick, S.; Lubell, W. D. *J. Org. Chem.* **1998**, *63*, 6572-6578.
26. Koskinen, A.M.P.; Rapoport, H. *J. Org. Chem.* **1989**, *54*, 1859-1866.

27. (a) McCafferty, D.G.; Friesen, D.A.; Danielson, E.; Wall, C.G.; Saderholm, M.J.; Erickson, B.W.; Meyer, T.J. *Proc. Natl. Acad. Sci. USA* **1996**, *93*, 8200-8204. (b) McCafferty, D.G.; Slate, C.A.; Nakhle, B.M.; Graham Jr., H.D.; Austell, T.L.; Vachet, R.W.; Mullis, B.H.; Erickson, B.W. *Tetrahedron* **1995**, *51*, 9859-9872. (c) Tamaki, M.; Han, G.; Hruby, V.J. *J. Org. Chem.* **2001**, *66*, 3593.
28. Zhang, R.; Brownewell, F.; Madalengoitia, J.S. *J. Am. Chem. Soc.* **1998**, *120*, 3894-3902.
29. Delaney, N.G.; Madison, V. *Int. J. Peptide Protein Res.* **1982**, *19*, 543-548.
30. Beausoleil, E.; Lubell, W. D. *J. Am. Chem. Soc.* **1996**, *118*, 12902-12908.
31. Halab, L.; Lubell, W. D. *J. Org. Chem.* **1999**, *64*, 3312-3321.
32. Halab, L.; Lubell, W. D. *J. Peptide Sci* **2001**, *7*, 92-104.
33. Beausoleil, E.; Lubell, W. D. *Biopolymers* **2000**, *53*, 249-256.
34. (a) Magaard, V.W.; Sanchez, R.M.; Bean, J.W.; Moore, M.L. *Tetrahedron Lett.* **1993**, *34*, 381-384. (b) An, S. S. A.; Lester, C. C.; Peng, J.-L.; Li, Y.-J.; Rothwarf, D. M.; Welker, E.; Thannhauser, T. W.; Zhang, L. S.; Tam, J. P.; Scheraga, H. A. *J. Am. Chem. Soc.* **1999**, *121*, 11558-11566.
35. (a) Hanessian, S.; Bernstein, N.; Yang, R.-Y.; Maguire, R. *Bioorg. Med. Chem. Lett.* **1999**, *9*, 1437-1442. (b) Gerona-Navarro, G.; Bonache, M.A.; Herranz, R.; García-López, M.T.; González-Muñiz, R. *J. Org. Chem.* **2001**, *66*, 3538-3547.
36. Hanessian, S.; Fu, J.-M.; Chiara, J.-L.; Di Fabio, R. *Tetrahedron Lett.* **1993**, *34*, 4157-4160.
37. Evans, M. C.; Johnson, R. L. *Tetrahedron* **2000**, *56*, 9801-9808.
38. (a) Hanessian, S.; Reinhold, U.; Gentile, G. *Angew. Chem. Int. Ed. Engl.* **1997**, *36*, 1881. (b) Hanessian, S.; Reinhold, U.; Saulnier, M.; Claridge, S. *Bioorg. Med. Chem. Lett.* **1998**, *8*, 2123-2128.
39. Computational analysis was performed on a Silicon Graphics computer using the Macromodel 3.5x program with the Amber force field. The structures were

- drawn and minimized using first the Steepest Descent (DS) procedure and Polack-Ribiere Conjugate Gradient (PRCG) until a 0.001 kJ/Å•mol gradient was reached followed by minimization of the resulting structures with the Monte Carlo method. Still, W.C.; Tempczyk, A.; Hawley, R.C.; Hendrickson, T. *J. Am. Chem. Soc.* **1990**, *112*, 6127-.
40. Shiosaki, K.; Rapoport, H. *J. Org. Chem.* **1985**, *50*, 1229-1239.
41. (a) Thaning, M.; Wistrand, L.-G. *Acta Chem. Scand.* **1992**, *46*, 194-199. (b) Wistrand, L.-G.; Skrinjar, M. *Tetrahedron* **1991**, *47*, 573-582.
42. Collado, I.; Ezquerro, J.; Pedregal, C. *J. Org. Chem.* **1995**, *60*, 5011-5015.
43. Bertz, S.H.; Dabbagh, G. *Tetrahedron* **1989**, *45*, 425-434.
44. Gosselin, F.; Lubell, W. D. *J. Org. Chem.* **2000**, *65*, 2163-2171.
45. *N*-BOC-5-Methoxyproline benzyl ester (**10**) was synthesized using the procedure described for reduction of *N*-BOC-pyroglutamate ethyl ester and formation of the corresponding aminal (see Ref. 42).  $^1\text{H}$  NMR ( $\text{CDCl}_3$ ) resonances for **10** as a 2:3 mixture of diastereomers are:  $\delta$  1.32 (s, 9 H), 1.46 (s, 9 H), 1.77-1.95 (m, 5 H), 2.10 (m, 1 H), 2.30 (m, 2 H), 3.32 (d, 3 H,  $J$  = 1.5), 3.37 (d, 3H,  $J$  = 1.5), 4.28-4.39 (m, 2 H), 5.04-5.28 (m, 6H), 7.33 (m, 10 H).
46. The *trans*-isomer was presumed to be the major product based on analogy with literature precedents using less bulky alkylcopper reagents (see Refs 41 and 42). From the spectrum of a 4:1 mixture,  $^1\text{H}$  NMR ( $\text{CDCl}_3$ ) resonances for the major isomer are as follows:  $\delta$  0.89 (s, 9 H), 1.35 (s, 9 H), 1.81 (m, 3 H), 2.30 (m, 1 H), 3.99 (d, 1 H,  $J$  = 8.7), 4.32 (d, 1 H,  $J$  = 9.4), 5.15 (m, 2 H), 7.36 (m, 5 H).
47. Evans, D.A.; Chapman, K.T.; Carreira, E.M. *J. Am. Chem. Soc.* **1988**, *110*, 3560-3578.
48. (a) Grandjean, C.; Rosset, S.; Célérier, J.P.; Lhommet, G. *Tetrahedron Lett.* **1993**, *34*, 4517-4518. (b) Rosset, S.; Célérier, J.P.; Lhommet, G. *Tetrahedron Lett.* **1991**, *32*, 7521-7524.

49. Polyak, F.; Lubell, W.D. *J. Org. Chem.* **2001**, *66*, 1171-1180.
50. Ley, S.V.; Norman, J.; Griffith, W.P.; Marsden, S.P. *Synthesis* **1994**, 639-666.
51. Mancuso, A.J.; Swern, D. *Synthesis* **1981**, 165-185
52. Corey E.J.; Kim, C.U. *J. Org. Chem.* **1973**, *38*, 1233-1234.
53. Jordis, U.; Sauter, F.; Siddiqi, S.M.; Küenborg, B.; Bhattacharya, K. *Synthesis* **1990**, 925-930.
54. (a) Langlois, N. *Tetrahedron: Asymmetry* **1998**, *9*, 1333-1336. (b) Carlsen, P.H.J.; Katsuki, T.; Martin, V.S.; Sharpless, K.B. *J. Org. Chem.* **1981**, *46*, 3936-3938.
55. Zhao, M.; Li, J.; Mano, E.; Song, Z.; Tschaen, D.M.; Grabowski, E.J.J.; Reider, P. *J. J. Org. Chem.* **1999**, *64*, 2564-3566.
56. (a) Lubell, W.D., Jamison, T.F.; Rapoport, H. *J. Org. Chem.* **1990**, *55*, 3511-3521. (b) Bal, B.S.; Childers, W.E., Jr.; Pinnick, H. *Tetrahedron* **1981**, *37*, 2091-2094.
57. (a) Pettit, G.R.; Singh, S.B.; Herald, D.L.; Lloyd-Williams, P.; Kantoci, D.; Burkett, D.D.; Barkóczy, J.' Hogan, F.; Wardlaw, T.R. *J. Org. Chem.* **1994**, *59*, 6287-6295. (b) Roux, F.; Maugras, I.; Poncet, J.; Jouin, P. *Tetrahedron* **1994**, *50*, 5345-5360. (c) Shioiri, T.; Hayashi, K.; Hamada, Y. *Tetrahedron* **1993**, *49*, 1913-1924. (d) Tomioka, K.; Kanai, M.; Koga, K. *Tetrahedron Lett.* **1991**, *32*, 2395-2398.

## **CHAPITRE 2**

**Synthèse et étude conformationnelle de  
dipeptides *N*-acétyles *N'*-méthylamides  
incorporant la proline et la 5-*tert*-butylproline,  
mimétique de repliement  $\beta$  de type VIa et VIb.**

## 2.1. Les repliements $\beta$ de type VI

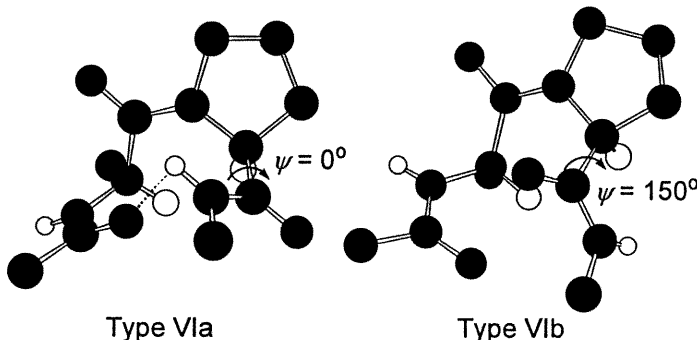


**Figure 1. Structures des repliements  $\beta$  de type VI.**

Les types de repliements  $\beta$ , comme mentionné précédemment, sont classés selon les valeurs des angles de torsion des résidus  $i + 1$  et  $i + 2$ .<sup>1</sup> Les repliements  $\beta$  de type VI sont des structures secondaires uniques, car ce sont les seuls repliements où une proline est située en position  $i + 2$  du tour  $\beta$  et que le lien amide  $N$ -terminal de la proline adopte une conformation *cis*.<sup>2</sup> Deux classes de repliements  $\beta$  de type VI ont été définies: le repliement  $\beta$  de type VIa et de type VIb (Figure 1).<sup>2</sup> Dans un repliement  $\beta$  de type VIa, l'angle dièdre  $\psi$  de la proline est proche de  $0^\circ$  et un pont d'hydrogène intramoléculaire existe entre l'oxygène du carbonyle du résidu  $i$  et l'hydrogène de l'amide du résidu  $i + 3$ . Cet angle  $\psi$  adopte une valeur de  $150^\circ$  dans la conformation de repliement  $\beta$  de type VIb ce qui éloigne les deux chaînes et proscrit la formation de pont d'hydrogène intramoléculaire.

Contrairement aux autres types de repliements  $\beta$ , les types VI se retrouvent rarement dans la nature. Ils sont présents sur la surface des protéines globulaires, tels que la ribonuclease S, l'hémoglobine, la thermolysine et l'immunoglobuline de Bence-Jones.<sup>2,3</sup> Plusieurs peptides cycliques biologiquement actifs possèdent une conformation de tour  $\beta$  de type VI, par exemple, le cycloleonuridine, un agent immunosuppresseur,<sup>4</sup> l'aureobasidine E, un antibiotique antifongique<sup>5</sup> et le phakellistin, un inhibiteur de croissance des cellules cancéreuses.<sup>6</sup>

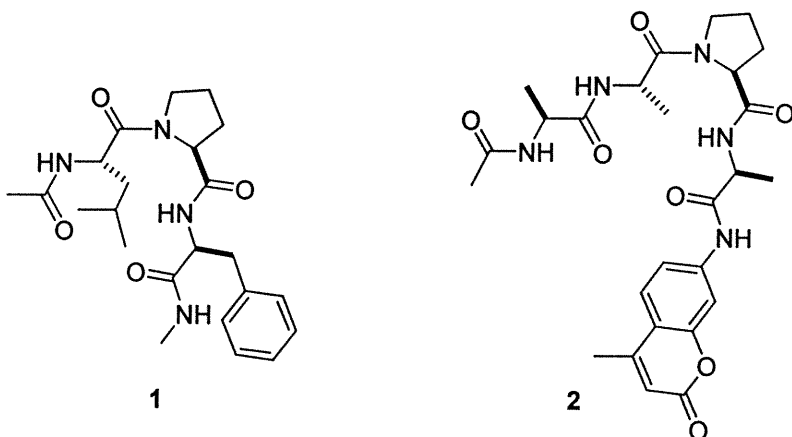


**Figure 2. Structures des substrats 1 et 2 qui adoptent une conformation de repliement  $\beta$  de type VI.**

La conformation de repliement  $\beta$  de type VI joue un rôle important dans la reconnaissance, la réactivité et la stabilité des peptides et protéines bioactives.<sup>7-11</sup> Les peptidyles prolyles isomérasées (PPIases), aussi connus comme les rotamases,<sup>10,12</sup> sont des enzymes qui catalysent l’isomérisation *cis-trans* du lien amide *N*-terminal de la proline en diminuant l’énergie d’activation d’une valeur de 19-20 à 5-6 kcal/mole dans une solution aqueuse et ainsi ils accélèrent le repliement de certaines protéines.<sup>13</sup> Il a été proposé que ces enzymes se liaient de préférence à des peptides possédant un repliement  $\beta$  de type VI.<sup>7,8</sup> Deux de ces enzymes ont bien été identifiés: le cyclophiline et le FKBP qui sont liés par les ligands immunosuppressifs cyclosporine A et FK506 respectivement.<sup>14</sup> L’interconversion conformationnelle *cis-trans* du lien amide *N*-terminale de la proline est une réaction d’intérêt, car elle a été identifiée comme l’étape limitante dans le repliement des protéines.<sup>15</sup> Le mécanisme de catalyse de l’isomérisation par les PPIases propose une stabilisation d’un intermédiaire possèdant un amide pyramidalisé.<sup>16</sup> Des études de modélisation moléculaire ont démontré que le tripeptide 1 se lie au rotamase FKBP en adoptant un repliement  $\beta$  de type VIa et que la catalyse du rotamase est effectuée par une diminution de la barrière d’isomérisation (Figure 2).<sup>7</sup> De plus, une étude de diffraction de rayons-X a illustré que le tétrapeptide 2 est lié au PPIase cyclophiline avec une géométrie de repliement  $\beta$  de type VIb (Figure 2).<sup>8</sup> Ces exemples et le mécanisme proposé pour l’isomérisation catalysée par PPIase suggèrent que les

conformations de repliement  $\beta$  de type VI doivent se lier aux PPIases et peuvent fonctionner comme des inhibiteurs compétitifs. Aussi, une conformation de tour  $\beta$  de type VI a été proposée comme une exigence pour le clivage catalytique de thrombine de la boucle V3 de la protéine HIV gp120.<sup>9</sup>

## 2.2. Outil pour stabiliser l'isomère *cis* N-terminale de la proline

Plusieurs stratégies ont été développées pour la préparation d'isostères conformationnellement rigides afin de contraindre le lien amide *N*-terminal de la proline en isomère *cis* ou *trans*.<sup>17</sup> Deux méthodes pour contraindre la flexibilité conformationnelle de la proline en isomère *cis* sont présentées: l'utilisation des prolines rigidifiées où l'amide *N*-terminal de la proline est fixé par un lien covalent et l'utilisation d'analogues de proline où l'équilibre conformationnel peut avoir lieu.

### 2.2.1. Utilisation des prolines rigidifiées

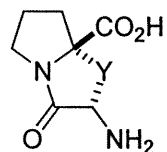


**Figure 3.** Structure générale d'une proline contrainte en isomère *cis*.

Le lien amide *N*-terminal de la proline peut être contraint dans une conformation *cis* en unissant les carbones  $\alpha$  de la proline et de l'acide aminé *N*-terminal de la proline pour former un lactame bicyclique, et ainsi éviter la possibilité d'isomérisation (Figure 3). Des groupements tels qu'un méthylène<sup>18</sup> (**3-4**), un amide<sup>19</sup> (**5**) et un hydrazide<sup>20</sup> (**6**) sont utilisés comme chaînes afin de construire le dipeptide bicyclique (Figure 4).

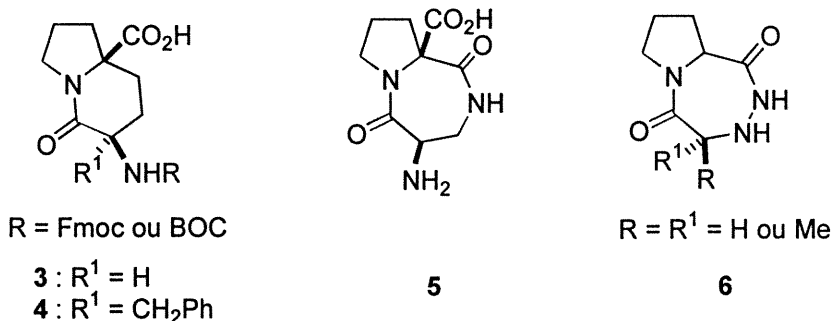


**Figure 4. Exemples représentatifs des lactames bicycliques.**

Dans le but de mimer le repliement  $\beta$  de type VI, seuls les bicycles **3** et **4** ont été incorporés dans des peptides. Ainsi, des études de RMN, d'IR et de modélisation moléculaire ont démontré que des tripeptides possèdant le bicycle **3** adoptent une conformation de repliement  $\beta$  de type VIa.<sup>18e</sup> De plus, les lactames **3** et **4** ont été incorporés dans des peptides biologiquement actifs.<sup>18a-b</sup> Le bicycle **3** a été introduit dans l'hormone bradykinine (**7**), un médiateur efficace de la dilatation des vaisseaux sanguins, de la contraction des muscles, de la douleur, de l'inflammation et de la perméabilité vasculaire.<sup>18a</sup> Afin de déterminer la conformation du peptide actif au récepteur, le lactame **3** a été remplacé aux résidus Ser<sup>6</sup>-Pro<sup>7</sup> où une flexibilité conformationnelle existe (Figure 5). Toutefois, lorsque le peptide **8** a été analysé pour sa capacité à déplacer la bradykinine du récepteur, il a démontré une très faible activité ainsi soutenant que le lien amide Ser<sup>6</sup>-Pro<sup>7</sup> adopte une conformation *trans*.<sup>18a</sup> Par ailleurs, les résidus Phe-Pro d'un analogue de l'hormone somatostatine (**9**), qui possède les mêmes activités biologiques que la somatostatine, mais une plus grande stabilité métabolique,<sup>21</sup> ont été remplacés par le mimétique *cis*-Phe-Pro **4** (Figure 5).<sup>18b</sup> Le peptide **10** a montré une grande affinité ( $\text{pIC}_{50} 8.6$ ) aux récepteurs de la somatostatine ainsi soutenant que le lien *cis*-Phe Pro adopte une conformation de repliement  $\beta$  de type VI dans le site actif du récepteur.<sup>18b</sup>

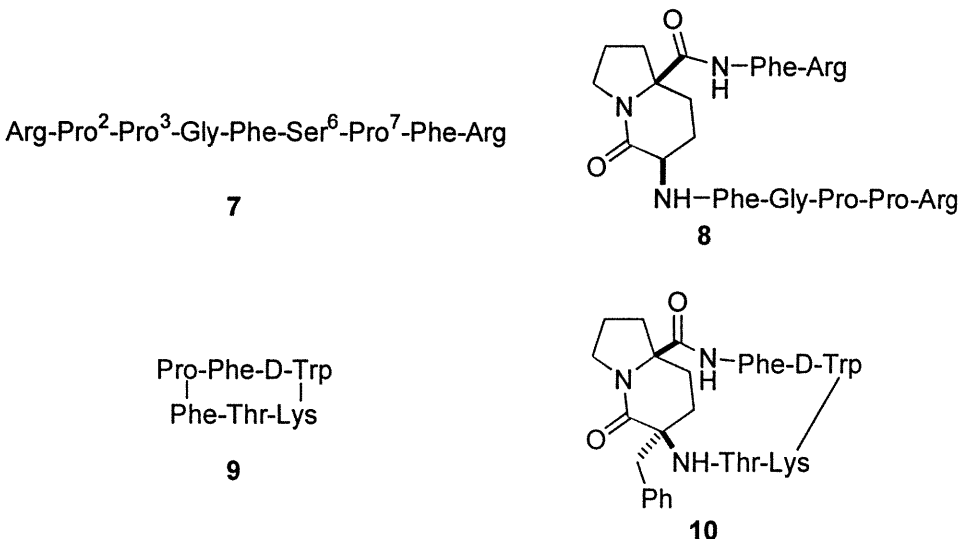


**Figure 5. Structures de la bradykinine, d'un analogue de la somatostatine et de leurs dérivés avec des prolines rigidifiées.**

Cependant à cause de la difficulté d'attacher des substituants sur les résidus du dipeptide lactame,<sup>18b</sup> les acides aminés azabicycloalcanes ne miment pas convenablement les pharmacophores des chaînes latérales. Par conséquent, ceci peut influencer la reconnaissance du peptide au niveau du récepteur. De plus, la stéréochimie des acides aminés azabicycloalcanes est fixée lors de leur synthèse. Ainsi, la formation de son épimère pour mimer un acide aminé avec la stéréochimie *R* *N*-terminale de la proline est complexe.

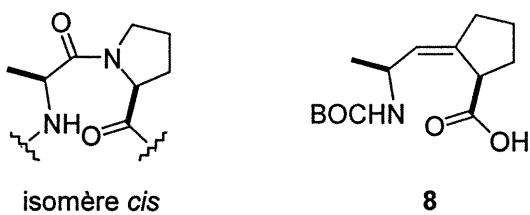


**Figure 6. Mimétique de l'isomère *cis* du lien prolylamide.**

Des isostères de l'amide hybridé sp<sup>2</sup> avec l'isomère *cis* ont été générés en utilisant des hétérocycles comme le tétrazole<sup>22</sup> et des oléfines<sup>23-24</sup> pour remplacer le lien amide. Un mimétique du dipeptide Ala-*cis*-Pro qui ne possède pas de proline mais qui utilise un (*Z*)-alcène comme isostère du lien amide a été reporté (Figure 6).<sup>24a</sup> L'oléfine 8 a été synthétisée de façon énantiomérisélective et régiosélective et elle a

été incorporée dans le tetrapeptide succinyl-Ala-Ala-Pro-Phe-*p*-nitroanilide, un substrat du PPIase cyclophiline.<sup>24</sup> Ce dernier a démontré une inhibition de l'activité de la cyclophiline avec un IC<sub>50</sub> de 6.5 μM.<sup>24</sup> En remplaçant le lien amide de la proline par une oléfine, la reconnaissance de ces peptides au niveau du récepteur peut ainsi être affectée.

### **2.2.2. Utilisation des analogues de prolines**

Pendant mes études de doctorat, l'utilisation de l'azaproline et des dérivés de proline diméthylé comme outil pour mimer un repliement  $\beta$  de type VI a été publiée.

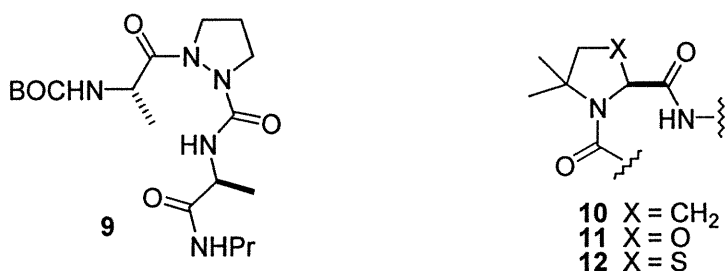


**Figure 7. Exemples d'analogues de proline où l'équilibre conformationnelle est possible.**

Le cycle de la proline peut être modifié en remplaçant le C<sub>α</sub> de la proline par un azote pour former un azaproline (Figure 7). Une fois incorporé dans un tripeptide, l'azaproline induit seulement l'isomère *cis* du lien amide N-terminal de la proline et ainsi le tripeptide **9** adopte une conformation de repliement β de type VIa tel qu'illustré par RMN, IR et rayon-X.<sup>25</sup> Bien que cette approche peut procurer une variété de mimétiques de tour β de type VI, l'azaproline n'est pas chirale et cette perte de chiralité peut influencer la bioactivité des peptides.

Des interactions stériques ont aussi été utilisées pour contraindre l'isomérisation du lien amide *N*-terminal de la proline. Deux groupements méthyles ont été incorporés à la position 5 de la proline<sup>26</sup> **10** et à la position 2 d'oxazolidine<sup>27</sup> **11** et de thiazolidine<sup>27</sup> **12** (Figure 7). En particulier, le dérivé thiazolidine 2,2-diméthylé peut induire seulement la conformation *cis* dans les peptides.<sup>27</sup> Cette

approche qui consiste à mimer le repliement  $\beta$  de type VI, bien qu'elle soit versatile, possède des inconvénients. Seulement une synthèse racémique est rapportée pour la 5,5-diméthylproline.<sup>26</sup> De plus, l'incorporation d'un hétéroatome dans le cycle pyrrolidine peut modifier la conformation du cycle et ainsi la réactivité au niveau du récepteur.

Les quatre articles qui suivent présentent l'efficacité de l'acide aminé (2*S*,5*R*)-5-*tert*-butylproline comme un outil pour mimer et reproduire la conformation de repliement  $\beta$  de type VI dans les dipeptides. Nous avons non seulement démontré l'utilisation des interactions stériques pour perturber l'isomérisation *cis-trans* mais nous avons aussi formé des mimétiques de repliement  $\beta$  de type VIa et VIb. En incorporant des acides aminés avec la stéréochimie *S* et *R* *N*-terminale de la 5-*tert*-butylproline, nous avons formé des mimétiques de repliement  $\beta$  de type VIa et VIb respectivement. Des études de RMN, de dichroïsme circulaire et de rayons-X ont montré que les dipeptides Ac-L-Xaa-5-*t*BuPro-NHMe et Ac-D-Xaa-5-*t*BuPro-NHMe adoptent respectivement des repliements  $\beta$  de type VIa et VIb. Dans le premier et le deuxième article, nous avons décrit la synthèse et l'analyse conformationnelle de dipeptides incorporant la 5-*tert*-butylproline et capables de mimer le repliement  $\beta$  de type VIa. Dans le troisième et le quatrième article, nous avons décrit la synthèse et l'analyse conformationnelle de dipeptides incorporant la 5-*tert*-butylproline et capables de mimer le repliement  $\beta$  de type VIb.

### 2.3. Références

1. (a) Richardson, J.S. *Adv. Protein Chem.* **1981**, *34*, 167. (b) Rose, G.D.; Giersch, L.M.; Smith, J.A. *Adv. Protein Chem.* **1985**, *37*, 1. (c) Smith, J.A.; Pease, L.G. *CRC Crit. Rev. Biochem.* **1980**, *8*, 315.
2. Revue dans: Müller, G.; Gurrath, M.; Kurz, M.; Kessler, H. *Proteins: Structure, Function and Genetics* **1993**, *15*, 235.
3. (a) Werner, M. H.; Wemmer, D. E. *Biochemistry* **1992**, *31*, 999. (b) Kim, E. E.; Varadarajan, R.; Wyckoff, H. W.; Richards, F. M. *Biochemistry* **1992**, *31*,

12304. (c) Epp, O.; Lattman, E. E.; Schiffer, M.; Huber, R.; Palm, W. *Biochemistry* **1975**, *14*, 4943.
4. Morita, H.; Gonda, A.; Takeya, K.; Itokawa, H.; Hirano, T.; Oka, K.; Shirota, O. *Tetrahedron* **1997**, *53*, 7469.
5. Fujikawa, A.; In, Y.; Inoue, M.; Ishida, T.; Nemoto, N.; Kobayashi, Y.; Kataoka, R.; Ikai, K.; Takesako, K.; Kato, I. *J. Org. Chem.* **1994**, *59*, 570.
6. Pettit, G. R.; Xu, J.-P.; Cichacz, Z. A.; Williams, M. D.; Dorsaz, A.-C.; Brune, D. C.; Boyd, M. R.; Cerny, R. L. *Bioorg. Med. Chem. Lett.* **1994**, *4*, 2091.
7. Fischer, S.; Michnick, S.; Karplus, M. *Biochemistry* **1993**, *32*, 13830.
8. Kallen, J.; Walkinshaw, M. D. *FEBS Lett.* **1992**, *300*, 286.
9. Johnson, M. E.; Lin, Z.; Padmanabhan, K.; Tulinsky, A.; Kahn, M. *FEBS Lett.* **1994**, *337*, 4.
10. Revue dans: Fischer, G. *Angew. Chem. Int. Ed. Engl.* **1994**, *33*, 1415.
11. Liu, J.; Chen, C.-M.; Walsh, C. T. *Biochemistry* **1991**, *30*, 2306.
12. (a) Rudd, K.E.; Sofia, H.J.; Koonin, E.V.; Plunkett, G.R.; Lazar, S.; Rouvière, P.E. *Trends Biochem. Sci.* **1995**, *20*, 12. (b) Rouvière, P.E.; Gross, C.A. *Genes and Development* **1996**, *10*, 3170.
13. (a) Drakenberg, T.; Forsen, S. *J. Phys. Chem.* **1970**, *74*, 1. (b) Roques, B.P.; Garbay-Jaureguiberry, C.; Combrisson, S.; Oberlin, R. *Biopolymers* **1977**, *16*, 937. (c) Cheng, H.N.; Bovey, F.A. *Biopolymers* **1977**, *16*, 1465.
14. (a) Revue dans: Schreiber, S.L. *Science* **1991**, *251*, 283. (b) Harding, M.W.; Galat, A.; Uehling, D.E.; Schreiber, S.L. *Nature* **1989**, *341*, 758. (c) Siekierka, J.J.; Hung, S.H.Y.; Poe, M.; Lin, C.S.; Sigal, N.H. *Nature* **1989**, *341*, 755. (d) Fischer, G.; Wittmann-Liebold, B.; Lang, K.; Kiehaber, T.; Schmid, F. *Nature* **1989**, *337*, 476.
15. (a) Revue dans: Schmid, F.X.; Mayr, L.M.; Mücke, M.; Schönbrunner, E.R. *Adv. Protein Chem.* **1993**, *44*, 25. (b) Schmid, F.X.; Baldwin, R.L. *Proc. Natl. Acad. Sci USA* **1978**, *75*, 4764. (c) Schmid, F.X.; Baldwin, R.L. *J. Mol. Biol.* **1979**, *133*, 185. (d) Brandts, J.F.; Halvorson, H.R.; Brennan, M. *Biochemistry* **1975**, *14*, 4953.
16. Revue dans: Stein R.L. *Adv. Protein Chem.* **1993**, *44*, 1.

17. (a) Hanessian, S.; McNaughton-Smith, G.; Lombart, H.-G.; Lubell, W. D. *Tetrahedron* **1997**, *53*, 12789. (b) Gillespie, P.; Cicariello, J.; Olson, G. L. *Biopolymers, Peptide Science* **1997**, *43*, 191. (c) Etzkorn, F.A.; Travins, J.M.; Hart, S.A. *Adv. Amino Acid Peptidomim.* **1999**, *2*, 125.
18. (a) Gramberg, D.; Robinson, J. A. *Tetrahedron Lett.* **1994**, *35*, 861. (b) Gramberg, D.; Weber, C.; Beeli, R.; Inglis, J.; Bruns, C.; Robinson, J. A. *Helv. Chim. Acta* **1995**, *78*, 1588. (c) Dumas, J.-P.; Germanas, J. P. *Tetrahedron Lett.* **1994**, *35*, 1493. (d) Kim, K.; Dumas, J.-P.; Germanas, J. P. *J. Org. Chem.* **1996**, *61*, 3138. (e) Kim, K.; Germanas, J. P. *J. Org. Chem.* **1997**, *62*, 2847.
19. Curran, T.P.; McEnaney, P.M. *Tetrahedron Lett.* **1995**, *36*, 191.
20. (a) Lenman, M.M.; Lewis, A.; Gani, D. *J. Chem. Soc., Perkin Trans. 1* **1997**, 2297. (b) Lenman, M.M.; Ingham, S.L.; Gani, D. *Chem. Commun.* **1996**, 85.
21. Veber, D.F.; Strachan, R.G.; Bergstrand, S.J.; Holly, F.W.; Glitzer, M.S.; Hirschmann, R.; Torchianan, M.; Saperstein, R. *J. Am. Chem. Soc.* **1976**, *98*, 2367.
22. (a) Zabrocki, J.; Dunbar, J.B.; Marshall, K.W.; Toth, M.V.; Marshall, G.R. *J. Org. Chem.* **1992**, *57*, 202. (b) Beusen, D.D.; Zabrocki, J.; Slomczynska, U.; Head, R.D.; Kao, J.L.-F.; Marshall, G.R. *Biopolymers* **1995**, *36*, 181.
23. Boros, L.G.; De Corte, B.; Gimi, R.H.; Welsh, J.T.; Wu, Y.; Handschumacher, R.E. *Tetrahedron Lett.* **1994**, *35*, 6033.
24. (a) Hart, S.A.; Sabat, M.; Etzkorn, F.A. *J. Org. Chem.* **1998**, *63*, 7580. (b) Hart, S.A.; Etzkorn, F.A. *J. Org. Chem.* **1998**, *64*, 2998.
25. Zouikri, M.; Vicherat, A.; Aubry, A.; Marraud, M.; Boussard, G. *J. Peptide Res.* **1998**, *52*, 19.
26. Magaard, V. W.; Sanchez, R. M.; Bean, J. W.; Moore, M. L. *Tetrahedron Lett.* **1993**, *34*, 381.
27. (a) Wittelsberger, A.; Keller, M.; Scarpellino, L.; Patiny, L.; Acha-Orbea, H.; Mutter, M. *Angew. Chem. Int. Ed. Engl.* **2000**, *39*, 1111. (b) Mutter, M., Wöhr, T.; Gioria, S.; Keller, M. *Biopolymers* **1999**, *51*, 121. (c) Keller, M.;

Sager, C.; Dumy, P.; Schutkowski, M.; Fischer, G. S.; Mutter, M. *J. Am. Chem. Soc.* **1998**, *120*, 2714.

## Article 2

Halab, L.; Lubell, W. D. "Steric Effects of 5-*tert*-Butylproline in Dipeptide Mimics of Type VI  $\beta$ -Turns." Publié dans *Peptides 1998*, Proceedings of the 25<sup>th</sup> European Peptide Symposium, S. Bajusz & F. Hudecz, Eds; Akadémia Kiadò: Budapest, Hungary, 1999, 356-357.

## Steric Effects of 5-*tert*-Butylproline in Dipeptide Mimics of Type VI $\beta$ -Turns.

Liliane Halab and William D. Lubell\*

Département de chimie, Université de Montréal

C. P. 6128, Succursale Centre-Ville, Montréal, Québec, Canada H3C 3J7

### 2.4. Introduction

In proteins, the  $\beta$ -turn is a common secondary structure. The type VI  $\beta$ -turn uniquely features an amide *cis*-isomer *N*-terminal to a proline residue at the  $i + 2$  position. Type VI  $\beta$ -turns have been suggested to play important roles in the recognition and the folding of bioactive peptides and proteins. For example, a type VI  $\beta$ -turn conformation has been postulated to be a requirement for thrombin catalyzed cleavage of the V3 loop of HIV gp120, a prerequisite to viral infection [1]. In addition, the peptidyl prolyl isomerase which isomerize X-Pro amide bonds and accelerate the folding of particular proteins have been proposed to bind preferably to peptides possessing type VI  $\beta$ -turn conformations [2].

We have shown that sterically bulky 5-position substituents destabilize the *N*-terminal amide *trans*-isomer and augment the *cis*-isomer population in *N*-(acetyl)-proline *N*<sup>1</sup>-methylamides [3]. We report now the synthesis and the analysis of dipeptide analogs incorporating (2*S*, 5*R*)-5-*tert*-butylproline (5-tBuPro) [4] that serve as conformationally restrained type VI  $\beta$ -turn mimics.

### 2.5. Results and Discussion

*N*-Acetyl dipeptide *N*<sup>1</sup>-methylamides containing (2*S*, 5*R*)-tBuPro at the *C*-terminal position were synthesized using solution-phase peptide chemistry. The allyl ester of 5-tBuPro was first prepared from *N*-(BOC)-5-tBuPro by alkylation with allyl bromide and DIEA in CH<sub>2</sub>Cl<sub>2</sub>. The *N*<sup>1</sup>-methylamide of 5-tBuPro was obtained by coupling *N*-(BOC)-5-tBuPro to CH<sub>3</sub>NH<sub>2</sub>·HCl using TBTU and DIEA in CH<sub>3</sub>CN. Dipeptides were synthesized by removal of the BOC group with 25% TFA in CH<sub>2</sub>Cl<sub>2</sub> and acylation with *N*-(BOC)-amino acids using BOP-Cl and DIEA in CH<sub>2</sub>Cl<sub>2</sub> (Table

1). Allyl ester cleavage was accomplished on the dipeptides in high yields using Pd(PPh<sub>3</sub>)<sub>4</sub> in THF with morpholine, and the *C*-terminal *N*<sup>t</sup>-methylamides were synthesized as described above. The *N*-(BOC)-dipeptide *N*<sup>t</sup>-methylamides were deprotected with 25% TFA in CH<sub>2</sub>Cl<sub>2</sub> and acetylated with Ac<sub>2</sub>O and K<sub>2</sub>CO<sub>3</sub> in CH<sub>2</sub>Cl<sub>2</sub> to furnish the *N*-acetyl dipeptide *N*<sup>t</sup>-methylamides.

The amide isomer population and NH chemical shifts of the *N*-acetyl dipeptide *N*<sup>t</sup>-methylamides were ascertained by proton NMR spectroscopy (Table 2). The major conformer in the dipeptides possessed an amide *cis*-isomer *N*-terminal to the 5-tBuPro residue. Changes in solvent polarity had limited effects on the amide *cis*-isomer population. In the case of Xaa = Gly, coalescence of the amide signals was observed in CDCl<sub>3</sub> and DMSO. As the steric bulk of the side-chain augmented, the amide *cis*-isomer population increased in D<sub>2</sub>O. The benzyl side-chain induced the highest population of amide *cis*-isomer. In the major conformer of the dipeptides, the signals for the NHXaa and NHMe protons were respectively between 6.0-6.4 and 8.3-8.5 ppm in CDCl<sub>3</sub>. The chemical shifts of the NHXaa signals were strongly influenced by changes in solvent polarity whereas those of the NHMe protons showed little variation. This demonstrated that the NHXaa protons were exposed to solvent and the NHMe protons were hydrogen bound in type VI β-turn conformations.

**Table 1. Acylation of (2*S*,5*R*)-5-tBuPro-R with *N*-(BOC)-amino acids (Xaa).**

R	Xaa	% yield	R	Xaa	% yield
OAll	Ala	68	NHMe	Ala	75
OAll	Leu	82	NHMe	Gly	87
OAll	Phe	94	NHMe	Met	64
OAll	Val	43	NHMe	Val	35

**Table 2. Solvent Effects on Ac-Xaa-(2S, 5R)-5-tBuPro-NHMe Conformation.**

Xaa	%cis X-Pro			$\Delta\delta$ NH CDCl <sub>3</sub> →DMSO (ppm)		$\Delta\delta$ NH CDCl <sub>3</sub> →H <sub>2</sub> O (ppm)	
	CDCl <sub>3</sub>	DMSO	H <sub>2</sub> O	NHMe	NHXaa	NHMe	NHXaa
Gly	-	-	55	-	-	-	-
Ala	83	79	79	0.28	2.39	0.28	2.22
Met	73	72	74	0.32	2.08	0.16	1.95
Leu	85	67	81	0.22	2.43	0.12	2.27
Phe	89	79	90	0.35	2.53	0.26	-
Val	89	73	81	0.32	2.13	0.13	1.86

**Acknowledgements:** This research was supported by NSERC (Canada) and FCAR (Québec). L. H. is grateful for awards supporting travel expenses from the Ichikizaki Fund for Young Chemists and from the ESCOM Science Foundation.

## 2.6. References

1. Johnson, M.E., Lin, Z., Padmanabhan, K., Tulinsky, A. and Kahn, M. *FEBS Lett.*, 337 (1994) 4.
2. Fischer, S., Michnick, S. and Karplus, M. *Biochemistry*, 32 (1993) 13830.
3. Beausoleil, E. and Lubell, W.D. *J. Am. Chem. Soc.*, 118 (1996) 12902.
4. Beausoleil, E., L'Archevêque, B., Bélec, L., Atfani, M. and Lubell, W.D. *J. Org. Chem.*, 61 (1996) 9447.

**Article 3**

**Halab, L.; Lubell, W. D. "Use of Steric Interactions to Control Peptide Turn Geometry. Synthesis of Type VI  $\beta$ -Turn Mimics with 5-*tert*-Butylproline." Publié dans *The Journal of Organic Chemistry* 1999, 64, 3312-3321.**

Use of Steric Interactions to Control Peptide Turn Geometry.  
Synthesis of Type VI  $\beta$ -Turn Mimics with 5-*tert*-Butylproline.

Liliane Halab and William D. Lubell\*

Département de chimie, Université de Montréal

C. P. 6128, Succursale Centre Ville, Montréal, Québec, Canada H3C 3J7

**2.7. Abstract**

The influences of steric interactions on peptide geometry were studied to develop a novel means for generating type VIa  $\beta$ -turn mimics. (2S, 5R)-5-*tert*-Butylproline and L-proline were respectively introduced at the C-terminal residue of *N*-(acetyl)dipeptide *N'*-methylamides **1** and **2**. The relative populations of prolyl *cis*- and *trans*-amide isomers in dipeptides **1** and **2** were measured in chloroform, DMSO and water by proton NMR spectroscopy. Although the *trans*-amide isomer was favored in prolyl peptide **2**, the Xaa-Pro peptide bond adopted preferably the *cis*-amide isomer in the case of 5-*tert*-butylprolyl peptide **1**. Measurements of the influence of solvent and temperature on the chemical shift values for the amide proton signals of **1** in the *cis*-amide conformer indicated that the *N'*-methylamide was engaged in a hydrogen bond with the acetamide carbonyl in a type VIa  $\beta$ -turn conformation. Analysis of *N*-(acetyl)leucyl-5-*tert*-butylproline *N'*-methylamide (**1d**) in the solid state by X-ray diffraction showed the *cis*-amide conformer which adopted a geometry characteristic of the central, *i* + 1 and *i* + 2 residues of an ideal type VIa  $\beta$ -turn. In contrast to prolyl peptides **2b** and **2d**, *N*-(acetyl)alanyl- and *N*-(acetyl)leucyl-5-*tert*-butylproline *N'*-methylamides (**1b** and **1d**) maintained ordered  $\beta$ -turn conformations in solution that were shown to be independent of solvent composition by a comparison of their circular dichroism spectra obtained in water and acetonitrile. The NMR, X-ray and CD data, all confirm that the steric interactions of the 5-*tert*-butylprolyl residue induced dipeptide **1** to adopt a type VIa  $\beta$ -turn conformation.

## 2.8. Introduction

The spatial requirements for peptide biology may be elucidated by employing constrained analogs of native secondary structures to probe relationships between conformation and activity. Because of the importance of  $\beta$ -turns in protein folding and recognition,<sup>1</sup> considerable effort has focused on developing conformationally restricted mimics of the backbone geometry, intramolecular hydrogen bonding and side-chain orientations exhibited by these secondary structures.<sup>2</sup> Among such designs, the use of modified prolines has often led to successful surrogates because of the high frequency of this amino acid at the central residues of the  $\beta$ -turn conformation.<sup>2,3</sup> We report now the use of the steric interactions of 5-*tert*-butylproline to generate conformationally rigid mimics of the type VIa  $\beta$ -turn.

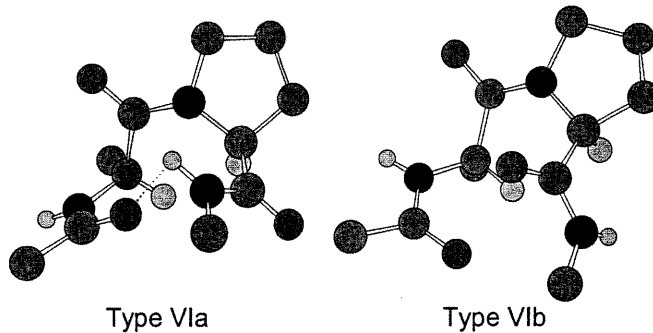


**Figure 1. Central,  $i + 1$  and  $i + 2$  residues of type VIa and VIb turn conformations found respectively in ribonuclease S<sup>5b</sup> and Bence-Jones protein.<sup>5c</sup> Only amide protons shown (N, black; C, dark gray; O, light gray; H, white).**

The type VI  $\beta$ -turn is a unique secondary structure that features an amide *cis*-isomer *N*-terminal to a prolyl residue situated at the  $i + 2$  position of the peptide bend.<sup>4</sup> Two classes of type VI  $\beta$ -turns have been defined based on the back-bone dihedral angle values of their central,  $i + 1$  and  $i + 2$  residues (Figure 1).<sup>1,4</sup> In the type VIa  $\beta$ -turn, the proline  $\psi$ -dihedral angle is near  $0^\circ$  and an intramolecular hydrogen bond exists between the carbonyl oxygen of the  $i$  and amide hydrogen of the  $i + 3$  residues. The proline  $\psi$ -dihedral angle is situated around  $150^\circ$  in the type VIb geometry which can not form an intramolecular hydrogen bond. Identified on the surfaces of globular proteins,<sup>5</sup> type VI  $\beta$ -turns are commonly located in cyclic

peptides possessing prolyl residues.<sup>6</sup> In addition, the minor *cis*-amide conformers of certain linear peptides, particularly those possessing aromatic amino acids *N*-terminal to proline and pipecolate residues, have been observed to adopt type VI  $\beta$ -turn geometry.<sup>7-10</sup>

Type VI  $\beta$ -turn conformations play important roles in the recognition and reactivity of bioactive peptides and proteins. For example, a type VI  $\beta$ -turn conformation has been suggested as a requirement for thrombin catalyzed cleavage of the V<sub>3</sub> loop of HIV gp120, a prerequisite to viral infection.<sup>11</sup> Furthermore, peptidyl prolyl isomerasases (PPIases) which catalyze the isomerization of Xaa-Pro amide bonds and thereby accelerate the folding of particular proteins have been proposed to bind preferably to peptides possessing type VI  $\beta$ -turn conformations.<sup>12,13</sup> Computational analysis revealed that the PPIase FKBP bound *N*-acetyl-Leu-Pro-Phe-methylamide in a type VIa  $\beta$ -turn.<sup>12</sup> In the solid state, the tetrapeptide substrate, *N*-acetyl-Ala-Ala-Pro-Ala-amidomethylcoumarin was shown by X-ray diffraction to adopt a type VIb  $\beta$ -turn geometry when bound to the PPIase cyclophilin.<sup>13</sup> In addition, the nature of the amino acid (Xaa) *N*-terminal to the prolyl residue was found to influence PPIase activity.<sup>14</sup>

Among the *cis*-amide prolyl peptide surrogates, competent replacements for the backbone geometry of the central residues of the type VIa  $\beta$ -turn have been synthesized by tethering the  $\alpha$ -carbon of the *N*-terminal amino acid residue to the proline 2-position in a dipeptide lactam.<sup>15,16</sup> These azabicycloalkane amino acids have been effectively used in constrained analogs of peptides that require a type VI  $\beta$ -turn for bioactivity.<sup>15b</sup> In model peptides, these dipeptide lactams have oriented the *N*- and *C*-terminal amides to form intramolecular hydrogen bonds in ten member  $\beta$ -turn and fourteen member  $\beta$ -hairpin secondary structures.<sup>16c,d</sup> Although they may replicate the backbone and hydrogen bonding elements of type VI  $\beta$ -turns, because of difficulties in appending substituents onto the *N*-terminal amino acid residue of dipeptide lactams, these azabicycloalkane amino acids do not effectively mimic side-chain pharmacophores that may influence peptide turn recognition.<sup>14</sup> A second

approach for replicating the type VIa  $\beta$ -turn, that may allow diversification at the  $i + 1$  position, has employed azaproline analogs in which the prolyl  $\alpha$ -carbon is replaced by nitrogen.<sup>17</sup> In the solid state, azaproline analogs adopted a type VIa conformation as demonstrated by X-ray diffraction.<sup>17a</sup> Furthermore, spectroscopic studies of *N*-(BOC)alanyl-azaprolinyl-alanine *N*-*iso*-propylamides by NMR in solution indicated that intramolecular hydrogen bonding was maintained in a type VIa  $\beta$ -turn conformation as solvent composition was changed from chloroform to DMSO.<sup>17b</sup> Although azaproline is not chiral and the configurations of the neighboring residues may influence the ring puckering and  $\psi$ -dihedral angle of this prolyl residue in peptides, this approach may provide a variety of type VI  $\beta$ -turn mimics should the pyrazolidine moiety be efficiently introduced into peptide structures. Type VI  $\beta$ -turn surrogates may also be procured from alternative strategies for replicating *cis*-amide geometry, such as cyclo-cystine<sup>18</sup> and cyclo-lanthione<sup>19</sup> derivatives, diazabicycloalkane amino acids<sup>20</sup> as well as heterocycle<sup>21</sup> olefin<sup>22</sup> and fluoro-olefin<sup>23</sup> amide bond replacements; however, less is known about the influence of these constraints on the overall peptide conformation. Moreover, approaches involving amide isosteres may not be readily amenable to the construction Xaa-Pro dipeptide surrogate libraries by diversification of the *N*-terminal amino acid.

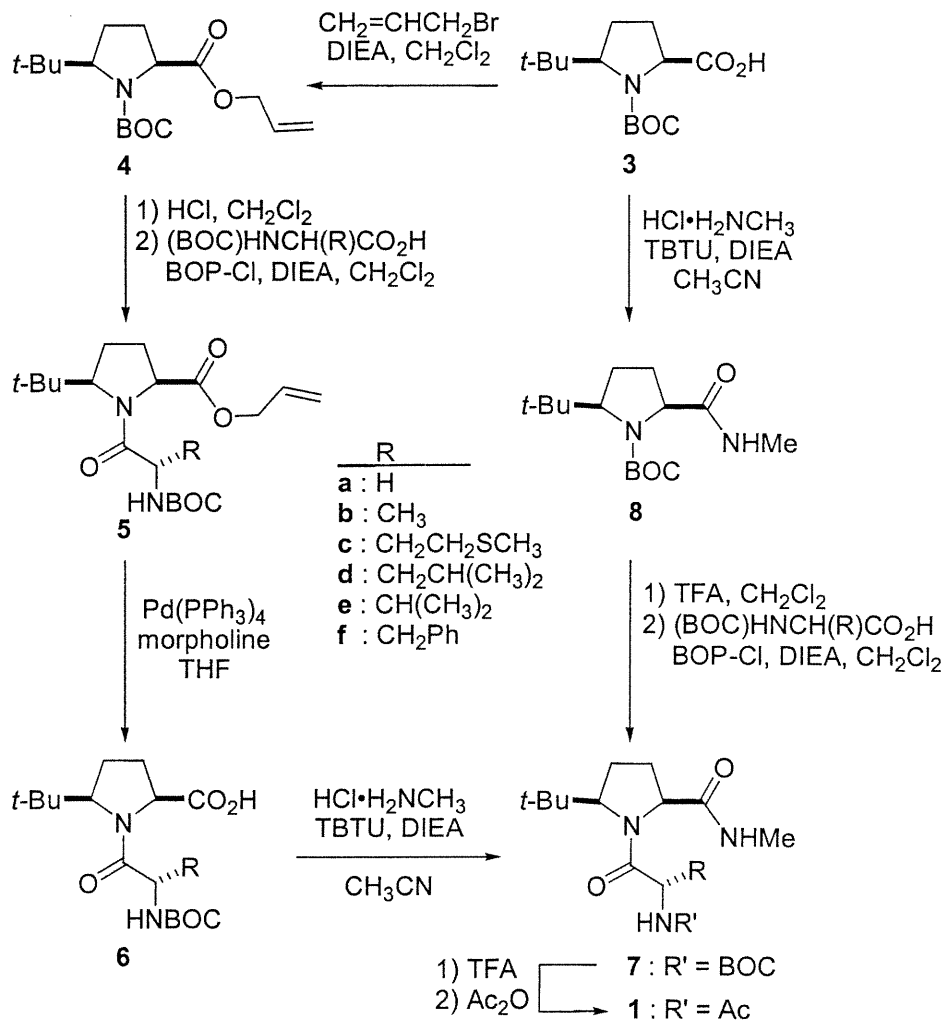
Towards an approach for generating libraries of conformationally constrained type VI  $\beta$ -turn mimics, we have employed 5-alkylprolines to control the prolyl amide isomer geometry. The steric interactions between a 5-*tert*-butyl substituent and the *N*-terminal residue disfavor the Xaa-Pro peptide bond *trans*-isomer and increase the *cis*-isomer population.<sup>24</sup> By studying analogs of *N*-(acetyl)proline *N*'-methylamide, we demonstrated that incorporation of 5-*tert*-butylproline into this model peptide increased the *cis*-isomer population, influenced the energy barrier for prolyl amide isomerization, as well as restricted the proline  $\psi$ -dihedral angle.<sup>24</sup> We have now incorporated (2*S*, 5*R*)-5-*tert*-butylproline at the *C*-terminal of a series of *N*-(acetyl)dipeptide *N*'-methylamides **1** in order to examine if the constraints on the prolyl  $\omega$ - and  $\psi$ -dihedral angles would stabilize the type VI  $\beta$ -turn geometry. Conformational analyses of dipeptides **1** by NMR experiments, X-ray diffraction and

circular dichroism spectroscopy, and comparison of **1** with dipeptide counterparts **2** possessing natural proline, all have shown that (*2S, 5R*)-*5-tert*-butylproline stabilized the type VIa  $\beta$ -turn geometry possessing an intramolecular hydrogen bond between the *N*<sup>o</sup>-methylamide proton and the acetamide carbonyl. By simply coupling a variety of different amino acid residues to the *N*-terminal of (*2S, 5R*)-*5-tert*-butylproline, we have demonstrated the means for generating a library of dipeptide surrogates that mimic the backbone geometry, hydrogen bonding and side-chain elements of type VIa  $\beta$ -turns. These *5-tert*-butylproline surrogates may thus reproduce both the structural and recognition elements of type VI  $\beta$ -turns.

## 2.9. Results

### 2.9.1. Synthesis of Ac-Xaa-Pro-NHMe Dipeptides **1** and **2**

(*2S, 5R*)-*N*-(BOC)-*5-tert*-Butylproline (**3**) was synthesized in seven steps from glutamic acid as an inexpensive chiral educt using our acylation / diastereoselective reductive amination sequence.<sup>25</sup> Two routes were investigated to introduce **3** into *N*-acetyl-Xaa-*5-tert*-butylproline *N*<sup>o</sup>-methylamides **1** (Scheme 1). In the first route, *N*-(BOC)-*5-tert*-butylproline allyl ester (**4**) was synthesized by alkylation of acid **3** with allyl bromide and DIEA in dichloromethane. Solvolysis of the BOC group with HCl gas in dichloromethane and coupling to *N*-(BOC)amino acids provided the *N*-(BOC)-dipeptide allyl esters **5** that were converted to *N*-(BOC)-dipeptides **6** by palladium catalyzed ester cleavage. We have introduced *N*-BOC-Xaa-*5-tert*-butylprolines **6** into peptide structures by conventional coupling techniques using both solution- and solid-phase strategies.<sup>26</sup> In the context of the present project, dipeptides **6** were coupled to methylamine using benzotriazol-1-yl-1,1,3,3-tetramethyluronium tetrafluoroborate (TBTU)<sup>27</sup> in DMF to furnish *N*-BOC-Xaa-*5-tert*-butylproline *N*<sup>o</sup>-methylamides **7**. The respective *N*-acetyl-Xaa-*5-tert*-butylproline *N*<sup>o</sup>-methylamides **1** were synthesized from **7** by solvolysis of the BOC group with trifluoroacetic acid and *N*-acetylation with acetic anhydride and potassium carbonate in dichloromethane.



Scheme 1. Synthesis of *N*-(acetyl)dipeptide *N'*-methylamides 1.

In the second route, *N*-(BOC)-5-*tert*-butylproline (3) was coupled to methylamine using TBTU in acetonitrile to provide *N*-(BOC)-5-*tert*-butylproline *N*'-methylamide (8).<sup>24</sup> Solvolysis of the BOC group with TFA in dichloromethane and coupling to *N*-(BOC)-amino acids provided *N*-BOC-Xaa-5-*tert*-butylproline *N*'-methylamides 7 that were acetylated as described above. Among the reagents explored for coupling to the *N*-terminal of 5-*tert*-butylproline allyl ester and 5-*tert*-butylproline *N*-methylamide, *N,N*-bis(2-oxo-3-oxazolidinyl)phosphonic chloride (BOPCl)<sup>28</sup> in CH<sub>2</sub>Cl<sub>2</sub> at 5 °C gave the best yields of protected dipeptides 5 and 7.<sup>29</sup> For comparison with dipeptides possessing natural L-proline, we synthesized *N*-(acetyl)alanyl-L-proline *N*'-methylamide (**2b**) and *N*-(acetyl)leucyl-L-proline *N*'-

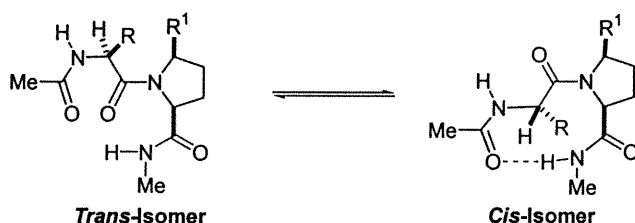
methylamide (**2d**) by respectively coupling *N*-(BOC)alanine and *N*-(BOC)leucine to proline *N*-methylamide, followed by BOC group solvolysis and acetylation as described in the experimental section.

### 2.9.2. Conformational Analysis of Prolyl Dipeptides **1** and **2** by NMR Spectroscopy

The relative populations of the amide *cis*- and *trans*-isomers *N*-terminal to the prolyl residues of peptides **1** and **2** were ascertained by NMR spectroscopy in chloroform, dimethyl sulfoxide and water. The amide populations of **1** and **2** could be determined for all peptides in water; however, coalescence of signals prevented their measurement for *N*-acetyl-glycyl-5-*tert*-butylproline *N*-methylamide (**1a**) in chloroform and DMSO at room temperature. The *cis*-isomer was assigned based on observation of the cross-peak arising from the nuclear Overhauser effect between the *N*-terminal amino acid and proline  $\alpha$ -hydrogens in the NOESY and ROESY spectra in DMSO. The populations of the amide isomers were measured by integration of the isomeric *tert*-butyl singlets and *N*-methyl doublets in the  $^1\text{H}$  NMR spectra of **1** and **2**. The *tert*-butyl singlet of the amide *trans*-isomer appeared always downfield from that of the *cis*-isomer. The ratios of amide isomers in **1b-f** and **2** for each solvent are listed as the percent of *cis*-isomer in Table 1.

As is typically observed for linear prolyl peptides,<sup>7-11</sup> the major conformer of peptides **2** possessed the *trans*-amide geometry *N*-terminal to the prolyl residue. On the other hand, the major conformer of peptides **1** adopted the *cis*-amide geometry *N*-terminal to the 5-*tert*-butylprolyl residue. *N*-Acetyl-glycyl-5-*tert*-butylproline *N*-methylamide (**1a**) exhibited only 55% *cis*-isomer population in water, which was similar to the amount of *cis*-isomer (48%) previously observed with (2*S*, 5*R*)-*N*-acetyl-5-*tert*-butylproline *N*-methylamide and indicated that the additional acetamide group had a limited influence on the prolyl amide equilibrium.<sup>24</sup> The presence of an alkyl substituent at the  $\alpha$ -position of the *N*-terminal amino acid residue augmented significantly the *cis*-isomer population in peptides **1b-f** (Table 1).

**Table 1. Influence of solvent on the chemical shifts and amide isomer equilibrium of 1 and 2.<sup>a</sup>**



entry	R	R <sup>1</sup>	%cis-isomer ± 3%			(CDCl <sub>3</sub> )		(CDCl <sub>3</sub> → DMSO)		(CDCl <sub>3</sub> → H <sub>2</sub> O)	
			H <sub>2</sub> O ; DMSO	CDCl <sub>3</sub>	δ NH <sup>Xaa</sup> , NH <sup>Me</sup>	δ NH <sup>Xaa</sup> , NH <sup>Me</sup>	Δδ NH <sup>Xaa</sup> ; NH <sup>Me</sup>				
1b	CH <sub>3</sub>	t-Bu	79	79	83	6.07	8.30	2.39	0.28	2.22	0.28
1c	CH <sub>2</sub> CH <sub>2</sub> SCH <sub>3</sub>	t-Bu	74	72	73	6.41	8.27	2.08	0.32	1.95	0.16
1d	CH <sub>2</sub> CH(CH <sub>3</sub> ) <sub>2</sub>	t-Bu	81	67	85	5.97	8.27	2.43	0.22	2.27	0.12
1e	CH(CH <sub>3</sub> ) <sub>2</sub>	t-Bu	81	73	89	6.18	8.48	2.13	0.32	1.86	0.13
1f	CH <sub>2</sub> Ph	t-Bu	90	79	89	6.09	8.37	2.53	0.35	-	0.26
2b	CH <sub>3</sub>	H	14	30	19	6.33	6.61	1.79	1.06	1.82	1.20
2d	CH <sub>2</sub> CH(CH <sub>3</sub> ) <sub>2</sub>	H	19	17	20	6.03	6.68	2.00	1.65	2.13	1.10

<sup>a</sup> Values are for the major conformer at 5 mM concentration.

Additional alkyl branching at the  $\beta$ - and  $\gamma$ -positions gave a relatively minor increase to the *cis*-isomer population. As previously noted in prolyl peptides,<sup>8-10</sup> the presence of an aromatic amino acid *N*-terminal to proline caused a notable increase in the population of the *cis*-isomer in water and *N*-acetyl-phenylalanyl-5-*tert*-butylproline *N*-methylamide (**1f**) exhibited the largest amounts of *cis*-amide among the examples studied.

In the major *cis*-amide conformer of peptides **1**, the signal for the *N*-methylamide proton was observed downfield relative to the signal for the acetamide proton in all three solvents. This downfield shift was most evident in chloroform in which the *N*-methylamide proton signal appeared between 8.27 and 8.48 ppm at the same time the acetamide proton signal came between 5.97 and 6.41 ppm (Table 1). The downfield shifted amide proton signal was indicative of an intramolecular hydrogen bond between the *N*-methylamide proton and the acetamide carbonyl in a type VI  $\beta$ -turn conformation.<sup>30</sup>

The signal for the *N*<sup>1</sup>-methylamide proton was not affected by changes in solvent relative to the signal for the acetamide proton in the NMR spectra for the *cis*-amide conformer of dipeptides **1**. The *N*<sup>1</sup>-methylamide proton signal was shifted 0.22-0.35 ppm downfield on switching solvent from chloroform to DMSO and 0.12-0.28 ppm downfield on changing solvent from chloroform to water (Table 1). On the contrary, the signal for the acetamide proton was shifted 2.08-2.53 ppm downfield on switching solvent from chloroform to DMSO and 1.86-2.27 ppm downfield on changing solvent from chloroform to water. The influence of solvent on the chemical shifts of the amide proton signals supported a type VI  $\beta$ -turn conformation for the *cis*-amide conformer of **1** by indicating that the *N*<sup>1</sup>-methylamide proton was engaged in an intramolecular hydrogen bond.<sup>30</sup>

**Table 2. Influence of temperature on the NH chemical shifts of *N*-(acetyl)dipeptide *N*<sup>1</sup>-methylamides **1** and **2** in DMSO.**

entry	R	R <sup>1</sup>	isomer	$\Delta\delta/\Delta T$ (–ppb/K)	
				NH <sup>Xaa</sup>	NH <sup>Me</sup>
<b>1b</b>	CH <sub>3</sub>	<i>t</i> -Bu	<i>cis</i>	5.6	3.7
			<i>trans</i>	4.9	4.4
<b>2b</b>	CH <sub>3</sub>	H	<i>cis</i>	6.3	4.3
			<i>trans</i>	5.7	4.4
<b>1d</b>	CH <sub>2</sub> CH(CH <sub>3</sub> ) <sub>2</sub>	<i>t</i> -Bu	<i>cis</i>	5.3	3.0
			<i>trans</i>	4.3	4.4
<b>2d</b>	CH <sub>2</sub> CH(CH <sub>3</sub> ) <sub>2</sub>	H	<i>cis</i>	6.1	4.1
			<i>trans</i>	5.6	5.3

A comparison of the measured temperature coefficients for the amide protons in peptides **1b**, **1d**, **2b** and **2d** in DMSO provided additional evidence for a type VI  $\beta$ -turn conformation in **1** (Table 2). In the case of the *cis*- and *trans*-conformers of Ac-Ala-Pro-NHMe (**2b**) and Ac-Leu-Pro-NHMe (**2d**), all of the amide proton signals exhibited chemical shift temperature coefficients that were less than –4 ppb/K, within the range for unstructured peptides.<sup>31</sup> Similarly, in the case of the corresponding *tert*-butylprolyl peptides **1b** and **1d**, the amide signals for the minor *trans*-amide conformer and the acetamide proton signal of the *cis*-amide conformer, all possessed chemical shift temperature coefficients less than –4 ppb/K in DMSO. Only the *N*<sup>1</sup>-

methylamide proton signal for the major *cis*-amide conformer of *tert*-butylprolyl peptides **1b** and **1d** exhibited a temperature coefficient that was greater than -4 ppb/K in DMSO. Although values greater than -3 ppb/K have been suggested to indicate a solvent shielded amide proton engaged in an intramolecular hydrogen bond in DMSO,<sup>31</sup> such temperature coefficients are usually measured on cyclic peptides and peptide structures larger than those studied in this report. The respective values of -3.7 ppb/K and -3.0 ppb/K for the *N*<sup>o</sup>-methylamide proton signal of the major *cis*-amide conformer of dipeptides **1b** and **1d** fall into the region between temperature coefficients associated with hydrogen bonded and solvent-exposed amide; however, their size is most probably due to the inability of the acetamide and *N*<sup>o</sup>-methyl groups in model peptides **1** to provide adequate solvent shielding of the hydrogen-bound *N*<sup>o</sup>-methylamide proton.

Smaller values were consistently measured for the vicinal coupling constant (<sup>3</sup>*J*<sub>NH,α</sub>) between the amide and α-protons of the *N*-terminal amino acid residue in the major *cis*-amide conformer of *tert*-butylprolyl peptides **1b-f** than were observed for the minor *trans*-amide conformer of **1** and the *cis*- and *trans*-amide conformers of **2**. For example, <sup>3</sup>*J*<sub>NH,α</sub> values were 0.8-3.5 Hz lower for the *cis*-amide than for the *trans*-amide conformer of **1b-f** in DMSO. The <sup>3</sup>*J*<sub>NH,α</sub> values varied from 5.2-6.4 Hz for the *cis*-amide conformers of **1b-f** in DMSO. Since the ideal φ-dihedral angle of -60° for the *i* + 1 residue in a type VIa β-turn corresponds to a <sup>3</sup>*J*<sub>NH,α</sub> of 4.2 Hz, the observed reduced coupling constant values support the hypothesis that the major *cis*-amide conformer of peptides **1b-f** adopts a significant population of type VI β-turn in solution.<sup>32</sup>

Evidence for the presence of a twisted amide geometry in solution was obtained by examining the chemical shift value for the carbonyl carbon of the *N*-terminal amino acid residue in peptide **1b**.<sup>33</sup> After assigning the amide carbonyl resonances by using two-dimensional HMBC NMR experiments,<sup>34</sup> we observed that 5-*tert*-butylprolyl peptide **1b** exhibited carbonyl chemical shift values for the *N*-

terminal amino acid residue that were 3.1 ppm downfield relative to those of prolyl peptide **2b** in water. Because inhibition of amide resonance by factors that distort the N-C(O) bond deshields the carbonyl carbon,<sup>33a</sup> the downfield-shifted <sup>13</sup>C NMR chemical shift value indicated that the prolyl amide bond of **1b** was twisted from planarity by steric interactions between the *N*-terminal residue and *5-tert*-butyl substituent.

### 2.9.3. X-Ray Crystallographic Analysis of *N*-Acetyl-L-leucyl-5-*tert*-butylproline *N'*-Methylamide (**1d**)

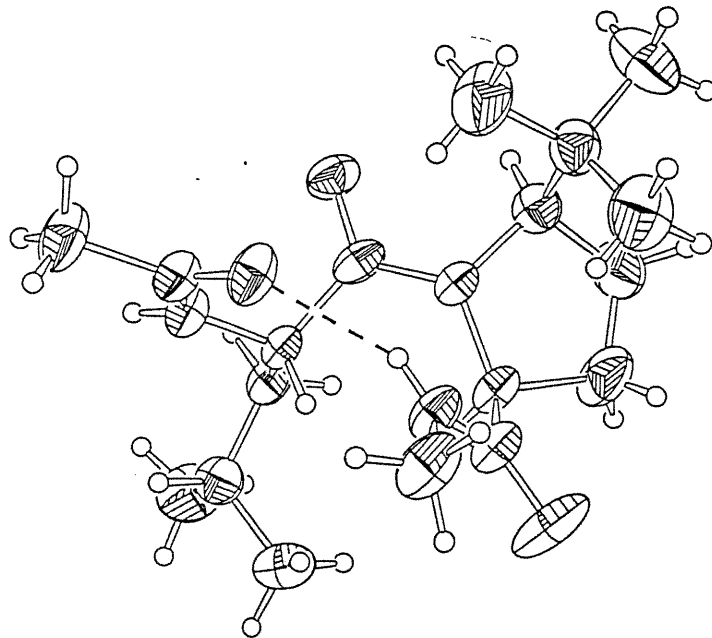


Figure 2. ORTEP view of Ac-Leu-5-*t*BuPro-NHMe **1d**. Ellipsoids drawn at 40% probability level. Hydrogens represented by spheres of arbitrary size.<sup>35</sup>

Table 3. Comparison of the Dihedral Angles of Ideal Type VIa  $\beta$ -Turn and X-Ray Structure of *N*-(Acetyl)Leucyl-5-*tert*-butylproline *N'*-Methylamide **1d**.

entry	$\phi_2$	$\psi_2$	$\omega$	$\phi_3$	$\psi_3$
Ideal Type VIa $\beta$ -Turn <sup>4</sup>	-60°	120°	0°	-90°	0°
Ac-Leu-5- <i>t</i> -BuPro-NHMe <b>1d</b> <sup>35</sup>	-61°	139°	17°	-95°	19°
Leu-Pro residues in X-ray of evolidine <sup>6d</sup>	-65°	151°	2°	-93°	13°

Crystals of *N*-acetyl-L-leucyl-5-*tert*-butylproline *N*-methylamide (**1d**) were grown from a mixture of ether and hexane. Crystallographic analysis of **1d** by X-ray diffraction demonstrated the presence of the amide *cis*-isomer *N*-terminal to the 5-*tert*-butylprolyl residue (Figure 2).<sup>35</sup> Furthermore, the dihedral angles of peptide **1d** resembled those of the central, *i* + 1 and *i* + 2 residues of a type VIa  $\beta$ -turn. For comparison, the dihedral values for the crystal structure of **1d** are listed in Table 3 with those of an ideal type VIa geometry,<sup>4</sup> and the values for the Leu-Pro residues found in the central positions of the type VIa  $\beta$ -turn in the X-ray structure of the cyclic peptide evolidine.<sup>6d</sup> An intramolecular hydrogen bond between the *N*-methylamide proton and the acetamide carbonyl oxygen was clearly inferred from their interatomic distance of 2.13 Å in the X-ray structure of **1d**.

The  $\omega$ ,  $\psi$  and  $\phi$  values for the dihedral angles of the 5-*tert*-butylprolyl residue in the X-ray structure of peptide **1d** were similar to those calculated for the energy minimum of the *cis*-isomer of *N*-acetyl-5-*tert*-butylproline *N*-methylamide.<sup>24</sup> A twisted amide conformation *N*-terminal to the 5-*tert*-butylprolyl residue was observed on measuring the  $\omega$ -dihedral angle value of 17.3° for **1d** in the X-ray structure and indicated that the bulky 5-position substituent skewed the amide bond away from planarity.<sup>33</sup> The twisted amide geometry was substantiated by the 1.36 Å carbonyl carbon to nitrogen bond distance for the amide *N*-terminal to the 5-*tert*-butylprolyl residue, which was longer than the 1.33 Å bond lengths for the other amides.<sup>33b</sup> The measured  $\psi$ -dihedral angle value of 18.5° placed the *N*-methylamide hydrogen at a 2.45 Å interatomic distance from the prolyl nitrogen. These constraints account for the observed acceleration of amide isomerization *N*-terminal to (2*S*, 5*R*)-5-*tert*-butylproline. Ground-state destabilization results from the bulky 5-*tert*-butyl substituent distorting the amide bond away from planarity. Stabilization of the pyramidalized amide transition state arises from the *N*-methylamide hydrogen interacting with the nitrogen lone pair of the rotating prolyl amide.<sup>12,36</sup> In the case of *N*-(acetyl)glycyl-5-*tert*-butylproline *N*-methylamide (**1a**), such an acceleration of the rate of prolyl amide isomerization was illustrated by the coalescence of the isomeric *cis*- and *trans*-amide signals in DMSO and chloroform at room temperature, because

amide isomerization *N*-terminal to proline proceeded faster in the non-protic and comparatively non-polar solvent than in water which stabilized the polar amide ground states relative to the less polar transition state.<sup>37</sup>

#### 2.9.4. Conformational Analysis of Dipeptides 1 and 2 by Circular Dichroism Spectroscopy

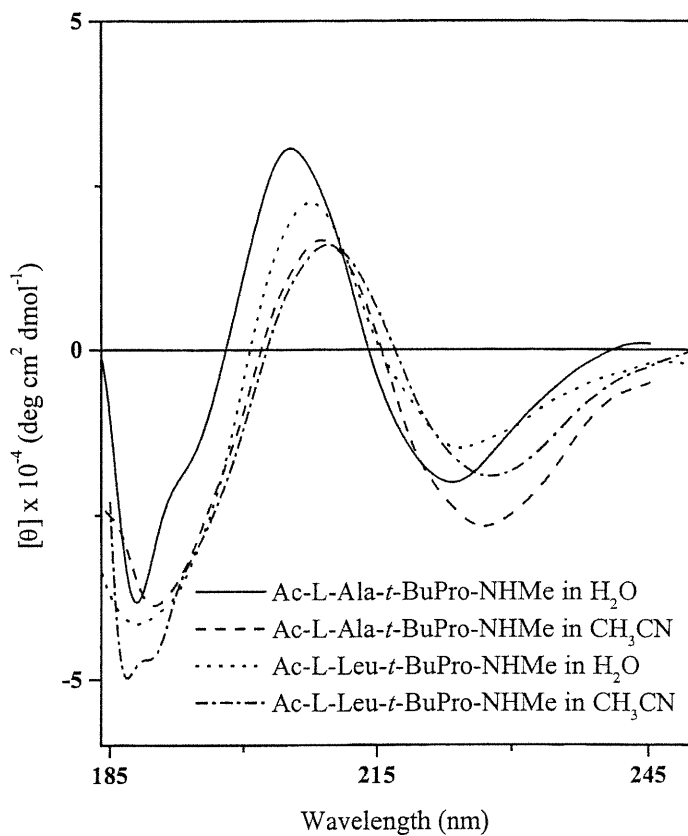


**Figure 3. Circular dichroism spectra of *N*-(acetyl)alanyl- and *N*-(acetyl)leucyl-5-*tert*-butylproline *N'*-methylamides (**1b** and **1d**) in water and acetonitrile.**

Circular dichroism (CD) spectra of **1b**, **1d**, **2b** and **2d** were measured in both water and acetonitrile to examine the influence of solvent composition on peptide conformation. The CD spectra of **1b** and **d** in acetonitrile exhibited a strong negative band at 188 nm, a strong positive band at 209 nm and a weak negative band at 227 nm (Figure 3). This type of CD curve shape has previously been assigned to  $\beta$ -turn conformations in studies of model peptides in water.<sup>38</sup> Aside from a slight blue

shift,<sup>39</sup> the shape of the CD curves for **1b** and **d** remained constant as solvent was changed from acetonitrile to water. The type VIa  $\beta$ -turn conformation adopted by 5-*tert*-butylprolyl peptide **1** was thus shown to be independent of solvent composition. On the other hand, the CD spectral characteristics of prolyl peptides **2** were similar to those reported for *N*-(acetyl)proline *N*-methylamide and varied significantly with changes in solvent composition exhibiting a n- $\pi^*$  band near 225 nm in acetonitrile that shifted to a significant  $\pi$ - $\pi^*$  band near 195 nm in water (Figure 4).<sup>40</sup>

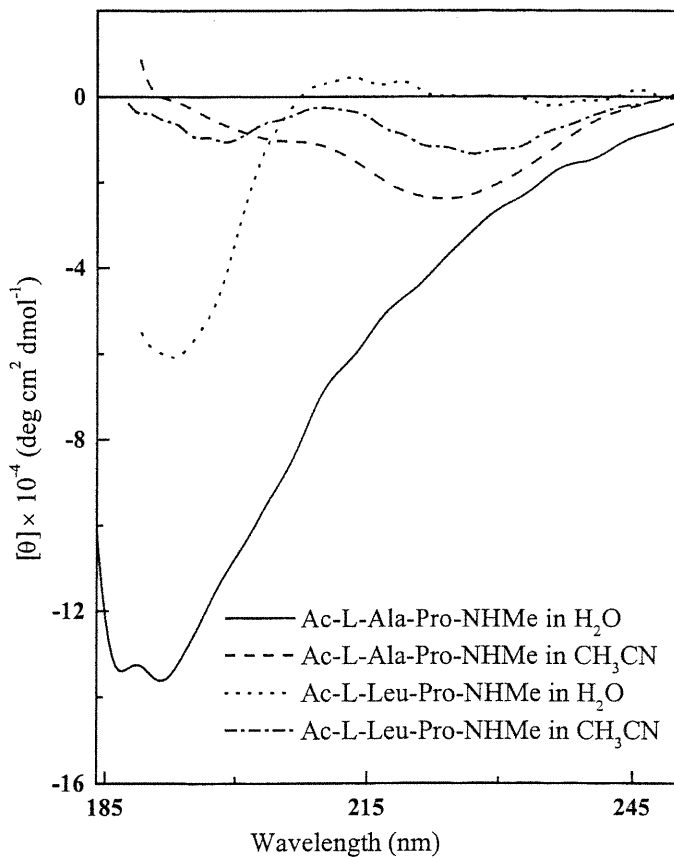


**Figure 4:** Circular dichroism spectra of *N*-(acetyl)alanyl- and *N*-(acetyl)leucyl-proline *N*-methylamides (**2b** and **2d**) in water and acetonitrile.

## 2.10. Discussion

Steric interactions have been employed to restrain peptide geometry and favor particular secondary structures. For example, amino *iso*-butyric acid (Aib) residues

can create steric interactions with neighboring residues that favor 3<sub>10</sub>- and  $\alpha$ -helical geometries such as those found in antibiotic peptides like althemethicin.<sup>41</sup> By similar interactions, the related  $\alpha,\alpha$ -dialkyl glycines induce 3<sub>10</sub>-helices and type III  $\beta$ -turn geometries in linear peptides.<sup>42</sup> In pioneering studies of substituted polyproline oligomers, the steric effects of 2-methylproline were found to stabilize polyproline type II helical conformation.<sup>43</sup> Recently, the combination of A<sup>1,3</sup>- and A<sup>1,2</sup>-strain of alkyl substituted olefin amide bond isosteres have been used to induce the formation of  $\beta$ -turn conformations exhibiting ten member intramolecular hydrogen bonds,<sup>44</sup> and a  $\beta$ -hairpin mimic possessing a fourteen member intramolecular hydrogen bond.<sup>45</sup> On the other hand, disruption of the  $\gamma$ -turn conformation has been caused by the placement of alkyl substituents at the 3-position of a central prolyl residue.<sup>46</sup>

In this report, we have demonstrated that the steric interactions of 5-*tert*-butylproline can induce the formation of type VI  $\beta$ -turn conformations. Although 5-alkylprolines and their related 4-aza- and 4-oxaproline analogues have previously been employed for augmenting the prolyl amide *cis*-isomer population in peptide structures,<sup>24,47,48</sup> prior to our examination, the influence of the 5-alkyl substituent on the prolyl peptide turn conformation had not been reported.

We synthesized *N*-(acetyl)dipeptide *N*-methylamides **1** and **2** possessing respectively (2*S*, 5*R*)-5-*tert*-butylproline and L-proline at the *C*-terminal residue. Conformational analysis of dipeptides **1** and **2** by NMR spectroscopy showed that the Xaa-Pro peptide bond adopted preferably the *cis*-amide isomer in 5-*tert*-butylprolyl peptides **1** in contrast to prolyl dipeptides **2** which preferred the *trans*-amide isomer in solution. The limited influence of solvent composition and temperature on the chemical shift value of the *N*-methylamide in the *cis*-amide conformer of dipeptide **1** indicated that it was engaged in an intramolecular hydrogen bond with the acetamide carbonyl in a type VIa  $\beta$ -turn conformation. The presence of significant type VI  $\beta$ -turn populations for *tert*-butylprolyl peptides **1b-f** in solution was also supported by the reduced value for the vicinal coupling constant between the  $\alpha$ - and amide protons

of the *N*-terminal amino acid residue in the major *cis*-amide conformer. Furthermore, in the solid state, *N*-acetyl-L-leucyl-5-*tert*-butylproline *N*<sup>o</sup>-methylamide (**1d**) existed in a type VIa  $\beta$ -turn geometry as shown by X-ray diffraction. Finally, because they exhibited circular dichroism spectra characteristic of  $\beta$ -turn conformation in both water and acetonitrile, *tert*-butylprolyl peptides **1b** and **1d** were shown to adopt type VIa  $\beta$ -turn geometry independent of solvent composition.

Steric interactions between the bulky 5-position substituent and the *N*-terminal residue contorted the (2*S*, 5*R*)-5-*tert*-butylprolyl amide away from the planar sp<sup>2</sup> hybridized geometry as illustrated by spectroscopic and crystallographic analysis. In the <sup>13</sup>C NMR spectrum of *N*-acetyl-L-alanyl-5-*tert*-butylproline *N*<sup>o</sup>-methylamide **1b**, the carbonyl carbon signal of the *N*-terminal residue was downfield shifted 3.1 ppm relative to the amide carbon resonance of its prolyl dipeptide counterpart **2b** in water. The *tert*-butylprolyl peptide bond exhibited a 17°  $\omega$ -dihedral angle and an extended N–C(O) bond length in the X-ray structure of dipeptide **1d**. Contortion from planarity is the primary force diminishing the barrier for 5-*tert*-butylprolyl amide isomerization. For example, amide isomerization *N*-terminal to (2*S*, 5*R*)-*N*-acetyl-5-*tert*-butylproline *N*<sup>o</sup>-methylamide was reduced by 3.7 kcal/mol compared to the barrier for *N*-(acetyl)proline *N*<sup>o</sup>-methylamide in water.<sup>24</sup> However, the 5-*tert*-butyl substituent influences the prolyl carboxylate to adopt a  $\psi$ -dihedral angle around  $\psi \approx 0^\circ$ , which may also lead to a lower barrier for amide isomerization by enabling stabilization of the pyramidalized transition state via interactions between the *C*-terminal amide NH with the nitrogen lone pair of the rotating *N*-terminal amide.<sup>12,36</sup>

In conclusion, we have developed a novel approach for mimicking type VIa  $\beta$ -turns that features the employment of (2*S*, 5*R*)-5-*tert*-butylproline to constrain the conformational liberty of *N*-(acetyl)dipeptide *N*<sup>o</sup>-methylamides **1**. An ensemble of spectroscopic and crystallographic data verified the presence of the type VIa  $\beta$ -turn geometry in both solution and the solid state. Because (2*S*, 5*R*)-5-*tert*-butylproline can now be conveniently introduced into peptide structures, we are presently

generating type VIa  $\beta$ -turn libraries in order to explore the importance of this structure in peptide chemistry and biology.<sup>26</sup>

### **2.11. Experimental Section**

**General.** Unless otherwise noted, all reactions were run under a nitrogen atmosphere and distilled solvents were transferred by syringe. THF was distilled from sodium/benzophenone, CH<sub>2</sub>Cl<sub>2</sub> was distilled over P<sub>2</sub>O<sub>5</sub>, CH<sub>3</sub>CN was distilled over CaH<sub>2</sub>, DIEA was distilled over ninhydrin and CaH<sub>2</sub>. Final reaction mixture solutions were dried over Na<sub>2</sub>SO<sub>4</sub>. Chromatography was on 230-400 mesh silica gel, and TLC was on aluminum-backed silica plates. Melting points are uncorrected. Mass spectral data, HRMS (EI and FAB), were obtained by the Université de Montréal Mass Spectroscopy facility.

**NMR Measurements.** <sup>1</sup>H and <sup>13</sup>C NMR experiments were performed on Bruker DMX600 and ARX400 spectrometers. The chemical shifts are reported in ppm ( $\delta$  units) downfield of the internal tetramethylsilane ((CH<sub>3</sub>)<sub>4</sub>Si). Coupling constants are in Hz. The chemical shifts for the carbons and the protons of the minor isomers are respectively reported in parentheses and in brackets. COSY, NOESY and ROESY spectra were obtained with 2048 by 512 data points. A mixing time of 500 ms was used for the NOESY and ROESY spectra. The temperature coefficients of the amide proton chemical shifts in DMSO-*d*<sub>6</sub> were measured for at least five different temperatures in 5 deg steps by varying the temperature between 298-328 K. The value of the temperature coefficient was obtained by a linear least-squares fit of the data.

**Circular Dichroism Measurements.** CD spectra of 0.1 mM solutions in H<sub>2</sub>O and CH<sub>3</sub>CN were measured on a Jasco J-710 spectropolarimeter using a circular quartz cell with a path length of 1 mm at 23°C. Spectra were run with a band width of 1 nm, a response time of 0.25 s and a scan speed of 100 nm min<sup>-1</sup>. Each measurement was

the average result of ten repeated scans in steps of 0.2 nm. Baseline spectra of the solvents were subtracted.

**(2S, 5R)-N-(BOC)-5-*tert*-butylproline allyl ester (4).** A solution of (2*S*, 5*R*)-*N*-(BOC)-5-*tert*-butylproline (0.71 g, 2.62 mmol, prepared according to reference 25) in CH<sub>2</sub>Cl<sub>2</sub> (26 mL) was treated with DIEA (1.0 mL, 5.76 mmol) and allylbromide (2.3 mL, 26.2 mmol), heated to a reflux, stirred for 18 h, cooled to rt, and evaporated. The residue was dissolved in EtOAc (50 mL) and the solution was washed with cold 0.1 M HCl (2 × 10 mL) and a phosphate buffer solution at pH 9.5 (15 mL), dried, and evaporated to give **4** (0.28 g, 98%) as an oil: [α]<sup>20</sup><sub>D</sub> -29.7° (c 0.5, CHCl<sub>3</sub>); <sup>1</sup>H NMR (CDCl<sub>3</sub>) δ 0.88 (s, 9 H), 1.35 (s, 9 H), 1.85 (m, 3 H), 2.17 (m, 1 H), 3.76 (m, 1 H), 4.24 (m, 1 H), 4.55 (m, 2 H), 5.30 (m, 2 H), 5.86 (m, 1 H); <sup>13</sup>C NMR (CDCl<sub>3</sub>) δ 26.4, 27.2, 28.0, 29.5, 36.2, 61.4, 65.1, 66.5, 79.7, 118.2, 131.8, 155.8, 172.8; HRMS calcd for C<sub>17</sub>H<sub>30</sub>O<sub>4</sub>N (MH<sup>+</sup>) 312.2175, found 312.2193.

**(2S, 5R)-5-*tert*-Butylproline allyl ester hydrochloride.** A solution of (2*S*, 5*R*)-*N*-(BOC)-5-*tert*-butylproline allyl ester (**4**, 1.91 g, 6.14 mmol) in CH<sub>2</sub>Cl<sub>2</sub> (60 mL) was saturated with HCl (g) bubbles at 0°C, stirred for 2 h at rt and evaporated to provide (2*S*, 5*R*)-5-*tert*-butylproline allyl ester hydrochloride in 99% (1.51 g) yield as a white precipitate: [α]<sup>20</sup><sub>D</sub> -24.6° (c 0.7, CHCl<sub>3</sub>); <sup>1</sup>H NMR (CD<sub>3</sub>OD) δ 1.12 (s, 9 H), 1.79 (m, 1 H), 2.13 (m, 1 H), 2.3-2.4 (m, 2 H), 3.55 (dd, 1 H, *J* = 6.3, 12.0), 4.58 (dd, 1 H, *J* = 3.8, 9.2), 4.77 (m, 2 H), 5.33 (m, 2 H), 6.00 (m, 1 H); <sup>13</sup>C NMR (CD<sub>3</sub>OD) δ 25.7, 26.7, 29.5, 33.1, 60.6, 68.4, 72.9, 120.0, 132.5, 170.1; HRMS calcd for C<sub>12</sub>H<sub>22</sub>O<sub>2</sub>N (MH<sup>+</sup>) 212.1651, found 212.1656. Anal. Calcd. for C<sub>12</sub>H<sub>22</sub>O<sub>2</sub>NCl: C, 58.17; H, 8.95; N, 5.65. Found: C, 58.20, H, 9.34, N, 5.65. (2*S*, 5*R*)-5-*tert*-Butylproline allyl ester trifluoroacetate was prepared by stirring a solution of allyl ester **4** (0.84 g, 2.70 mmol) in 1:3 TFA:CH<sub>2</sub>Cl<sub>2</sub> at rt for 2 h to give an oil (0.86 g, 98%) after evaporation of the volatiles: <sup>1</sup>H NMR (CDCl<sub>3</sub>) δ 1.08 (s, 9 H), 1.65 (m, 1

H), 2.04 (m, 1 H), 2.33 (m, 1 H), 2.50 (m, 1 H), 3.65 (m, 1 H), 4.59 (dd, 1 H, *J* = 2.1, 9.9 ), 4.74 (m, 2 H), 5.36 (m, 2 H), 5.91 (m, 1 H).

**General Procedure for Peptide Coupling to 5-*tert*-Butylproline Residues.** A solution of (2*S*, 5*R*)-5-*tert*-butylproline allyl ester hydrochloride (355 mg, 1.43 mmol), *N*-(BOC)amino acid (1.72 mmol) and DIEA (1.0 mL, 5.72 mmol) in CH<sub>2</sub>Cl<sub>2</sub> (14 mL) was cooled to 0°C, treated with BOP-Cl (430 mg, 1.72 mmol), stirred for 1 h and let warm to rt with stirring for 18 h. Brine (5 mL) was added to the reaction solution which was extracted with CH<sub>2</sub>Cl<sub>2</sub> (2 × 10 mL). The combined organic layers were washed with 0.1 M HCl (2 × 5 mL), 5% NaHCO<sub>3</sub> (2 × 5 mL) and brine (10 mL), dried and evaporated to a residue that was purified by chromatography on silica gel using 35% EtOAc in hexane as eluant. Evaporation of the collected fractions afforded *N*-(BOC)dipeptide allyl ester **5**. The same protocol was used to couple *N*-(BOC)amino acids and (2*S*, 5*R*)-5-*tert*-butylproline *N*-methylamide trifluoroacetate to provide *N*-(BOC)dipeptide *N*-methylamides **7**.

***N*-(BOC)-L-alanyl-(2*S*, 5*R*)-5-*tert*-butylproline allyl ester (5b)** was obtained in 68% yield as an oil; [α]<sup>20</sup><sub>D</sub> -92.4° (c 0.85, CHCl<sub>3</sub>); <sup>1</sup>H NMR (CDCl<sub>3</sub>) δ [0.83 (s, 3.7 H)] 0.93 (s, 5.3 H), [1.17 (d, 1.2 H, *J* = 6.4)] 1.26 (d, 1.8 H, *J* = 6.5), 1.33 (s, 5.3 H) [1.35 (s, 3.7 H)], 1.75-1.98 (m, 3 H), 2.25 (m, 1 H), 4.12 (d, 1 H, *J* = 7.9), 4.31 (m, 1 H), 4.55-4.65 (m, 3 H), 4.95 (d, 1 H, *J* = 8.8), 5.27 (m, 2 H), 5.83 (m, 1 H); <sup>13</sup>C NMR (CDCl<sub>3</sub>) δ 18.1 (19.0), 25.6, (27.3) 27.5, 28.0 (28.1), 28.8, 35.7 (36.0), 46.5 (47.9), (59.8) 60.4, 65.1 (66.3), 66.6, (79.0) 79.4, 117.9 (118.9), (131.3) 131.8, (154.3) 154.9, (171.2) 171.5, (173.7) 174.8; HRMS calcd for C<sub>20</sub>H<sub>35</sub>O<sub>5</sub>N<sub>2</sub> (MH<sup>+</sup>) 383.2546, found 383.2560.

***N*-(BOC)-L-leucyl-(2*S*, 5*R*)-5-*tert*-butylproline allyl ester (5d)** was obtained in 82% yield as an oil; [α]<sup>20</sup><sub>D</sub> -91.8° (c 1, CHCl<sub>3</sub>); <sup>1</sup>H NMR (CDCl<sub>3</sub>) δ 0.89-1.01 (s, 15 H), 1.41 (m, 10 H), 1.70-1.93 (m, 3 H), 2.04 (m, 1 H), 2.30-2.35 (m, 2 H), 4.19 (d, 1 H, *J* = 8.6), 4.38 (m, 1 H), 4.63-4.74 (m, 4 H), 5.21-5.35 (m, 2 H), 5.92 (m, 1 H); <sup>13</sup>C

NMR ( $\text{CDCl}_3$ )  $\delta$  21.5 (21.7), (25.8) 27.3, 27.4 (29.1), (23.4) 27.6, (24.2) 28.0, (24.3) 28.1, 35.6 (36.1), 40.5 (43.3), 49.4 (50.4), (59.9) 60.4, (66.4) 65.2, 66.5 (66.6), (78.8) 79.3, 118.0 (118.9), (131.5) 131.8, (154.7) 155.2, (171.3) 171.5, (173.9) 174.6; HRMS calcd for  $\text{C}_{23}\text{H}_{41}\text{O}_5\text{N}_2$  ( $\text{MH}^+$ ) 425.3015, found 425.3023.

***N-(BOC)-L-valyl-(2S, 5R)-5-tert-butylproline allyl ester (5e)*** was obtained in 43% yield as an oil;  $[\alpha]^{20}_{\text{D}} -72.5^\circ$  (c 0.88,  $\text{CHCl}_3$ );  $^1\text{H}$  NMR ( $\text{CDCl}_3$ )  $\delta$  0.89-1.01 (m, 15 H), 1.41 (s, 9 H), 1.75-2.32 (m, 5 H), 4.20 (m, 1 H), 4.42 (m, 1 H), 4.55-4.75 (m, 3 H), 5.33 (m, 2 H), 5.89 (m, 1 H);  $^{13}\text{C}$  NMR ( $\text{CDCl}_3$ )  $\delta$  17.5 (17.9), 19.4 (19.8), 26.0 (28.9), 27.4 (27.5), (27.7) 28.1, 28.2, (31.1) 32.5, (35.6) 36.2, 56.5 (56.6), 60.0 (60.1), (65.4) 66.4, (66.2) 66.5, 78.9 (79.6), 118.3 (118.9), (131.6) 131.8, 155.0 (155.3), 171.4 (171.7), 173.2 (173.7); HRMS calcd for  $\text{C}_{22}\text{H}_{39}\text{O}_5\text{N}_2$  ( $\text{MH}^+$ ) 411.2859, found 411.2852.

***N-(BOC)-L-phenylalanyl-(2S, 5R)-5-tert-butylproline allyl ester (5f)*** was obtained in 94% yield as a white solid: mp 118-119°C;  $[\alpha]^{20}_{\text{D}} -67.4^\circ$  (c 0.84,  $\text{CHCl}_3$ );  $^1\text{H}$  NMR ( $\text{CDCl}_3$ )  $\delta$  0.81 (s, 7.4 H) [0.96 (s, 1.6 H)], [1.28 (s, 1.6 H)] 1.42 (s, 7.4 H), 1.51-1.65 (m, 2 H), 1.83 (m, 1 H), 2.05 (m, 1 H), 2.83 (m, 1 H), 3.02 (m, 1 H), 3.48 (t, 1 H,  $J = 8.4$ ), 4.07 (d, 0.8 H,  $J = 8.5$ ) [4.29 (d, 0.2 H,  $J = 7.9$ )], 4.62 (m, 3 H), 4.91 (br s, 1 H), 5.29 (m, 2 H), 5.84 (m, 1 H), 7.19-7.27 (m, 5 H);  $^{13}\text{C}$  NMR ( $\text{CDCl}_3$ )  $\delta$  25.4, 27.3 (27.5), (27.4) 28.0, (28.1) 28.2, (35.6) 36.0, (38.3) 41.0, (52.0) 53.7, 59.5 (60.5), (65.3) 66.2, 66.6, 79.2 (79.5), (118.1) 118.8, (126.4) 126.9, (128.2) 128.6, 129.3, 131.4 (131.8), 136.4 (136.9), 154.4 (154.9), 171.4 (171.5), 172.8 (173.7); HRMS calcd for  $\text{C}_{26}\text{H}_{39}\text{O}_5\text{N}_2$  ( $\text{MH}^+$ ) 459.2859, found 459.2872.

***N-(BOC)-glycyl-(2S, 5R)-5-tert-butylproline N'-methylamide (7a)*** was obtained in 87% yield as a white solid: mp 63-66°C;  $[\alpha]^{20}_{\text{D}} -113.7^\circ$  (c 0.86,  $\text{CHCl}_3$ );  $^1\text{H}$  NMR ( $\text{CDCl}_3$ )  $\delta$  0.92 (s, 9 H), 1.45 (s, 9 H), 1.85 (m, 2 H), 2.04 (m, 0.7 H) [2.20 (m, 0.3)], [2.35 (m, 0.3 H)] 2.63 (m, 0.7 H), 2.80 (m, 3 H), 3.71 (d, 0.7 H,  $J = 8.1$ ) [3.85 (m, 0.3

H)], 4.11 (m, 1 H), [4.30 (m, 0.3 H)] 4.68 (t, 0.7 H,  $J = 8.5$ ), 5.40 (br s, 1 H), [6.81 (br s, 0.3 H)] 7.24 (br s, 0.7 H);  $^{13}\text{C}$  NMR ( $\text{CDCl}_3$ )  $\delta$  24.7 (25.6), 26.1, 26.5, 27.4, 28.1, 35.6 (35.9), (42.9) 43.3, 61.7, (67.2) 67.6, 79.6, 155.6, (171.4) 171.7, 172.2; HRMS calcd for  $\text{C}_{17}\text{H}_{32}\text{O}_4\text{N}_3$  ( $\text{MH}^+$ ) 342.2393, found 342.2399.

**N-(BOC)-L-alanyl-(2S, 5R)-5-tert-butylproline N'-methylamide (7b)** was obtained in 75% yield as a white solid: mp 100-101 °C;  $[\alpha]^{20}\text{D} -81.5^\circ$  (c 0.6,  $\text{CHCl}_3$ );  $^1\text{H}$  NMR ( $\text{CDCl}_3$ )  $\delta$  0.81 (s, 7.6 H) [0.84 (s, 1.4 H)], 1.16 (d, 2.6 H,  $J = 6.8$ ) [1.27 (d, 0.4 H,  $J = 6.6$ )], 1.34 (s, 9 H), 1.75 (m, 2 H), 2.15 (m, 1 H), 2.33 (m, 1 H), [2.72 (d, 0.4 H,  $J = 6.5$ )] 2.75 (d, 2.6 H,  $J = 4.6$ ), 4.07 (m, 1 H), 4.22 (m, 2 H), 5.29 (d, 1 H,  $J = 3.8$ ), 8.32 (br s, 1 H);  $^{13}\text{C}$  NMR ( $\text{CDCl}_3$ )  $\delta$  16.2 (18.2), (24.9) 25.2, 26.2, 27.4, 28.0, (26.3) 29.1, (35.1) 35.6, (46.6) 48.9, (61.5) 61.9, 67.0 (67.5), (79.7) 80.3, 156.4, 171.7, 175.6; HRMS calcd for  $\text{C}_{18}\text{H}_{34}\text{O}_4\text{N}_3$  ( $\text{MH}^+$ ) 356.2549, found 356.2556.

**N-(BOC)-L-methionyl-(2S, 5R)-5-tert-butylproline N'-methylamide (7c)** was obtained in 64% yield as a white solid: mp 102-103°C;  $[\alpha]^{20}\text{D} -88.4^\circ$  (c 0.9,  $\text{CHCl}_3$ );  $^1\text{H}$  NMR ( $\text{CDCl}_3$ )  $\delta$  0.86 (s, 6.4 H) [0.93 (s, 2.6 H)], 1.42 (s, 9 H), 1.83 (m, 3 H). 2.01-2.09 (m, 5 H), 2.56 (m, 3 H), [2.78 (d, 0.9 H,  $J = 4.7$ )] 2.83 (d, 2.1 H,  $J = 4.4$ ), 4.28 (m, 2 H), 4.44 (m, 1 H), 5.12 (d, 1 H,  $J = 7.8$ ), 8.29 (br s, 1 H);  $^{13}\text{C}$  NMR ( $\text{CDCl}_3$ )  $\delta$  (14.0) 15.6, (25.1) 25.2, 26.1 (26.2), (26.3) 27.1, (27.4) 28.0, 28.7, 30.3, 30.7, (35.1) 35.6, (50.5) 52.5, (61.5) 61.8, 67.0 (67.5), (80.0) 80.6, (155.1) 157.0, 171.3 (171.9), 174.6 (175.2); HRMS calcd for  $\text{C}_{20}\text{H}_{38}\text{O}_4\text{N}_3\text{S}$  ( $\text{MH}^+$ ) 416.2583, found 416.2593.

**N-(BOC)-L-valyl-(2S, 5R)-5-tert-butylproline N'-methylamide (7e)** was obtained in 35% yield as a white solid: mp 56-58°C;  $[\alpha]^{20}\text{D} -80.8^\circ$  (c 0.57,  $\text{CHCl}_3$ );  $^1\text{H}$  NMR ( $\text{CDCl}_3$ )  $\delta$  0.86 (m 9 H), 0.96 (d, 3 H,  $J = 6.9$ ), 1.03 (d, 3 H,  $J = 6.7$ ), 1.43 (s, 9 H), 1.61 (m, 1 H), 1.84 (m, 3 H), 2.57 (m, 1 H), 2.81 (d, 3 H,  $J = 4.6$ ), 3.95 (t, 1 H,  $J = 8.0$ ), 4.32 (t, 1 H,  $J = 7.3$ ), 4.46 (dd, 1 H,  $J = 3.5, 8.1$ ), 4.99 (d, 1 H,  $J = 8.5$ ), 8.48

(br s, 1 H);  $^{13}\text{C}$  NMR ( $\text{CDCl}_3$ )  $\delta$  (17.9) 18.3, 19.5 (20.0), (24.9) 25.2, 26.0, (26.2) 27.1, (27.6) 28.0, 28.1, 30.5 (31.1), (35.0) 35.6, (56.9) 58.6, (61.3) 61.7, 66.7 (66.9), (79.8) 80.4, 156.9, 171.1 (172.0), 175.0; HRMS calcd for  $\text{C}_{20}\text{H}_{38}\text{O}_4\text{N}_3$  ( $\text{MH}^+$ ) 384.2862, found 384.2872.

**General Procedure for Allyl Ester Removal.** A solution of allyl ester **5** (1.0 g, 2.18 mmol) in THF (22 mL) was treated with morpholine (1.9 mL, 21.8 mmol) and  $\text{Pd}(\text{PPh}_3)_4$  (25 mg, 0.2 mmol), stirred for 3 h at rt and evaporated. The residue was dissolved in  $\text{CH}_2\text{Cl}_2$  (40 mL), washed with 0.1 M HCl ( $2 \times 15$  mL) and brine ( $2 \times 15$  mL), dried and evaporated to a residue that was purified by chromatography on silica gel using 5% MeOH in  $\text{CHCl}_3$  as eluant. Evaporation of the collected fractions afforded *N*-(BOC)dipeptide **6**.

***N*-(BOC)-L-leucyl-(2*S*, 5*R*)-5-*tert*-butylproline (6d)** was isolated in 79% yield as a white solid: mp 152-153°C;  $[\alpha]^{20}\text{D} -170.4^\circ$  (c 0.6,  $\text{CHCl}_3$ );  $^1\text{H}$  NMR ( $\text{CDCl}_3$ )  $\delta$  0.86-0.91 (m, 15 H), 1.36 (s, 9 H), 1.42 (m, 1 H), 1.66-1.86 (m, 3 H), 2.01 (m, 1 H), 2.34 (m, 2 H), [4.19 (m, 0.3 H)] 4.44 (m, 1.2 H), 4.62 (m, 1 H), 5.21 (d, 0.6 H,  $J = 9.5$ ) [5.68 (d, 0.4 H,  $J = 8.9$ )];  $^{13}\text{C}$  NMR ( $\text{CDCl}_3$ )  $\delta$  21.4 (21.6), 23.4, 24.1 (24.3), (25.6) 26.0, 26.5 (29.0), (27.3) 27.5, 28.1, 35.3 (35.9), 40.1 (41.9), 49.5 (51.1), (60.2) 61.4, (66.9) 67.4, 79.6 (80.0), 155.3 (156.0), 172.8 (173.0), (174.5) 176.8; HRMS calcd for  $\text{C}_{20}\text{H}_{37}\text{O}_5\text{N}_2$  ( $\text{MH}^+$ ) 385.2702, found 385.2710.

***N*-(BOC)-L-phenylalanyl-(2*S*, 5*R*)-5-*tert*-butylproline (6f)** was isolated in 64% yield as a white solid: mp 149-151°C;  $[\alpha]^{20}\text{D} -66.7^\circ$  (c 0.88,  $\text{CHCl}_3$ );  $^1\text{H}$  NMR ( $\text{CDCl}_3$ )  $\delta$  0.90 (s, 6.3 H) [1.03 (s, 2.7 H)], [1.29 (s, 2.7 H)] 1.39 (s, 6.3 H), 1.48 (m, 1 H), 1.76-1.96 (m, 3 H), 2.87 (m, 2 H), 3.75 (t, 1 H,  $J = 8.7$ ), 4.06 (d, 1 H,  $J = 8.5$ ), 4.35 (d, 1 H,  $J = 7.5$ ), 5.60 (m, 1 H), 7.24 (m, 5 H);  $^{13}\text{C}$  NMR ( $\text{CDCl}_3$ )  $\delta$  26.7 (28.0), 28.3, (28.6) 28.8, (28.5) 30.2, (36.7) 37.2, (38.7) 41.0, (54.2) 55.3, 62.8 (63.8), 68.0

(68.3), (80.4) 80.9, (127.5) 128.0, (129.3) 129.7, (130.5) 130.6, 138.0 (138.9), 157.1 (157.4), 174.5 (176.0), 179.5.

**General Procedure for Amidation of the Dipeptides.** A solution of *N*-(BOC)dipeptide **6** (104 mg, 0.26 mmol) in CH<sub>3</sub>CN (2.6 mL) was treated with DIEA (181  $\mu$ L, 1.0 mmol), methylamine hydrochloride (21 mg, 0.31 mmol) and TBTU (100 mg, 0.31 mmol), stirred at rt for 18 h, and partitioned between brine (2 mL) and EtOAc (10 mL). The organic phase was washed with 0.1 M HCl (2  $\times$  3 mL), 5% NaHCO<sub>3</sub> (2  $\times$  3 mL), and brine (4 mL), dried and evaporated to yield the *N*-(BOC)dipeptide methylamide **7**.

***N*-(BOC)-L-leucyl-(2*S*, 5*R*)-5-*tert*-butylproline *N*<sup>t</sup>-methylamide (7d)** was isolated in 97% yield as a white solid: mp 152-153°C;  $[\alpha]^{20}_D$  -95.9° (c 0.75, CHCl<sub>3</sub>); <sup>1</sup>H NMR (CDCl<sub>3</sub>)  $\delta$  0.87-0.94 (m, 15 H), 1.25 (m, 1 H), 1.42 (s, 9 H), 1.72-1.84 (m, 4 H), 2.17 (m, 1 H), 2.44 (m, 1 H), [2.78 (d, 0.5 H, *J* = 4.7) 2.83 (d, 2.5 H, *J* = 4.6), 4.12 (m, 1 H), 4.28 (m, 2 H), 4.92 (d, 1 H, *J* = 7.7), 8.32 (br s, 1 H); <sup>13</sup>C NMR (CDCl<sub>3</sub>)  $\delta$  21.3 (21.5), 23.4 (23.5), (24.3) 24.5, (24.8) 25.2, 26.1 (26.2), 27.2 (27.5), 28.0, 29.0 (29.6), (35.0) 35.7, 40.0 (41.0), (49.5) 51.9, (61.5) 61.7, 67.0 (67.5), (79.8) 80.4, (155.1) 157.1, 171.5 (172.0), 175.2 (176.2); HRMS calcd for C<sub>21</sub>H<sub>40</sub>O<sub>4</sub>N<sub>3</sub> (MH<sup>+</sup>) 398.3019, found 398.3031.

***N*-(BOC)-L-phenylalanyl-(2*S*, 5*R*)-5-*tert*-butylproline *N*<sup>t</sup>-methylamide (7f)** was isolated in 49% yield as a white solid: mp 51-52°C;  $[\alpha]^{20}_D$  -28.6° (c 0.5, CHCl<sub>3</sub>); <sup>1</sup>H NMR (CDCl<sub>3</sub>)  $\delta$  0.82 (s, 9 H), 1.15 (m, 1 H), [1.36 (s, 1.4 H)] 1.43 (s, 7.6 H), 1.59 (m, 2 H), 2.08 (m, 1 H), 2.76 (d, 3 H, *J* = 4.6), 2.92 (m, 2 H), 3.57 (dd, 1 H, *J* = 4.4, 8.9), 4.25 (dd, 1 H, *J* = 5.2, 8.6), 4.37 (m, 1 H), 5.12 (d, 1 H, *J* = 7.0), 7.17-7.33 (m, 5 H), 8.38 (br s, 1 H); <sup>13</sup>C NMR (CDCl<sub>3</sub>)  $\delta$  25.0, 25.9, 27.1, 27.9, 28.0, 35.6, 38.4, 54.5, 61.6, 66.9, 80.7, 127.5, 129.0, 129.3, 135.2, 156.2, 171.3, 174.6; HRMS calcd for C<sub>24</sub>H<sub>38</sub>O<sub>4</sub>N<sub>3</sub> (MH<sup>+</sup>) 432.2862, found 432.2871.

**General Procedure for Acetamide Synthesis.** A solution of *N*-(BOC)dipeptide *N*<sup>t</sup>-methylamide **7** (62 mg, 0.16 mmol) in 1:3 TFA:CH<sub>2</sub>Cl<sub>2</sub> (1.6 mL) was stirred at rt for 2 h, and evaporated on a rotary evaporator. The resulting dipeptide *N*<sup>t</sup>-methylamide trifluoroacetate was dissolved in CH<sub>2</sub>Cl<sub>2</sub> (1.6 mL), treated with K<sub>2</sub>CO<sub>3</sub> (0.22 mg, 1.6 mmol) and Ac<sub>2</sub>O (148 μL, 1.6 mmol), stirred for 18 h, filtered, washed with CH<sub>2</sub>Cl<sub>2</sub> (3 × 3 mL) and evaporated to give the *N*-acetyl-dipeptide *N*<sup>t</sup>-methylamide **1**.

***N*-Acetyl-glycyl-(2*S*, 5*R*)-5-*tert*-butylproline *N*<sup>t</sup>-methylamide (1a)** was isolated in 93% yield as a white solid: mp 71–73°C; [α]<sup>20</sup><sub>D</sub> –99.5° (c 0.46, CHCl<sub>3</sub>); mixture of 1:1 rotamers <sup>1</sup>H NMR (CDCl<sub>3</sub>) δ 0.93 (s, 9 H), 1.27 (m, 1 H), 1.64 (m, 2 H), 1.85 (m, 1 H), 2.05 (s, 3 H), 2.82 (m, 3 H), 3.74 (d, 1 H, *J* = 9.5), 4.20 (m, 2 H), 4.66 (m, 1 H), 6.43 (br s, 1 H), 7.14 (br s, 1 H); <sup>13</sup>C NMR (CDCl<sub>3</sub>) δ 13.9, 22.5, 22.7, 25.0, 25.7, 26.2, 26.5, 27.4, 29.5, 30.2, 31.4, 35.6, 36.0, 42.2, 42.4, 61.7, 61.9, 67.4, 67.7, 170.2, 170.9, 171.1, 171.7, 171.9; HRMS calcd for C<sub>14</sub>H<sub>26</sub>O<sub>3</sub>N<sub>3</sub> (MH<sup>+</sup>) 284.1974, found 284.1968.

***N*-Acetyl-L-alanyl-(2*S*, 5*R*)-5-*tert*-butylproline *N*<sup>t</sup>-methylamide (1b)** was isolated in 97% yield as a white solid: mp 119–121°C; [α]<sup>20</sup><sub>D</sub> –60.3° (c 0.36, CHCl<sub>3</sub>); <sup>1</sup>H NMR (CDCl<sub>3</sub>) δ 0.89 (s, 7.5 H) [0.93 (s, 1.5 H)], 1.31 (d, 2.5 H, *J* = 6.9) [1.39 (d, 0.5 H, *J* = 6.6)], 1.85 (m, 2 H), [1.97 (s, 0.5 H)] 2.01 (s, 2.5 H), 2.22 (m, 1 H), 2.45 (m, 1 H), [2.80 (d, 0.5 H, *J* = 4.7)] 2.86 (d, 2.5 H, *J* = 4.6), 4.32 (m, 3 H), 6.54 (d, 1 H, *J* = 6.1), 8.35 (br s, 1 H); <sup>13</sup>C NMR (CDCl<sub>3</sub>) δ (15.8) 16.0, 22.1 (22.6), (24.5) 25.2, 26.2 (26.4), 27.3 (27.5), 28.9, 35.6, 48.5, (61.6) 62.0, 67.4 (68.0), (169.8) 171.5, 171.7 (171.9), 175.4 (176.3); HRMS calcd for C<sub>15</sub>H<sub>28</sub>O<sub>3</sub>N<sub>3</sub> (MH<sup>+</sup>) 298.2131, found 298.2120.

***N*-Acetyl-L-methionyl-(2*S*, 5*R*)-5-*tert*-butylproline *N*<sup>t</sup>-methylamide (1c)** was isolated in 99% yield as a white solid: mp 53–56°C; [α]<sup>20</sup><sub>D</sub> –71.7° (c 0.4, CHCl<sub>3</sub>);

<sup>1</sup>H NMR (CDCl<sub>3</sub>) δ 0.85 (s, 6.6 H) [0.93 (s, 2.4 H)], 1.82 (m, 2 H), 1.96 (m, 4 H), 2.07 (s, 5 H), 2.53 (m, 3 H), [2.76 (d, 0.8 H, *J* = 4.6)] 2.83 (d, 2.2 H, *J* = 4.6), 4.23 (dd, 1 H, *J* = 5.3, 8.2), 4.48 (m, 2 H), 7.72 (d, 1 H, *J* = 6.2), 8.41 (br s, 1 H); <sup>13</sup>C NMR (CDCl<sub>3</sub>) δ (15.5) 15.6, 22.2 (22.5), 25.1 (25.5), (26.2) 26.3, 27.2, (27.4) 28.4, 30.3, 30.5, (35.1) 35.5, (49.7) 52.1, (61.6) 61.7, 67.4 (67.8), (170.1) 171.0, (171.8) 172.2, 174.5 (175.2); HRMS calcd for C<sub>17</sub>H<sub>32</sub>O<sub>3</sub>N<sub>3</sub> (MH<sup>+</sup>) 358.2131, found 358.2152.

***N*-Acetyl-L-leucyl-(2*S*, 5*R*)-5-*tert*-butylproline *N*'-methylamide (1d)** was isolated in 98% yield as a white solid: mp 172-173°C; [α]<sup>20</sup>D -88.2° (c 0.3, CHCl<sub>3</sub>); <sup>1</sup>H NMR (CDCl<sub>3</sub>) δ 0.88 (s, 7.7 H) [0.91 (s, 1.3 H)], 0.92 (d, 3 H, *J* = 4.0), 0.97 (d, 3 H, *J* = 6.6), 1.29 (m, 1 H), 1.58-1.72 (m, 3 H), 1.85 (m, 1 H), [1.98 (s, 0.4 H)] 2.04 (s, 2.6 H), 2.17 (m, 1 H), 2.48 (m, 1 H), [2.79 (d, 0.4 H, *J* = 4.6)] 2.87 (d, 2.6 H, *J* = 4.6), 4.29 (m, 3 H), 5.96 (d, 1 H, *J* = 6.9), 8.26 (br s, 1 H); <sup>13</sup>C NMR (CDCl<sub>3</sub>) δ 21.2 (21.4), 22.4 (22.7), 23.3 (23.5), (24.4) 24.8, 25.2, 26.3 (26.4), 27.3 (27.6), 28.7, (35.0) 35.6, 39.5 (40.7), (48.6) 51.5, (61.5) 61.8, 67.3 (67.9), 171.2, (171.8) 172.0, 174.8; HRMS calcd for C<sub>18</sub>H<sub>34</sub>O<sub>3</sub>N<sub>3</sub> (MH<sup>+</sup>) 340.2600, found 340.2611.

***N*-Acetyl-L-valyl-(2*S*, 5*R*)-5-*tert*-butylproline *N*'-methylamide (1e)** was isolated in 97% yield as a white solid: mp 166-167°C; [α]<sup>20</sup>D -93.8° (c 0.3, CHCl<sub>3</sub>); <sup>1</sup>H NMR (CDCl<sub>3</sub>) δ 0.86 (s, 8 H), 0.97 (m, 4 H), 1.05 (d, 3 H, *J* = 6.7), 1.81-2.06 (m, 7 H), 2.59 (m, 1 H), [2.80 (d, 0.3 H, *J* = 4.6)] 2.84 (d, 2.7 H, *J* = 4.6), 4.18 (t, 1 H, *J* = 7.5), 4.30 (t, 1 H, *J* = 7.3), 4.50 (m, 1 H), 6.18 (d, 1 H, *J* = 6.2), 8.48 (br s, 1 H); <sup>13</sup>C NMR (CDCl<sub>3</sub>) δ (18.0) 18.7, 19.3 (19.9), 22.6, (25.0) 25.2, 26.2 (26.5), 27.2, 27.9, 30.5, (35.0) 35.5, (55.6) 58.1, (61.3) 61.8, 67.0 (67.2), (169.2) 170.9, 171.5 (171.8), 174.3 (175.1); HRMS calcd for C<sub>17</sub>H<sub>32</sub>O<sub>3</sub>N<sub>3</sub> (MH<sup>+</sup>) 326.2444, found 326.2455.

***N*-Acetyl-L-phenylalanyl-(2*S*, 5*R*)-5-*tert*-butylproline *N*'-methylamide (1f)** was isolated in 94% yield as a white solid: mp 81-82°C; [α]<sup>20</sup>D -32.2° (c 1, CHCl<sub>3</sub>); <sup>1</sup>H

NMR ( $\text{CDCl}_3$ )  $\delta$  0.83 (s, 9 H), 1.16 (m, 1 H), 1.51-1.67 (m, 2 H), [1.90 (s, 0.3 H)] 2.00 (s, 2.7 H), 2.13 (m, 1 H), 2.79 (d, 3 H,  $J$  = 4.6), 2.97-3.09 (m, 2 H), 3.71 (dd, 1 H,  $J$  = 4.5, 8.9), 4.25 (dd, 1 H,  $J$  = 4.9, 8.7), 4.57 (m, 1 H), 6.72 (d, 1 H,  $J$  = 5.6), 7.20-7.35 (m, 5 H), 8.37 (br s, 1 H);  $^{13}\text{C}$  NMR ( $\text{CDCl}_3$ )  $\delta$  22.6 (22.7), 24.9 (25.1), 26.2 (26.4), 27.2 (27.5), 27.8, 35.5, 38.1 (38.4), 54.0, (61.5) 61.7, 67.3 (67.9), (127.0) 127.6, (128.4) 129.1, 129.2 (129.3), 134.5, 171.2, 173.9; HRMS calcd for  $\text{C}_{21}\text{H}_{32}\text{O}_3\text{N}_3$  ( $\text{MH}^+$ ) 374.2444, found 374.2449.

***N*-Acetyl-L-alanylproline *N'*-methylamide and *N*-Acetyl-L-leucylproline *N'*-methylamide**

were synthesized in solution phase from *N*-(BOC)-L-proline *N'*-methylamide using the TBTU coupling and acetylation conditions as described above.

***N*-Acetyl-L-alanylproline *N'*-methylamide (2a):** mp 176-177°C;  $[\alpha]^{20}\text{D} -145.0^\circ$  (c 0.5,  $\text{CHCl}_3$ );  $^1\text{H}$  NMR ( $\text{CDCl}_3$ )  $\delta$  [1.31 (d, 0.6 H,  $J$  = 7.0)] 1.36 (d, 2.4 H,  $J$  = 6.9), [1.78 (m, 0.2 H)] 1.92 (m, 0.8 H), 2.00 (s, 2.4 H) [2.01 (s, 0.6 H)], 2.03 (m, 1 H), [2.09 (m, 0.2 H)] 2.14 (m, 0.8 H), 2.34 (m, 0.8 H) [2.55 (m, 0.2 H)], 2.79 (d, 2.4 H,  $J$  = 3.9) [2.85 (d, 0.7 H,  $J$  = 3.8)], 3.57 (m, 1 H), 3.68 (m, 1 H), [4.31 (m, 0.2 H,  $J$  = 8.2)] 4.53 (dd, 0.8 H,  $J$  = 2.9, 8.1), [4.25 (m, 0.2 H)] 4.76 (m, 0.8 H), 6.53 (d, 0.8 H,  $J$  = 6.3) [6.65 (br s, 0.2 H)], 6.72 (br s, 0.8 H) [7.58 (br s, 0.2 H)];  $^{13}\text{C}$  NMR ( $\text{CDCl}_3$ )  $\delta$  (16.3) 17.8, (22.3) 22.8, (21.8) 24.8, 26.0 (26.4), 27.7 (31.3), 46.5 (48.0), (46.7) 47.2, 59.8 (60.7), 169.5 (170.9), (171.1) 171.5, (172.0) 172.4; HRMS calcd for  $\text{C}_{11}\text{H}_{20}\text{O}_3\text{N}_3$  ( $\text{MH}^+$ ) 242.1505, found 242.1498.

***N*-Acetyl-L-leucylproline *N'*-methylamide (2b):** mp 90-91°C;  $[\alpha]^{20}\text{D} -130.3^\circ$  (c 1,  $\text{CHCl}_3$ );  $^1\text{H}$  NMR ( $\text{CDCl}_3$ )  $\delta$  0.94 (m, 6 H), 1.53 (m, 1 H), 1.67 (m, 1 H), 1.88 (m, 3 H), 2.00 (s, 2.4 H) [2.02 (s, 0.6 H)], 2.15 (m, 1 H), 2.35 (m, 1 H), 2.77 (d, 2.4 H,  $J$  = 4.8) [2.85 (d, 0.6 H,  $J$  = 4.7)], 3.56 (m, 1 H), 3.76 (m, 1 H), 4.50 (dd, 1 H,  $J$  = 2.7, 8.1), 4.81 (m, 1 H), 6.18 (d, 0.8 H,  $J$  = 8.4) [6.29 (d, 0.2 H,  $J$  = 6.1)], 6.72 (br s, 0.8

H) [7.52 (br s, 0.2 H)];  $^{13}\text{C}$  NMR ( $\text{CDCl}_3$ )  $\delta$  (21.1) 21.6, (22.3) 22.8, 23.2 (23.3), 24.6 (24.7), (21.8) 24.8, 26.0 (26.5), 27.4 (31.2), 39.8 (41.4), (46.7) 47.2, 49.0 (50.9), 59.6 (60.8), 170.0 (170.6), 171.5 (171.6), (172.0) 172.8; HRMS calcd for  $\text{C}_{14}\text{H}_{26}\text{O}_3\text{N}_3$  ( $\text{MH}^+$ ) 284.1974, found 284.1966.

**Acknowledgment:** This research was supported in part by the Natural Sciences and Engineering Research Council of Canada, the Ministère de l'Éducation du Québec, and the DuPont Educational Aid Program. We thank Sylvie Bilodeau and Dr. M. T. Phan Viet of the Regional High-Field NMR Laboratory for their assistance. The crystal structure analysis of compound **1d** was performed by Francine Bélanger-Gariépy at l'Université de Montréal X-ray facility.

**Supporting Information Available:**  $^1\text{H}$  and  $^{13}\text{C}$  NMR spectra of **1a-f**, **2b** and **2d**; COSY and NOESY spectra and plots of temperature versus amide N–H chemical shift for **1b** and **2b**, and crystallographic data for **1d**. This material is available free of charge via the Internet at <http://pubs.acs.org>.

## 2.12. References

1. Reviews and leading articles on  $\beta$ -turns include: (a) Wilmot, C. M.; Thornton, J. M. *J. Mol. Biol.* **1988**, *203*, 221. (b) Rose, G. D.; Giersch, L. M.; Smith, J. A. *Advan. Protein Chem.* **1985**, *37*, 1. (c) Richardson, J. S. *Advan. Protein Chem.* **1981**, *34*, 167. (d) Lewis, P. N.; Momany, F. A.; Scheraga, H. A. *Biochem. Biophys. Acta* **1973**, *303*, 211. (e) Venkatachalam, C. M. *Biopolymers* **1968**, *6*, 1425.
2. Reviewed in: (a) Hanessian, S.; McNaughton-Smith, G.; Lombart, H.-G.; Lubell, W. D. *Tetrahedron* **1997**, *53*, 12789. (b) Gillespie, P.; Cicariello, J.; Olson, G. L. *Biopolymers, Peptide Science* **1997**, *43*, 191.
3. Examples include: (a) Takeuchi, Y.; Marshall, G. R. *J. Am. Chem. Soc.* **1998**, *120*, 5363. (b) Baures, P. W.; Ojala, W. H.; Gleason, W. B.; Johnson, R. L. *J. Peptide Res.* **1997**, *50*, 1. (c) Lombart, H.-G.; Lubell, W. D. *J. Org. Chem.* **1996**, *61*, 9437. (d) Chalmers, D. K.; Marshall, G. R. *J. Am. Chem. Soc.* **1995**,

- 117, 5927. (e) Genin, M. J.; Mishra, R. K.; Johnson, R. L. *J. Med. Chem.* **1993**, *36*, 3481. (f) Hinds, M. G.; Welsh, J. H.; Brennand, D. M.; Fisher, J.; Glennie, M. J.; Richards, N. G. J.; Turner, D. L.; Robinson, J. A. *J. Med. Chem.* **1991**, *34*, 1777.
4. Müller, G.; Gurrath, M.; Kurz, M.; Kessler, H. *Proteins: Structure, Function and Genetics* **1993**, *15*, 235.
5. Reviewed in reference 4. (a) Werner, M. H.; Wemmer, D. E. *Biochemistry* **1992**, *31*, 999. (b) Kim, E. E.; Varadarajan, R.; Wyckoff, H. W.; Richards, F. M. *Biochemistry* **1992**, *31*, 12304. (c) Epp, O.; Lattman, E. E.; Schiffer, M.; Huber, R.; Palm, W. *Biochemistry* **1975**, *14*, 4943.
6. Recent examples include: (a) segetalin A, Morita, H.; Yun, Y. S.; Takeya, K.; Itokawa, H.; Shiro, M. *Tetrahedron* **1995**, *51*, 5987. (b) cycloleonurinin, Morita, H.; Gonda, A.; Takeya, K.; Itokawa, H.; Hirano, T.; Oka, K.; Shiota, O. *Tetrahedron* **1997**, *53*, 7469. (c) aureobasidin E, Fujikawa, A.; In, Y.; Inoue, M.; Ishida, T.; Nemoto, N.; Kobayashi, Y.; Kataoka, R.; Ikai, K.; Takesako, K.; Kato, I. *J. Org. Chem.* **1994**, *59*, 570. (d) evolidine, Eggleston, D. S.; Baures, P. W.; Peishoff, C. E.; Kopple, K. D. *J. Am. Chem. Soc.* **1991**, *113*, 4410. (e) phakellistatin, Pettit, G. R.; Xu, J.-P.; Cichacz, Z. A.; Williams, M. D.; Dorsaz, A.-C.; Brune, D. C.; Boyd, M. R.; Cerny, R. L. *Bioorg. Med. Chem. Lett.* **1994**, *4*, 2091.
7. Recent examples include: (a) tuftsin, Valdeavella, C. V.; Blatt, H. D.; Pettitt, B. M. *Int. J. Peptide Protein Res.* **1995**, *46*, 372. (b) decorin/DS-PGII, Wang, Y.; Scott, P. G.; Sejbal, J.; Kotovych, G. *Can. J. Chem.* **1996**, *74*, 389.
8. (a) Yao, J.; Brüschweiler, R.; Dyson, H. J.; Wright, P. E. *J. Am. Chem. Soc.* **1994**, *116*, 12051. (b) Dyson, H. J.; Rance, M.; Houghten, R. A.; Lerner, R. A.; Wright, P. E. *J. Mol. Biol.* **1988**, *201*, 161.
9. Oka, M.; Montelione, G. T.; Scheraga, H. A. *J. Am. Chem. Soc.* **1984**, *106*, 7959.
10. (a) Wu, W.-J.; Raleigh, D. P. *Biopolymers* **1998**, *45*, 381. (b) Wu, W.-J.; Raleigh, D. P. *J. Org. Chem.* **1998**, *63*, 6689.

11. Johnson, M. E.; Lin, Z.; Padmanabhan, K.; Tulinsky, A.; Kahn, M. *FEBS Lett.* **1994**, *337*, 4.
12. Fischer, S.; Michnick, S.; Karplus, M. *Biochemistry* **1993**, *32*, 13830.
13. Kallen, J.; Walkinshaw, M. D. *FEBS Lett.* **1992**, *300*, 286.
14. Reviewed in: (a) Fischer, G. *Angew. Chem. Int. Ed. Engl.* **1994**, *33*, 1415. (b) Liu, J.; Chen, C.-M.; Walsh, C. T. *Biochemistry* **1991**, *30*, 2306.
15. (a) Gramberg, D.; Robinson, J. A. *Tetrahedron Lett.* **1994**, *35*, 861. (b) Gramberg, D.; Weber, C.; Beeli, R.; Inglis, J.; Bruns, C.; Robinson, J. A. *Helv. Chim. Acta* **1995**, *78*, 1588.
16. (a) Dumas, J.-P.; Germanas, J. P. *Tetrahedron Lett.* **1994**, *35*, 1493. (b) Kim, K.; Dumas, J.-P.; Germanas, J. P. *J. Org. Chem.* **1996**, *61*, 3138. (c) Kim, K.; Germanas, J. P. *J. Org. Chem.* **1997**, *62*, 2847. (d) Kim, K.; Germanas, J. P. *J. Org. Chem.* **1997**, *62*, 2853.
17. (a) Didierjean, C.; Del Duca, V.; Benedetti, E.; Aubry, A.; Zouikri, M.; Marraud, M.; Boussard, G. *J. Peptide Res.* **1997**, *50*, 451. (b) Zouikri, M.; Vicherat, A.; Aubry, A.; Marraud, M.; Boussard, G. *J. Peptide Res.* **1998**, *52*, 19.
18. (a) Brady, S. F.; Paleveda, W. J. Jr.; Arison, B. H.; Saperstein, R.; Brady, E. J.; Raynor, K.; Reisine, T.; Veber, D. F.; Freidinger, R. M. *Tetrahedron* **1993**, *49*, 3449. (b) Cumberbatch, S.; North, M.; Zagotto, G. *Tetrahedron* **1993**, *49*, 9049. (c) Cumberbatch, S.; North, M.; Zagotto, G. *J. Chem. Soc., Chem. Commun.* **1993**, 641. (d) Horne, A.; North, M.; Parkinson, J. A.; Sadler, I. H. *Tetrahedron* **1993**, *49*, 5891.
19. Ösapay, G.; Zhu, Q.; Shao, H.; Chadha, R. K.; Goodman, M. *Int. J. Peptide Protein Res.* **1995**, *46*, 290.
20. (a) Curran, T. P.; McEnaney, P. M. *Tetrahedron Lett.* **1995**, *36*, 191. (b) Lenman, M. M.; Ingham, S. L.; Gani, D. *Chem. Commun.* **1996**, 85.
21. (a) Zabrocki, J.; Dunbar, J. B.; Marshall, K. W.; Toth, M. V.; Marshall, G. R. *J. Org. Chem.* **1992**, *57*, 202. (b) Garofolo, A.; Tarnus, C.; Remy, J.-M.; Leppik, R.; Piriou, F.; Harris, B.; Pelton, J. T. In *Peptides: Chemistry, Structure and Biology*, J.E. Rivier and G.R. Marshall, Editors; ESCOM Science Publishers

- B.V.: Leiden, The Netherlands, 1990, 833-834. (c) Beusen, D. D.; Zabrocki, J.; Slomczynska, U.; Head, R. D.; Kao, J. L.-F.; Marshall, G. R. *Biopolymers* **1995**, *36*, 181. (d) Abell, A. D.; Foulds, G. J. *J. Chem. Soc., Perkin Trans. I* **1997**, 2475.
22. (a) Hart, S. A.; Sabat, M.; Etzkorn, F. A. *J. Org. Chem.* **1998**, *63*, 7580. (b) Andres, C. J.; Macdonald, T. L.; Ocain, T. D.; Longhi, D. *J. Org. Chem.* **1993**, *58*, 6609.
23. Welch, J. T.; Lin, J. *Tetrahedron* **1996**, *52*, 291.
24. Beausoleil, E.; Lubell, W. D. *J. Am. Chem. Soc.* **1996**, *118*, 12902.
25. Beausoleil, E.; L'Archevêque, B.; Bélec, L.; Atfani, M.; Lubell, W. D. *J. Org. Chem.* **1996**, *61*, 9447.
26. Halab, L.; Beausoleil, E.; Bélec, L.; L'Archevêque, B.; Gosselin, F.; Lubell, W. D. unpublished results.
27. (a) Knorr, R.; Trzeciak, A.; Bannwarth, W.; Gillessen, D. *Tetrahedron Lett.* **1989**, *30*, 1927. The crystal structure of HBTU, the corresponding PF<sub>6</sub> salt, substantiates a guanidinium-1-N-oxide salt for TBTU: (b) Abdelmoty, I.; Albericio, F.; Carpino, L. A.; Foxman, B.; Kates, S.A. *Lett. Peptide Sci.* **1994**, *1*, 57.
28. (a) Van Der Auwera, C.; Anteunis, M. J. O. *Int. J. Peptide Protein Res.* **1987**, *29*, 574. (b) Tung, R. D.; Rich, D. H. *J. Am. Chem. Soc.* **1985**, *107*, 4342.
29. Preliminary results were reported in part in: Halab, L.; Lubell, W. D. In *Peptides 1998 (Proceedings of the 25th European Peptide Symp.)*, S. Bajusz & F. Hudecz, Eds; Akadémia Kiadó, Budapest, Hungary, 1999, In Press.
30. Reviewed in: Dyson, H. J.; Wright, P. E. *Annu. Rev. Biophys. Biophys. Chem.* **1991**, *20*, 519.
31. Reviewed in: Kessler, H. *Angew Chem. Int. Ed. Engl.* **1982**, *21*, 512.
32. (a) Karplus, M. *J. Am. Chem. Soc.* **1963**, *85*, 2870. (b) Bystrov, V. F.; Ivanov, V. T.; Portnova, S. L.; Balashova, T. A.; Ovchinnikov, Yu. A. *Tetrahedron* **1973**, *29*, 873.
33. The use of carbon NMR spectroscopy to study twisted amide geometry is presented in: (a) Bennet, A. J.; Somayaji, V.; Brown, R. S.; Santarsiero, B. D. *J.*

- Am. Chem. Soc.* **1991**, *113*, 7563. The relationship between bond length and twisted amide geometry is described in: (b) Shao, H.; Jiang, X.; Gantzel, P.; Goodman, M. *Chemistry & Biology* **1994**, *1*, 231 and the characterization and reactivity of other distorted amides is discussed in refs 15-19 therein. (c) Bennet, A. J.; Wang, Q.-P.; Slebocka-Tilk, H.; Somayaji, V.; Brown, R. S. *J. Am. Chem. Soc.* **1990**, *112*, 6383. (d) Kirby, A. J.; Komarov, I. V.; Feeder, N. *J. Am. Chem. Soc.* **1998**, *120*, 7101.
34. Bax, A.; Summers, M. F. *J. Am. Chem. Soc.* **1986**, *108*, 2093.
  35. The structure of **1d** was solved at l'Université de Montréal X-ray facility using direct methods (SHELXS96) and refined with NRCVAX and SHELXL96: C<sub>18</sub>H<sub>33</sub>N<sub>3</sub>O<sub>3</sub>; M<sub>r</sub> = 339.474; orthorhombic, colorless crystal; space group P2<sub>1</sub>2<sub>1</sub>2<sub>1</sub>; unit cell dimensions (Å) a = 9.110 (3), b = 10.860 (5), c = 20.435 (10); volume of unit cell (Å<sup>3</sup>) 2021.7 (15); Z = 4; R<sub>1</sub> = 0.0505 for I>2 sigma(I), wR<sub>2</sub> = 0.1140 for all data; GOF = 0.986. The author has deposited the atomic coordinates for the structure of **1d** with the Cambridge Crystallographic Data Center. The coordinates can be obtained, on request, from the Cambridge Crystallographic Data Center, 12 Union Road, Cambridge, CB2 1EZ, UK.
  36. (a) Fischer, S.; Dunbrack, Jr. R. L.; Karplus, M. *J. Am. Chem. Soc.* **1994**, *116*, 11931. (b) Cox, C.; Young, Jr. V. G.; Lectka, T. *J. Am. Chem. Soc.* **1997**, *119*, 2307. (c) Beausoleil, E.; Sharma, R.; Michnick, S.; Lubell, W. D. *J. Org. Chem.* **1998**, *63*, 6572. (d) Cox, C.; Lectka, T. *J. Am. Chem. Soc.* **1998**, *120*, 10660.
  37. Reviewed in: Stein, R. L. *Adv. Protein Chem.* **1993**, *44*, 1.
  38. (a) Deslauriers, R.; Evans, D. J.; Leach, S. J.; Meinwald, Y. C.; Minasian, E.; Némethy, G.; Rae, I. D.; Scheraga, H. A.; Somorjai, R. L.; Stimson, E. R.; Van Nispen, J. W.; Woody, R. W. *Macromolecules* **1981**, *14*, 985. (b) Reviewed in: Brahms, S.; Brahms, J. *J. Mol. Biol.* **1980**, *138*, 149.
  39. Lambert, J. B.; Shurvell, H. F.; Lightner, D. A.; Cooks, R. G. *Organic Structural Spectroscopy*; Prentice Hall: Upper Saddle River, N. J. 1998; pp 281-283.
  40. Madison, V.; Kopple, K. D. *J. Am. Chem. Soc.* **1980**, *102*, 4855.

41. (a) Pispisa, B.; Palleschi, A.; Amato, M. E.; Segre, A. L.; Venanzi, M. *Macromolecules* **1997**, *30*, 4905. (b) Fox, R. O. Jr.; Richards, F. M. *Nature* **1982**, *300*, 325.
42. For representative examples see: (a) Benedetti, E.; Di Blasio, B.; Iacovino, R.; Menchise, V.; Saviano, M.; Pedone, C.; Bonora, G. M.; Ettorre, A.; Graci, L.; Formaggio, F.; Crisma, M.; Valle, G.; Toniolo, C. *J. Chem. Soc., Perkin Trans. 2* **1997**, 2023. (b) Toniolo, C.; Crisma, M.; Formaggio, F.; Benedetti, E.; Santini, A.; Iacovino, R.; Saviano, M.; Di Blasio, B.; Pedone, C.; Kamphuis, J. *Biopolymers* **1996**, *40*, 519. (c) Prasad, S.; Rao, R. B.; Balaram, P. *Biopolymers* **1995**, *35*, 11. (d) Toniolo, C.; Benedetti, E. *Macromolecules* **1991**, *24*, 4004; and references therein.
43. Overberger, C. G.; Jon, Y. S. *J. Polym. Sci.: Polym. Chem. Ed.* **1977**, *15*, 1413.
44. (a) Gardner, R. R.; Liang, G.-B.; Gellman, S. H. *J. Am. Chem. Soc.* **1995**, *117*, 3280. (b) Wipf, P.; Henninger, T. C.; Geib, S. J. *J. Org. Chem.* **1998**, *63*, 6088.
45. Schopfer, U.; Stahl, M.; Brandl, T.; Hoffmann, R. W. *Angew Chem. Int. Ed. Engl.* **1997**, *36*, 1745.
46. (a) Beausoleil, E.; Sharma, R.; Michnick, S.; Lubell, W. D. In *Peptides 1996 (Proceedings of the 24th European Peptide Symposium)*, R. Ramage and R. Epton, Editors; ESCOM, Leiden, The Netherlands, 1997, pp 241-242; (b) Delaney, N. G.; Madison, V. *J. Am. Chem. Soc.* **1982**, *104*, 6635. (c) Samanen, J.; Zuber, G.; Bean, J.; Eggleston, D.; Romoff, T.; Kopple, K.; Saunders, M.; Regoli, D. *Int. J. Peptide Protein Res.* **1990**, *35*, 501.
47. 5-Alkylproline examples include: (a) Delaney, N. G.; Madison, V. *Int. J. Peptide Protein Res.* **1982**, *19*, 543; (b) Magaard, V. W.; Sanchez, R. M.; Bean, J. W.; Moore, M. L. *Tetrahedron Lett.* **1993**, *34*, 381. (c) Overberger, C. G.; David, K.-H. *Macromolecules* **1972**, *5*, 373. (d) Overberger, C. G.; Han, M. J. *J. Polym. Sci.: Polym. Chem. Ed.* **1975**, *13*, 2251. (e) Overberger, C. G.; Han, M. J. *Pure Appl. Chem.* **1974**, *39*, 33. (f) Ahn, K.-D.; Overberger, C. G. *J. Polym. Sci.: Polym. Chem. Ed.* **1983**, *21*, 1699. (g) Yang, W. W.-Y.; Overberger, C. G.; Venkatachalam, C. M. *J. Polym. Sci.: Polym. Chem. Ed.* **1983**, *21*, 1741. (h) Yang, W. W.-Y.; Overberger, C. G.; Venkatachalam, C. M.

- J. Polym. Sci.: Polym. Chem. Ed.* **1983**, *21*, 1751. (i) McGrady, K. A. W.; Overberger, C. G. *Polym. Prepr. (Am. Chem. Soc., Div. Polym. Chem.)* **1987**, *28*, 429.
48. 5-Alkyl-4-thiaproline analogs: (a) Nefzi, A.; Schenk, K.; Mutter, M. *Protein and Peptide Lett.* **1994**, *1*, 66. (b) Savrda, J. In *Peptides 1976* Loffet, A. ed. Edition de l'Université de Bruxelles, Brussels, 1976, p. 653. 5-Alkyl-4-thia- and 4-oxaproline analogs: (c) Keller, M.; Sager, C.; Dumy, P.; Schutkowski, M.; Fischer, G. S.; Mutter, M. *J. Am. Chem. Soc.* **1998**, *120*, 2714. (d) Dumy, P.; Keller, M.; Ryan, D. E.; Rohwedder, B.; Wöhr, T.; Mutter, M. *J. Am. Chem. Soc.* **1997**, *119*, 918.

## Article 4

Halab, L.; Lubell, W. D. "The Effects of Stereochemistry and Sequence on 5-*tert*-Butylproline Type VI  $\beta$ -Turns Mimics." Publié dans *Peptides* 1999, Proceedings of the 16<sup>th</sup> APS, G.B. Fields, J.P. Tam & G. Barany, Eds; Kluwer Academic: Minnesota, USA, 2000, 305-306.

## The effects of stereochemistry and sequence on 5-*tert*-butylproline type VI $\beta$ -turn mimics.

Liliane Halab and William D. Lubell\*

Département de chimie, Université de Montréal,  
C. P. 6128, Succursale Centre Ville, Montréal, Québec, Canada H3C 3J7

### 2.13. Introduction

Steric interactions can control peptide geometry favoring particular secondary structures. We have examined the effects of steric bulk on peptide turn geometry by synthesizing *N*-acetyl-L-Xaa-5-*tert*-butylproline *N'*-methylamides and their natural proline counterparts which were analyzed by NMR and CD spectroscopy as well as X-ray diffraction [1]. The prolyl amide *trans*-isomer was favored in the peptides containing natural proline, which were found not to adopt specific turn geometries in solution. In contrast, the L-Xaa-Pro amide *cis*-isomer was favored in the case of the 5-*tert*-butylprolyl peptides, which adopted preferably type VIa  $\beta$ -turn conformations. Because the type II'  $\beta$ -turn conformation is often adopted by peptides possessing D-amino acids *N*-terminal to proline at the central turn residues [2], we have now synthesized *N*-acetyl-D-Xaa-5-*tert*-butylproline *N'*-methylamides in order to examine if by favoring the prolyl amide *cis*-isomer, the bulky 5-*tert*-butyl substituent could disrupt the type II' geometry and induce a type VI  $\beta$ -turn.

### 2.14. Results and Discussion

(2*S*, 5*R*)-5-*tert*-Butylproline was introduced into Ac-D-Xaa-5-*t*BuPro-NHMe analogs with the protocols developed on the L-Xaa series [1]. Couplings of D-*N*-(BOC)amino acid, to 5-*t*BuPro-NHMe with BOP-Cl and DIEA in DCM gave lower yields (32-60%) than with the L-amino acids (75-94%). The prolyl isomers were assigned by two dimensional NMR experiments. Integration of the *N*-methyl doublets in the proton spectra in CDCl<sub>3</sub>, DMSO and water indicated that the major conformer possessed a *cis*-isomer *N*-terminal to 5-*t*BuPro (Table 1). In CDCl<sub>3</sub> and water, the D-Xaa-5-*t*BuPro *cis*-isomer population was lower than that observed in the

L-series. In DMSO, the highest (>90%) *cis*-isomer populations were observed when the D-amino acid side-chain was aliphatic.

**Table 1. Solvent effect on amide isomer equilibrium of Ac-Xaa-(2*S*,5*R*)-5-tBuPro-NHMe.**

D-Xaa (L-Xaa)	CDCl <sub>3</sub>	% <i>cis</i> Xaa-5- <i>t</i> BuPro	10% D <sub>2</sub> O/H <sub>2</sub> O
		DMSO- <i>d</i> <sub>6</sub>	
D-Ala (L-Ala)	71 (83)	91 (79)	68 (79)
D-Leu (L-Leu)	60 (85)	93 (67)	78 (81)
D-Phe (L-Phe)	82 (89)	73 (79)	58 (90)

The influence of solvent composition on the chemical shift of the NH signals was used to identify amides engaged in intramolecular hydrogen bonds (Table 2). In the major *cis*-amide conformer of the D-series, the signal for the *N*<sup>l</sup>-methylamide proton was observed downfield (7.29-7.37 ppm) relative to that for the acetamide proton (6.19-6.43 ppm) in CDCl<sub>3</sub>. The downfield shift of the signal for the *N*<sup>l</sup>-methylamide proton was indicative of an intramolecular hydrogen bond between the NHMe proton and the acetamide carbonyl in a type VIa β-turn conformation. This hydrogen bond was inferred to be weaker than in the L-series where the *N*<sup>l</sup>-methylamide proton was shifted much further downfield (8.27-8.37 ppm). In both series, the signal for the NHXaa proton was strongly shifted (1.71-2.53 ppm) with changes in solvent relative to the signal for the NHMe proton which was shifted 0.22-1.12 ppm downfield on switching solvents from CDCl<sub>3</sub> to DMSO and 0.12-0.60 ppm downfield on changing from CDCl<sub>3</sub> to water. In contrast, the minor amide *trans*-conformer in the D-series exhibited amide proton signals that shifted 1.12-2.08 ppm with changes in solvent polarity indicating a greater exposure to solvent. Although less pronounced than in the L-series, the influences of solvent on the NH chemical shift suggested the presence of a ten-member hydrogen-bond indicative of a type VIa β-turn for the *cis*-amide conformer in the Ac-D-Xaa-*t*BuPro-NHMe series.

As previously observed in the L-series, the steric interactions from the 5-*tert*-butyl substituent in the Ac-D-Xaa-*t*BuPro-NHMe series created a predominant prolyl amide *cis*-isomer population that appeared to adopt a type VIa turn geometry. In the D-series, the prolyl amide equilibrium was influenced more dramatically by solvent than in the L-series indicating that the type VIa turn was less stable than in the L-series presumably because of a greater interaction between the D-amino acid side-chain and the *tert*-butyl group. We are presently examining the D-series by CD spectroscopy as well as preparing D-Xaa analogs possessing natural L-proline in order to enhance our understanding of the steric and stereochemical components that influence the prolyl amide equilibrium.

**Table 2. Solvent effects on NH chemical shifts of Ac-Xaa-(2S,5R)-5-tBuPro-NHMe.**

Xaa	CDCl <sub>3</sub>		CDCl <sub>3</sub> →DMSO		CDCl <sub>3</sub> →H <sub>2</sub> O	
	δ NHXaa	NHMe	Δδ NHXaa	NHMe	Δδ NHXaa	NHMe
<b>Major <i>tert</i>-Butylprolyl Amide <i>Cis</i>-Conformer</b>						
D-Ala (L-Ala)	6.43 (6.07)	7.34 (8.30)	1.71 (2.39)	0.62 (0.28)	1.71 (2.22)	0.51 (0.28)
D-Leu (L-Leu)	6.19 (5.97)	7.29 (8.27)	1.89 (2.43)	0.71 (0.22)	1.94 (2.27)	0.60 (0.12)
D-Phe (L-Phe)	6.32 (6.09)	7.37 (8.37)	1.86 (2.53)	1.12 (0.35)	-	0.16 (0.26)
<b>Minor <i>tert</i>-Butylprolyl Amide <i>Trans</i>-Conformer</b>						
D-Ala	6.13	6.20	1.82	1.35	1.92	1.23
D-Leu	5.97	6.31	1.92	1.26	2.08	1.12
D-Phe	-	6.06	-	2.01	-	1.78

**Acknowledgements:** This research was supported by NSERC (Canada), FCAR (Québec) and the DuPont Educational Aid Program. L. H. is grateful for an award supporting travel expenses from the APS Travel Grant Committee.

## 2.15. References

1. Halab, L. and Lubell, W. D., J. Org. Chem. 64 (1999) 3312.
2. Haque, T. S., Little, J. C., and Gellman, S. H., J. Am. Chem. Soc. 118 (1996) 6975.

**Article 5**

**Halab, L.; Lubell, W. D. "Influence of N-Terminal Residue Stereochemistry on the prolyl Amide Geometry and the Conformation of 5-*tert*-Butylproline Type VI  $\beta$ -Turn Mimics." Publié dans *The Journal of Peptide Science* 2001, 7, 92-104.**

# Influence of *N*-Terminal Residue Stereochemistry on the Prolyl Amide Geometry and the Conformation of 5-*tert*-Butylproline Type VI $\beta$ -Turn Mimics.

Liliane Halab and William D. Lubell\*

Département de chimie, Université de Montréal

C. P. 6128, Succursale Centre Ville, Montréal, Québec, Canada H3C 3J7

## 2.16. Abstract

The effects of *N*-terminal amino acid stereochemistry on prolyl amide geometry and peptide turn conformation were investigated by coupling both L- and D-amino acids to (2*S*, 5*R*)-5-*tert*-butylproline and L-proline to generate respectively *N*-(acetyl)dipeptide *N*<sup>1</sup>-methylamides **1** and **2**. Prolyl amide *cis*- and *trans*-isomers were respectively favored for peptides **1** and **2** as observed by proton NMR spectroscopy in water, DMSO and chloroform. The influence of solvent composition on amide proton chemical shift indicated an intramolecular hydrogen bond between the *N*<sup>1</sup>-methylamide proton and the acetamide carbonyl for the major conformer of dipeptides (*S*)-**1**, that became less favorable in (*R*)-**1** and **2**. The coupling constant (<sup>3</sup>*J*<sub>NH, $\alpha$</sub> ) values for the *cis*-isomer of (*R*)-**1** indicated a  $\phi_2$  dihedral angle value characteristic of a type VIb  $\beta$ -turn conformation in solution. X-ray crystallographic analysis of *N*-acetyl-D-leucyl-5-*tert*-butylproline *N*<sup>1</sup>-methylamide (*R*)-**1b** showed the prolyl residue in a type VIb  $\beta$ -turn geometry possessing an amide *cis*-isomer and  $\psi_3$ -dihedral angle having a value of 157° that precluded an intramolecular hydrogen bond. Intermolecular hydrogen bonding between the leucyl residues of two turn structures within the unit cell positioned the *N*-terminal residue in a geometry where their  $\phi_2$  and  $\psi_2$ -dihedral angle values were not characteristic of an ideal type VIb turn. The circular dichroism spectra of *tert*-butylprolyl peptides (*S*)- and (*R*)-**1b** were found to be uninfluenced by changes in solvent composition from water to acetonitrile. The

type B spectrum exhibited by (*S*)-**1b** has been previously assigned to a type VIa  $\beta$ -turn conformation (Halab, L. & Lubell, W. D. J. Org. Chem. 1999, 64, 3312-3321). The type C spectrum exhibited by the (*R*)-**1b** has previously been associated with type II'  $\beta$ -turn and  $\alpha$ -helical conformations in solution and appears now to be also characteristic for a type VIb geometry.

**Key words:** *cis*-amide bond; 5-*tert*-butylproline; stereochemistry; steric interactions; type VI  $\beta$ -turn mimics

### 2.17. Introduction

Turns play essential roles in protein folding and recognition [1, 2]. Conformationally constrained turn mimics are thus valuable tools for replicating these secondary structures to study their effects in such phenomenon [3, 4]. Modified prolines have been particularly useful in the preparation of turn mimics because of the high preference of proline at the central residues of  $\beta$ -turn structures [3-6]. Specific turn geometries have been achieved by using alkylprolines to affect the energy barrier for prolyl amide isomerization as well as the conformation about the proline residue [7-18].

Conformational preferences of peptide turns are contingent on the configuration of their amino acid components. For example, studies of the influence of stereochemistry on the conformation and amide equilibrium of peptides possessing sequences incorporating a D-amino acid at the *N*-terminal position of a proline residue have demonstrated preferences for the amide *trans*-isomer as well as type II and II'  $\beta$ -turn geometry [2]. In the dipeptide H-D-Phe-Pro-OH, only the prolyl amide *trans*-isomer was observed by NMR spectroscopy whereas the incorporation of L-Phe augmented the *cis*-isomer population in D<sub>2</sub>O [19]. In the case of linear peptides, X-ray diffraction has shown that *N*-pivaloyl-D-alanyl-proline *N*'-isopropylamide adopted

a type II'  $\beta$ -turn conformation with an intramolecular hydrogen bond between the oxygen of the pivaloyl carbonyl and the hydrogen of the isopropylamide [20]. Spectroscopic and crystallographic data of depsipeptides Ac-X-Pro-Glyco-D-Leu-NMe<sub>2</sub> and Ac-X-Pro-D-Lac-D-Leu-NMe<sub>2</sub> (where X = L- or D-Val, Glyco = glycolic acid and Lac = lactic acid) have shown them to adopt type II  $\beta$ -turn conformations in CD<sub>2</sub>Cl<sub>2</sub>, CD<sub>3</sub>CN and DMSO-d<sub>6</sub> when X = D-Val [21]. In these cases, greater amounts (15-25%) of prolyl amide *cis*-isomer were observed in DMSO relative to the other two solvents [21].

The influences of an *N*-terminal residue with D-stereochemistry on the conformations about proline residues have also been studied with cyclic peptides both in solution and in the crystalline state. For example, *cyclo*-(X-Pro-Y)<sub>2</sub> was shown by a combination of NMR, CD and X-ray experiments to adopt type II or II'  $\beta$ -turn conformations when a D-residue preceded the proline (X = D-Ala, D-Phe) [22]. The cyclic pentapeptide, *cyclo*-(Gly<sup>1</sup>-Pro-Gly<sup>2</sup>-D-Ala-Pro) adopted a  $\gamma$ -turn conformation about the D-Ala-Pro-Gly residues with an intramolecular H-bond between the carbonyl oxygen of D-Ala<sup>4</sup> and the amide hydrogen of Gly<sup>1</sup> as observed in the crystal state and in solution [23-24].

A rare turn conformation is the type VI  $\beta$ -turn secondary structure which features uniquely an amide *cis*-isomer *N*-terminal to a proline residue situated at the *i* + 2 position of the peptide bend (Fig. 1) [25]. The type VI  $\beta$ -turn is classified into type VIa and type VIb conformations which have been defined based on the dihedral angle values of the central *i* + 1 and *i* + 2 residues [25]. In the type VIa  $\beta$ -turn, an intramolecular hydrogen bond is found between the *i* residue carbonyl oxygen and the *i* + 3 residue amide hydrogen. This intramolecular hydrogen bond cannot be formed in the type VIb  $\beta$ -turn because of the proline  $\psi$ -dihedral angle value. Type VI  $\beta$ -turn

conformations play important roles in the recognition and reactivity of bioactive peptides and proteins [26-30].

Previously, we demonstrated that the steric interactions of 5-*tert*-butylproline can influence the prolyl amide isomer geometry in peptides [7-12, 14]. Incorporation of (2*S*, 5*R*)-5-*tert*-butylproline [31] at the *C*-terminal of a series of *N*-acetyl-dipeptide *N*<sup>l</sup>-methylamides (*S*)-1 has led to a means for reproducing the structural elements of type VIa  $\beta$ -turns. For example, replacement of proline by (2*S*, 5*R*)-5-*tert*-butylproline in *N*-acetyl-L-Xaa-L-proline *N*<sup>l</sup>-methylamides (*S*)-2 (Xaa = Gly, Ala, Met, Leu, Val, Phe) perturbed the naturally favored prolyl amide *trans*-isomer and promoted a dominant *cis*-isomer population as shown by NMR experiments in chloroform, DMSO and water [9-10]. Conformational analyses of the *N*-acetyl-L-Xaa-5-*tert*-butylproline *N*<sup>l</sup>-methylamides (Xaa = Ala, Leu) by circular dichroism spectroscopy exhibited characteristic type B spectrum for a  $\beta$ -turn conformation in both water and acetonitrile, and indicated that the *tert*-butylprolyl type VIa  $\beta$ -turn geometry was adopted independent of solvent composition [9]. Furthermore, crystallographic analysis of *N*-acetyl-L-leucyl-5-*tert*-butylproline *N*<sup>l</sup>-methylamide by X-ray diffraction demonstrated the presence of an amide *cis*-isomer in a geometry characteristic of the central *i* + 1 and *i* + 2 residues of an ideal type VIa  $\beta$ -turn [9]. An intramolecular hydrogen bond between the *N*<sup>l</sup>-methylamide and the acetamide carbonyl was inferred from their interatomic distance (2.13 Å) in the X-ray structure.

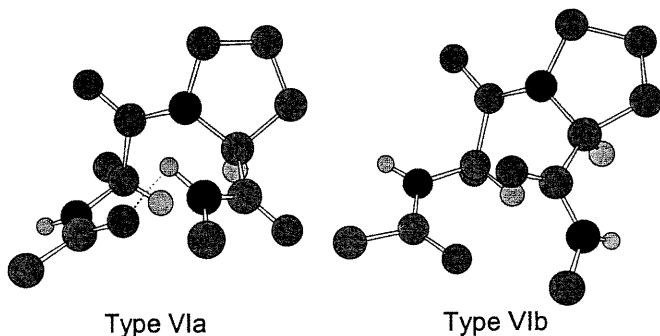


**Figure 1.** Type VIa and VIb turn conformation found respectively in the central  $i + 1$  and  $i + 2$  residues of Ribonuclease S and Bence-Jones protein (N, black; C, dark gray; O, light gray; H, white).

The influence of the *N*-terminal residue stereochemistry on the conformation of dipeptides possessing (2*S*, 5*R*)-5-*tert*-butylproline has now been investigated through a comparison of *N*-acetyl-D-Xaa-5-*tert*-butylproline *N*<sup>′</sup>-methylamides (*R*)-1 and *N*-acetyl-D-Xaa-proline *N*<sup>′</sup>-methylamide (*R*)-2 (Xaa = **a**, Ala; **b**, Leu and **c**, Phe). Employing 5-*tert*-butyproline to sterically disfavor the prolyl amide *trans*-isomer, we have explored its potential to disrupt the type II and II'  $\beta$ -turn conformations, expected for the natural D-Xaa-Pro diastereomers, to induce a type VI geometry. Conformational analyses of dipeptides **1** and **2** by proton NMR and circular dichroism spectroscopy, as well as X-ray diffraction, all have shown that (*R*)-1**a-c** preferred the prolyl amide *cis*-isomer in a turn geometry that was less likely to adopt an intramolecular hydrogen bond relative to its diastereomeric counterpart (*S*)-1**a-c**. Changing the stereochemistry at the *N*-terminal residue of 5-*tert*-butylproline peptides seems thus to disrupt the hydrogen-bond of the type VIa  $\beta$ -turn conformation adopted by *N*-acetyl-L-Xaa-5-*tert*-butylproline *N*<sup>′</sup>-methylamides (*S*)-1**a-c** and gives rise to an alternative type VI  $\beta$ -turn conformation.

## 2.18. Results and Discussion

### 2.18.1. Synthesis of dipeptides 1 and 2

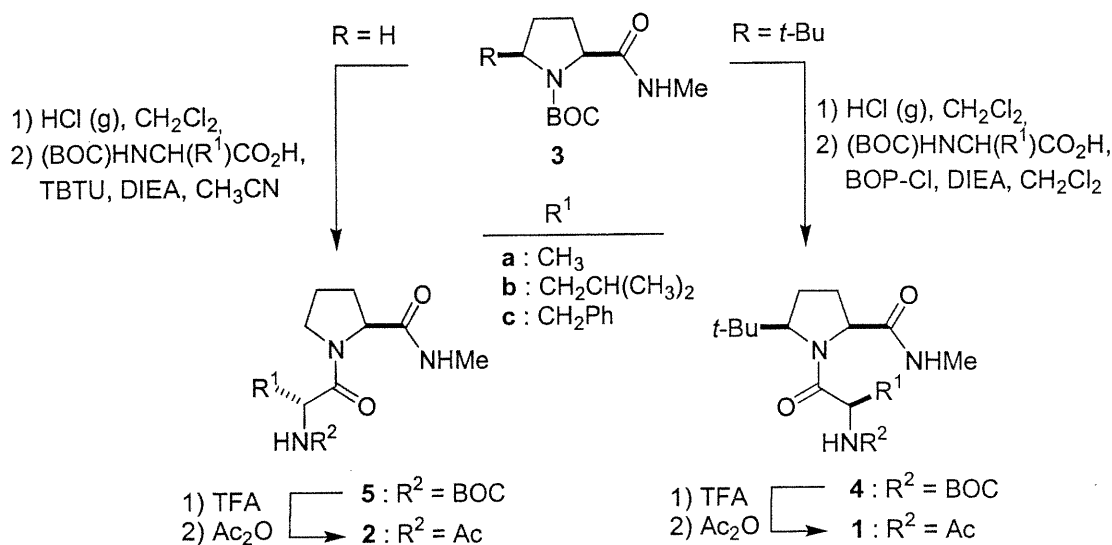


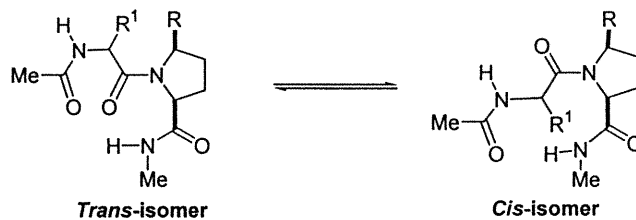
Figure 2. Synthesis of *N*-(Acetyl)Dipeptide *N'*-methylamides 1 and 2.

Dipeptide analogs Ac-D-Xaa-5-*t*-BuPro-NHMe (*R*)-1a-c were synthesized using D-amino acids and protocols described previously for the respective L-Xaa series (*S*)-1a-c [9-10]. The D-*N*-BOC-amino acids were coupled to the *N*-terminal of 5-*tert*-butylproline *N'*-methylamide using BOP-Cl, DIEA in dichloromethane in lower yields (60-64%) than had been obtained with the L-*N*-BOC-amino acids (75-94%, Fig. 2). The *N*-acetyl-D-Xaa-5-*tert*-butylproline *N'*-methylamides (*R*)-1a-c (Xaa = Ala, Leu, Phe) were finally produced by solvolysis of the BOC group with trifluoroacetic acid and *N*-acetylation with acetic anhydride and potassium carbonate in dichloromethane [11]. For comparison, dipeptides possessing natural L-proline (*N*-acetyl-D-Xaa-L-proline *N'*-methylamides (*R*)-2a-c) were synthesized by coupling D-*N*-(BOC)-amino acids to proline *N'*-methylamide using TBTU, and DIEA in acetonitrile, followed by BOC group removal and acetylation of the amine as described for the *tert*-butylproline analogs.

### 2.18.2. Conformational analysis of dipeptides 1 and 2 by NMR spectroscopy

A series of solvents were used to study the influence of environment on the conformation of prolyl dipeptides **1** and **2**. The relative populations of the amide *cis*- and *trans*-isomers *N*-terminal to the prolyl residues of peptides **1** and **2** were measured by integration of the isomeric *tert*-butyl singlets or *N*<sup>1</sup>-methyl doublets in their proton NMR spectra in CDCl<sub>3</sub>, DMSO-*d*<sub>6</sub> and water. The *tert*-butyl singlet of the amide *cis*-isomer appeared always upfield from that of the *trans*-isomer in the *tert*-butylprolyl peptides. The cross-peak between the *N*-terminal amino acid and proline  $\alpha$ -hydrogens arising from the nuclear Overhauser effect in the NOESY and ROESY spectra confirmed the assignment of the *cis*-isomer in dipeptides **1** and **2**.

**Table 1. Influence of solvent on the chemical shifts and amide isomer equilibrium of **1** and **2**.<sup>a</sup>**



entry	<i>N</i> -terminal residue	R	% <i>cis</i> -isomer $\pm$ 3% D <sub>2</sub> O ; DMSO ; CDCl <sub>3</sub>			(CDCl <sub>3</sub> ) $\delta$ NH <sup>Xaa</sup> ; NH <sup>Me</sup>	(CDCl <sub>3</sub> $\rightarrow$ DMSO) $\Delta\delta$ NH <sup>Xaa</sup> ; NH <sup>Me</sup>	(CDCl <sub>3</sub> $\rightarrow$ D <sub>2</sub> O) $\Delta\delta$ NH <sup>Xaa</sup> ; NH <sup>Me</sup>	
(S)-1a	L-Ala	<i>t</i> -Bu	79	79	83	6.07	8.30	2.39	0.28
(R)-1a	D-Ala	<i>t</i> -Bu	68	91	71	6.43	7.34	1.71	0.62
(S)-1b	L-Leu	<i>t</i> -Bu	81	67	85	5.97	8.27	2.43	0.22
(R)-1b	D-Leu	<i>t</i> -Bu	78	93	60	6.19	7.29	1.89	0.71
(S)-1c	L-Phe	<i>t</i> -Bu	90	79	89	6.09	8.37	2.53	0.35
(R)-1c	D-Phe	<i>t</i> -Bu	58	73	82	6.32	7.37	1.86	1.12
(S)-2a	L-Ala	H	14	30	19	6.33	6.61	1.79	1.06
(R)-2a	D-Ala	H	19	36	6	6.30	6.90	1.90	0.63
(S)-2b	L-Leu	H	19	17	20	6.03	6.68	2.00	1.65
(R)-2b	D-Leu	H	29	48	9	6.19	6.95	1.97	0.57
(R)-2c	D-Phe	H	14	39	4	6.31	6.91	2.07	0.59
								2.03	0.73
								2.03	0.65

<sup>a</sup> Values are for the major conformer at 5 mM concentration, 25 °C, determined by 600 MHz NMR.

In the proline dipeptides (*R*)-**2a-c**, as is typically observed for linear prolyl peptides [32-35], the *trans*-amide geometry *N*-terminal to the prolyl residue was the major conformer. On the other hand, the incorporation of 5-*tert*-butylproline into the dipeptides favored the *cis*-amide geometry *N*-terminal to the 5-*tert*-butylprolyl residue. In CDCl<sub>3</sub> and water, the D-Xaa-5-*t*-BuPro *cis*-isomer population was lower for (*R*)-**2a-c** than that observed in the L-series (*S*)-**2a-c**. Switching solvent from CDCl<sub>3</sub> to DMSO augmented more significantly the *cis*-isomer population in the D-series than had been previously observed in the dipeptide counterparts with L-amino acids (Table 1). In DMSO, the highest (>90%) *cis*-isomer populations were observed when the D-amino acid side-chain was aliphatic.

The influence of solvent composition on the chemical shifts of the NH signals was used to identify amides engaged in intramolecular hydrogen bonds (Table 1). In the major *cis*-amide conformer of peptides **1** and the major *trans*-amide conformer of **2**, the signal for the *N*<sup>1</sup>-methylamide proton was always observed downfield relative to the signal for the acetamide proton in all three solvents. This downfield shift was most evident in chloroform in which the *N*<sup>1</sup>-methylamide proton signals were shifted furthest downfield for (*S*)-**1** (8.27-8.37 ppm) relative to (*R*)-**1** (7.29-7.37 ppm), (*R*)-**2** (6.90-6.95 ppm) and (*S*)-**2** (6.61-6.68 ppm). In contrast, the acetamide proton signal varied between 5.97-6.43 ppm for all four series (Table 1). The downfield shifted amide proton signal can be used to suggest an intramolecular hydrogen bond between the *N*<sup>1</sup>-methylamide proton and the acetamide carbonyl in a type VIa β-turn conformation for (*S*)-**1**. Taking into consideration that the chemical shift of the amide protons represents an average value from a conformational equilibrium, we may conclude that relative to (*S*)-**1**, the D-Xaa-5-*tert*-butylproline dipeptide (*R*)-**1** is less likely to adopt a type VIa β-turn possessing an intramolecular hydrogen bond. An opposite influence of stereochemistry on the preference for an intramolecular

hydrogen bond may also be suggested from the results with the proline dipeptides **2**, where a type II'  $\beta$ -turn is better accommodated in the D-series (*R*)-**2** relative to its diastereomer (*S*)-**2** [22, 36].

In all cases, the signal for the *N*<sup>o</sup>-methylamide proton was less affected by changes in solvent relative to the signal for the acetamide proton in the NMR spectra for the major amide *cis*-isomer of **1** and major amide *trans*-isomer of **2**. The signal for the acetamide proton of dipeptides **1** and **2** was strongly shifted (1.71-2.53 ppm) with changes in solvent. On switching solvents from CDCl<sub>3</sub> to DMSO, the signal for the *N*<sup>o</sup>-methylamide proton was less shifted downfield (0.22-0.35 ppm) for (*S*)-**1** relative to (*R*)-**1** (0.62-1.12 ppm), (*R*)-**2** (0.57-0.63 ppm) and (*S*)-**2** (1.06-1.65 ppm). Similarly, on changing from CDCl<sub>3</sub> to water, the signal for the *N*<sup>o</sup>-methylamide proton was less shifted downfield (0.12-0.28 ppm) for (*S*)-**1** relative to (*R*)-**1** (0.16-0.60 ppm), (*R*)-**2** (0.65-0.75 ppm) and (*S*)-**2** (1.10-1.20 ppm, Table 1).

In the *tert*-butylproline dipeptides, the influences of solvent on the *N*<sup>o</sup>-methylamide NH chemical shift were more pronounced in the D-series (*R*)-**1** relative to (*S*)-**1**. Since independence from solvent composition is characteristic of an amide proton engaged in a shielded environment such as an intramolecular hydrogen-bond, this result also indicated a greater preference for a type VIa  $\beta$ -turn conformation in the *cis*-amide conformer of the L-series (*S*)-**1** relative to the D-series (*R*)-**1**. The opposite trend was again observed in the proline dipeptides **2**, where the *N*<sup>o</sup>-methylamide proton was less shifted downfield in the D-series indicative of its greater preference for an intramolecular hydrogen bond in a  $\beta$ -turn.

The coupling constant (<sup>3</sup>J<sub>NH, $\alpha$</sub> ) between the amide and  $\alpha$ -protons of the *N*<sup>o</sup>-terminal amino acid residue can be used to determine the  $\phi$ -dihedral angle value in solution [37]. The <sup>3</sup>J<sub>NH, $\alpha$</sub>  values for the major amide *cis*-isomer of the *tert*-butylprolyl dipeptides (*S*)-**1** were 1.0-2.5 Hz lower than for the major amide *cis*-isomer of the

*tert*-butylprolyl dipeptides (*R*)-**1**. In DMSO, the  $^3J_{\text{NH},\alpha}$  values varied from 5.2 to 5.5 Hz for the amide *cis*-isomer of (*S*)-**1** and from 6.2 to 8.0 Hz for the major conformer of (*R*)-**1**. Since the ideal  $-60^\circ$  and  $-120^\circ$   $\phi$ -dihedral angle values for the *i* + 1 residue in a type VIa and VIb  $\beta$ -turn correspond respectively to  $^3J_{\text{NH},\alpha}$  coupling constant of 4.2 Hz and 6.9 Hz, the observed values support the hypothesis that the major *cis*-isomer of (*S*)-**1** and (*R*)-**1** adopt respectively type VIa and VIb  $\beta$ -turn geometry in solution. In the prolyl dipeptides in DMSO, the  $^3J_{\text{NH},\alpha}$  values (6.7–7.2 Hz) for the major amide *trans*-isomer of (*R*)-**2** corresponded with the ideal  $\phi_2$ -dihedral angle value of  $60^\circ$  inside a type II'  $\beta$ -turn conformation.

### 2.18.3. Conformational analysis of dipeptides 1 and 2 by circular dichroism spectroscopy

To examine the influence of solvent composition on peptide conformation, circular dichroism (CD) spectra of dipeptides **1b** and **2b** were measured in water and acetonitrile (Fig. 3). The CD spectra of the *N*-acetyl-L-leucyl-*tert*-butylproline *N*<sup>l</sup>-methylamide (*S*)-**1b** (Fig. 3A) exhibited a strong negative band at 188 nm, a strong positive band at 209 nm and a weak negative band at 227 nm [9]. The shape of the CD curves for (*S*)-**1b** remained constant as solvent was changed from acetonitrile to water [9]. Because this CD curve shape had been classified as a type B spectrum [38], previously assigned to  $\beta$ -turn conformations [39], we concluded that a type VIa  $\beta$ -turn conformation was adopted by the *tert*-butylprolyl peptide (*S*)-**1b** that was shown to be independent of solvent composition [9]. Modifying the stereochemistry on the *N*-terminal amino acid of 5-*tert*-butylproline had an important effect on the CD spectra. The CD curves of *N*-acetyl-D-leucyl-*tert*-butylproline *N*<sup>l</sup>-methylamide (*R*)-**1b** (Fig. 3B) were characterized by a minimum at 205 nm in both water and acetonitrile and a shape similar to a type C spectrum [38]. Type C curves were also observed for *N*-acetyl-D-leucyl-proline *N*<sup>l</sup>-methylamide (*R*)-**2b** which exhibited minima at 200 nm and 206 nm in water that converged to a single band at 206 nm in acetonitrile (Fig. 3D). Type C curves have been reported for cyclic peptides such as

gramicidin S that possess D-Xaa-L-Pro sequences and adopt type II'  $\beta$ -turn conformations [40, 41].

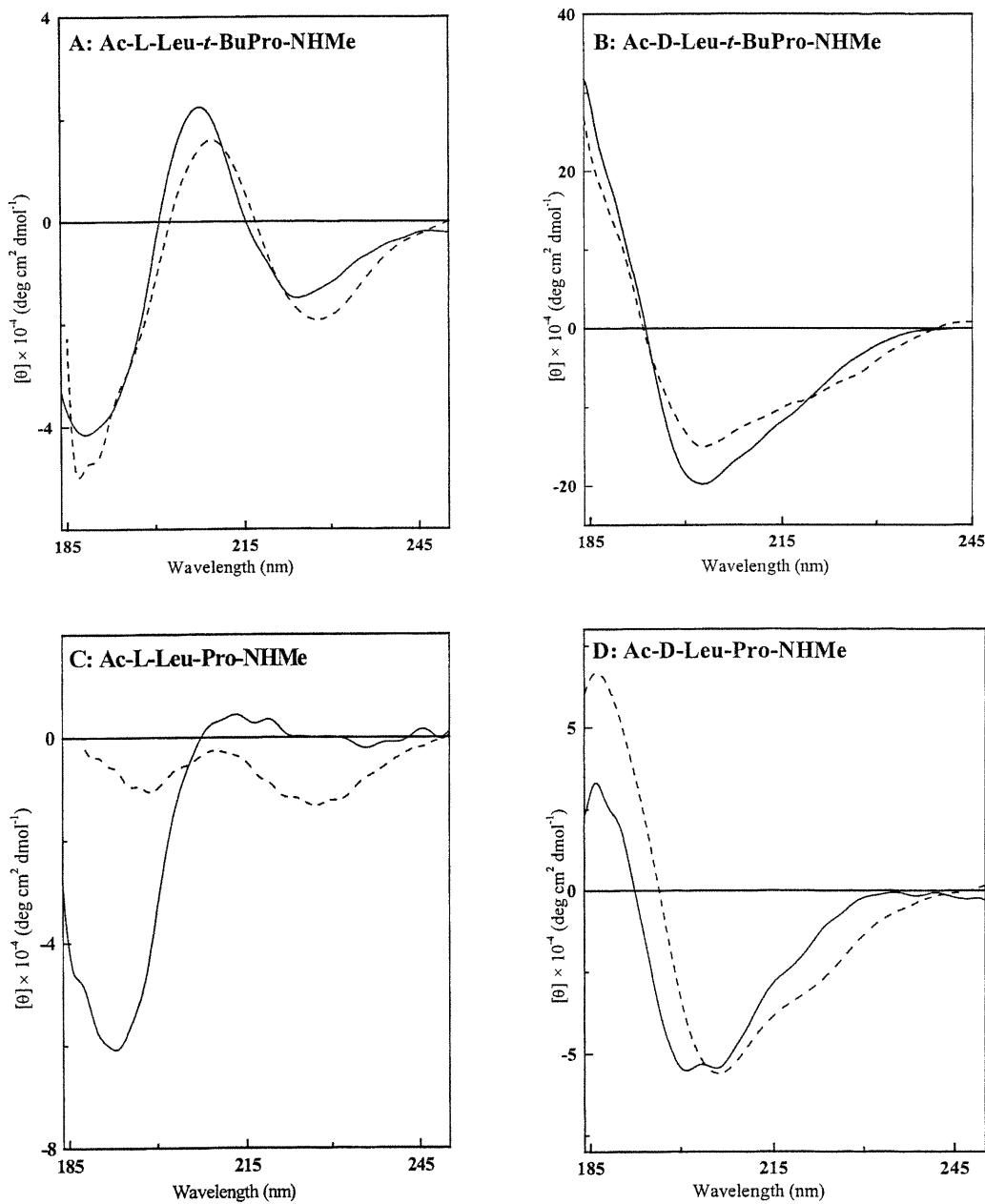


**Figure 3. Circular dichroism spectra of *N*-(acetyl)dipeptide *N'*-methylamides (*S*)-1b (A), (*R*)-1b (B), (*S*)-2b (C) and (*R*)-2b (D) in water (—) and acetonitrile (----).**

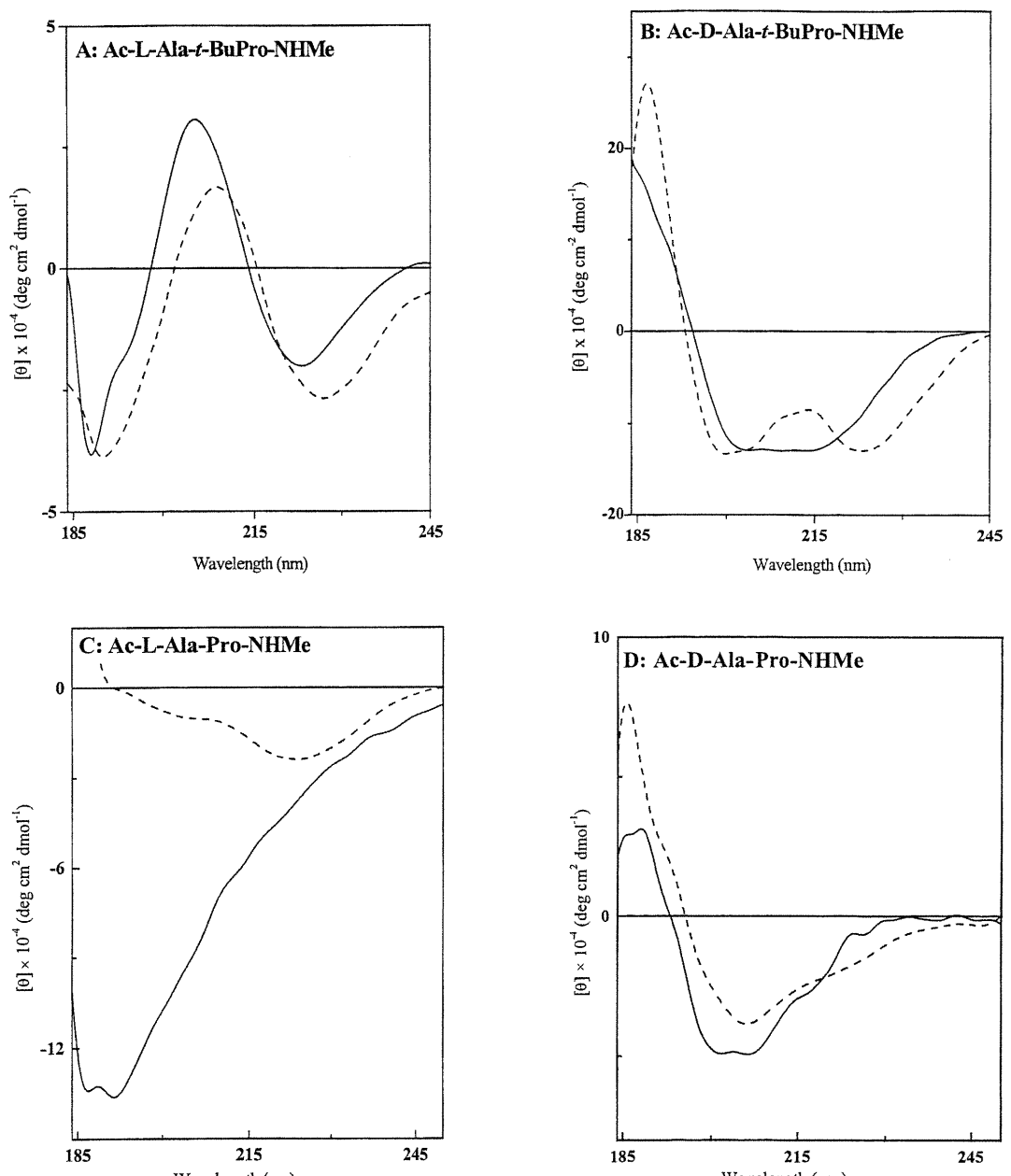


**Figure 4. Circular dichroism spectra of *N*-(acetyl)dipeptide *N'*-methylamides (*S*)-1a (A), (*R*)-1a (B), (*S*)-2a (C) and (*R*)-2a (D) in water (—) and acetonitrile (----).**

On the other hand, the CD spectra of the prolyl peptide (*S*)-2b varied significantly with changes in solvent composition and exhibited a n- $\pi^*$  band near 225 nm in

acetonitrile and a significant  $\pi-\pi^*$  band near 195 nm in water (Fig. 3C) [9], similar to CD spectra reported for *N*-(acetyl)proline *N*'-methylamide [42]. The similarity of the CD curves of (*R*)-**1b** and (*R*)-**2b** also indicated that the prolyl amide geometry has a limited influence on the molecular ellipticity exhibited by the D-Xaa-Pro residues within the peptide. A similar set of CD curves was obtained from examination of dipeptides **1a** and **2a** in which alanine preceded the prolyl residues (Fig. 4).

#### 2.18.4. X-ray crystallographic analysis of dipeptide (*R*)-**1b**

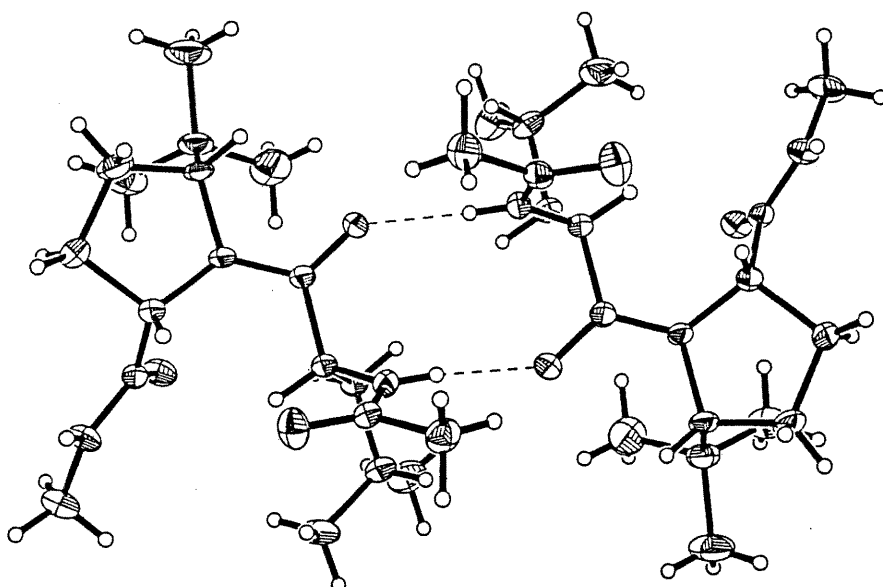


Figure 5. Two dipeptide turn structures (*R*)-**1b** and (*R*)-**1b'** engaged in intermolecular hydrogen-bonds between their leucyl residues in the crystal structure. Ellipsoids drawn at 40% probability level. Hydrogens represented by spheres of arbitrary size.#

**Table 2. Comparison of the Dihedral Angles of Ideal Type VI  $\beta$ -Turn and X-Ray Structure of *N*-(Acetyl)-D-Leucyl-5-*tert*-butylproline *N'*-Methylamide (*R*)-1b.**

entry		$\phi_2$	$\psi_2$	$\omega$	$\phi_3$	$\psi_3$
Ideal Type VIa $\beta$ -Turn [25]		-60°	120°	0°	-90°	0°
Ac-L-Leu-5- <i>t</i> -BuPro-NHMe ( <i>S</i> )-1b [9]		-61°	139°	17°	-95°	19°
L-Leu-Pro residues in X-ray of evolidine [43]		-65°	151°	2°	-93°	13°
Ideal Type VIb $\beta$ -Turn [25]		-120°	120°	0°	-60°	150°
Ac-D-Leu-5- <i>t</i> -BuPro-NHMe ( <i>R</i> )-1b		93°	-141°	29°	-81°	157°
( <i>R</i> )-1b'		95°	-139°	29°	-82°	164°
L-Leu-Pro residues in X-ray of Bence-Jones immunoglobulin [44]		-88°	154°	-27°	-56°	149°

*N*-Acetyl-D-leucyl-5-*tert*-butylproline *N'*-methylamide (*R*)-1b was crystallized from a mixture of ethyl acetate and hexane. The analysis of the crystal structure by X-ray diffraction revealed a unit cell with 8 molecules which adopted one of two similar turn conformations. Intermolecular hydrogen bonds were observed between the *N*-(acetyl)leucyl residues with the leucine carbonyl oxygen and the acetamide nitrogen at an interatomic distance of 2.86 - 2.87 Å (Fig. 5) as well as between the *N*'-methylamide residues with the carbonyl oxygen and the nitrogen at an equal interatomic distance (2.86 - 2.87 Å). Both turn structures possessed *cis*-amide bonds *N*-terminal to the 5-*tert*-butylproline residues with significantly twisted dihedral angle values of  $\omega = 28.9^\circ$  and  $29.0^\circ$ . In addition, no intramolecular hydrogen bond was observed between the methylamide nitrogen and the acetamide oxygen in the crystal structure of (*R*)-1b.

For comparison, the dihedral angles of peptides (*S*)-**1b** and (*R*)-**1b** are illustrated in Table 2 with the ideal values of type VIa and VIb  $\beta$ -turn conformations [9, 25], as well as those for the L-Leu-Pro residues of the cyclic peptide evolidine [43] and the Bence-Jones immunoglobulin [44] which adopt respectively a type VIa and VIb  $\beta$ -turns as observed in their X-ray structures. The  $\phi_3$  and  $\psi_3$  dihedral angle values of peptide (*R*)-**1b** were similar to the values of a type VIb geometry. However, the  $\phi_2$  and  $\psi_2$  dihedral angle of peptide (*R*)-**1b** possessed opposite values from those of the type VIb structure, an effect that could be attributed to the intermolecular hydrogen bonds in the unit cell. The distance between the carbons of the acetamide methyl group and the methylamide at the *i* and *i* + 3 residues is 7.5 Å indicative of a  $\beta$ -turn conformation.<sup>§</sup> The sterically bulky 5-*tert*-butyl substituent exhibited an influence on the amide bond *N*-terminal to the prolyl residue that distorted it from planarity. The X-ray structure of (*S*)-**1b** had shown the presence of a twisted amide geometry *N*-terminal to the 5-*tert*-butylprolyl residue with an  $\omega$ -dihedral angle value of 17° [9]. A more important effect was observed for (*R*)-**1b**, where the  $\omega$ -dihedral angle value was 29°.

### 2.19. Conclusions

Comparing the effects of 5-*tert*-butylproline and L-proline at the *C*-terminal of *N*-(acetyl)dipeptide *N*-methylamides in which the *N*-terminal residue was varied using both L- and D-amino acids, we have itemized the influences of steric bulk and stereochemistry on prolyl amide geometry and peptide turn conformation. Proton NMR experiments indicated that prolyl dipeptides (*S*)-**2** and (*R*)-**2**, both adopted dominant amide *trans*-isomer geometry in chloroform, DMSO and water. Further, analysis by CD spectroscopy in water and acetonitrile revealed that prolyl peptides (*S*)-**2a** and (*S*)-**2b** possessed conformations that were dependent on solvent composition. On the other hand, type C curves were obtained for prolyl peptides (*R*)-

**2a** and **(R)-2b** that were unaffected by changes in solvent composition. The type C curve shape had previously been assigned to a type II'  $\beta$ -turn conformation in cyclic peptides [41]. Prolyl peptide **(R)-2** was thus assumed to adopt a predominant type II'  $\beta$ -turn conformation in solution, where its diastereomer **(S)-2** exhibited no preferred conformation.

The stereochemistry of the *N*-terminal residue in peptides possessing *5-tert*-butylproline was shown to exhibit a significant effect on their conformation. Spectral analysis by NMR experiments in various solvents indicated that *5-tert*-butylprolyl peptide **(S)-1** adopted predominantly the amide *cis*-isomer in a type VIa  $\beta$ -turn conformation whereas a type VIb  $\beta$ -turn conformation was exhibited by *5-tert*-butylprolyl dipeptide **(R)-1**. This shift from type VIa to VIb  $\beta$ -turn conformation on switching the *N*-terminal amino acid stereochemistry from L- to D-configuration was also suggested by the significant differences in the CD curve shapes for **(S)**- and **(R)**-**1a** and **1b**: Ac-Xaa-*5-tert*BuPro-NHMe (Xaa = Ala, Leu) exhibited respectively type B and type C spectrum with L- and D-Xaa residues. The conformations adopted by **(S)**- and **(R)-1** were also shown by CD analysis to be independent of solvent composition. Because both B and C curve types have been associated with  $\beta$ -turn conformations possessing respectively L- and D-amino acids at the *i* + 1 position, we may infer that a similar change in stereochemistry has given rise to this switch in type VI  $\beta$ -turn geometry for the *tert*-butylproline dipeptides. Accordingly, the different conformations adopted by the peptides **(S)**- and **(R)-1b** was supported by their X-ray structures. In the solid state, *N*-acetyl-L-leucyl-*5-tert*-butylproline *N'*-methylamide (**S)-1b** adopted a type VIa  $\beta$ -turn conformation with an intramolecular hydrogen bond between the acetamide oxygen and the methylamide hydrogen [9]. The *tert*-butylprolyl residue in the X-ray structure of *N*-acetyl-D-leucyl-*5-tert*-butylproline *N'*-methylamide (**R)-1b** adopted a type VIb geometry; however, the  $\phi_2$  and  $\psi_2$ -dihedral

angle values deviated from that of an ideal type VIb conformation, perhaps due to intermolecular hydrogen bonds within the unit cell. Thus, replacement of proline by 5-*tert*-butylproline in *N*-acetyl dipeptide *N'*-methylamides provided respectively type VIa and VIb  $\beta$ -turn conformations when the *N*-terminal amino acids possessed L-configuration and D-configuration. Steric interactions have thus been used to destabilize the natural predisposition for type II'  $\beta$ -turn geometry and in turn augment the population of a rare type VI  $\beta$ -turn conformation. These results demonstrate further the importance of steric interactions and stereochemistry for dictating peptide secondary structure.

## 2.20. Experimental Section

**General.** Unless otherwise noted, all reactions were run under a nitrogen atmosphere and distilled solvents were transferred by syringe. CH<sub>2</sub>Cl<sub>2</sub> was distilled over P<sub>2</sub>O<sub>5</sub>, CH<sub>3</sub>CN was distilled over CaH<sub>2</sub>, and DIEA was distilled over ninhydrin and CaH<sub>2</sub>. Final reaction mixture solutions were dried over Na<sub>2</sub>SO<sub>4</sub>. Chromatography was on 230-400 mesh silica gel, and TLC was on aluminium-backed silica plates. Melting points are uncorrected. Mass spectral data, HRMS (EI and FAB), were obtained by the Université de Montréal Mass Spectroscopy facility.

**NMR Measurements.** <sup>1</sup>H and <sup>13</sup>C NMR experiments were performed on Brucker DMX600 and ARX400 spectrometers. The chemical shifts are reported in ppm ( $\delta$  units) downfield of the internal tetramethylsilane ((CH<sub>3</sub>)<sub>4</sub>Si). Coupling constants are in hertz. The chemical shifts for the carbons and the protons of the minor isomers are respectively reported in parentheses and in brackets. All 2D NMR experiments were carried out at a concentration of 5 mM. COSY, NOESY, and ROESY spectra were obtained with 2048 by 512 data points. A mixing time of 500 ms was used for the NOESY and ROESY spectra.

**Circular Dichroism Measurements.** CD spectra of 0.1 mM solutions of peptides in H<sub>2</sub>O and CH<sub>3</sub>CN were measured on a Jasco J-710 spectropolarimeter using a circular quartz cell with a path length of 1 mm at 23 °C. Band intensities are expressed as molar ellipticities [θ]. Spectra were run with a bandwidth of 1 nm, a response time of 0.25 s, and a scan speed of 100 nm min<sup>-1</sup>. Each measurement was the average result of 10 repeated scans in steps of 0.2 nm. Baseline spectra of the solvents were subtracted.

**General Procedure for Coupling to 5-*tert*-Butylproline *N*-Methylamide.** A solution of (2*S*, 5*R*)-5-*tert*-butylproline *N*-methylamide hydrochloride (100 mg, 0.45 mmol) prepared according to reference (9), *N*-(BOC)-D-amino acid (0.54 mmol) and DIEA (0.3 mL, 1.8 mmol) in CH<sub>2</sub>Cl<sub>2</sub> (4.5 mL) was cooled to 0 °C, treated with BOP-CI (138 mg, 0.54 mmol), stirred for 1 h and allowed to warm to room temperature with stirring for 18 h. Brine was added and the solution was extracted with EtOAc. The combined organic layers were washed with 0.1 M HCl (2 × 10 mL), 5% NaHCO<sub>3</sub> (2 × 10 mL) and brine (10 mL), dried and evaporated to a residue that was purified by chromatography on silica gel using 35% EtOAc in hexane as eluent. Evaporation of the collected fractions furnished *N*-(BOC)-dipeptide *N*-methylamides.

***N*-(BOC)-(2*R*)-Alanyl-(2*S*, 5*R*)-5-*tert*-butylproline *N*-Methylamide (R)-4a** was obtained in 60% yield as a white solid: mp 165-166 °C; [α]<sup>20</sup><sub>D</sub> -122.9° (c 0.5, CHCl<sub>3</sub>); <sup>1</sup>H NMR (CDCl<sub>3</sub>) δ 0.86 (s, 5 H) [0.89 (s, 4 H)], 1.18 (d, 1.7 H, *J* = 6.6) [1.23 (d, 1.3 H, *J* = 6.5)], [1.33 (s, 4 H)] 1.37 (s, 5 H), 1.80 (m, 1 H), 1.98 (m, 2 H), [2.22 (m, 0.4 H)] 2.56 (m, 0.6 H), 2.71 (d, 1.7 H, *J* = 4.7) [2.78 (d, 1.3 H, *J* = 4.0)], [3.52 (d, 0.4 H, *J* = 4.0)] 3.67 (d, 0.6 H, *J* = 8.2), 4.22 (m, 1 H), 4.52 (t, 1 H, *J* = 8.5), 4.50-1.72 (m, 1 H), [5.25 (m, 0.4 H)] 5.38 (d, 0.6 H, *J* = 6.0), [6.48 (br s, 0.4 H)] 7.33

(br s, 0.6 H);  $^{13}\text{C}$  NMR ( $\text{CDCl}_3$ )  $\delta$  (19.0) 19.2, 25.0 (25.7), 26.1 (30.7), 26.2, 27.3, 28.1, 35.3 (36.1), (47.6) 48.1, 61.7 (62.2), (65.7) 67.5, 79.4, 154.6 (155.3), 171.7 (172.6), 175.8 (176.4); HRMS calcd for  $\text{C}_{18}\text{H}_{34}\text{O}_3\text{N}_3$  ( $\text{MH}^+$ ) 340.2600, found 340.2618.

**N-(BOC)-(2*R*)-Leucyl-(2*S*, 5*R*)-5-*tert*-butylproline *N*-Methylamide (*R*)-4b** was obtained in 62% yield as a white solid: mp 156-157 °C;  $[\alpha]^{20}\text{D} -99.6^\circ$  (c 0.6,  $\text{CHCl}_3$ );  $^1\text{H}$  NMR ( $\text{CDCl}_3$ )  $\delta$  0.81-0.99 (m, 15 H), 1.12 (m, 1 H), [1.36 (s, 3 H)] 1.40 (s, 6 H), 1.60-1.88 (m, 3 H), 2.01 (m, 1.4 H) [2.21 (m, 0.6 H)], 2.59 (m, 1 H), 2.75 (d, 2.1 H,  $J = 4.7$ ) [2.80 (d, 0.9 H,  $J = 4.5$ ), [3.70 (d, 0.3 H,  $J = 7.9$ )] 4.23 (m, 0.7 H), 4.54 (dd, 0.7 H,  $J = 7.7, 9.5$ ) [4.60 (m, 0.3 H)], 4.78 (t, 1 H,  $J = 8.4$ ), [5.03 (d, 0.3 H,  $J = 9.4$ )] 5.23 (d, 0.7 H,  $J = 8.3$ ), [6.46 (br s, 0.3 H)] 7.34 (br s, 0.7 H);  $^{13}\text{C}$  NMR ( $\text{CDCl}_3$ )  $\delta$  (20.8) 21.6, (23.1) 23.4, (24.2) 24.4, 25.0 (25.8), 26.0 (30.9), 26.2, 27.2, 28.1, 35.2 (36.1), (41.7) 43.5, (50.2) 50.7, 61.6 (62.2), (65.8) 67.4, 79.4, 155.0 (155.8), 171.8 (172.5), 176.0 (176.2); HRMS calcd for  $\text{C}_{21}\text{H}_{40}\text{O}_4\text{N}_3$  ( $\text{MH}^+$ ) 398.3019, found 398.3007.

**N-(BOC)-(2*R*)-Phenylalanyl-(2*S*, 5*R*)-5-*tert*-butylproline *N*-Methylamide (*R*)-4c** was obtained in 64% yield as an oil:  $[\alpha]^{20}\text{D} -124.4^\circ$  (c 0.2,  $\text{CHCl}_3$ );  $^1\text{H}$  NMR ( $\text{CDCl}_3$ )  $\delta$  0.71 (s, 7.2 H) [0.88 (s, 1.8 H)], [1.26 (s, 1.8 H)] 1.38 (s, 7.2 H), 1.47 (m, 2 H), 2.27 (m, 1 H), 2.69 (d, 3 H,  $J = 4.3$ ), 2.79 (m, 1 H), 3.05 (dd, 1 H,  $J = 4.8, 12.4$ ), 3.22 (d, 1 H,  $J = 8.3$ ), 4.29 (m, 1.6 H) [4.36 (m, 0.4 H)], [4.66 (t, 0.2 H,  $J = 8.5$ )] 4.92 (m, 0.8 H), [5.22 (d, 0.2 H,  $J = 8.7$ )] 5.43 (d, 0.8 H,  $J = 8.4$ ), 7.13-7.24 (m, 5 H), [6.31 (br s, 0.2 H)] 7.38 (br s, 0.8 H);  $^{13}\text{C}$  NMR ( $\text{CDCl}_3$ )  $\delta$  24.6 (25.8), 24.8 (30.3), 26.2, 26.6 (27.4), 28.1, 35.0 (36.0), (39.2) 41.3, 53.6, 61.4 (62.3), (66.2) 67.9, 79.7, (126.4) 127.0, (128.1) 128.6, 129.0 (129.2), 135.8 (137.2), 154.4 (155.4), 171.7 (172.4), (175.1) 174.4; HRMS calcd for  $\text{C}_{24}\text{H}_{38}\text{O}_4\text{N}_3$  ( $\text{MH}^+$ ) 432.2862, found 432.2849.

**General Procedure for Acetamide Synthesis.** A solution of *N*-(BOC)dipeptide *N*<sup>t</sup>-methylamide (20.5 mg, 0.05 mmol) in 25% TFA in CH<sub>2</sub>Cl<sub>2</sub> (1 mL) was stirred for 1 h and the solvent was evaporated. The residue was dissolved in CH<sub>2</sub>Cl<sub>2</sub> (1 mL), treated with K<sub>2</sub>CO<sub>3</sub> (65.6 mg, 0.5 mmol) and acetic anhydride (45 mL, 0.5 mmol) and stirred for 18 h. The solution was filtered, washed with CH<sub>2</sub>Cl<sub>2</sub> (2 × 5 mL) and evaporated to give the *N*-acetyl dipeptide *N*<sup>t</sup>-methylamide.

***N*-Acetyl-(2*R*)-alanyl-(2*S*, 5*R*)-5-*tert*-butylproline *N*<sup>t</sup>-Methylamide (*R*)-1a** was isolated in 98% yield as a white solid: mp 186-187 °C; [α]<sup>20</sup><sub>D</sub> -125.7° (c 0.4, CHCl<sub>3</sub>); <sup>1</sup>H NMR (CDCl<sub>3</sub>) δ 0.94 (s, 6.3 H) [1.0 (s, 2.7 H)], 1.29 (d, 2.1 H, *J* = 6.7) [1.35 (d, 0.9 H, *J* = 6.4)], 1.88 (m, 2 H), [1.99 (s, 0.9 H)] 2.05 (s, 2.1 H), 2.09 (m, 1 H), [2.29 (m, 0.3 H)] 2.69 (m, 0.7 H), 2.84 (d, 2.1 H, *J* = 4.6) [2.90 (d, 0.9 H, *J* = 4.4)], 3.79 (d, 0.7 H, *J* = 8.6) [4.30 (d, 0.3 H, *J* = 8.7)], [4.55 (t, 0.3 H, *J* = 7.0)] 4.60 (t, 0.7 H, *J* = 8.5), [4.73 (t, 0.3 H, *J* = 9.2)] 5.13 (m, 0.7 H), [6.20 (br s, 0.3 H)] 6.43 (d, 0.7 H, *J* = 6.8), [6.13 (br s, 0.3 H)] 7.34 (br s, 0.7 H); <sup>13</sup>C NMR (CDCl<sub>3</sub>) δ (18.4) 19.0, (22.6) 23.1, 25.2 (25.8), 26.1 (30.7), (26.2) 27.2, 27.3, 35.4 (36.2), (46.9) 47.1, 62.0 (62.2), (65.8) 67.6, 169.0 (170.2), 171.6 (172.7), 175.6 (175.9); HRMS calcd for C<sub>15</sub>H<sub>28</sub>O<sub>3</sub>N<sub>3</sub> (MH<sup>+</sup>) 298.2131, found 298.2120.

***N*-Acetyl-(2*R*)-leucyl-(2*S*, 5*R*)-5-*tert*-butylproline *N*<sup>t</sup>-Methylamide (*R*)-1b** was isolated in 92% yield as a white solid that was recrystallized from EtOAc and hexane: [α]<sup>20</sup><sub>D</sub> -73.8° (c 0.1, CHCl<sub>3</sub>); <sup>1</sup>H NMR (CDCl<sub>3</sub>) δ [0.87 (d, 1.2 H, *J* = 6.3)] 0.95 (d, 1.8 H, *J* = 8.5), [0.93 (d, 1.2 H, *J* = 6.2)] 1.05 (d, 1.8 H, *J* = 6.5), 0.96 (s, 5.4 H) [1.01 (s, 3.6 H)], [1.20 (m, 0.4 H)] 1.50 (m, 0.6 H), 1.79-1.96 (m, 2 H), [2.01 (s, 1.2 H)] 2.06 (s, 1.8 H), 2.08-2.16 (m, 2 H), 2.25 (m, 1 H), 2.65-2.75 (m, 1 H), 2.83 (d, 1.8 H, *J* = 4.8) [2.88 (d, 1.2 H, *J* = 4.8)], 3.80 (d, 0.6 H, *J* = 8.0) [4.27 (d, 0.4 H, *J* = 8.5)], 4.56-4.69 (m, 1.4 H), 5.21 (m, 0.6 H), [5.97 (d, 0.4 H, *J* = 9.4)] 6.19 (d, 0.6 H, *J* =

8.5), [6.31 (br s, 0.4 H)] 7.29 (br s, 0.6 H);  $^{13}\text{C}$  NMR ( $\text{CDCl}_3$ )  $\delta$  (20.9) 21.6, (22.9) 23.1, (23.2) 23.4, (24.4) 24.6, 25.1 (30.8), (25.9) 26.0, 26.1 (26.3), 27.2 (27.3), 35.3 (36.2), (41.4) 43.5, (49.3) 49.4, 61.8 (62.4), (65.8) 67.5, 169.3, 171.7 (172.6), 175.7; HRMS calcd for  $\text{C}_{18}\text{H}_{34}\text{O}_3\text{N}_3$  ( $\text{MH}^+$ ) 340.2600, found 340.2594.

**N-Acetyl-(2*R*)-phenylalanyl-(2*S*, 5*R*)-5-*tert*-butylproline *N*<sup>1</sup>-Methylamide (*R*)-1c** was isolated in 94% yield as a white solid: mp 96-97 °C;  $[\alpha]^{20}\text{D} -108.0^\circ$  (c 0.2,  $\text{CHCl}_3$ );  $^1\text{H}$  NMR ( $\text{CDCl}_3$ )  $\delta$  0.67 (m, 1 H), 0.79 (s, 7.2 H) [0.98 (s, 1.8 H)], 0.90 (m, 1 H), 1.58 (m, 1 H), 2.07 (s, 1.6 H) [1.91 (s, 1.4 H)], 2.38 (m, 1 H), 2.83 (d, 1.6 H,  $J = 4.8$ ), 2.85-2.89 (m, 2.4 H), 3.19 (dd, 0.8,  $J = 4.9, 12.7$ ) [3.27 (dd, 0.4 H,  $J = 5.0, 14.0$ )], 3.35 (dd, 0.8 H,  $J = 1.4, 8.7$ ) [4.74 (m, 0.2 H)], [4.33 (d, 0.2 H,  $J = 8.7$ ) 4.40 (m, 0.8 H), [4.80 (t, 0.2 H,  $J = 8.4$ ) 5.36 (m, 1 H), 6.36 (d, 1 H,  $J = 8.1$ ), 7.19-7.36 (m, 5 H), [6.06 (br s, 0.2 H)] 7.37 (br s, 0.8 H);  $^{13}\text{C}$  NMR ( $\text{CDCl}_3$ )  $\delta$  23.2, 24.7 (24.8), 26.3 (26.5), 26.7, 27.4, 35.2, 41.0, 52.5, 61.7, 68.0, 127.3, (128.4) 128.7, (128.5) 129.2, 135.7, 168.9, 171.7, 174.4; HRMS calcd for  $\text{C}_{21}\text{H}_{32}\text{O}_3\text{N}_3$  ( $\text{MH}^+$ ) 374.2444, found 374.2434.

**General Protocol For The Synthesis of *N*-Acetyl Dipeptide *N*<sup>1</sup>-Methylamides Possessing Natural Proline.** A solution of *N*-(BOC)-D-amino acid (2.1 mmol) in  $\text{CH}_3\text{CN}$  (10 mL) was treated with DIEA (0.7 mL, 4.4 mmol), proline *N*<sup>1</sup>-methylamide hydrochloride (150 mg, 1.1 mmol) and TBTU (0.68 g, 2.2 mmol), stirred at room temperature for 18 h, and partitioned between brine (10 mL) and EtOAc (10 mL). The organic phase was washed with 0.1 M HCl (2 × 8 mL), 5% NaHCO<sub>3</sub> (2 × 8 mL), and brine (10 mL), dried, and evaporated to a residue that was purified by chromatography on silica gel (35% EtOAc in hexane). The *N*-(BOC)dipeptide *N*<sup>1</sup>-methylamide was treated with 25% TFA in  $\text{CH}_2\text{Cl}_2$  (10 mL) for 1 h and evaporated.

The resulting dipeptide *N*<sup>o</sup>-methylamide trifluoroacetate was dissolved in CH<sub>2</sub>Cl<sub>2</sub> and treated in the same acetylation conditions as described above.

***N*-Acetyl-(2*R*)-alanylproline *N*<sup>o</sup>-Methylamide (*R*)-2a** was isolated as a white precipitate in 56% overall yield for the 3 steps:  $[\alpha]^{20}_D -61.6^\circ$  (c 0.7, CHCl<sub>3</sub>); <sup>1</sup>H NMR (CDCl<sub>3</sub>) δ [1.31 (d, 0.18 H, *J* = 6.8)] 1.39 (d, 2.82 H, *J* = 6.9), 1.94-2.04 (m, 1 H), 2.05 (s, 3 H), 2.06-2.15 (m, 2 H), 2.42 (m, 1 H), 2.81 (d, 2.82 H, *J* = 4.8) [2.90 (d, 0.18 H, *J* = 4.7)], 3.51 (q, 0.94 H, *J* = 6.9, 9.4) [3.66 (m, 0.06 H), 3.92 (m, 1 H), 4.62 (m, 1.88 H) [4.71 (m, 0.12 H)], 6.30 (d, 1 H, *J* = 5.1), 6.90 (br s, 1 H); <sup>13</sup>C NMR (CDCl<sub>3</sub>) δ 16.1, 22.3, 24.0, 26.2, 29.0, 46.9, 47.6, 60.6, 171.3, 171.5, 172.5; HRMS calcd for C<sub>11</sub>H<sub>20</sub>O<sub>3</sub>N<sub>3</sub> (MH<sup>+</sup>) 242.1505, found 242.1498.

***N*-Acetyl-(2*R*)-leucylproline *N*<sup>o</sup>-Methylamide (*R*)-2b** was isolated as an oil in 52% overall yield for the 3 steps:  $[\alpha]^{20}_D -52.4^\circ$  (c 0.5, CHCl<sub>3</sub>); <sup>1</sup>H NMR (CDCl<sub>3</sub>) δ [0.89 (d, 0.3 H, *J* = 6.6), 0.93 (d, 0.3 H, *J* = 6.6)] 1.01 (d, 5.4 H, *J* = 6.6), 1.52 (m, 1 H), 1.73 (m, 1 H), 2.03 (m, 1 H), 2.05 (s, 3 H), 2.41 (m, 1 H), 2.79 (d, 2.7 H, *J* = 4.8) [2.88 (d, 0.3 H, *J* = 4.8)], 3.50 (m, 0.9 H) [4.63 (m, 0.1 H), 4.00 (m, 1 H), 4.60 (m, 1.8 H) [4.65 (m, 0.1 H), 4.73 (m, 0.1 H)], 6.19 (d, 1 H, *J* = 6.6), 6.95 (br s, 1 H); <sup>13</sup>C NMR (CDCl<sub>3</sub>) δ 21.6, 22.2, 23.2, 23.9, 24.5, 26.1, 29.1, 39.6, 46.8, 50.6, 60.7, 171.5, 172.0, 172.6; HRMS calcd for C<sub>14</sub>H<sub>26</sub>O<sub>3</sub>N<sub>3</sub> (MH<sup>+</sup>) 284.1974, found 284.1983.

***N*-Acetyl-(2*R*)-phenylalanylproline *N*<sup>o</sup>-Methylamide (*R*)-2c** was isolated as an oil in 75% overall yield for the 3 steps:  $[\alpha]^{20}_D -107.2^\circ$  (c 0.6, CHCl<sub>3</sub>); <sup>1</sup>H NMR (CDCl<sub>3</sub>) δ 1.60 (m, 1 H), 1.65 (m, 1 H), 1.84 (m, 1 H), 2.04 (s, 3 H), 2.26 (m, 1 H), 2.63 (m, 1 H), [2.76 (d, 0.1 H, *J* = 5.1)] 2.78 (d, 2.9 H, *J* = 4.8), 3.05 (m, 2 H), 3.66 (m, 1 H), 4.49 (d, 1 H, *J* = 8.1), 4.71 (m, 1 H), 6.31 (d, 1 H, *J* = 5.9), 6.91 (br s, 1 H), 7.25-7.36 (m, 5 H); <sup>13</sup>C NMR (CDCl<sub>3</sub>) δ 22.1, 23.6, 26.1, 28.9, 37.3, 46.6, 54.1,

60.5, 127.2, 128.5, 129.1, 135.6, 171.6, 171.8; HRMS calcd for C<sub>17</sub>H<sub>24</sub>O<sub>3</sub>N<sub>3</sub> (MH<sup>+</sup>) 318.1818, found 318.1832.

**Acknowledgment:** This research was supported in part by the Natural Sciences and Engineering Research Council of Canada, the Ministère de l'Éducation du Québec, and the DuPont Educational Aid Program. We thank Sylvie Bilodeau and Dr. M. T. Phan Viet of the Regional High-Field NMR Laboratory for their assistance. The crystal structure analysis of compounds (*S*)- and (*R*)-**1b** were performed by Francine Bélanger-Gariépy at l'Université de Montréal X-ray facility.

**Notes:** § The interatomic distance between the  $\alpha$ -carbons of the *i* and *i* + 3 residues in a  $\beta$ -turn conformation has been defined to be between 4-7 Å [45].

# The structure of (*R*)-**1b** was solved at l'Université de Montréal X-ray facility using direct methods (SHELXS96) and refined with NRCVAX and SHELXL96: [C<sub>18</sub>H<sub>33</sub>N<sub>3</sub>O<sub>3</sub>]<sub>2</sub> [C<sub>4</sub>H<sub>8</sub>O<sub>2</sub>]; M<sub>r</sub> = 767.052; orthorhombic, colorless crystal; space group P2<sub>1</sub>2<sub>1</sub>2<sub>1</sub>; unit cell dimensions (Å) a = 9.685 (3), b = 18.001 (11), c = 26.586 (17); volume of unit cell (Å<sup>3</sup>) 4635 (4); Z = 4; R<sub>1</sub> = 0.0619 for F<sup>2</sup>>2 sigma(F<sup>2</sup>), wR<sub>2</sub> = 0.1534 for all data; GOF = 1.056. The author has deposited the atomic coordinates for the structure of (*R*)-**1b** with the Cambridge Crystallographic Data Center. The coordinates can be obtained, on request, from the Cambridge Crystallographic Data Center, 12 Union Road, Cambridge, CB2 1EZ, UK.

## 2.21. References

1. Wilmot, C. M. & Thornton, J. M. (1988) Analysis and prediction of the different types of  $\beta$ -turn in proteins. *J. Mol. Biol.* **203**, 221-232.
2. Rose, G. D., Giersch, L. M. & Smith, J. A. (1985) Turns in peptides and proteins. *Advan. Protein Chem.* **37**, 1-109.

3. Hanessian, S., McNaughton-Smith, G., Lombart, H.-G. & Lubell, W. D. (1997) Design and synthesis of conformationally constrained amino acids as versatile scaffolds and peptide mimetics. *Tetrahedron* **53**, 12789-12854.
4. Gillespie, P., Cicariello, J. & Olson, G. L. (1997) Conformation analysis of dipeptide mimetics. *Biopolymers, Peptide Science* **43**, 191-217.
5. Takeuchi, Y. & Marshall, G. R. (1998) Conformational analysis of reverse-turn constraints by N-methylation and N-hydroxylation of amide bonds in peptides and non-peptide mimetics. *J. Am. Chem. Soc.* **120**, 5363-5372.
6. Baures, P. W., Ojala, W. H., Gleason, W. B. & Johnson, R. L. (1997) Conformational analysis of homochiral and heterochiral diprolines as  $\beta$ -turn-forming pepidomimetics: Unsubstituted and substituted models. *J. Pept. Res.* **50**, 1-13.
7. Beausoleil, E. & Lubell, W. D. (1996) Steric effects on the amide isomer equilibrium of prolyl peptides. Synthesis and conformational analysis of *N*-acetyl-5-*tert*-butylproline *N'*-methylamides. *J. Am. Chem. Soc.* **118**, 12902-12908.
8. Beausoleil, E., Sharma, R., Michnick, S. & Lubell, W. D. (1998) Alkyl 3-position substituents retard the isomerization of prolyl and hydroxyprolyl amides in water. *J. Org. Chem.* **63**, 6572-6578.
9. Halab, L. & Lubell, W. D. (1999) Use of steric interactions to control peptide turn geometry. Synthesis of type VI  $\beta$ -turn mimics with 5-*tert*-butylproline. *J. Org. Chem.* **64**, 3312-3321.
10. Halab, L. & Lubell, W. D. (1999) Steric effects of 5-*tert*-butylproline in dipeptide mimics of type VI  $\beta$ -turns. In *Peptides 1998, Proc. Eur. Pept. Symp., 25th* (Bajusz, S. & Hudecz, F., eds). Akadémia Kiadò, Budapest, Hungary, pp. 356-357.

11. Halab, L. & Lubell, W. D. (2000) The effects of stereochemistry and sequences on 5-*tert*-butylproline type VI  $\beta$ -turn mimics. In *Peptides 1999, Proc. Am. Pept. Symp., 16th* (Fields, G. B. & Barany, G., eds.) in press.
12. Beausoleil, E. & Lubell, W. D. (2000) An examination of the steric effects of 5-*tert*-butylproline on the conformation of polyproline and the cooperative nature of type II to type I helical interconversion. *Biopolymers* **53**, 249-256.
13. Overberger, C. G. & Jon, Y. S. J. (1977) Synthesis and solution properties of poly(2-methylproline). *J. Polym. Sci.: Polym. Chem. Ed.* **15**, 1413-1421.
14. Bélec, L., Slaninova, J. & Lubell, W. D. (2000) A study of the relationship between biological activity and prolyl amide isomer geometry in oxytocin using 5-*tert*-butylproline to augment the Cys<sup>6</sup>-Pro<sup>7</sup> amide *cis*-isomer population. *J. Med. Chem.* **43**, 1448-1455.
15. Keller, M., Sager, C., Dumy, P., Schutkowski, M., Fischer, G. S. & Mutter, M. (1998) Enhancing the proline effect: Pseudo-prolines for tailoring *cis/trans* isomerization. *J. Am. Chem. Soc.* **120**, 2714-2720.
16. Delaney, N. G. & Madison, V. (1982) Unusual *cis-trans* isomerism in *N*-acetyl, *N*-methylamide derivatives of *syn*- and *anti*-5-methylproline. *Int. J. Peptide Protein Res.* **19**, 543-548.
17. Magaard, V. W., Sanchez, R. M., Bean, J. W. & Moore, M. L. (1993) A convenient synthesis of the conformationally constrained amino acid 5,5-dimethylproline. *Tetrahedron Lett.* **34**, 381-384.
18. An, S. S. A., Lester, C. C., Peng, J.-L., Li, Y.-J., Rothwarf, D. M., Welker, E., Thannhauser, T. W., Zhang, L. S., Tam, J. P. & Scheraga, H. A. (1999) Retention of the *cis* proline conformation in tripeptide fragments of bovine pancreatic Ribonuclease A containing a non-natural proline analogue, 5,5-dimethylproline. *J. Am. Chem. Soc.* **121**, 11558-11566.

19. Wüthrich, K., Grathwohl, C. & Schwyzer, R. (1974) Cis, trans, and nonplanar peptide bonds in oligopeptides:  $^{13}\text{C}$  NMR studies. *Peptides Polypeptides and Proteins*. Wiley-Interscience, pp.300-307.
20. Aubry, A., Protas, J., Boussard, G. & Marraud, M. (1979) Conformation repliée à l'état solide de la *N*-pivaloyl-D-alanyl- L-proline *N*-isopropylamide. *Acta Cryst. B* **35**, 694-699.
21. Haque, T. S., Little, J. C. & Gellman, S. H. (1996) Stereochemical requirements for  $\beta$ -hairpin formation: Model studies with four-residue peptides and depsipeptides. *J. Am. Chem. Soc.* **118**, 6975-6985.
22. Giersch, L. M., Deber, C. M., Madison, V., Niu, C.-H. & Blout, E. R. (1981) Conformations of (X- L-Pro-Y)<sub>2</sub> cyclic hexapeptides. Preferred  $\beta$ -turn conformers and implications for  $\beta$ -turns in proteins. *Biochemistry* **20**, 4730-4738.
23. Karle, I. L. (1978) Crystal structure and conformation of cyclo-(glycylprolylglycyl-D-alanylprolyl) containing 4→1 and 3→1 intramolecular hydrogen bonds. *J. Am. Chem. Soc.* **100**, 1286-1289.
24. Pease, L. G., Niu, C. H. & Zimmermann, G. (1979) Solution conformation of cyclo-(Gly-Pro-Ser-D-Ala-Pro). Hydrogen-bonded reverse turns in cyclic pentapeptides. *J. Am. Chem. Soc.* **101**, 184-191.
25. Müller, G., Gurrath, M., Kurz, M. & Kessler, H. (1993)  $\beta$ VI turns in peptides and proteins: A model peptide mimicry. *Proteins: Structure, Function and Genetics* **15**, 235-251.
26. Johnson, M. E., Lin, Z., Padmanabhan, K., Tulinsky, A. & Kahn, M. (1994) Conformational rearrangements required of the V3 loop of HIV-1 gp120 for proteolytic cleavage and infection. *FEBS Lett.* **337**, 4-8.

27. Fischer, S., Michnick, S. & Karplus, M. (1993) A mechanism for rotamase catalysis by the FK506 binding protein (FKBP). *Biochemistry* **32**, 13830-13837.
28. Kallen, J. & Walkinshaw, M. D. (1992) The X-ray structure of a tetrapeptide bound to the active site of human cyclophilin A. *FEBS Lett.* **300**, 286-290.
29. Fischer, G. (1994) Peptidyl-prolyl *cis/trans* isomerases and their effectors. *Angew. Chem. Int. Ed. Engl.* **33**, 1415-1436.
30. Liu, J., Chen, C.-M. & Walsh, C. T. (1991) Human and Escherichia coli cyclophilins: Sensitivity to inhibition by *Biochemistry* **30**, 2306-2310.
31. Beausoleil, E., L'Archevêque, B., Bélec, L., Atfani, M. & Lubell, W. D. (1996) 5-*tert*-Butylproline. *J. Org. Chem.* **61**, 9447-9454.
32. Yao, J., Brüschweiler, R., Dyson, H. J. & Wright, P. E. (1994) Differential side chain hydration in a linear peptide containing a type VI turn. *J. Am. Chem. Soc.* **116**, 12051-12052.
33. Dyson, H. J., Rance, M., Houghten, R. A., Lerner, R. A. & Wright, P. E. (1988) Folding of immunogenic peptide fragments of proteins in water solution. *J. Mol. Biol.* **201**, 161-200.
34. Oka, M., Montelione, G. T. & Scheraga, H. A. (1984) Chain-folding initiation structures in Ribonuclease A: Conformational free energy calculations on Ac-Asn-Pro-Tyr-NHMe, Ac-Tyr-Pro-Asn-NHMe, and related peptides. *J. Am. Chem. Soc.* **106**, 7959-7969.
35. Wu, W.-J. & Raleigh, D. P. (1998) Local control of peptide conformation: Stabilization of *cis* proline peptide bonds by aromatic proline interactions. *Biopolymers* **45**, 381-394.
36. Chalmers, D. K. & Marshall, G. R. (1995) Pro-D-NMe-amino acid and D-Pro-NMe-amino acid: Simple, efficient reverse-turn constraints. *J. Am. Chem. Soc.* **117**, 5927-5937.

37. Pardi, A., Billeter, M., Wüthrich, K. (1984) Calibration of the angular dependence of the amide proton-C<sup>α</sup> proton coupling constants,  $^3J_{\text{NH}\alpha}$ , in a globular protein. *J. Mol. Biol.* **180**, 741-751.
38. Woody, R. W. (1974) Studies of theoretical circular dichroism of polypeptides: Contributions of β-turns. In *Peptides, Polypeptides and Proteins* (Blout, E. R., Bovey, F. A., Goodman, M. & Lotan, N., Eds). John Wiley, Inc., New York, pp. 338-348.
39. Brahms, S. & Brahms, J. (1980) Determination of protein secondary structure in solution by vacuum ultraviolet circular dichroism. *J. Mol. Biol.* **138**, 149-178.
40. Kawai, M. & Nagai, U (1978) Comparison of conformation and antimicrobial activity of synthetic analogs of Gramicidin S: Stereochemical consideration of the role of D-phenylalanine in the antibiotic. *Biopolymers* **17**, 1549-1565.
41. Bush, C. A., Sarkar, S. K. & Kopple, K. D. (1978) Circular Dichroism of β Turns in Peptides and Proteins. *Biochemistry* **17**, 4951-4954.
42. Madison, V. & Kopple, K. D. (1980) Solvent-dependent conformational distributions of some dipeptides. *J. Am. Chem. Soc.* **102**, 4855-4863.
43. Eggleston, D. S., Baures, P. W., Peishoff, C. E. & Kopple, K. D. (1991) Conformations of cyclic heptapeptides: Crystal structure and computational studies of evolidine. *J. Am. Chem. Soc.* **113**, 4410-4416.
44. Epp, O., Lattman, E. E., Schiffer, M., Huber, R. & Palm, W. (1975) The molecular structure of a dimer composed of the variable portions of the Bence-Jones protein REI refined at 2.0-Å resolution. *Biochemistry* **14**, 4943-4952.
45. Venkatachalam, C. M. (1968) Stereochemical criteria for polypeptides and proteins. V. Conformation of a system of three linked peptide units. *Biopolymers* **6**, 4951-4954.

## **CHAPITRE 3**

**Repliement  $\beta$  de type VI: Effet de séquence et  
formation d'épinglé  $\beta$ .**

Dans ce chapitre, l'importance de la séquence d'acides aminés d'un peptide sur sa conformation sera décrite. De plus, l'incorporation de mimétiques de repliement  $\beta$  de type VIa dans des tétrapeptides par synthèse peptidique sur support solide sera présentée afin d'étudier l'effet de la séquence sur la stabilisation de ces peptides dans la conformation d'épingle  $\beta$ .

### 3.1. Séquence et conformation

La conformation d'un peptide dépend de sa structure primaire et ainsi de sa séquence d'acides aminés. L'observation courante de certains acides aminés à l'intérieur de séquences spécifiques a amené au développement d'une approche statistique pour déterminer la structure secondaire des protéines.<sup>1</sup> En effet, des analyses statistiques ont été rapportées basées sur les structures rayons-X des peptides et des protéines montrant les préférences de séquences d'acides aminés dans les différents types de repliement  $\beta$ .<sup>2</sup> Par exemple, dans le repliement  $\beta$  de type I, la position  $i$  du tour est favorisée par des résidus possédant une chaîne latérale pouvant participer dans des ponts d'hydrogène tels que l'acide aspartique, l'asparagine, la sérine ou la cystéine.<sup>2</sup> La proline est l'acide aminé le plus commun à la position  $i + 1$ .<sup>2</sup> Cependant, il est encore difficile de prédire la structure secondaire d'un peptide avec sa séquence d'acide aminé puisque la structure secondaire d'un peptide dépend de son milieu.<sup>3</sup>

Les articles qui suivent présentent l'effet de la séquence d'acide aminé sur la conformation des mimétiques de repliement  $\beta$  de type VIa. Une étude de la possibilité d'induire une géométrie d'épingle  $\beta$  en utilisant les interactions stériques de la 5-*tert*-butylproline a été réalisée. Dans une série de dipeptides *N*-acétyle *N'*-méthylamide, Ac-Xaa-5-*t*BuPro-NHMe, une augmentation de la population d'isomère *cis* a été observée par la variation de la chaîne latérale de l'acide aminé Xaa, d'un groupement pouvant former un pont d'hydrogène à un groupement alkyle à un groupement aromatique. Nous avons démontré que les interactions stériques de la 5-*tert*-butylproline peuvent favoriser la formation de repliement  $\beta$  de type VIa dans des tétrapeptides *N*-acétyle méthylester. Encore une fois, l'importance de la séquence

du térapéptide a été démontrée en étudiant l'effet des différents acides aminés à chaque position.

### **3.2. L'Épinglé $\beta$**

À ce point, nous avons voulu présenter une description de la conformation d'une épingle  $\beta$  afin que le lecteur ait une plus grande connaissance de cette structure secondaire. L'épingle  $\beta$  est une forme simple de la conformation de feuillets plissés  $\beta$  antiparallèles. C'est une structure secondaire qui est définie par deux chaînes polypeptidiques antiparallèles, reliées entre eux par une boucle. Les différents types d'épingles  $\beta$  sont classés selon le motif de pont d'hydrogène et le nombre de résidus impliqués dans le tour (Figure 1).<sup>4a</sup> L'épingle  $\beta$  le plus commun possède deux résidus dans le tour (Figure 1a).<sup>4a</sup> Pour chaque classe d'épingle  $\beta$ , deux catégories existent dépendante sur le nombre de ponts d'hydrogène. Ainsi, deux numéros X : Y sont utilisés pour classer les épingles  $\beta$ . Si les résidus près de la boucle forment deux ponts d'hydrogène, alors X = Y. Si le premier pont d'hydrogène n'est pas formé, alors Y = X + 2. Alors, le plus court peptide adoptant la conformation d'épingle  $\beta$  devrait posséder quatre résidus d'acides aminés et la formation de deux ponts d'hydrogène intramoléculaire. La région de connectivité du tour est induite par des replis  $\beta$  dans les protéines.<sup>4b</sup> D'après les banques de données cristallines des protéines, la formation d'épingle  $\beta$  est induite principalement par les replis  $\beta$  de type I' et II'.<sup>4</sup>

#### **3.2.1. Épinglé $\beta$ induit par la séquence du peptide**

Peu d'exemples sont connus de peptides courts et linéaires contenant des acides L-aminés dans leur séquence qui se replient pour adopter une conformation d'épingle  $\beta$ . À part un exemple d'un peptide naturel, un fragment de la protéine tendamistat, qui adoptent un épingle  $\beta$  dans l'eau, le design de peptides a fourni une plus grande capacité de comprendre la conformation d'épingle  $\beta$ .<sup>5</sup>

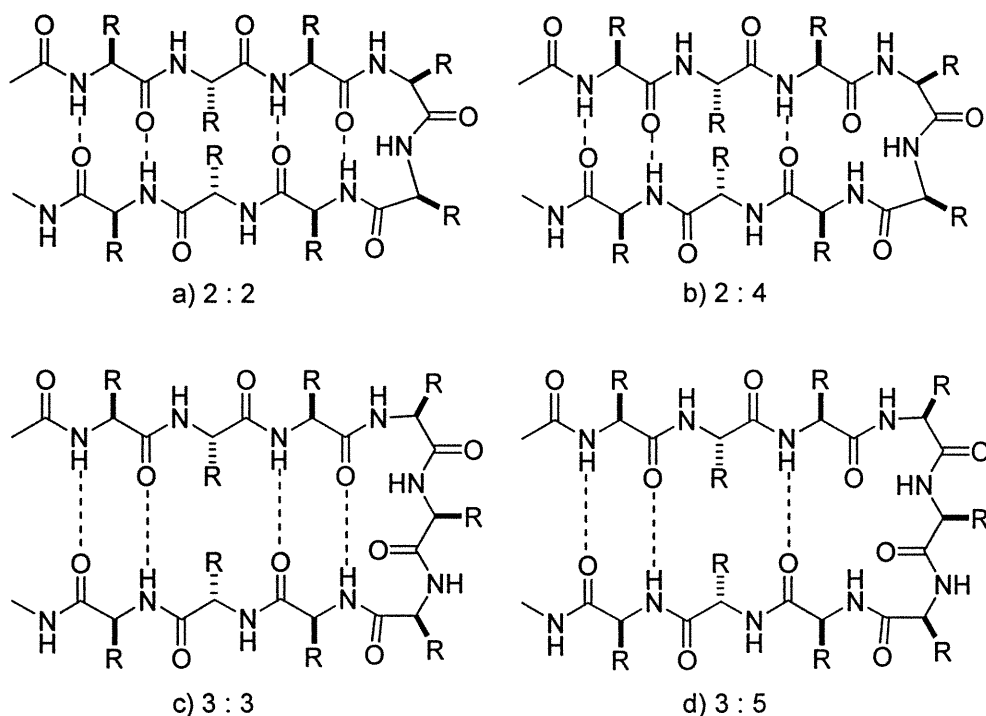


**Figure 1.** Représentation des différentes classes de structures épingle  $\beta$ .

Deux stratégies ont été présentées récemment pour l'induction d'épingle  $\beta$  dans des peptides avec une boucle de deux résidus. L'utilisation des séquences L-Asn-Gly<sup>6</sup> et D-Pro-Xaa<sup>7-8</sup> dans des peptides stabilisent la conformation d'épingle  $\beta$  en milieu aqueux. Selon les banques de données de rayons-X des protéines, ces deux séquences favorisent la formation de repliement  $\beta$  de type I' ou II' dans des peptides.<sup>2</sup>

### **3.2.2. Mimétique d'épinglé $\beta$**

Une approche alternative pour le design d'épingle  $\beta$  et ainsi de feuillets plissés  $\beta$  consiste à introduire des mimétiques pour contraindre la conformation du squelette peptidique. Des structures basées sur des noyaux aromatiques tels que le biphenyle (1),<sup>9b</sup> le dibenzofurane (2)<sup>9c</sup> et les analogues de 3<sup>10</sup> ont été introduits dans des peptides (Figure 2). Ces derniers ont démontré une stabilisation de structure  $\beta$  par la formation de ponts d'hydrogène intramoléculaire des chaînes peptidiques.<sup>9</sup>

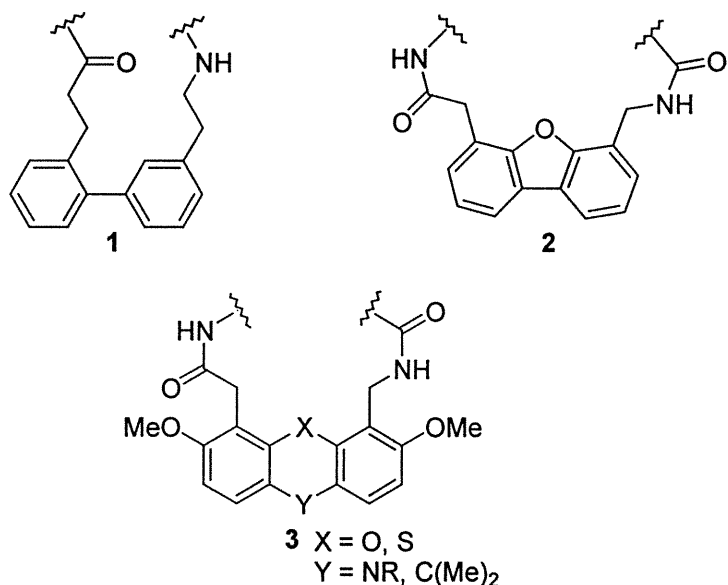


**Figure 2.** Représentation de mimétiques d'épingles  $\beta$  basés sur des systèmes aromatiques.

D'autres mimétiques ont aussi été développés afin de stabiliser la boucle et induire la conformation d'épingle  $\beta$  (Figure 3). Il a été montré par la spectroscopie IR et RMN dans le dichlorométhane que le peptide **4** qui possède deux résidus d'acide nipécolique, un acide  $\beta$ -aminé, induit la conformation d'épingle  $\beta$ .<sup>11</sup> Le peptide **5** qui contient une diurée permet également de stabiliser une conformation en épingle  $\beta$  dans le chloroforme (analyse RMN).<sup>12</sup> D'autres stratégies ont impliqué l'incorporation d'alcène di- ou tétra-substitué dans des peptides (**6-7**) afin de stabiliser une conformation d'épingle  $\beta$ .<sup>13</sup>

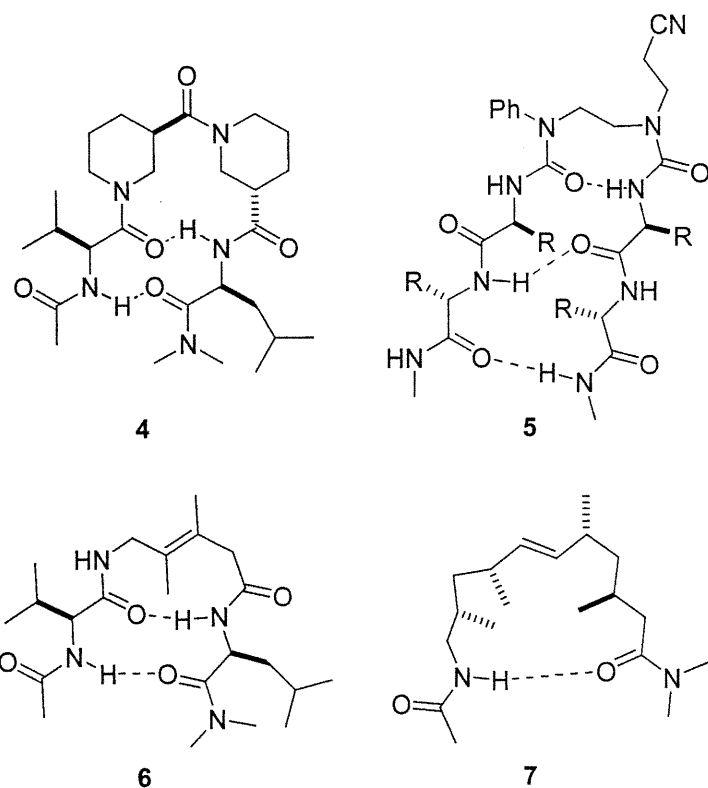


**Figure 3.** Représentations de mimétiques d'épingle  $\beta$ .

D'autre part, des analogues basés sur la proline ont été synthétisés et incorporés dans des peptides pour induire une conformation d'épingle  $\beta$  (Figure 4).<sup>10,14</sup> Le lactame bicyclique **8**, un mimétique de repliement  $\beta$  de type VI, a induit une stabilisation d'épingle  $\beta$  dans des peptides linéaires et cycliques.<sup>10</sup>

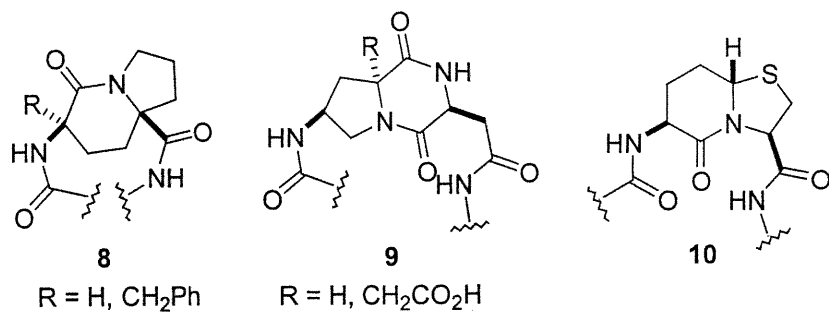


**Figure 4.** Représentation de mimétiques d'épingles  $\beta$  basés sur des prolines.

### 3.3. Références

1. (a) Guzzo, A.V. *Biophys. J.* **1965**, *5*, 809. (b) Prothero, J.W. *Biophys. J.* **1966**, *6*, 367. (c) Chou, P.Y.; Fasman, G.D. *Adv. Enzymol.* **1978**, *47*, 45.
2. (a) Wilmot, C.M.; Thornton, J.M. *J. Mol. Biol.* **1988**, *203*, 221. (b) Hutchinson, E.G.; Thornton, J.M. *Protein Sci.* **1994**, *3*, 2207.
3. Forsythe, K.H.; Hopfinger, A.J. *Macromolecules* **1973**, *6*, 423.
4. (a) Sibanda, B.L.; Thornton, J.M. *J. Mol. Biol.* **1993**, *229*, 428. (b) Sibanda, B.L.; Thornton, J.M. *Nature* **1985**, *316*, 170.
5. Revue dans: (a) Gellman, S.H. *Curr. Opin. Chem. Biol.* **1998**, *2*, 717. (b) Lacroix, E.; Kortemme, T.; Lopez de la Paz, M.; Serrano, L. *Curr. Opin. Struct. Biol.* **1999**, *9*, 487.
6. (a) Ramírez-Alvarado, M.; Blanco, F.J.; Serrano, L. *Nat. Struct. Biol.* **1996**, *3*, 604. (b) Kortemme, T.; Ramírez-Alvarado, M.; Serrano, L. *Science* **1998**, *281*, 253. (c) de Alba, E.; Jimenez, M.A.; Rico, M. *J. Am. Chem. Soc.* **1997**, *119*, 175. (d) Maynard, A.J.; Searle, M.S. *J. Chem. Soc., Chem. Commun.* **1997**, 1297. (e) Colley, C.S.; Griffiths-Jones, S.R.; George, M.W.; Searle, M.S. *J. Chem. Soc., Chem. Commun.* **2000**, 593.
7. (a) Stanger, H.E.; Gellman, S.H. *J. Am. Chem. Soc.* **1998**, *120*, 4236. (b) Schenck, H.L.; Gellman, S.H. *J. Am. Chem. Soc.* **1998**, *120*, 4869. (c) Fisk, J.D.; Powell, D.R.; Gellman, S.H. *J. Am. Chem. Soc.* **2000**, *122*, 5443. (d) Fisk, J.D.; Gellman, S.H. *J. Am. Chem. Soc.* **2001**, *123*, 343. (e) Haque, T.S.; Little, J.C.; Gellman, S.H. *J. Am. Chem. Soc.* **1994**, *116*, 4105. (f) Haque, T.S.; Little, J.C.; Gellman, S.H. *J. Am. Chem. Soc.* **1996**, *118*, 6975.
8. (a) Das, C.; Raghorthama, S.; Balaram, P. *J. Chem. Soc., Chem. Commun.* **1999**, 967. (b) Das, C.; Raghorthama, S.; Balaram, P. *J. Am. Chem. Soc.* **1998**, *120*, 5812. (c) Raghorthama, S.R.; Awasthi, S.K.; Balaram, P. *J. Chem. Soc., Perkin Trans. 2* **1998**, 137.

9. (a) Revue dans: Schneider, J.P.; Kelly, J.W. *Chem. Rev.* **1995**, *95*, 2169. (b) Nesloney, C.L.; Kelly, J.W. *J. Am. Chem. Soc.* **1996**, *118*, 5836. (c) Tsang, K.Y.; Diaz, H.; Graciani, N.; Kelly, J.W. *J. Am. Chem. Soc.* **1994**, *116*, 3988.
10. Robinson, J.A. *Synlett* **1999**, 429.
11. (a) Huck, B.R.; Fisk, J.D.; Gellman, S.H. *Org. Lett.* **2000**, *2*, 2607. (b) Chung, Y.J.; Christianson, L.A.; Stanger, H.E.; Powell, D.R.; Gellman, S.H. *J. Am. Chem. Soc.* **1998**, *120*, 10555.
12. (a) Revue dans: Nowick, J.S. *Acc. Chem. Soc.* **1999**, *32*, 287. (b) Holmes, D.L.; Smith, E.M.; Nowick, J.S. *J. Am. Chem. Soc.* **1997**, *119*, 7665.
13. (a) Gardner, R.R.; Liang, G.-B.; Gellman, S.H. *J. Am. Chem. Soc.* **1995**, *117*, 3280. (b) Schopfer, U.; Stahl, M.; Brandl, T.; Hoffmann, R.W. *Angew. Chem. Int. Ed. Engl.* **1997**, *36*, 1745.
14. (a) Sato, K.; Nagai, U. *J. Chem. Soc., Perkin Trans I* **1986**, 1231. (b) Bach, II, A.C.; Markwalder, J.A.; Ripka, W.C. *Int. J. Peptide Protein Res.* **1991**, *38*, 314.

**Article 6**

Halab, L.; Lubell, W. D. "Stabilization of Type VIa  $\beta$ -Turn in Tetrapeptides." Publié dans *Peptides 2000 Proceedings of the 26<sup>th</sup> European Peptide Symposium*, J. Martinez & J.-A. Fehrentz, Eds; Montpellier, France, 2001, 815-816.

## Stabilization of Type VIa $\beta$ -Turn in Tetrapeptides

Liliane Halab and William D. Lubell\*

*Département de chimie, Université de Montréal*

*C. P. 6128, Succursale Centre-Ville, Montréal, Québec, Canada H3C 3J7*

### **3.4. Introduction**

The steric interactions of (2S, 5R)-5-*tert*-butylproline (5-*t*BuPro) have previously been employed to stabilize type VI  $\beta$ -turns in *N*-(acetyl)-dipeptide *N*-methylamides [1]. In Ac-Xaa-5-*t*BuPro-NHMe dipeptides, the prolyl amide *cis*-isomer was present in the dominant conformer which was shown by NMR, CD and X-ray analysis to adopt respectively type VIa and VIb  $\beta$ -turns as the *N*-terminal residue stereochemistry varied from L- to D-configuration [2]. To probe further the factors stabilizing type VIa  $\beta$ -turns in peptides, we have now incorporated 5-*t*BuPro into a series of tetrapeptides possessing the general structure of Ac-Ala-Xaa-5-*t*BuPro-Yaa-ZMe. Using this model peptide, we have investigated the importance of the nature of the amino acids on either side of the 5-*t*BuPro residue. Moreover, replacement of the *N*-methylamide (Z = NH) with its methyl ester counterpart (Z = O) had a significant influence on peptide folding.

### **3.5. Results and Discussion**

Tetrapeptides containing Pro and 5-*t*BuPro were synthesized using a combination of solution- and solid-phase peptide chemistry. In solution, *N*-(BOC)-Xaa-5-*t*BuPro (Xaa = Ala, Leu, Phe) dipeptides were synthesized by acylation of 5-*t*BuPro-OBn with *N*-(BOC)-Xaa, BOP-Cl and DIEA in CH<sub>2</sub>Cl<sub>2</sub> followed by benzyl ester cleavage with H<sub>2</sub>, Pd/C in MeOH. Oxime resin was used as the solid support. The BOC protected amino acids and dipeptides were coupled using TBTU and DIEA in DMF. The BOC protection was removed with 25% TFA in CH<sub>2</sub>Cl<sub>2</sub> followed by neutralization with 10% DIEA in CH<sub>2</sub>Cl<sub>2</sub>. Acetylation was performed with Ac<sub>2</sub>O and DIEA in CH<sub>2</sub>Cl<sub>2</sub>. The final tetrapeptides were cleaved from oxime resin to furnish the *C*-terminal *N*-methylamides and methyl esters by respectively using CH<sub>3</sub>NH<sub>2</sub> in

CHCl<sub>3</sub> and Ca(OAc)<sub>2</sub> in MeOH:THF at 40 °C. The tetrapeptides were isolated in 21–61% overall yields (based on initial resin loading) after purification on C<sub>18</sub> reverse-phase HPLC.

The amide isomer populations were ascertained by measuring the integrals for the *N*<sup>1</sup>-methylamide and methyl ester signals in the proton NMR spectra (Table 1). The *cis*-isomer population in the 5-*t*BuPro-tetrapeptides varied from 43% to 84% in water. In the *N*-acetyl tetrapeptide *N*<sup>1</sup>-methylamides, a significant augmentation of the *cis*-isomer population occurred when Phe was *N*-terminal to 5-*t*BuPro such that the major conformation possessed an amide *cis*-isomer. On the contrary, variations C-terminal to 5-*t*BuPro caused no significant effect on the isomer population. Replacement of the *N*<sup>1</sup>-methylamide by its methyl ester counterpart augmented significantly (16–26%) the 5-*t*BuPro-tetrapeptide *cis*-isomer population.

Temperature coefficient values for the amide NH protons in four tetrapeptides were measured in water to determine the presence of hydrogen-bonds in turn and hairpin conformations (Table 2). Because the values were significantly greater for the Ala and Yaa amide proton signals relative to the Xaa amide and NHMe proton signals, we may infer that the major *cis*-amide isomer of the 5-*t*BuPro tetrapeptides adopts a type VI β-hairpin conformation. On the other hand, the values for the amides of the Pro tetrapeptides were not indicative of a particular conformation for the major *trans*-conformer of Ac-Ala-Phe-Pro-Ala-NHMe, yet may support a β-turn conformation centered at the Phe-Pro residue of Ac-Ala-Phe-Pro-Ala-OMe.

These preliminary results demonstrate that the Phe-5-*t*BuPro tetrapeptides possessed dominant *cis*-isomer populations and stabilized type VIa β-hairpin conformations. Replacement of the methyl amide at the *C*-terminus by its methyl ester counterpart removed a competing hydrogen-bond donor and enhanced the stability of the type VIa β-hairpin geometry as indicated by an increase of *cis*-conformer population and an augmentation in the temperature coefficient values of

particular amide NH protons. These elements are now being used to design longer peptides that adopt predictable conformations in water.

**Table 1. Amide isomer equilibrium of 5-*tert*-butylprolyl tetrapeptides in 10% D<sub>2</sub>O/H<sub>2</sub>O.**

Peptides	% <i>cis</i> -isomer	Peptides	% <i>cis</i> -isomer
Ac-Ala-Leu-5- <i>t</i> BuPro-Leu-NHMe	50	Ac-Ala-Phe-5- <i>t</i> BuPro-Phe-NHMe	62
Ac-Ala-Leu-5- <i>t</i> BuPro-Phe-NHMe	43	Ac-Ala-Phe-5- <i>t</i> BuPro-Leu-NHMe	65
Ac-Ala-Ala-5- <i>t</i> BuPro-Ala-NHMe	49	Ac-Ala-Phe-5- <i>t</i> BuPro-Ala-NHMe	68
Ac-Ala-Ala-5- <i>t</i> BuPro-Leu-NHMe	44	Ac-Ala-Phe-Pro-Ala-NHMe	22
Ac-Ala-Ala-5- <i>t</i> BuPro-Phe-NHMe	47	Ac-Ala-Phe-5- <i>t</i> BuPro-Ala-OMe	84
Ac-Ala-Ala-5- <i>t</i> BuPro-Phe-OMe	73	Ac-Ala-Phe-Pro-Ala-OMe	9

**Table 2. Influence of temperature on amide NH chemical shifts in the major tetrapeptide conformer in 10% D<sub>2</sub>O/H<sub>2</sub>O.**

Peptides	-Δδ/ΔT (ppb/K)			
	Ala	Xaa	Yaa	NHMe
Ac-Ala-Phe-5- <i>t</i> BuPro-Ala-NHMe	7.7	8.8	6.9	8.4
Ac-Ala-Phe-5- <i>t</i> BuPro-Ala-OMe	6.9	10.0	4.9	-
Ac-Ala-Phe-Pro-Ala-NHMe	7.2	7.8	10.4	7.1
Ac-Ala-Phe-Pro-Ala-OMe	9.5	8.6	6.1	-

### Acknowledgements

This research was supported by NSERC (Canada) and FCAR (Québec). L. H. is grateful for an award supporting travel expenses from the EPS Travel Grant Committee.

### 3.6. References

1. Halab, L. and Lubell, W. D. *J. Org. Chem.*, 64 (1999) 3312.
2. Halab, L. and Lubell, W. D. *J. Peptide Sci.*, (2000) In press.

**Article 7**

**Halab, L.; Lubell, W. D. "Effect of Sequence Peptide Geometry in 5-*tert*-Butylprolyl Type VI  $\beta$ -Turn Mimics."**  
**Accepté dans *The Journal of the American Chemical Society* 2002.**

**Effect of Sequence on Peptide Geometry in 5-*tert*-Butylprolyl  
Type VI  $\beta$ -Turn Mimics.**

**Liliane Halab and William D. Lubell\***

*Département de chimie, Université de Montréal*

*C. P. 6128, Succursale Centre Ville, Montréal, Québec, Canada H3C 3J7*

**3.7. Abstract**

The influence of sequence on turn geometry was examined by incorporating (2*S*,5*R*)-5-*tert*-butylproline (5-*t*BuPro) into a series of dipeptides and tetrapeptides. (2*S*,5*R*)-5-*tert*-butylproline and proline were respectively introduced at the *C*-terminal residue of *N*-acetyl dipeptide *N*<sup>1</sup>-methylamides **1** and **2**. The conformational analysis of these analogues was studied using NMR and CD spectroscopy as well as X-ray diffraction to examine the factors that control the prolyl amide equilibrium and stabilize type VI  $\beta$ -turn conformation. The high *cis*-isomer population with aromatic residues *N*-terminal to proline was shown to result from a stacking interaction between the partial positive charged prolyl amide nitrogen and the aromatic  $\pi$ -system as seen in the crystal structure of **1c**. The effect of sequence on the prolyl amide equilibrium of 5-*t*BuPro-tetrapeptides (Ac-Xaa-Yaa-5-*t*BuPro-Zaa-XMe **13** and **14**) was studied by varying the amino acids at the Xaa, Yaa and Zaa positions. High (>80%) *cis*-isomer populations were obtained with alkyl groups at the Xaa position, an aromatic residue at the Yaa position, and either an alanine or a lysine residue at the Zaa position of the 5-*t*BuPro-tetrapeptide methyl esters in water. Tetrapeptides Ac-Ala-Phe-5-*t*BuPro-Zaa-OMe (Zaa = Ala, Lys) **14d** and **14f** with high *cis*-isomer content adopted type VIa  $\beta$ -turn conformations as shown by their NMR and CD spectra. Although a pattern of amide proton temperature coefficient values indicative of a hairpin geometry was observed in peptides **14d** and **14f**, the value magnitudes did not indicate strong hydrogen-bonding in water.

### 3.8. Introduction

Reverse turns play important roles in protein folding.<sup>1</sup> Local sequence-specific interactions can initiate the folding process by enhancing turn structures that nucleate hairpins and thereby stabilize  $\beta$ -pleated sheets.<sup>2</sup> On the other hand, *cis-trans* isomerization about prolyl amide bonds in turn regions can be a rate limiting step in the folding mechanism.<sup>3</sup> The factors that favor specific isomer geometry about prolyl amides can thus contribute significantly toward controlling peptide folding.

The type VI  $\beta$ -turn is a relatively rare secondary structure that features uniquely an amide *cis*-isomer *N*-terminal to a proline residue situated at the  $i + 2$  position of the peptide bend.<sup>4</sup> Type VI  $\beta$ -turns play important roles in protein folding.<sup>5-7</sup> They have been shown to be recognition sites for peptidyl prolyl isomerases (PPIases) which can accelerate protein folding by catalyzing the conversion of the *cis*-isomer to its more thermodynamically stable *trans*-conformation.<sup>5,6</sup> Type VI  $\beta$ -turns have also been implicated in other important recognition events of bioactive proteins. For example, a type VI  $\beta$ -turn conformation has been proposed for thrombin-catalyzed cleavage of the V<sub>3</sub> loop of HIV gp120, a prerequisite to viral infection.<sup>7</sup> In addition, in the X-ray structure of the ribonuclease S protein, a type VIa  $\beta$ -turn was located at the central position of a hairpin conformation.<sup>4</sup>

Type VI  $\beta$ -turns are classified into two types based on the dihedral angle values of their central  $i + 1$  and  $i + 2$  residues.<sup>4</sup> In the type VIa  $\beta$ -turn, the proline  $\psi$ -dihedral angle is equal to 0° and a ten membered intramolecular hydrogen bond exists between the carbonyl oxygen of the  $i$  residue and the amide hydrogen of the  $i + 3$  residue. This intramolecular hydrogen bond is not present in the type VIb  $\beta$ -turn in which the proline  $\psi$ -dihedral angle value is equal to 150°.

As a minor isomer, the prolyl amide *cis*-isomer is often difficult to observe in natural peptides.<sup>8</sup> Minor *cis*-conformers may, however, exhibit significant effects on the transport, metabolism and reactivity of biologically active peptides.<sup>9</sup> To enhance the *cis*-isomer population, several approaches have been tried to stabilize this geometry by the means of conformational constraint using structural links and steric interactions.<sup>10-18</sup> Alternatively, double bond isosteres have been employed to mimic the spatial orientation presented by the *cis*-conformer.<sup>19</sup> These approaches have achieved effective replication of the backbone geometry of the type VI  $\beta$ -turn as well as analogues exhibiting inhibitory activity of PPIases.<sup>20</sup> Moreover, stabilization of a hairpin conformation has been achieved in a model linear tetrapeptide possessing an indolizidinone amino acid mimic of the central residues of type VIa  $\beta$ -turn as demonstrated by NMR in DMSO and IR spectroscopy in dichloromethane.<sup>14d</sup> These approaches have succeeded in replicating *cis*-conformer geometry; however, an important aspect of prolyl amides that many such examples by design fail to mimic has been the conformational equilibrium exhibited by prolyl peptides.

We have synthesized and used (2*S*,5*R*)-5-*tert*-butylproline (5-*t*BuPro) to explore both prolyl amide *cis*-isomer geometry as well as the amide equilibrium *N*-terminal to proline in various peptides.<sup>21-23</sup> In Ac-Xaa-5-*t*BuPro-NHMe, the 5-*t*BuPro residue stabilized type VIa and VIb  $\beta$ -turn conformations contingent upon the stereochemistry of the *N*-terminal residue.<sup>22</sup> Dipeptides possessing Ala and Leu residues adopted type VIa and VIb  $\beta$ -turn conformations when the *N*-terminal amino acid possessed respectively L- and D-configuration as shown by NMR and CD spectroscopy as well as X-ray analysis.<sup>22</sup> Furthermore, the presence of phenylalanine at the *N*-terminal of 5-*t*BuPro caused a remarkable increase in *cis*-isomer population (Ac-Phe-5-*t*BuPro-NHMe exhibited >90% prolyl amide *cis*-isomer in water).<sup>22</sup>

As well as its power to augment the *cis*-isomer population, the 5-*tert*-butyl substituent influences the barrier for amide isomerization.<sup>21b</sup> In the case of the (2*S*,5*R*)-diastereomer, the sterically bulky *tert*-butyl group interacts with the *N*-terminal residue such as to twist the amide bond away from planarity.<sup>22</sup> In *N*-acetyl proline *N*-methylamides, twisting of the prolyl amide was among factors that caused a reduction in the barrier for isomerization of 3.7 kcal/mol in the (2*S*,5*R*)-5-*t*BuPro analogue relative to its proline counterpart.<sup>21b</sup> The influences of sequence and stereochemistry on the amide equilibrium become thus more apparent in (2*S*,5*R*)-5-*t*BuPro peptides, because of the combination of the reduced isomerization barrier and the enhanced *cis*-isomer population.

We have synthesized a diverse array of 5-*t*BuPro peptides by employing BOP-Cl as coupling reagent to attach different amino acid electrophiles onto the sterically hindered prolyl residue. This synthesis achievement has allowed us to explore the influence of sequence on the equilibrium *N*-terminal to the prolyl residues. Study of the effect of sequence on isomer equilibrium in natural prolyl peptides has previously shown that aromatic residues adjacent to proline caused an augmentation in the *cis*-isomer population.<sup>8,24-26</sup> Although aromatic residues *N*-terminal to proline have been shown to cause a 10-fold reduction in the *cis* to *trans* isomerization rate,<sup>3</sup> to the best of our knowledge, little has been reported about the factors by which aromatic residues augment the *cis*-isomer population and increase the isomerization energy barrier. Amino acid residues possessing side-chains with hydrogen-bond acceptor and donor moieties have been shown to stabilize turn conformations when adjacent to proline.<sup>1a</sup> We report now the influence of hydrogen-bonding residues on the prolyl amide equilibrium and the *cis*-isomer population.

Examining the influence of sequence on turn geometry, we have introduced 5-*t*BuPro into a series of dipeptide and tetrapeptide analogues possessing aromatic and hydrogen-donor and acceptor residues. By studying the conformations of these analogues using NMR and CD spectroscopy as well as X-ray diffraction, we have itemized factors that control the prolyl amide equilibrium and stabilize type VI  $\beta$ -turn geometry. The high *cis*-isomer populations and preponderance of type VIa  $\beta$ -turn conformation brought about by aromatic amino acid residues has been shown to result from an interaction between the pyrrolidine ring and the aromatic  $\pi$ -system in the *cis*-amide as observed in the X-ray structure of Ac-Tyr-5-*t*BuPro-NHMe. Furthermore, hydrogen-bonding residues situated *N*-terminal to 5-*t*BuPro were found to destabilize the amide *cis*-isomer. Studying tetrapeptide analogues, we have examined the propensity for type VIa  $\beta$ -turns to nucleate hairpins. A combination of aromatic residues at the *N*-terminal and small alkyl groups at the *C*-terminal of tetrapeptide esters has led to high populations of *cis*-conformers that exhibited hydrogen-bonding characteristics of  $\beta$ -hairpins.

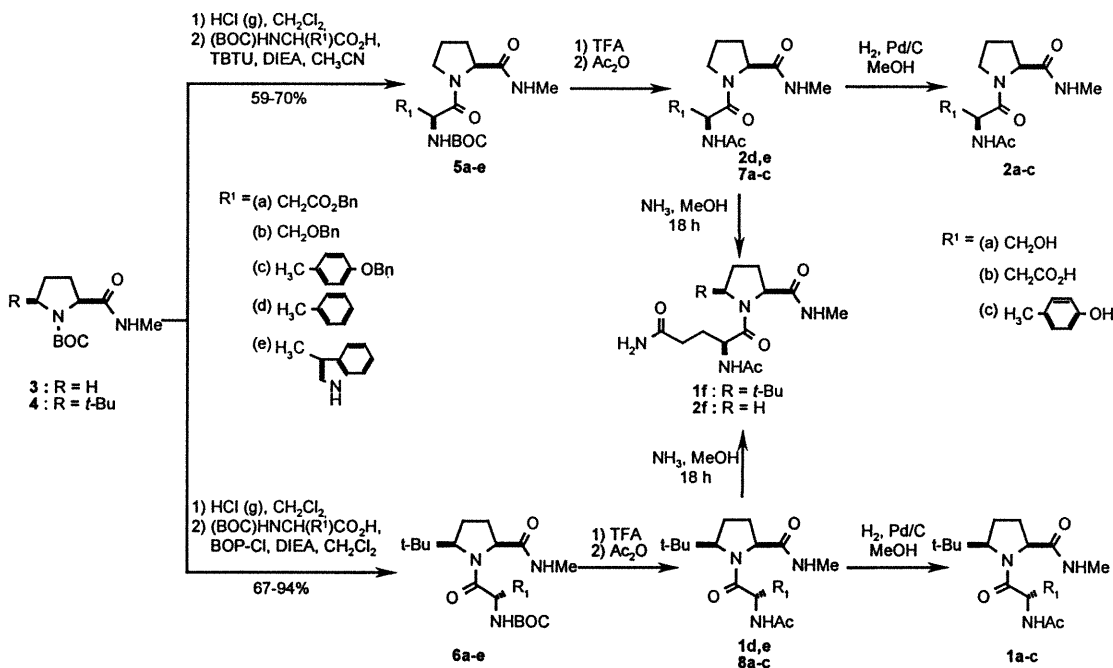
### 3.9. Results and Discussion

#### 3.9.1. Synthesis of dipeptides 1 and 2.

Dipeptides Ac-Xaa-5-*t*BuPro-NHMe (**1a-f**) were normally synthesized using BOC and benzyl (Bn) protecting groups for the respective protection of the amine and side-chain groups. The protected amino acids were coupled to the *N*-terminal of 5-*t*BuPro-NHMe<sup>21a</sup> using BOP-Cl and DIEA in dichloromethane to furnish dipeptides **6** in 67-94% yield (Scheme 1). For comparison, dipeptides possessing natural proline, Ac-Xaa-Pro-NHMe (**2a-f**), were synthesized by coupling similarly protected amino acids to proline *N*<sup>1</sup>-methylamide using TBTU and DIEA in acetonitrile which furnished dipeptides **5** in 59-70% yield. Removal of the BOC group with TFA in dichloromethane followed by acetylation of the amine with Ac<sub>2</sub>O and potassium

carbonate in dichloromethane provided *N*-acetyl dipeptide *N'*-methylamides. The benzyl ester and ether groups of the *N*-acetyl *O*-benzyl dipeptide *N'*-methylamides **7a-c** and **8a-c** were then deprotected by hydrogenation using 1 atm of H<sub>2</sub> with Pd/C in methanol and afforded the *N*-acetyl dipeptide *N'*-methylamides **1a-c** and **2a-c** in 92-99% yield. Because of the low yields obtained in coupling reactions with *N*-BOC-asparagine, the 5-*t*BuPro and Pro dipeptides **1f** and **2f** were synthesized by converting their respective aspartic benzyl ester, **7a** and **8a** to the corresponding amide, **1f** and **2f** using liquid ammonia in methanol in 97-99% yield (Scheme 1).

**Scheme 1.** Synthesis of *N*-(Acetyl)Dipeptide *N'*-Methylamides **1a-f** and **2a-f**.

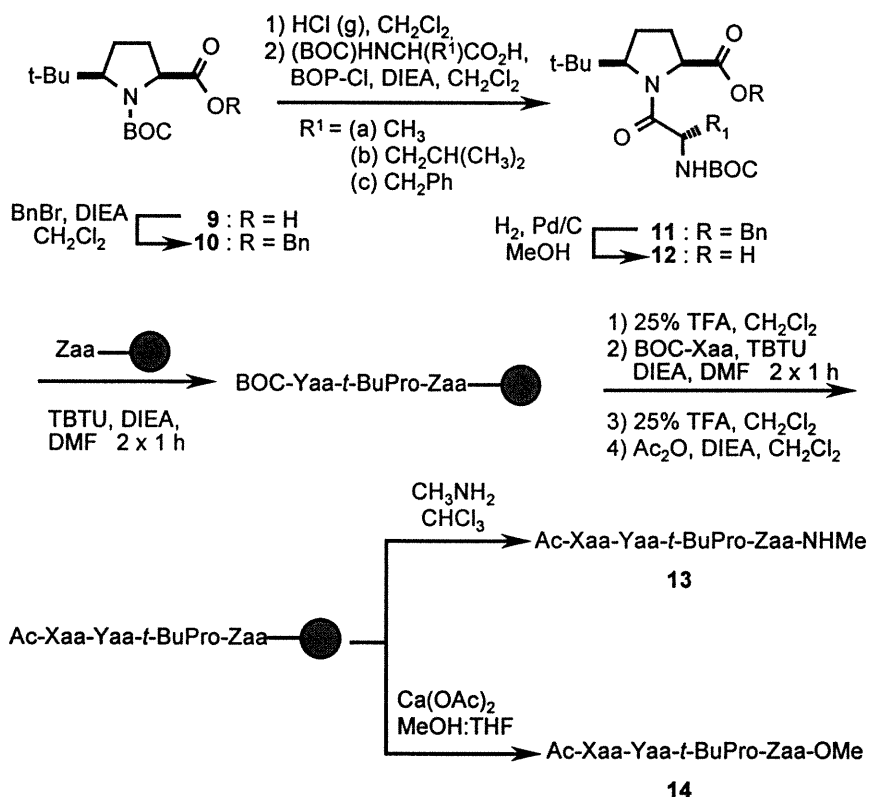


### 3.9.2. Synthesis of tetrapeptides.

Longer peptide sequences have been synthesized with 5-*t*BuPro using a combination of solution and solid-phase chemistry.<sup>21c,22c,23</sup> Tetrapeptides **13-16** were prepared on oxime resin<sup>27a</sup> by employing a BOC-protected dipeptide possessing 5-*t*BuPro at the C-terminal (Scheme 2). The first *N*-(BOC)amino acid was loaded onto oxime resin

using DCC in dichloromethane for 18 h.<sup>27</sup> The loading of the resin (mmol/g) was then determined by treatment of a precise amount of the resin with n-propylamine in chloroform<sup>27b</sup> and subsequent measurement of the weight and purity of the resulting *N*-(BOC)amino *N*-propylamide as assessed by NMR spectroscopy. Sequential elongation involved deprotections using TFA in dichloromethane, couplings of *N*-(BOC)amino acids using TBTU and DIEA in DMF and acetylation using Ac<sub>2</sub>O and DIEA in CH<sub>2</sub>Cl<sub>2</sub>.

**Scheme 2. Solid-Phase Synthesis of 5-*tert*-Butylprolyl Tetrapeptides 13 and 14.**



The sterically hindered 5-*tert*-butylproline was introduced into the peptides as a dipeptide unit that was synthesized in solution. Protection of *N*-BOC-5-*t*BuPro with benzyl bromide and DIEA in dichloromethane at reflux for 18 h gave ester **10** which was exposed to HCl (g) in dichloromethane to remove the BOC group and then coupled to *N*-(BOC)amino acids using BOP-Cl to provide the *N*-(BOC)dipeptide

benzyl esters **11a-c**. The benzyl group was removed by hydrogenation to afford the *N*-(BOC)dipeptides **12a-c** that were coupled to the resin using TBTU and the solid-phase protocol described above.

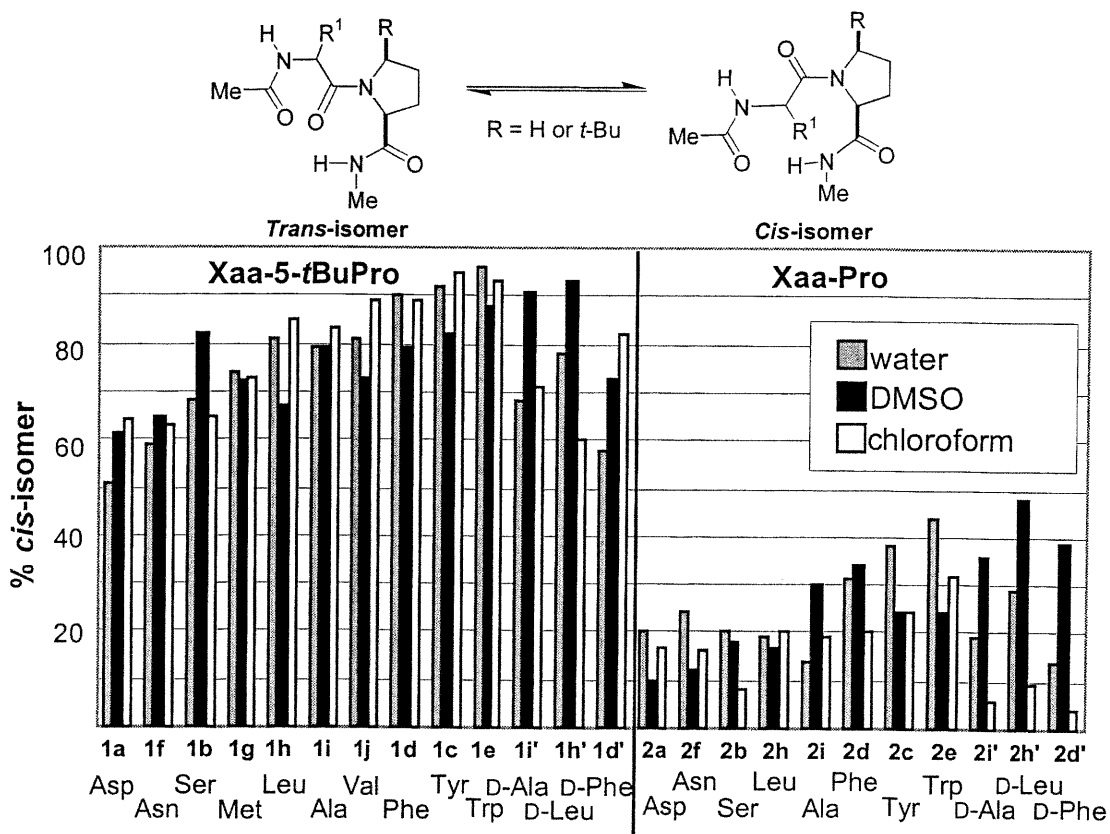
The peptides were cleaved from the resin to afford the peptide *N*-methylamides and methyl esters by using respectively methylamine in chloroform and calcium acetate in MeOH:THF at 40°C.<sup>28</sup> The final peptides **13-16** were obtained in 21-61% overall yields after purification by C18 reverse-phase HPLC and lyophilization. The purity of the peptides **13-16** was examined by analytical HPLC and their compositions were verified by fast atom bombardment mass spectrometry.

### **3.9.3. Conformational analysis of the dipeptides**

#### **NMR spectroscopy.**

The conformation of peptides **1** and **2** was analyzed by NMR spectroscopy in chloroform, DMSO and water. The relative populations of the amide *cis*- and *trans*-isomers *N*-terminal to the prolyl residues were measured by integration of the isomeric *tert*-butyl singlets and *N*-methyl doublets in the <sup>1</sup>H NMR spectra. As previously noted, the *tert*-butyl singlet of the amide *cis*-isomer appeared always upfield from that of the *trans*-isomer in the 5-*tert*-butylprolyl peptides **1**. Nuclear Overhauser effect experiments were used to confirm the assignment of the *cis*-isomer in dipeptides **1** and **2** on the basis of observation of a cross-peak between the *N*-terminal amino acid and the proline  $\alpha$ -hydrogens in the NOESY and ROESY spectra.

**Figure 1. Amide Equilibrium of *N*-Acetyl Dipeptide *N'*-Methylamides.<sup>a</sup>**



<sup>a</sup> The data for *N*-acetyl dipeptide *N'*-methylamides with alkyl and D-amino acid residues were obtained from Refs 22.

In the prolyl dipeptides **2**, the amide *trans*-isomer geometry *N*-terminal to the prolyl residue was the major conformer (Figure 1) in all three solvents, as observed in linear prolyl peptides.<sup>7,25,26,29,30</sup> Aromatic residues *N*-terminal to proline exhibited a 2-3 fold increase in the *cis*-isomer population relative to their alanine counterpart. The largest amount of *cis*-amide (44%) was observed with Ac-L-Trp-Pro-NHMe among the prolyl peptides in water. On the contrary, the 5-*tert*-butylprolyl peptides **1** adopted the amide *cis*-isomer in the major conformer (Figure 1). The presence of an aromatic amino acid *N*-terminal to 5-*tert*-butylproline caused a significant increase in the *cis*-isomer population. The highest *cis*-isomer population (96%) was observed for Ac-L-Trp-*t*BuPro-NHMe in water. Relative to their aliphatic and aromatic amino acid counterparts, hydrogen-bond donor and acceptor residues *N*-terminal to 5-*tert*-

butylproline gave lower *cis*-isomer populations. An increase in *cis*-isomer population was observed when the aromatic residue was varied from phenylalanine to tyrosine to tryptophan in 5-*tert*-butylprolyl dipeptides, which has also been the trend in prolyl peptides.<sup>26,27a</sup> This tendency may be caused by the increase in electron density in the aromatic rings which interacts effectively with the partial positive charge of the prolyl nitrogen thus increasing the *cis*-isomer population.

In 5-*t*BuPro-peptides **1c-e** and **1g-j** which have amino acids of L-configuration possessing aliphatic and aromatic side-chains, the *cis*-isomer population was augmented on switching solvent from DMSO to water and from DMSO to chloroform. On the contrary, higher *cis*-isomer populations were observed in DMSO relative to water when the *N*-terminal residue was of L-configuration possessing a side-chain capable of forming hydrogen bonds (**1a**, **1b**, and **1f**), as well as when a D-amino acid residue was *N*-terminal to 5-*t*BuPro (**1d'**, **1h'** and **1i'**). In the natural prolyl peptides which possess D-amino acid residues (**2d'**, **2h'** and **2i'**), a large increase of *cis*-isomer was also observed in DMSO relative to water and chloroform. However, in the prolyl peptides possessing a side-chain capable of forming hydrogen bonds (**2a**, **2b**, and **2f**), higher *cis*-isomer was found in water relative to DMSO.

The influence of solvent composition on the chemical shifts of the amide signals was used to identify amides engaged in intramolecular hydrogen bonds. In the major amide *cis*-isomer of peptides **1**, the signal for the *N*-methylamide proton appeared always downfield relative to that for the acetamide proton in chloroform. The *N*-methylamide proton signals appeared between 7.29 and 8.52 ppm whereas the acetamide proton signals came between 5.97 and 7.21 ppm for the *cis*-isomer of peptides **1**. The downfield shifted amide proton signal suggested an intramolecular

hydrogen bond between the *N*<sup>t</sup>-methylamide and acetamide in a type VIa  $\beta$ -turn conformation. In contrast, the signals of the *N*<sup>t</sup>-methylamide and acetamide of the major *trans*-conformer of prolyl peptides **2** showed no significant differences in their chemical shifts which appeared between 6.03 and 7.17 ppm. Solvent changes from chloroform to water and to DMSO caused little changes in the chemical shift of the *N*<sup>t</sup>-methylamide proton signal of peptide **1**, which moved 0.04-0.60 ppm and 0.17-1.12 ppm downfield, respectively. The signals for the acetamide proton of peptides **1** and **2** and the *N*<sup>t</sup>-methylamide proton of peptide **2** shifted significantly (0.40-2.55 ppm) with changes in solvent. In conclusion, the influence of solvent composition on the chemical shift of the amide signals demonstrated the *N*<sup>t</sup>-methylamide proton of the *cis*-isomer of peptide **1** to be in an intramolecular hydrogen bond of a type VIa  $\beta$ -turn conformation.

#### 3.9.4. Circular dichroism spectroscopy.

Circular dichroism (CD) spectra of peptides **1a-f** and **2a-f** were measured in water and acetonitrile to study the influence of solvent composition on peptide conformation. The CD spectra of 5-*tert*-butylprolyl peptides possessing aromatic side-chains **1c-e** exhibited a strong negative band at  $190 \pm 5$  nm, a strong positive band at  $205 \pm 6$  nm and a weak negative band at  $230 \pm 10$  nm in water (Figure 2A). When changing the solvent from water to acetonitrile, the shape of the CD curves of peptides **1c-e** remained unchanged (Figure 2B). This type of CD curve has been identified previously as a class B CD spectra which we have previously assigned to type VIa  $\beta$ -turn conformations.<sup>22,31</sup> Similar curve shapes were obtained for 5-*tert*-butylprolyl peptides **1a**, **1b** and **1f** which possessed hydrogen-bond donor and acceptor side-chains (Figure 3A and 3B). The CD spectra of the prolyl peptides possessing aromatic side-chains **2c-e** varied significantly with changes in solvent composition and exhibited no distinct CD curve shapes (Figure 2C and 2D).

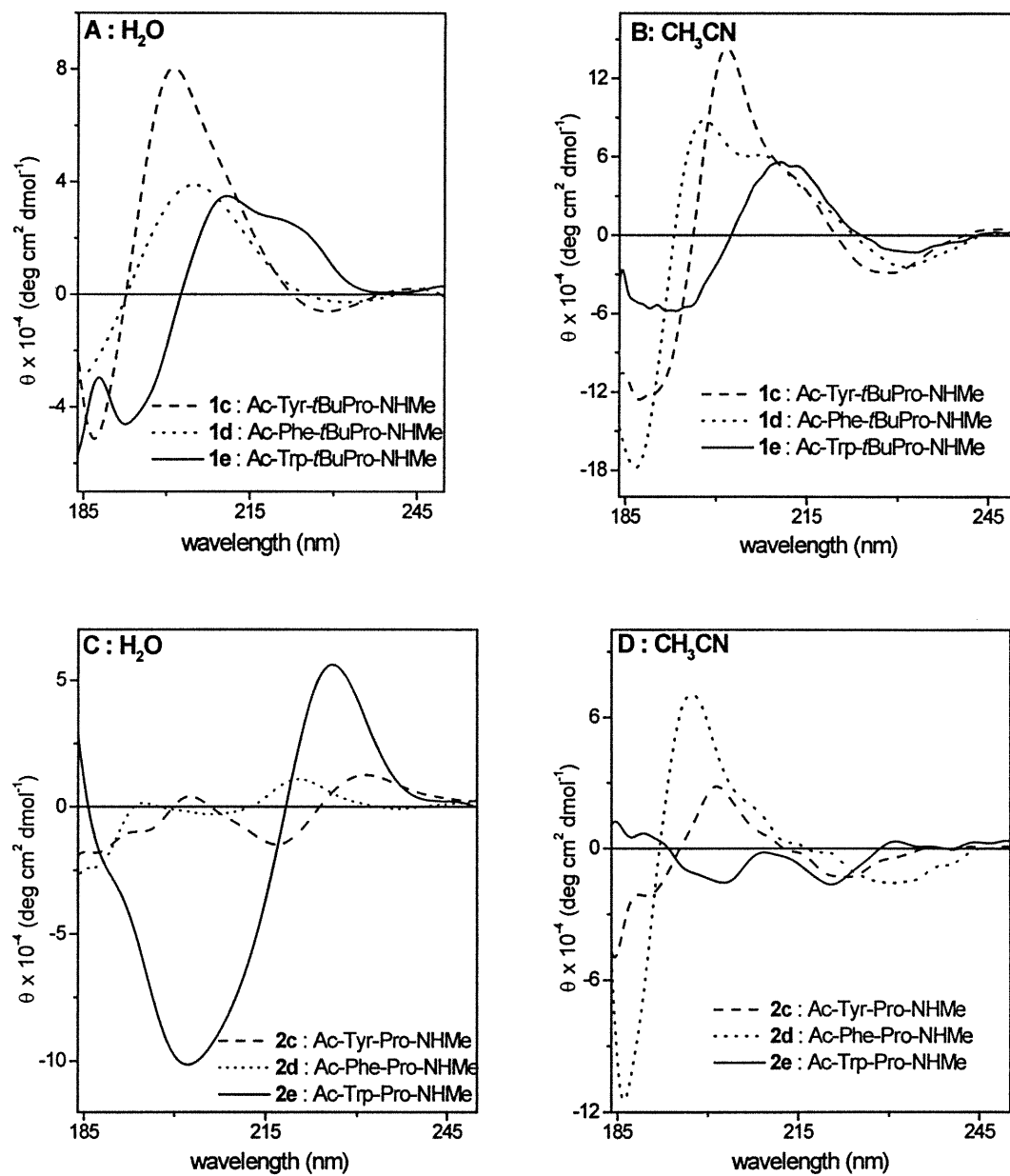


**Figure 2. Circular dichroism spectra of dipeptides **1c-e** (A, in water and B, in acetonitrile) and **2c-e** (C, in water and D, in acetonitrile) at 0.1 mM.**

On the other hand, the CD curves of prolyl peptides **2a** and **2f** which possessed Asp and Asn residues with hydrogen-bonding side-chains were characterized by a minima at around  $210 \pm 2$  nm and  $220 \pm 2$  nm in acetonitrile that

converged to a single band at around 205 nm in water (Figure 3C and 3D). This type of CD curve has been assigned to a class C CD spectra that has been reported for peptides adopting prolyl amide *trans*-isomers in type II'  $\beta$ -turn conformations.<sup>22,31,32</sup>

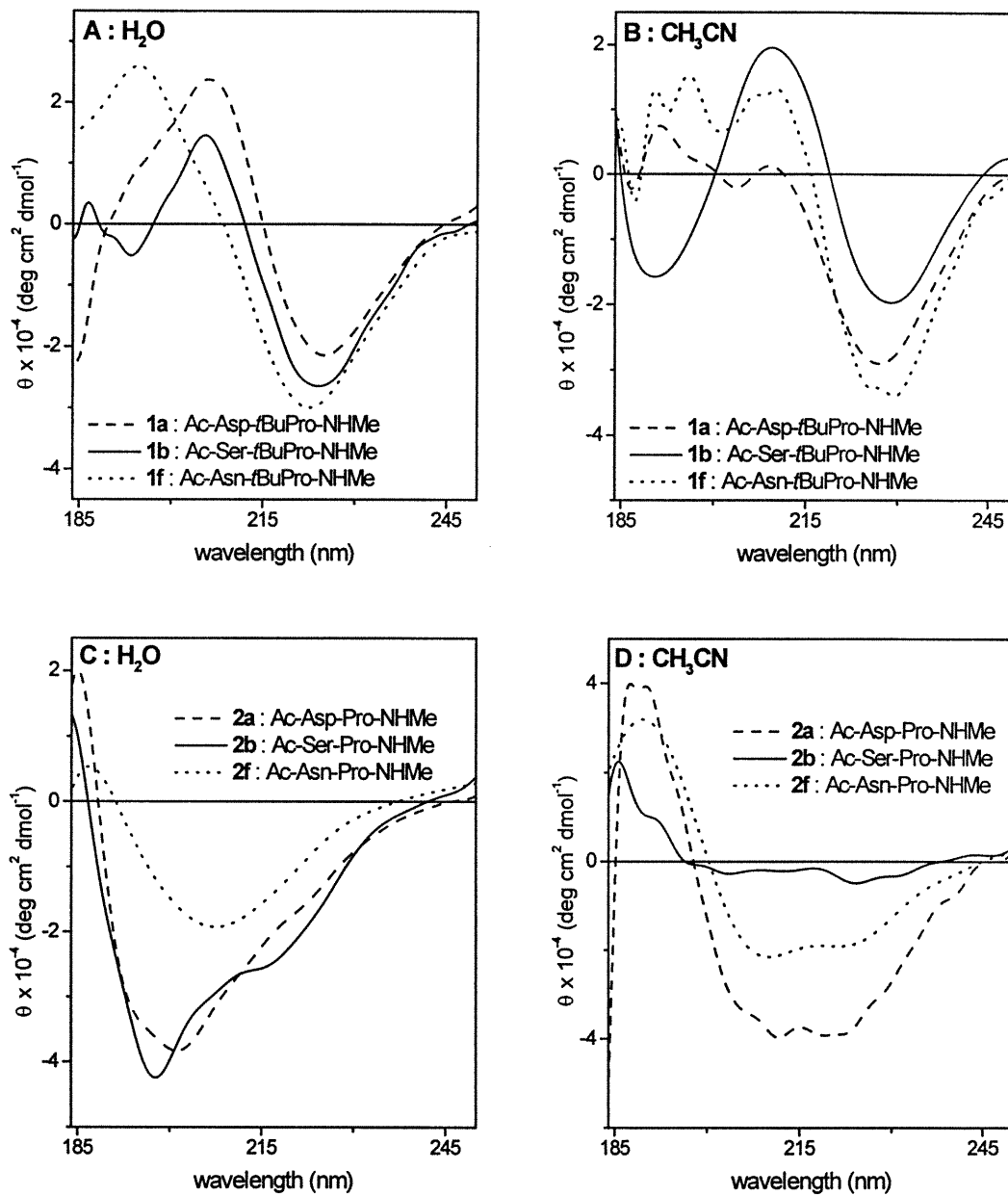


**Figure 3. Circular dichroism spectra of dipeptides 1a-b, 1f (A, in water and B, in acetonitrile) and 2a-b, 2f (C, in water and D, in acetonitrile) at 0.1 mM..**

### 3.9.5. X-ray crystallographic analysis.

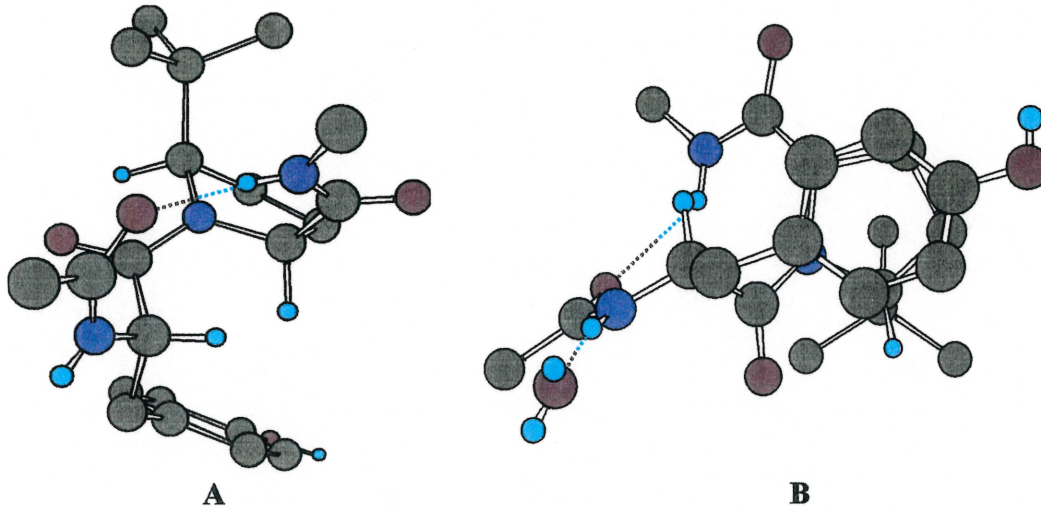


**Figure 4. A) Ball and stick representation of the X-ray structure of Ac-L-Tyr-5-*t*BuPro-NHMe 1c.<sup>33</sup> B) Side-view of the X-ray structure of 1c.**

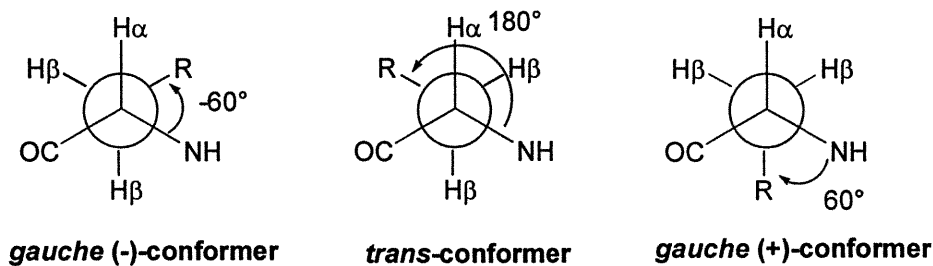
**Table 1. Comparison of the Dihedral Angles of Ideal Type VIa  $\beta$ -Turn and X-Ray Structure of *N*-(Acetyl)tyrosyl-5-*tert*-butylproline *N*<sup>o</sup>-Methylamide 1c.**

entry	$\phi_2$	$\psi_2$	$\omega$	$\phi_3$	$\psi_3$
Ideal Type VIa $\beta$ -Turn	-60°	120°	0°	-90°	0°
Ac-L-Tyr-5- <i>t</i> BuPro-NHMe (A)	-58°	137°	8°	-101°	26°
Ac-L-Tyr-5- <i>t</i> BuPro-NHMe (B)	-58°	137°	13°	-94°	11°
Ac-L-Leu-5- <i>t</i> BuPro-NHMe	-61°	139°	17°	-95°	19°
Ideal Type VIb $\beta$ -Turn	-120°	120°	0°	-60°	150°
Ac-D-Leu-5- <i>t</i> BuPro-NHMe	93°	-141°	29°	-81°	157°

Crystals of *N*-acetyl-L-tyrosyl-5-*tert*-butylproline *N*<sup>o</sup>-methylamide were obtained from a mixture of MeOH, EtOAc and hexane. The analysis of the crystal structure by X-ray diffraction revealed a unit cell with a molecule of water and two molecules of 1c which adopted similar turn conformations.<sup>33</sup> The crystallographic

analysis of **1c** demonstrated the presence of an amide *cis*-isomer *N*-terminal to the 5-*tert*-butylprolyl residue with twisted dihedral angle values of  $\omega = 8.5^\circ$  and  $\omega = 13.0^\circ$  (Figure 4). As previously shown, the sterically bulky 5-*tert*-butyl substituent influenced the amide bond *N*-terminal to the 5-*tert*-butylprolyl residue that distorted it from planarity.<sup>22a-b</sup> Furthermore, an intramolecular hydrogen bond could be inferred to exist between the *N*-methylamide proton and the acetamide carbonyl oxygen from measurement of an interatomic distance of 2.08 and 2.18 Å in the X-ray structure of **1c**. The dihedral angles of peptide **1c** resembled those of the central *i* + 1 and *i* + 2 residues of an ideal type VIa  $\beta$ -turn. For comparison, the dihedral angles of peptide **1c**, the ideal values of type VIa and VIb  $\beta$ -turn conformations as well as those for Ac-L-Leu-*t*BuPro-NHMe and Ac-D-Leu-*t*BuPro-NHMe are listed in Table 1. The  $\psi_3$  dihedral angle of dipeptide **1c** placed the *N*<sup>1</sup>-methylamide hydrogen at a 2.4 Å interatomic distance from the prolyl nitrogen, which has also been observed in the X-ray structure of Ac-L-Leu-*t*BuPro-NHMe. The interaction between the prolyl amide nitrogen and the *N*<sup>1</sup>-methylamide hydrogen has been suggested to stabilize the pyramidalized amide in the transition state and thereby accelerate isomerization *N*-terminal to proline.<sup>42</sup>

**Figure 5. Rotamers around the  $C\alpha-C\beta$  axis in amino acids**



In the structure of peptide **1c**, the side-chain adopted a  $\chi_1$  dihedral angle value of 172°. This *trans*-conformer positioned the tyrosyl aromatic ring beneath the proline ring (distance of 3.4-4.9 Å between the proline nitrogen and the tyrosyl

phenyl group, Figure 5). Prior to our work, computational study had suggested that the amino-aromatic interactions occur between positively charged or  $\delta(+)$  amine groups in side-chains and the  $\delta(-)$   $\pi$ -electrons of the aromatic ring of Phe, Tyr and Trp when they are separated by 3.4 to 6.0 Å.<sup>34</sup> Stacking interactions between the aromatic and pyrrolidine rings can be found in the crystal structures of proteins and cyclic peptides possessing aromatic residues *N*-terminal to proline.<sup>8,35</sup> For example, in the X-ray structure of the hexapeptide cyclo(L-Phe-L-Pro-D-Ala)<sub>2</sub>, the L-Phe-L-Pro amide bonds are in the *cis*-isomer with the  $\chi_1$  dihedral angle of the Phe residue in the *trans*-conformer (Figure 5).<sup>35a</sup> Interactions between the aromatic and proline rings in the amide *cis*-isomer of prolyl peptides containing aromatic residue have been observed by NMR spectra in which the chemical shift of the  $\alpha$ -proton of proline was shifted upfield.<sup>36</sup>

### 3.9.6. Conformational analysis of the tetrapeptides

The conformations of tetrapeptides Ac-Xaa-Yaa-5-*t*BuPro-Zaa-XMe **13-14** and Ac-Xaa-Yaa-Pro-Zaa-XMe **15-16** were studied by NMR spectroscopy in 9:1 H<sub>2</sub>O/D<sub>2</sub>O. The signals in the <sup>1</sup>H NMR were assigned using COSY, TOCSY and ROESY experiments. The relative populations of the prolyl amide *cis*- and *trans*-isomers of tetrapeptides **13-16** were measured by integration of the *tert*-butyl singlets and the *N*-methylamide or methyl ester signals in the proton NMR spectra (Table 2).

The *cis*-isomer geometry was found to be stabilized by aliphatic residues such as alanine and valine relative to the hydrogen-bonding residue serine at the *i* position (Figure 6). In the natural hexapeptides Xaa-Tyr-Pro-Tyr-Asp-Val, an alanine residue (57%) gave rise to higher *cis*-isomer populations than a serine residue (52%) at the Xaa position.<sup>25d</sup> Protein X-ray analysis in contrast has shown the highest occurrence

of serine at the *i* position in peptides possessing proline at the *i* + 1 position in the amide *cis*-conformer.<sup>37</sup>

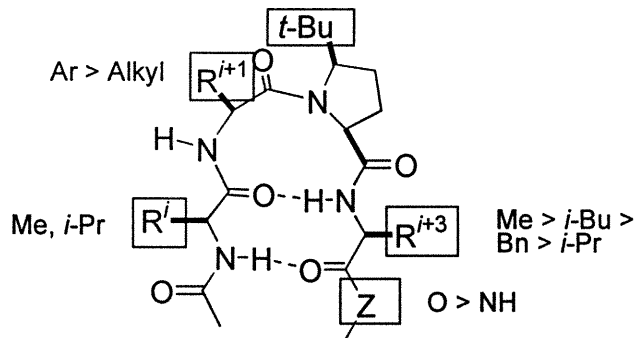
**Table 2. Amide Isomer Equilibrium of Tetrapeptides Ac-Xaa-Yaa-5-*t*BuPro-Zaa-XMe and Ac-Xaa-Yaa-Pro-Zaa-XMe in 10% D<sub>2</sub>O/H<sub>2</sub>O.**

entry	Xaa	Yaa	Zaa	X	% <i>cis</i> -isomer
<b>13a</b>	Ala	Ala	5- <i>t</i> BuPro	NH	49
<b>13b</b>	Ala	Ala	5- <i>t</i> BuPro	NH	44
<b>13c</b>	Ala	Ala	5- <i>t</i> BuPro	NH	47
<b>14a</b>	Ala	Ala	5- <i>t</i> BuPro	O	73
<b>13d</b>	Ala	Leu	5- <i>t</i> BuPro	NH	50
<b>13e</b>	Ala	Leu	5- <i>t</i> BuPro	NH	43
<b>13f</b>	Ala	Phe	5- <i>t</i> BuPro	NH	62
<b>12g</b>	Ala	Phe	5- <i>t</i> BuPro	NH	65
<b>13h</b>	Ala	Phe	5- <i>t</i> BuPro	NH	52
<b>14b</b>	Ala	Phe	5- <i>t</i> BuPro	O	68
<b>14c</b>	Ala	Phe	5- <i>t</i> BuPro	O	79
<b>13i</b>	Ala	Phe	5- <i>t</i> BuPro	NH	68
<b>14d</b>	Ala	Phe	5- <i>t</i> BuPro	O	84
<b>13j</b>	Ser	Phe	5- <i>t</i> BuPro	NH	70
<b>14e</b>	Ser	Phe	5- <i>t</i> BuPro	O	73
<b>14f</b>	Val	Phe	5- <i>t</i> BuPro	O	80
<b>15</b>	Ala	Phe	Pro	NH	22
<b>16</b>	Ala	Phe	Pro	O	9

As observed in the 5-*t*BuPro-dipeptides, a significant augmentation of the *cis*-isomer population occurred when an aromatic residue was at the *i*+1 position *N*-terminal to 5-*t*BuPro in the *N*-acetyl tetrapeptide *N*<sup>1</sup>-methylamides. When the 5-*t*BuPro residue was replaced by proline, the *cis*-isomer population decreased from 68-

84% to 9-22% (Table 2). Thus, the steric interactions between the *tert*-butyl substituent and the side-chain of the *N*-terminal residue disfavored the prolyl amide *trans*-isomer and increased the *cis*-isomer population. At the *i*+3 position of tetrapeptides, alanine and lysine were found to give rise to higher amide *cis*-isomer populations relative to the  $\beta$ -branched alkyl residue valine. In protein X-ray data, alanine at the *C*-terminal to position gave rise to the highest *cis*-conformer population.<sup>37</sup> Among the modifications to 5-*t*BuPro-tetrapeptides, the most significant increase in *cis*-isomer population was observed when the *N*<sup>o</sup>-methylamide was replaced by its methyl ester counterpart. For example, the *cis*-isomer population of tetrapeptide 13c (47%) was augmented 26% on conversion to its methyl ester 14a (73%, Table 2). This augmentation may be caused by the removal of a competitive hydrogen-bonding conformation in the tetrapeptides *N*<sup>o</sup>-methylamides that favor the prolyl amide *trans*-isomer.

**Figure 6. Influence of sequence on the amide equilibrium in 5-*t*BuPro-tetrapeptides.**



The coupling constant values ( $^3J_{\text{NH}-\text{CaH}}$ ) for the *i* + 1 and *i* + 2 residues of tetrapeptides 14d and 14f exhibiting the highest *cis*-isomer populations were characteristic of turn structure.<sup>38</sup> The  $^3J_{\text{NH}-\text{CaH}}$  coupling constant value for the Phe residue in tetrapeptides 14d and 14f was 3.7 Hz and in good agreement with a 4 Hz

coupling constant corresponding to the  $\phi$  dihedral angle of  $-60^\circ$  for the  $i + 1$  residue in a type VIa  $\beta$ -turn conformation. The  $^3J_{\text{NH-C}\alpha\text{H}}$  coupling constant values for the other residues in the tetrapeptides **14d** and **14f** were in the range of 6.2-8.4 Hz. Sequential  $\text{H}\alpha\text{N}(i, i + 1)$  NOEs were observed for all expected residues in the tetrapeptide **14d**. In the ROESY spectra of tetrapeptide **14d**, an additional  $\text{H}\alpha\text{N}(i, i + 2)$  NOE was observed between the  $\alpha$ -hydrogen of Phe and amide proton of the *C*-terminal Ala characteristic of a  $\beta$ -turn conformation.

**Table 3. Influence of temperature on the NH chemical shifts of the major isomer of the tetrapeptides **13i**, **14d**, **14f**, **15** and **16** in water and in DMSO.**

Peptides	$-\Delta\delta/\Delta T$ (ppb/K)			
	NHXaa	NHPhe	NHZaa	NHMe
Ac-Ala-Phe-5- <i>t</i> BuPro-Ala-NHMe ( <b>13i</b> )	7.7	8.8	6.9	8.4
Ac-Ala-Phe-5- <i>t</i> BuPro-Ala-OMe ( <b>14d</b> )	6.9 (6.0) <sup>b</sup>	10.0 (6.9) <sup>b</sup>	4.9 (4.7) <sup>b</sup>	-
Ac-Ala-Phe-Pro-Ala-NHMe ( <b>15</b> )	7.2	7.8	10.4	7.1
Ac-Ala-Phe-Pro-Ala-OMe ( <b>16</b> )	9.5	8.6	6.1	-
Ac-Val-Phe-5- <i>t</i> BuPro-Ala-OMe ( <b>14f</b> )	6.0 <sup>b</sup>	6.7 <sup>b</sup>	4.5 <sup>b</sup>	-

<sup>a</sup>Determined by 600 MHz NMR in 10%  $\text{D}_2\text{O}/\text{H}_2\text{O}$  at 5 mM concentration. <sup>b</sup> Values are in DMSO.

The temperature coefficient values ( $\Delta\delta/\Delta T$ ) were measured for the amide protons in peptide **14d**, which possessed the highest *cis*-isomer population, its amide counterpart **13i**, and their respective prolyl analogues **16** and **15** in 10%  $\text{D}_2\text{O}/\text{H}_2\text{O}$  (Table 3). The amide protons of the alanine residues at the Xaa and Zaa positions of 5-*t*BuPro-peptide **13i** and **14d** exhibited lower temperature coefficient values than the phenylalanine and *N*<sup>1</sup>-methylamide amide protons, which may indicate their participation in intramolecular hydrogen bonds. This tendency was not observed in the prolyl tetrapeptides **15** and **16** where the chemical shift variation with temperature for the amide protons were in the range of  $-6.1$  to  $-10.4$  ppb/K. The temperature coefficient values were measured in DMSO for the amide protons in 5-*t*BuPro-

tetrapeptides **14d** and **14f**, which possessed high *cis*-isomer populations. The amide proton of the alanine residue at the Zaa position of peptide **14d** exhibited similar temperature coefficient values in DMSO ( $-4.7 \text{ ppb/K}$ ) and water ( $-4.9 \text{ ppb/K}$ ). In DMSO, peptides **14d** and **14f** exhibited similar temperature coefficient values. Although temperature coefficient values greater than  $-3 \text{ ppb/K}$  in DMSO have been suggested to indicate amide protons engaged in intramolecular hydrogen-bonds, such values are normally measured in cyclic and larger peptides than those reported here.<sup>39</sup> The pattern of the temperature coefficient magnitudes in **13i**, **14d** and **14f** did conform to a hairpin-like structure; however, the values themselves suggested solvent exposed amides presumably due to the flexibility of the linear tetrapeptide.

The CD spectra of tetrapeptides **14d** and **14f** exhibited a minima at 230 nm, a maxima at 215 nm, an intense minima at 200 nm and a maxima at 190 nm in water (Figure 7). This type of CD curve has been classified as a class D CD spectrum which has been previously assigned to a  $\beta$ -turn conformation.<sup>31</sup>

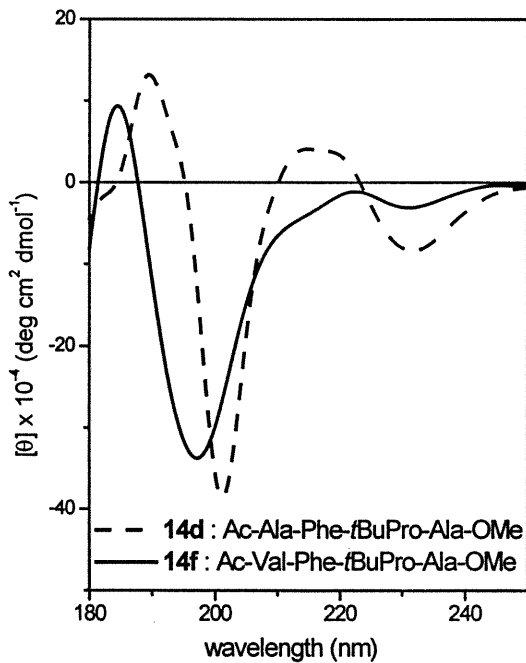


Figure 7. Circular dichroism spectra of tetrapeptides **14d** and **14f** in water at 0.1 mM.

### 3.10. Discussion

We have studied the influence of sequence and stereochemistry of the residue *N*-terminal to 5-*t*BuPro by the preparation and analysis of a series of dipeptide and tetrapeptide analogues (Ac-Xaa-5-*t*BuPro-NHMe and Ac-Xaa-Yaa-5-*t*BuPro-Zaa-XMe). All of the 5-*t*BuPro-dipeptide analogues adopted predominant *cis*-isomer conformations about the prolyl amide bond. In the dipeptide series, the turn type was contingent on the configuration of the amino acid *N*-terminal to 5-*t*BuPro and adopted respectively type VIa and VIb  $\beta$ -turn conformations when the *N*-terminal amino acid was of L- and D-configuration.<sup>22a-b</sup>

In the *N*-acetyl dipeptide *N'*-methylamides, the *cis*-isomer population increased as the amino acid *N*-terminal to 5-*t*BuPro was varied from a hydrogen-bonding residue to an alkyl residue to an aromatic residue. This pattern was also observed in the natural prolyl dipeptides where aromatic residues gave higher *cis*-isomer populations than alkyl and hydrogen-bonding residues. The augmentation of *cis*-isomer with aromatic residues *N*-terminal to proline appears to be caused by the interaction between the  $\delta(+)$  amine of 5-*t*BuPro and the aromatic ring of the tyrosyl side-chain which adopted a  $\chi_1$  value of 172° as observed in the X-ray structure of **1c**. This stacking interaction cannot be achieved in the *trans*-isomer geometry because the side-chain  $\chi_1$  dihedral angle adopts a *gauche*-conformer.<sup>36</sup> In the dipeptides possessing hydrogen bonding side-chains (**1a**, **1b**, **2a**, and **2b**), a hydrogen-bond between the *N'*-methylamide hydrogen and the carbonyl oxygen of the side-chain in an Asx-turn may favor the *trans*-isomer and therefore decrease the *cis*-isomer population.<sup>40</sup>

The influence of solvent composition on the *cis*-isomer equilibrium was contingent on the sequence of the dipeptide. Alkyl and aromatic residues in L-Xaa-5-

*t*BuPro dipeptides gave higher *cis*-isomer population in water than DMSO presumably due to favorable hydrophobic interactions between the proline ring and the *N*-terminal residue in the *cis*-conformer. The downfield shift for the *N*-methylamide proton signal of 5-*t*BuPro-dipeptides **1** was indicative of an intramolecular hydrogen bond between the *N*-methylamide proton and the acetamide carbonyl in a type VIa  $\beta$ -turn conformation. The presence of a type VIa  $\beta$ -turn geometry for 5-*t*BuPro-dipeptides in solution, independent of solvent composition, was supported by the circular dichroism spectra of dipeptides **1a-f** in water and acetonitrile. In chloroform, the intramolecular hydrogen bond in the type VIa  $\beta$ -turn conformation may be stabilized resulting in an increased *cis*-isomer population in 5-*t*BuPro dipeptides with L-configuration possessing alkyl and aromatic residues; in DMSO, the *cis*-isomer population was reduced presumably by the disruption of this intramolecular hydrogen bond. In the prolyl peptides possessing hydrogen-bonding residue (**2a**, **2b** and **2f**), higher *cis*-populations were observed in water which may compete with the side-chain hydrogen donor perturbing the intramolecular hydrogen bonding that stabilized a *trans*-conformer.

In the solid state, *N*-acetyl-L-tyrosyl-5-*tert*-butylproline *N*-methylamide (**1c**) existed in a type VIa  $\beta$ -turn conformation as shown by X-ray diffraction. In addition, the aromatic and proline rings were stacked in the crystal structure in a way that may stabilize the *cis*-isomer geometry by an interaction between the partial positive charge of the amide nitrogen and the electron-rich aromatic  $\pi$ -system. The *tert*-butyl substituent distorted the prolyl amide from planarity which may result in lowering of the prolyl amide isomerization energy barrier. Stabilization of the transition state for prolyl isomerization may also occur from interaction between the lone pair of the pyramidalized prolyl amide nitrogen and the *N*-methylamide hydrogen, which were inferred to be separated by 2.4 Å in the crystal structure of **1c**.<sup>6a,41</sup> A second

stabilizing force in the transition state may arise from the aromatic side-chain of tyrosine because as the prolyl amide carbonyl rotates, it may interact with the aromatic ring protons which from the crystal structure were inferred to be at a distance of 3.7-4.6 Å. Such a C-H···O interaction between the side-chains of the aromatic residues in the binding pocket of the PPIase FKPB and the tertiary amide carbonyl of its substrate have previously been suggested to stabilize the transition state for enzyme-catalyzed isomerization.<sup>6a</sup> The increased *cis*-isomer population and relative increase in the prolyl amide isomerization energy barrier that have been observed in natural prolyl peptides possessing aromatic amino acids, both however, appear to be due to ground-state stabilization through interactions between the δ(+) nitrogen and π-aromatic system.

The effect of sequence on the prolyl amide equilibrium of 5-*t*BuPro-tetrapeptides (Ac-Xaa-Yaa-5-*t*BuPro-Zaa-XMe) was studied by varying the amino acids at the Xaa, Yaa and Zaa positions. The highest *cis*-isomer populations were obtained with alkyl groups at the Xaa position, an aromatic residue at the Yaa position and either an alanine or a lysine residue at the Zaa position of the 5-*t*BuPro-tetrapeptide methyl esters. It has been previously illustrated that replacement of amide bonds with esters in peptides prevented the formation of undesired hydrogen-bonding conformations.<sup>42</sup> In natural prolyl peptides, high *cis*-isomer populations have been obtained by placing aromatic residues at both the *N*- and *C*-termini of proline.<sup>25</sup> In the 5-*t*BuPro-tetrapeptide **13f**, a combination of Phe residues at the *N*- and *C*-termini to 5-*t*BuPro did not produce the highest *cis*-isomer populations. On the contrary, amino acids with linear alkyl groups, such as alanine and lysine, at the *C*-terminal of 5-*t*BuPro-tetrapeptide *N*-methylamides **13g** and **13i** produced higher *cis*-isomer populations. Alkyl-branched residues at the *C*-terminal of 5-*t*BuPro may not favor the *cis*-isomer because of the steric interactions with the *tert*-butyl substituent.

Turn formation in peptides has been illustrated by the presence of a significant  $\text{H}\alpha\text{N}(i, i+2)$  NOE connectivity.<sup>25</sup> A strong  $\text{H}\alpha\text{N}(i, i+2)$  NOE was observed between the  $\alpha$ -hydrogen of Phe and amide proton of the C-terminal Ala in tetrapeptide **14d**. The circular dichroism spectra of peptides **14d** and **14f** exhibited a similar curve shape that has been classified as a type D CD spectrum, assigned to  $\beta$ -turn conformations.<sup>31</sup> Thus, peptide **14d** adopted a type VIa  $\beta$ -turn conformation in water.

The temperature coefficient study of tetrapeptides **13i**, **14d** and **14f** in water and DMSO did not provide values that corresponded to intramolecular hydrogen bonding amide protons. However, a pattern was observed where the amide protons of the residues at the Xaa and Zaa positions of 5-*t*BuPro-peptides **13i**, **14d** and **14f** exhibited lower temperature coefficient values than the phenylalanine and *N*-methylamide amide protons. Polar solvents such as water and DMSO are known to perturb intramolecular hydrogen-bonds in peptides. Steric interactions of 5-*tert*-butylproline could not stabilize a hairpin conformation in a linear tetrapeptide relative to the stabilizing structural link in an indolizidinone amino acid type VIa  $\beta$ -turn mimic.<sup>14d</sup> Although a type VIa  $\beta$ -turn was located at the central position of a hairpin conformation about residues 92-94 in the X-ray structure of the ribonuclease S protein, the type VIa  $\beta$ -turn conformation has rarely been observed to stabilize a hairpin geometry in natural peptides.<sup>4,45</sup> Our data reflect the difficulty of stabilizing a hydrogen-bonded network in a small peptide possessing an amide *cis*-isomer in polar solvents.

Proteins folding implicates a set of conformational changes and multiple transition states to adopt finally the low energy native structure. Different interactions are involved in this dynamic process such as hydrophobic effect, solvation of polar groups and hydrogen bonding which involve both van der Waals

and electrostatic interactions.<sup>44</sup> Prolyl amide isomerization in proteins can be a rate-limiting step in the folding mechanism. Although the *trans*-isomer geometry has been shown to be of lower energy, the *cis*-isomer may be augmented by the hydrophobic stacking interaction of the *N*-terminal residue to proline with the pyrrolidine ring as observed in the X-ray structure of **1c**. The prolyl amide *cis*-isomers in proteins may thus begin folding processes by a series of hydrophobic interactions prior to isomerization to the more stable *trans*-isomer.

In conclusion, we have demonstrated that the prolyl amide equilibrium was influenced by the sequence in the 5-*t*BuPro-dipeptides and tetrapeptides. X-ray analysis of Ac-L-Tyr-*t*BuPro-NHMe has illustrated the stabilization of the prolyl amide *cis*-isomer by a stacking interaction of the aromatic and pyrrolidine rings. By using steric constraints of a *tert*-butyl substituent, we were able to favor a type VIa  $\beta$ -turn conformation in *N*-acetyl tetrapeptide methylesters. The major conformer adopted a prolyl amide *cis*-isomer in the 5-*t*BuPro-tetrapeptide methylesters, possessing a prolyl amide *cis*-isomer and a ten-membered intramolecular hydrogen bond. Incorporation of these type VI  $\beta$ -turn mimics into larger peptides is being pursued to provide more understanding of the impact of prolyl amide *cis*-isomers and type VI  $\beta$ -turns on the folding of peptide structures.

### 3.11. Experimental Section

**General.** Solvents and reagents were purified as previously described. NMR and CD data were measured as described in Ref. 22. Mass spectral data, HRMS (EI and FAB), were obtained by the Université de Montréal Mass Spectroscopy facility.

**General Procedure for Coupling to 5-*tert*-Butylproline *N*<sup>o</sup>-Methylamide.** A solution of (2*S*,5*R*)-5-*tert*-butylproline *N*<sup>o</sup>-methylamide hydrochloride (0.37 mmol)

prepared according to Ref. 21a and 22a, *N*-(BOC)amino acid (0.74 mmol) and DIEA (0.26 mL, 1.5 mmol) in CH<sub>2</sub>Cl<sub>2</sub> (4 mL) was cooled to 0 °C, treated with BOP-Cl (188 mg, 0.74 mmol), stirred for 1 h and allowed to warm to room temperature with stirring for 18 h. Brine was added and the solution was extracted with EtOAc. The combined organic layers were washed with 0.1 M HCl (2 x 10 mL), 5% NaHCO<sub>3</sub> (2 x 10 mL) and brine (10 mL), dried and evaporated to a residue that was purified by chromatography on silica gel using 35% EtOAc in hexane as eluant. Evaporation of the collected fractions furnished *N*-(BOC)dipeptide *N*<sup>1</sup>-methylamides.

***N*-BOC-*O*-Benzyl-(*S*)-aspartyl-(2*S*,5*R*)-5-*tert*-butylproline *N*<sup>1</sup>-methylamide (6a)** was obtained in 87% yield as an oil in a 1:1 mixture of conformers: [α]<sup>20</sup>D -95.4° (*c* 0.3, CHCl<sub>3</sub>); <sup>1</sup>H NMR (CDCl<sub>3</sub>) δ 0.84 (s, 4.5 H) [0.93 (s, 4.5 H)], 1.39 (s, 9 H), 1.76 (m, 1.5 H), 2.01 (m, 1.5 H), 2.41 (m, 1 H), [2.60 (dd, 0.5 H, *J* = 7.1, 15.9)] 2.91 (dd, 0.5 H, *J* = 7.7, 16.2), [4.23 (m, 1 H)] 4.55 (m, 1 H), 5.08 (d, 2 H, *J* = 7.7), [4.69 (t, 0.5 H, *J* = 8.9)] 5.13 (m, 0.5 H), [5.33 (d, 0.5 H, *J* = 10.0)] 5.47 (d, 0.5 H, *J* = 7.8), 7.31 (m, 5 H), [7.05 (br s, 0.5 H)], 8.04 (br s, 0.5 H); <sup>13</sup>C NMR (CDCl<sub>3</sub>) δ 25.2 (25.5), 26.0 (26.2), 26.4 (28.7), 27.1 (27.4), 28.0, (35.4) 35.6, 36.1 (37.0), (48.4) 49.8, 61.4 (62.3), (66.4) 66.8, 67.0 (67.3), (80.3) 80.7, (128.0) 128.1, (128.2) 128.3, 128.4, 135.0 (135.3), (154.6) 156.0, 169.6 (170.8), 171.2 (171.9), (173.5) 173.8; HRMS calcd for C<sub>26</sub>H<sub>40</sub>O<sub>6</sub>N<sub>3</sub> (MH<sup>+</sup>) 490.2917, found 490.2904.

***N*-BOC-*O*-Benzyl-(*S*)-seryl-(2*S*,5*R*)-5-*tert*-butylproline *N*<sup>1</sup>-methylamide (6b)** was obtained in 94% yield as an oil: [α]<sup>20</sup>D -44.1° (*c* 0.5, CHCl<sub>3</sub>); <sup>1</sup>H NMR (CDCl<sub>3</sub>) δ 0.86 (s, 7.9 H) [0.89 (s, 1.1 H)], 1.42 (s, 7.9 H) [1.44 (s, 1.1 H)], 1.75 (m, 2 H), 2.10 (m, 1 H), 2.35 (m, 1 H), [2.74 (d, 0.4 H, *J* = 5.0)] 2.81 (d, 2.6 H, *J* = 4.6), 3.61 (m, 2 H), 4.28 (m, 1 H), 4.46 (m, 3 H), 4.73 (m, 1 H), 5.10 (d, 0.9 H, *J* = 7.2) [5.39 (d, 0.1 H, *J* = 6.6)], 7.23-7.47 (m, 4 H), 7.56 (m, 0.9 H) [7.58 (m, 0.1 H)], 7.99 (br s, 0.9 H)

[8.24 (br s, 0.1 H)];  $^{13}\text{C}$  NMR ( $\text{CDCl}_3$ )  $\delta$  25.9, 26.5, 27.7, 28.5, 28.8, 36.1, 53.3, 62.3, 67.6, 69.9, 74.2, 81.2, 128.2, 128.5, 128.9, 130.2, 130.4, 172.3, 174.6; HRMS calcd for  $\text{C}_{25}\text{H}_{40}\text{O}_5\text{N}_3$  ( $\text{MH}^+$ ) 462.2968, found 462.2983.

**N-BOC-O-Benzyl-(S)-tyrosyl-(2*S,5R*)-5-*tert*-butylproline *N*'-methylamide (6c)** was obtained in 86% yield as a foam:  $[\alpha]^{20}\text{D}$   $-22.0^\circ$  (*c* 0.3, MeOH);  $^1\text{H}$  NMR ( $\text{CDCl}_3$ )  $\delta$  0.82 (s, 9 H), 1.15 (m, 2 H), 1.42 (s, 9 H), 1.56 (m, 1 H), 2.06 (m, 1 H), 2.76 (d, 3 H, *J* = 4.6), 2.85 (m, 2 H), 3.61 (dd, 1 H, *J* = 4.4, 8.8), 4.22 (dd, 1 H, *J* = 5.2, 8.6), 4.31 (m, 1 H), 5.04 (m, 2 H), 5.18 (d, 1 H, *J* = 6.9), 6.89 (m, 2 H), 7.08 (d, 2 H, *J* = 8.6), 7.28-7.43 (m, 5 H), 8.45 (br s, 1 H);  $^{13}\text{C}$  NMR ( $\text{CDCl}_3$ )  $\delta$  25.5, 26.5, 27.6, 28.5, 35.4, 36.1, 38.0, 55.1, 62.1, 67.4, 70.3, 81.1, 115.8, 127.7, 127.8, 128.4, 129.0, 130.9, 137.2, 156.8, 158.5, 172.0, 175.2; HRMS calcd for  $\text{C}_{31}\text{H}_{44}\text{O}_5\text{N}_3$  ( $\text{MH}^+$ ) 538.3281, found 538.3258.

**N-BOC-(S)-Tryptophyl-(2*S,5R*)-5-*tert*-butylproline *N*'-methylamide (6e)** was obtained in 67% yield as a foam;  $[\alpha]^{20}\text{D}$   $-12.8^\circ$  (*c* 0.4, MeOH);  $^1\text{H}$  NMR ( $\text{CDCl}_3$ )  $\delta$  0.79 (s, 9 H), 0.86 (m, 2 H), 1.26 (m, 1 H), 1.44 (s, 9 H), 1.84 (m, 1 H), 2.75 (d, 3 H, *J* = 4.6), 3.08 (dd, 1 H, *J* = 5.4, 13.6), 3.19 (dd, 1 H, *J* = 10.3, 13.5), 3.52 (m, 1 H), 4.11 (m, 1 H), 4.37 (m, 1 H), 5.27 (d, 1 H, *J* = 6.7), 7.04 (d, 1 H, *J* = 2.1), 7.11 (m, 1 H), 7.19 (t, 1 H, *J* = 7.0), 7.31 (d, 1 H, *J* = 8.0), 7.55 (d, 1 H, *J* = 7.8), 8.45 (br s, 1 H), 8.79 (br s, 1 H);  $^{13}\text{C}$  NMR ( $\text{CDCl}_3$ )  $\delta$  23.0, 24.5, 25.6, 26.3, 26.5, 26.6, 36.3, 55.1, 61.9, 67.7, 81.3, 110.1, 112.0, 119.4, 120.6, 123.2, 124.1, 127.4, 136.8, 157.1, 172.7, 176.1; HRMS calcd for  $\text{C}_{26}\text{H}_{39}\text{O}_4\text{N}_4$  ( $\text{MH}^+$ ) 471.2971, found 471.2990.

**General Procedure for Acetamide Synthesis.** A solution of *N*-(BOC)dipeptide *N*'-methylamide (20.5 mg, 0.05 mmol) in 25% TFA in  $\text{CH}_2\text{Cl}_2$  (1 mL) was stirred for 1 h and the solvent was evaporated. The residue was dissolved in  $\text{CH}_2\text{Cl}_2$  (1 mL),

treated with  $K_2CO_3$  (65.6 mg, 0.5 mmol) and acetic anhydride (45 mL, 0.5 mmol) and stirred for 18 h. The solution was filtered, washed with  $CH_2Cl_2$  ( $2 \times 5$  mL) and evaporated to give the *N*-acetyl dipeptide *N'*-methylamide.

***N*-Acetyl-*O*-benzyl-(*S*)-aspartyl-(2*S*,5*R*)-5-*tert*-butylproline *N'*-methylamide (8a)** was isolated in 94% yield as an oil in a 1:1 mixture of conformers:  $[\alpha]^{20}_D -107.6^\circ$  (*c* 0.1,  $CHCl_3$ );  $^1H$  NMR ( $CDCl_3$ )  $\delta$  [0.87 (d, 1.2 H, *J* = 6.3)] 0.95 (d, 1.8 H, *J* = 8.5), [0.93 (d, 1.2 H, *J* = 6.2)] 1.05 (d, 1.8 H, *J* = 6.5), 0.96 (s, 5.4 H) [1.01 (s, 3.6 H)], [1.20 (m, 0.4 H)] 1.50 (m, 0.6 H), 1.79-1.96 (m, 2 H), [2.01 (s, 1.2 H)] 2.06 (s, 1.8 H), 2.08-2.16 (m, 2 H), 2.25 (m, 1 H), 2.65-2.75 (m, 1 H), 2.83 (d, 1.8 H, *J* = 4.8) [2.88 (d, 1.2 H, *J* = 4.8)], 3.80 (d, 0.6 H, *J* = 8.0) [4.27 (d, 0.4 H, *J* = 8.5)], 4.56-4.69 (m, 1.4 H), 5.21 (m, 0.6 H), [5.97 (d, 0.4 H, *J* = 9.4)] 6.19 (d, 0.6 H, *J* = 8.5), [6.31 (br s, 0.4 H)] 7.29 (br s, 0.6 H);  $^{13}C$  NMR ( $CDCl_3$ )  $\delta$  22.4 (22.6), 25.2 (25.9), (26.1) 26.2, 27.2 (27.5), (26.7) 28.7, (35.4) 35.6, 35.7 (36.8), (47.1) 49.3, (61.5) 62.1, (66.6) 67.0, 67.3 (67.6), (128.1) 128.2, 128.3, (128.4) 128.5, 134.9 (135.2), (169.4) 169.5, (170.7) 171.0, 171.1 (171.8), 172.9 (173.4); HRMS calcd for  $C_{23}H_{34}O_5N_3$  ( $MH^+$ ) 432.2498, found 432.2494.

***N*-Acetyl-*O*-benzyl-(*S*)-seryl-(2*S*,5*R*)-5-*tert*-butylproline *N'*-methylamide (8b)** was isolated in 94% yield as an oil:  $[\alpha]^{20}_D -46.8^\circ$  (*c* 1.0,  $CHCl_3$ );  $^1H$  NMR ( $CDCl_3$ )  $\delta$  0.86 (s, 8.8 H) [0.89 (s, 0.2 H)], 1.82 (m, 3 H), 1.99 (s, 2.9 H) [2.03 (s, 0.1 H)], 2.36 (m, 1 H), 2.83 (d, 3 H, *J* = 4.6), 3.66 (m, 2 H), 4.26 (dd, 1 H, *J* = 5.0, 8.1), 4.46 (m, 2 H), 4.67 (m, 2 H), 6.85 (d, 1 H, *J* = 5.7), 7.24-7.60 (m, 5 H), 8.31 (br s, 1 H);  $^{13}C$  NMR ( $CDCl_3$ )  $\delta$  23.0, 25.8, 26.7, 27.8, 28.7, 36.1, 53.0, 62.4, 67.9, 69.6, 74.2, 128.2, 128.6, 130.0, 137.2, 171.9, 172.1, 173.8; HRMS calcd for  $C_{22}H_{34}O_4N_3$  ( $MH^+$ ) 404.2549, found 404.2556.

**N-Acetyl-O-benzyl-(S)-tyrosyl-(2S,5R)-5-tert-butylproline N'-methylamide (8c)** was isolated in 99% yield as an oil:  $[\alpha]^{20}_D -12.7^\circ$  (*c* 1.0, MeOH);  $^1\text{H}$  NMR (CDCl<sub>3</sub>) δ 0.82 (s, 9 H), 1.19 (m, 1 H), 1.52 (m, 1 H), 1.60 (m, 1 H), 1.99 (s, 3 H), 2.10 (m, 1 H), 2.79 (d, 3 H, *J* = 4.6), 2.95 (m, 2 H), 3.75 (dd, 1 H, *J* = 4.4, 8.9), 4.22 (dd, 1 H, *J* = 4.9, 8.7), 4.52 (m, 1 H), 5.05 (m, 2 H), 6.90 (d, 3 H, *J* = 8.6), 7.10 (d, 2 H, *J* = 8.6), 7.27-7.43 (m, 5 H), 8.50 (br s, 1 H);  $^{13}\text{C}$  NMR (CDCl<sub>3</sub>) δ 23.0, 25.4, 26.7, 27.7, 28.3, 36.0, 37.7, 54.7, 62.2, 67.8, 70.4, 115.9, 127.6, 127.8, 128.4, 129.0, 130.6, 130.9, 137.1, 158.6, 171.8, 174.7; HRMS calcd for C<sub>28</sub>H<sub>38</sub>O<sub>4</sub>N<sub>3</sub> (MH<sup>+</sup>) 480.2862, found 480.2859.

**N-Acetyl-(S)-tryptophyl-(2S,5R)-5-tert-butylproline N'-methylamide (1e)** was obtained in 97% yield as a solid: mp 132-134°C;  $[\alpha]^{20}_D -30.5^\circ$  (*c* 0.5, CHCl<sub>3</sub>);  $^1\text{H}$  NMR (CDCl<sub>3</sub>) δ 0.82 (s, 9 H), 0.90 (m, 1 H), 1.03 (m, 1 H), 1.40 (m, 1 H), 1.92 (m, 1 H), 2.06 (s, 3 H), [2.73 (d, 0.2 H, *J* = 4.3)] 2.79 (d, 2.8 H, *J* = 4.2), 3.14 (dd, 1 H, *J* = 5.8, 13.8), 3.28 (m, 1 H), 3.67 (m, 1 H), 4.14 (dd, 1 H, *J* = 4.9, 7.2), 4.60 (m, 1 H), 6.20 (d, 1 H, *J* = 3.9), 7.13 (m, 2 H), 7.24 (t, 1 H, *J* = 7.5), 7.38 (d, 1 H, *J* = 8.0), 7.58 (d, 1 H, *J* = 7.9), 8.21 (br s, 1 H), 8.35 (br s, 1 H);  $^{13}\text{C}$  NMR (CDCl<sub>3</sub>) δ 20.0, 21.9, 23.8, 24.8, 25.2, 25.5, 33.0, 51.8, 58.8, 64.9, 106.6, 108.9, 115.9, 117.4, 120.0, 121.1, 124.2, 133.7, 169.0, 169.5, 172.6; HRMS calcd for C<sub>23</sub>H<sub>33</sub>O<sub>3</sub>N<sub>4</sub> (MH<sup>+</sup>) 413.2553, found 413.2545.

**General Procedure for Benzyl Group Deprotection.** A solution of *N*-acetyl-*O*-benzyl-dipeptide *N'*-methylamide **8a-c** (110.0 mg, 0.26 mmol) in MeOH (3 mL) was treated with Pd/C (26 mg, 10% by weight) under 1 atm of H<sub>2</sub> and stirred for 18 h at room temperature. The solution was filtered onto Celite, washed with MeOH and the filtrate was evaporated to furnish *N*-acetyl dipeptide *N'*-methylamide **1a-c**.

**N-Acetyl-(S)-aspartyl-(2*S*,5*R*)-5-*tert*-butylproline *N'*-methylamide (1a)** was isolated in 95% yield as a foam:  $[\alpha]^{20}_D -79.3^\circ$  (*c* 0.3, MeOH);  $^1\text{H}$  NMR (CDCl<sub>3</sub>) mixture of three isomers  $\delta$  0.92 (s, 6 H) [1.00 (s, 1 H)] [1.10 (s, 2 H)], 1.86 (m, 1 H), [2.02 (s, 1 H)] 2.04 (s, 2 H), 2.26 (m, 1 H), 2.40 (m, 1 H), 2.62 (m, 1 H), [2.80 (d, 1.1 H, *J* = 4.3)] 2.86 (d, 1.9 H, *J* = 4.3), 3.11 (q, 1 H, *J* = 7.4, 14.8), [3.45 (dd, 0.4 H, *J* = 6.4, 11.5)] 3.69 (m, 0.6 H), 4.29 (m, 0.6 H) [4.36 (m, 0.4 H)], 4.59 (m, 1.2 H) [4.66 (m, 0.4 H), 5.40 (m, 0.4 H)], [6.88 (m, 0.4 H)] 7.21 (br s, 0.6 H), [7.07 (br s, 0.15 H)] [7.98 (br s, 0.25 H)] 8.36 (br s, 0.6 H);  $^{13}\text{C}$  NMR (CDCl<sub>3</sub>)  $\delta$  (18.6) 22.8, 25.8 (27.4), (23.0) 26.8, 27.8 (28.1), 29.7 (31.2), 36.0, 36.1 (37.1), (47.8) 50.0, 62.5 (71.2), 68.2 (77.6), 171.0, 172.2, 172.7, 174.1; HRMS calcd for C<sub>16</sub>H<sub>28</sub>O<sub>5</sub>N<sub>3</sub> (MH<sup>+</sup>) 342.2029, found 342.2021.

**N-Acetyl-(S)-seryl-(2*S*,5*R*)-5-*tert*-butylproline *N'*-methylamide (1b)** was isolated in 94% yield as a foam:  $[\alpha]^{20}_D -51.9^\circ$  (*c* 0.5, MeOH);  $^1\text{H}$  NMR (CDCl<sub>3</sub>)  $\delta$  0.86 (s, 9 H), 1.82 (m, 1 H), 2.00 (s, 3 H), 2.16 (m, 1 H), 2.33 (m, 1 H), 2.79 (d, 3 H, *J* = 4.5), 3.75 (m, 1 H), 4.25 (m, 1 H), 4.46 (m, 1 H), 4.71 (m, 1 H), 7.30 (d, 1 H, *J* = 4.9), 8.47 (br s, 1 H);  $^{13}\text{C}$  NMR (CDCl<sub>3</sub>)  $\delta$  22.3, 25.3, 26.2, 27.3, 28.9, 35.6, 54.8, 61.4, 61.8, 67.4, 171.8, 172.3, 173.4; HRMS calcd for C<sub>15</sub>H<sub>27</sub>O<sub>4</sub>N<sub>3</sub> (MH<sup>+</sup>) 313.2002, found 313.2008.

**N-Acetyl-(S)-tyrosyl-(2*S*,5*R*)-5-*tert*-butylproline *N'*-methylamide (1c)** was isolated in 92% yield as a solid: mp 106-108 °C;  $[\alpha]^{20}_D -13.2^\circ$  (*c* 0.3, MeOH);  $^1\text{H}$  NMR (CDCl<sub>3</sub>)  $\delta$  0.85 (s, 9 H), 1.40 (m, 1 H), 1.50 (m, 1 H), 1.55 (m, 1 H), 1.98 (s, 3 H), 2.00 (m, 1 H), 2.75 (d, 3 H, *J* = 4.6), 2.88 (m, 2 H), 3.71 (dd, 1 H, *J* = 5.1, 8.8), 4.29 (dd, 1 H, *J* = 4.4, 8.6), 4.46 (m, 1 H), 6.05 (d, 1 H, *J* = 5.8), 6.81 (d, 2 H, *J* = 8.4), 7.07 (d, 2 H, *J* = 8.4), 8.52 (br s, 1 H);  $^{13}\text{C}$  NMR (CDCl<sub>3</sub>)  $\delta$  (19.7) 19.8, 22.4, (23.6) 23.8, 24.8 (25.0), 25.8, 33.0, 34.8, (51.9) 52.0, 59.0, 65.0, (112.9) 113.5, 123.1,

(127.7) 127.9, (153.2) 154.0, 169.1, 169.2, (169.8) 172.0; HRMS calcd for C<sub>21</sub>H<sub>31</sub>O<sub>4</sub>N<sub>3</sub> (MH<sup>+</sup>) 389.2314, found 389.2304.

**General Procedure for Asparaginyl Dipeptide Synthesis.** A solution of *N*-acetyl-*O*-benzyl-(2*S*)-aspartyldipeptide *N*<sup>t</sup>-methylamide **7a** and **8a** (100.0 mg, 0.23 mmol) in MeOH (2 mL) was treated with NH<sub>3</sub> (g) bubbles at 0°C and stirred for 18 h at room temperature. The solution was evaporated and triturated with Et<sub>2</sub>O to give *N*-acetyldipeptide *N*<sup>t</sup>-methylamide **1f** and **2f**.

***N*-Acetyl-(*S*)-asparaginyl-(2*S*,5*R*)-5-*tert*-butylproline *N*<sup>t</sup>-methylamide (1f)** was isolated in 97% yield as a foam: [α]<sup>20</sup><sub>D</sub> -70.9° (*c* 0.3, MeOH); <sup>1</sup>H NMR (CDCl<sub>3</sub>) δ 0.92 (s, 5.4 H) [1.0 (s, 3.6 H)], 1.80-1.90 (m, 2 H), [2.02 (s, 1.2 H)] 2.05 (s, 1.8 H), 2.15 (m, 1 H), 2.41-2.58 (m, 2 H), 2.63 (dd, 1 H, *J* = 6.0, 15.0), [2.81 (d, 1.2 H, *J* = 4.6)] 2.85 (d, 1.8 H, *J* = 4.6), 4.26 (m, 1 H), 4.73 (m, 1 H), 4.58 (q, 0.6 H, *J* = 5.5, 8.6) [5.39 (q, 0.4 H, *J* = 7.0, 14.8)], [5.51 (br s, 0.4 H)] 5.66 (br s, 0.6 H), [5.87 (br s, 0.4 H)] 6.22 (br s, 0.6 H), [6.33 (d, 0.4 H, *J* = 8.2)] 7.06 (d, 0.6 H, *J* = 5.9), [7.11 (br s, 0.4 H)] 8.10 (br s, 0.6 H); <sup>13</sup>C NMR (CD<sub>3</sub>OD:CDCl<sub>3</sub>) δ 21.9 (22.1), 25.2 (26.7), 25.9 (26.0), 27.1 (27.4), (26.9) 28.7, (35.4) 35.6, 36.2 (37.0), 49.8 (49.9), (61.4) 61.8, 67.5 (67.8), (170.4) 171.6, (171.7) 171.9, 172.0 (172.6), 173.5 (173.9); HRMS calcd for C<sub>16</sub>H<sub>29</sub>O<sub>4</sub>N<sub>4</sub> (MH<sup>+</sup>) 341.2202, found 341.2200.

***N*-Acetyl-(*S*)-asparaginyl-(*S*)-proline *N*<sup>t</sup>-methylamide (2f)** was isolated in 99% yield as an oil: [α]<sup>20</sup><sub>D</sub> -122.5° (*c* 0.8, MeOH); <sup>1</sup>H NMR (CDCl<sub>3</sub>) δ 2.02 (m, 5 H), 2.09 (m, 1 H), 2.12 (m, 1 H), [2.49 (m, 0.2 H)] 2.70 (dd, 0.8 H, *J* = 3.8, 14.8), 2.78 (d, 3 H, *J* = 4.6), 2.92 (dd, 0.8 H, *J* = 9.0, 14.8) [3.03 (m, 0.2 H)], 3.75 (m, 2 H), 4.61 (m, 1 H), 5.05 (m, 0.8 H) [5.13 (m, 0.2 H)], 5.43 (br s, 1 H), 6.00 (br s, 1 H), [6.17 (d, 0.2

H,  $J = 7.8$ )] 6.51 (d, 0.8 H,  $J = 7.7$ ), [6.89 (br s, 0.2 H)] 7.17 (br s, 0.8 H); HRMS calcd for C<sub>12</sub>H<sub>20</sub>O<sub>4</sub>N<sub>4</sub> (MH<sup>+</sup>) 284.1484, found 284.1494.

**General Protocol For The Synthesis of *N*-Acetyl Dipeptide *N'*-Methylamides Possessing Natural Proline.** A solution of *N*-(BOC)amino acid (1.4 mmol) in CH<sub>3</sub>CN (6 mL) was treated with DIEA (0.49 mL, 2.8 mmol), proline *N'*-methylamide hydrochloride (115 mg, 0.7 mmol) prepared according to Ref. 22a and TBTU (0.45 g, 1.4 mmol), stirred at room temperature for 18 h, and partitioned between brine (10 mL) and EtOAc (10 mL). The organic phase was washed with 0.1 M HCl (2 x 8 mL), 5% NaHCO<sub>3</sub> (2 x 8 mL), and brine (10 mL), dried, and evaporated to a residue that was purified by chromatography on silica gel (35% EtOAc in hexane). The *N*-(BOC)dipeptide *N'*-methylamide **5a-e** was treated with 25% TFA in CH<sub>2</sub>Cl<sub>2</sub> (10 mL) for 1 h and evaporated. The resulting dipeptide *N'*-methylamide trifluoroacetate was dissolved in CH<sub>2</sub>Cl<sub>2</sub> and treated in the same acetylation and benzyl deprotection conditions as described above.

***N*-Acetyl-(*S*)-aspartyl-(*S*)-proline *N'*-methylamide (2a)**

was isolated as an oil in 50% overall yield for the four steps:  $[\alpha]^{20}_D -97.8^\circ$  (*c* 1.3, MeOH); <sup>1</sup>H NMR (CDCl<sub>3</sub>)  $\delta$  1.47 (m, 3 H), [2.02 (s, 0.5 H)] 2.03 (s, 2.5 H), 2.27 (m, 1 H), 2.75 (d, 2.5 H,  $J = 4.7$ ) [2.83 d, 0.5 H,  $J = 4.7$ ], 2.98 (m, 1 H), 3.10 (m, 1 H), 3.84 (m, 2 H), 4.58 (dd, 1 H,  $J = 2.6, 7.7$ ), 5.15 (m, 1 H), [6.21 (d, 0.2 H,  $J = 9.5$ )] 6.87 (d, 0.8 H,  $J = 8.1$ ), 6.98 (br s, 0.8 H) [7.18 (br s, 0.2 H)]; <sup>13</sup>C NMR (CDCl<sub>3</sub>)  $\delta$  21.0 (21.2), (23.9) 24.2, 25.2 (25.4), 29.5 (29.7), (35.5) 46.1, 47.5, (51.4) 51.8, (60.0) 60.9, 171.3, 171.8, 172.0; HRMS calcd for C<sub>12</sub>H<sub>19</sub>O<sub>5</sub>N<sub>3</sub> (MH<sup>+</sup>) 285.1325, found 285.1328.

***N*-Acetyl-(*S*)-seryl-(*S*)-proline *N'*-methylamide (2b)**

was isolated as a foam in 65% overall yield for the four steps:  $[\alpha]^{20}_D -85.1^\circ$  (*c* 0.4, MeOH); <sup>1</sup>H NMR (CDCl<sub>3</sub>)  $\delta$

1.60 (br s, 1 H), 1.98-2.19 (m, 7 H), 2.83 (d, 2.8 H,  $J = 4.8$ ) [2.85 (d, 0.2 H,  $J = 4.6$ )], 3.71 (m, 2 H), 3.87 (m, 1 H), 4.02 (dd, 1 H,  $J = 4.5, 11.1$ ), 4.55 (m, 1 H), 4.94 (dd, 1 H,  $J = 6.1, 12.1$ ), 6.32 (br s, 0.9 H) [7.19 (m, 0.1 H)], 6.54 (d, 0.9 H,  $J = 7.0$ ) [7.19 (m, 0.1 H)];  $^{13}\text{C}$  NMR ( $\text{CD}_3\text{OD}:\text{CDCl}_3$ )  $\delta$  22.6 (22.9), (22.4) 24.9, 26.5 (26.7), 26.8 (31.8), (47.3) 48.1, 52.7, (60.9) 61.1, 171.2, 173.0; HRMS calcd for  $\text{C}_{11}\text{H}_{19}\text{O}_4\text{N}_3$  ( $\text{MH}^+$ ) 257.1376, found 257.1373.

**N-Acetyl-(S)-tyrosyl-(S)-proline N'-methylamide (2c)** was isolated as a solid in 49% overall yield for the four steps: mp 93-95°C;  $[\alpha]^{20}\text{D} -32.0^\circ$  ( $c$  0.4, MeOH);  $^1\text{H}$  NMR ( $\text{CDCl}_3$ )  $\delta$  1.81-1.94 (m, 3 H), 2.03 (s, 2.4 H) [2.04 (s, 0.6 H)], [2.20 (m, 0.2 H)] 2.33 (m, 0.8 H), 2.78 (d, 2.4 H,  $J = 4.8$ ) [2.81 (d, 0.6 H,  $J = 4.7$ )], [2.93 (m, 0.4 H)] 2.99 (m, 1.6 H), 3.10 (m, 1 H), [3.49 (m, 0.2 H)] 3.61 (q, 0.8 H,  $J = 8.2, 17.7$ ), [4.34 (m, 0.2 H)] 4.52 (dd, 0.8 H,  $J = 2.4, 7.7$ ), 4.97 (q, 1 H,  $J = 7.8, 14.2$ ), 5.90 (br s, 1 H), [6.02 (d, 0.2 H,  $J = 5.4$ )] 6.25 (d, 0.8 H,  $J = 8.0$ ), 6.48 (br s, 0.8 H) [7.39 (br s, 0.2 H)], 6.78 (d, 2 H,  $J = 8.5$ ), 7.05 (d, 2 H,  $J = 8.4$ );  $^{13}\text{C}$  NMR ( $\text{CDCl}_3$ )  $\delta$  (26.1) 26.4, (26.1) 28.9, 32.9 (35.0), 41.4 (41.8), (50.9) 51.8, 56.8 (58.3), 64.6 (65.0), (119.7) 120.0, (130.3) 131.1, 134.5 (134.6), 160.3 (160.7), 175.5 (176.0), 175.9 (176.3), 176.6; HRMS calcd for  $\text{C}_{17}\text{H}_{23}\text{O}_4\text{N}_3$  ( $\text{MH}^+$ ) 333.1688, found 333.1675.

**N-Acetyl-(S)-phenylalanyl-(S)-proline N'-methylamide (2d)** was isolated as a solid in 53% overall yield for the three steps: mp 102-104°C;  $[\alpha]^{20}\text{D} -37.6^\circ$  ( $c$  0.6, MeOH);  $^1\text{H}$  NMR ( $\text{CDCl}_3$ )  $\delta$  1.82 (m, 2 H), [1.93 (s, 0.6 H)] 1.94 (s, 2.4 H), 2.23 (m, 1 H), 2.67 (d, 2.4 H,  $J = 4.8$ ) [2.73 (d, 0.6 H,  $J = 4.7$ )], 2.97-3.10 (m, 3 H), 3.41 (m, 0.8 H) [3.55 (d, 0.2 H,  $J = 7.8$ )], 3.64 (m, 1 H), [4.41 (m, 0.2 H)] 4.46 (m, 0.8 H), 4.99 (m, 1 H), [6.00 (br s, 0.2 H)] 6.23 (d, 0.8 H,  $J = 8.3$ ), 6.38 (br s, 0.8 H) [7.44 (br s, 0.2 H)], 7.16-7.29 (m, 5 H);  $^{13}\text{C}$  NMR ( $\text{CDCl}_3$ )  $\delta$  22.8, (21.6) 24.6, 26.0 (26.4), 27.4 (30.4), (38.3) 38.6, (46.4) 47.3, 51.7 (53.6), 59.9 (60.8), 127.1 (127.4), 128.4

(128.8), (129.1) 129.2, (135.2) 135.7, (166.2) 169.6, (170.6) 170.8, 171.5; HRMS calcd for C<sub>17</sub>H<sub>23</sub>O<sub>3</sub>N<sub>3</sub> (M) 317.1739, found 317.1742.

**N-Acetyl-(S)-tryptophyl-(S)-proline N'-methylamide (2e)** was isolated as a foam in 55% overall yield for the three steps:  $[\alpha]^{20}_D -28.6^\circ$  (*c* 0.4, MeOH); <sup>1</sup>H NMR (CDCl<sub>3</sub>) δ 1.44 (m, 1 H), 1.83 (m, 2 H), [2.06 (s, 0.9 H)] 2.03 (s, 2.1 H), 2.27 (m, 1 H), 2.65 (d, 2.1 H, *J* = 4.8) [2.77 (d, 0.9 H, *J* = 4.7)], 3.17 (m, 1 H), 3.20-3.42 (m, 2 H), 3.60 (m, 1 H), [4.44 (m, 0.3 H)] 4.48 (m, 0.7 H), 5.14 (m, 1 H), [6.14 (br s, 0.3 H)] 6.29 (br s, 0.7 H), 7.02-7.41 (m, 5 H), [7.58 (d, 0.3 H, *J* = 7.8)] 7.71 (d, 0.7 H, *J* = 7.8), 8.14 (br s, 0.7 H) [8.20 (br s, 0.3 H)]; <sup>13</sup>C NMR (CDCl<sub>3</sub>) δ (23.0) 23.4, (22.1) 25.1, 26.6 (27.0), 28.6 (28.8), 28.9 (30.4), (47.2) 48.0, 51.8 (54.7), 60.7 (60.9), (109.7) 109.8, (111.9) 112.0, 118.8 (119.0), (120.0) 120.1, 122.5 (122.8), 123.9 (124.1), (127.3) 127.7, 136.5 (136.6), 170.5 (171.5), (171.8) 172.1, (172.4) 172.5; HRMS calcd for C<sub>19</sub>H<sub>24</sub>O<sub>3</sub>N<sub>4</sub> (MH<sup>+</sup>) 356.1848, found 356.1843.

**(2*S*,5*R*)-*N*-(BOC)-5-*tert*-Butylproline benzyl ester (10).** A solution of (2*S*,5*R*)-*N*-(BOC)-5-*tert*-butylproline (1.01 g, 3.7 mmol, prepared according to reference 21a) in CH<sub>2</sub>Cl<sub>2</sub> (25 mL) was treated with DIEA (1.3 mL, 7.4 mmol) and benzylbromide (2.2 mL, 18.5 mmol), heated to a reflux, stirred for 18 h, cooled to rt, and evaporated. The residue was dissolved in EtOAc (50 mL) and the solution was washed with cold 0.1 M HCl (2 x 10 mL) and a phosphate buffer solution at pH 9.5 (15 mL), dried, and evaporated to give **10** (1.3 g, 96%) as an oil:  $[\alpha]^{20}_D -39.1^\circ$  (*c* 0.7, CHCl<sub>3</sub>); <sup>1</sup>H NMR (CDCl<sub>3</sub>) δ 0.89 (s, 9 H), 1.37 (br s, 9 H), 1.79-1.97 (m, 3 H), 2.20 (m, 1 H), 3.78 (br s, 1 H), 4.27 (m, 1 H), 5.10 (m, 2H), 7.32 (m, 5 H); <sup>13</sup>C NMR (CDCl<sub>3</sub>) δ 27.0, 27.9, 28.6, 30.1, 36.8, 62.0, 66.9, 67.1, 80.2, 128.7, 128.8, 128.9, 136.2, 156.4, 173.4; LRMS calcd for C<sub>21</sub>H<sub>32</sub>O<sub>4</sub>N (MH<sup>+</sup>) 362.0, found 362.2.

**(2*S*,5*R*)-5-*tert*-Butylproline benzyl ester hydrochloride.** A solution of (2*S*,5*R*)-*N*-(BOC)-5-*tert*-butylproline benzyl ester (**x**, 1.3 g, 3.6 mmol) in CH<sub>2</sub>Cl<sub>2</sub> (36 mL) was treated with HCl (g) bubbles at 0°C, stirred for 2 h at rt and evaporated to provide (2*S*,5*R*)-5-*tert*-butylproline benzyl ester hydrochloride in 99% (1.07 g) yield as a white precipitate: <sup>1</sup>H NMR (CD<sub>3</sub>OD) δ 0.94 (s, 9 H), 1.45 (m, 1 H), 1.84 (m, 1 H), 2.21 (m, 2 H), 3.40 (m, 1 H), 4.36 (m, 1 H), 4.56 (s, 2 H), 7.30 (m, 5 H).

***N*-(BOC)-(S)-Alanyl-(2*S*,5*R*)-5-*tert*-butylproline benzyl ester (11a)** was synthesized from 5-*t*BuPro benzyl ester using BOP-Cl coupling conditions as described above and obtained in 74% yield as an oil; [α]<sup>20</sup><sub>D</sub> -85.6° (c 0.3, CHCl<sub>3</sub>); <sup>1</sup>H NMR (CDCl<sub>3</sub>) δ [0.79 (s, 3.6 H)] 0.92 (s, 5.4 H), [1.22 (d, 1.2 H, *J* = 5.6)] 1.30 (d, 1.8 H, *J* = 6.4), 1.37 (s, 5.4 H) [1.39 (s, 3.6 H)], 1.83-2.29 (m, 4 H), [4.14 (d, 0.4 H, *J* = 7.5)] 4.33 (d, 0.6 H, *J* = 7.1), [4.42 (t, 0.8 H, *J* = 7.9)] 4.67 (t, 1.2 H, *J* = 8.5), 4.90 (d, 0.6 H, *J* = 8.4) [5.37 (d, 0.4 H, *J* = 6.8)], 5.15 (m, 2 H), 7.23 (m, 5 H); <sup>13</sup>C NMR (CDCl<sub>3</sub>) δ 18.8 (19.6), 26.2 (28.1), 27.9 (29.4), (27.8) 28.1, 28.7 (28.8), 36.3 (36.5), 47.1 (48.5), 60.5 (61.0), 67.0 (68.1), 67.4, 80.1, 128.5, 128.6, 128.9 (129.1), 136.2, 172.0, 172.3, 175.4; LRMS calcd for C<sub>24</sub>H<sub>37</sub>O<sub>5</sub>N<sub>2</sub> (MH<sup>+</sup>) 433.6, found 433.4.

***N*-(BOC)-(S)-Leucyl-(2*S*,5*R*)-5-*tert*-butylproline benzyl ester (11b)** was synthesized from 5-*t*BuPro benzyl ester using BOP-Cl coupling conditions as described above and was obtained in 86% yield as an oil; [α]<sup>20</sup><sub>D</sub> -88.7° (c 0.6, CHCl<sub>3</sub>); <sup>1</sup>H NMR (CDCl<sub>3</sub>) δ 0.79-0.93 (m, 15 H), 1.45 (m, 10 H), 1.58-2.30 (m, 6 H), [4.11 (m, 0.5 H)] 4.38 (m, 1.5 H), 4.70 (m, 2 H), 5.07-5.37 (m, 2 H), 7.30 (m, 5 H); <sup>13</sup>C NMR (CDCl<sub>3</sub>) δ 22.0 (22.2), 24.1 (24.8), (26.4) 27.8, 28.1 (29.7), (27.9) 28.2, 28.6, 28.7, 36.2 (36.6) 41.2, 49.9, 60.9, 67.1, 67.2, 80.0, 128.5, 128.8, 129.3,

136.1, 155.8, 172.3, 175.2; HRMS calcd for C<sub>27</sub>H<sub>43</sub>O<sub>5</sub>N<sub>2</sub> (MH<sup>+</sup>) 475.3172, found 475.3181.

**N-(BOC)-(S)-Phenylalanyl-(2*S*,5*R*)-5-*tert*-butylproline benzyl ester (11c)** was synthesized from 5-*t*BuPro benzyl ester using BOP-Cl coupling conditions as described above and was obtained in 92% yield as an oil: [α]<sup>20</sup><sub>D</sub> -64.9° (*c* 0.5, CHCl<sub>3</sub>); <sup>1</sup>H NMR (CDCl<sub>3</sub>) δ 0.68 (s, 7.2 H) [0.89 (s, 1.8 H)], [1.25 (s, 1.8 H)] 1.38 (s, 7.2 H), 1.54 (m, 2 H), 1.74-2.2 (m, 2 H), 2.82-3.06 (m, 2 H), 3.49 (t, 1 H, *J* = 8.4), 4.02 (d, 0.8 H, *J* = 8.5) [4.26 (m, 0.2 H)], 4.58 (m, 0.8 H) [4.61 (m, 0.2 H)], 5.2 (m, 2 H), 5.40 (d, 1 H *J* = 8.5), 7.25 (m, 10 H); <sup>13</sup>C NMR (CDCl<sub>3</sub>) δ 29.5 (27.9), 27.8 (28.1), (28.6) 28.8, 28.7 (30.1), (36.2) 36.5, (38.8) 41.5, 52.6 (54.3), 60.1 (61.1), 66.8 (67.2), (67.0) 67.8, 79.8 (80.0), (127.0) 127.5, (128.6) 128.8, 128.9, 129.0, 129.2, 129.9, 135.6 (136.2), 136.9 (137.5), 155.1 (155.6), 172.0 (172.3), 173.4 (174.3); LRMS calcd for C<sub>30</sub>H<sub>41</sub>O<sub>5</sub>N<sub>2</sub> (MH<sup>+</sup>) 509.7, found 509.4.

**N-(BOC)-L-Alanyl-(2*S*,5*R*)-5-*tert*-butylproline (12a)** was synthesized from **11a** using benzyl deprotection conditions as described above and was obtained in 92% yield as an oil; [α]<sup>20</sup><sub>D</sub> -169.2° (*c* 0.6, CHCl<sub>3</sub>); <sup>1</sup>H NMR (CDCl<sub>3</sub>) δ 0.90 (s, 6.3 H) [0.88 (s, 2.7 H)], 1.35 (m, 12 H), 1.81-2.56 (m, 4 H), [4.18 (d, 0.3 H, *J* = 5.2)] 4.44 (m, 0.7 H), 4.61 (t, 1 H, *J* = 9.2), 4.71 (m, 1 H), 4.99 (d, 0.7 H, *J* = 7.7) [5.61 (d, 0.3 H, *J* = 6.9)], 9.45 (br s, 1 H); <sup>13</sup>C NMR (CDCl<sub>3</sub>) δ 18.4 (18.5), 26.0 (26.1), 26.7 (29.5), 27.9, 28.6, 35.9 (36.5), 47.3 (49.0), (60.8) 62.5, (67.5) 68.5, 80.7 (81.2), 155.5, 172.2 (173.6), (174.7) 178.4; LRMS calcd for C<sub>17</sub>H<sub>31</sub>O<sub>5</sub>N<sub>2</sub> (MH<sup>+</sup>) 343.0, found 343.3.

**N-(BOC)-(S)-Leucyl-(2*S,5R*)-5-*tert*-butylproline (12b)** was synthesized from **11b** using benzyl deprotection conditions as described above and was isolated in 99% yield as a solid; spectroscopic values were identical with those reported in Ref. 22a.

**N-(BOC)-(S)-Phenylalanyl-(2*S,5R*)-5-*tert*-butylproline (12c)** was synthesized from **11c** using benzyl deprotection conditions as described above and was isolated in 99% yield as a solid; spectroscopic values were identical with those reported in Ref. 22a.

**Peptide Synthesis.** The synthesis of the tetrapeptides were carried out manually by a stepwise solid-phase procedure using oxime resin. Serine and lysine were introduced as BOC-L-Ser(Bn)-OH and BOC-L-Lys(Cbz)-OH. Couplings were performed with BOC-protected amino acids (200 mol%), TBTU (200 mol%) and DIEA (400 mol%) in DMF for 1h. The resin was agitated with N<sub>2</sub> bubbles during the coupling, rinsing and deprotection sequences. Coupling reactions were monitored by Kaiser ninhydrin test. In cases of incomplete couplings, the resin was resubmitted to the same coupling conditions. Deprotections were performed with 25% TFA in CH<sub>2</sub>Cl<sub>2</sub> (2 x 30 min) and the resin was free-based with 10% DIEA in CH<sub>2</sub>Cl<sub>2</sub> (2 x 5 min). *N*-terminal acetylation of the peptides was accomplished by treating the resin with Ac<sub>2</sub>O (1000 mol%) and DIEA (1000 mol%) in CH<sub>2</sub>Cl<sub>2</sub> for 1 h. The tetrapeptide *N*-methylamides were obtained by cleaving the peptides from the resin with 10% methylamine in CHCl<sub>3</sub> upon agitation with a mechanical shaker for 24 h. The tetrapeptide methylesters were obtained by treating the resin with Ca(OAc)<sub>2</sub> in MeOH:THF (1:4) at 40°C for 48 h. The crude material was purified with semi-preparative RP-HPLC (Higgins C18 column, 20 x 250 mm, particle size 5 μm) with solvent A, H<sub>2</sub>O (0.05% TFA) and solvent B, 75% CH<sub>3</sub>CN/H<sub>2</sub>O (0.05% TFA). Analytical RP-HPLC was performed on a Higgins C18 (4.6 x 250 mm, particle size 5 μm) using a gradient of 0-90% eluant B (CH<sub>3</sub>CN 0.003% TFA) in A (H<sub>2</sub>O 0.03%

TFA) over 30 min with a flow rate of 1.5 mL/min and the detector centered at 214 nm; retention times ( $t_R$ ) are reported in minutes.

**N-Acetyl-(S)-alanyl-(S)-alanyl-(2*S,5R*)-5-*tert*-butylprolyl-(S)-alanine N'-methylamide (13a).** The peptide was cleaved from the resin (430 mg) according to the procedure described above to afford 66 mg of product. Purification of 56 mg of the peptide by RP-HPLC and collection of the pure fractions afforded 11 mg (21% overall yield) of product shown to be of >95% purity by RP-HPLC ( $t_R$  = 21.0); LRMS calcd for  $C_{21}H_{38}N_5O_5$  ( $MH^+$ ) 440.0 found 440.2; HRMS calcd for  $C_{21}H_{38}N_5O_5$  ( $MH^+$ ) 440.2873, found 440.2883.

**N-Acetyl-(S)-alanyl-(S)-alanyl-(2*S,5R*)-5-*tert*-butylprolyl-(S)-leucine N'-methylamide (13b).** The peptide was cleaved from the resin (452 mg) according to the procedure described above to afford 82 mg of product. Purification of 58 mg of the peptide by RP-HPLC and collection of the pure fractions afforded 21.8 mg (37% overall yield) of product shown to be of >95% purity by RP-HPLC ( $t_R$  = 25.6); LRMS calcd for  $C_{24}H_{44}N_5O_5$  ( $MH^+$ ) 482.0 found 482.4; HRMS calcd for  $C_{24}H_{44}N_5O_5$  ( $MH^+$ ) 482.3343, found 482.3365.

**N-Acetyl-(S)-alanyl-(S)-alanyl-(2*S,5R*)-5-*tert*-butylprolyl-(S)-phenylalanine N'-methylamide (13c).** The peptide was cleaved from the resin (594 mg) according to the procedure described above to afford 110 mg of product. Purification of 50 mg of the peptide by RP-HPLC and collection of the pure fractions afforded 21.0 mg (42% overall yield) of product shown to be of >95% purity by RP-HPLC ( $t_R$  = 26.5); LRMS calcd for  $C_{27}H_{42}N_5O_5$  ( $MH^+$ ) 516.0 found 516.1; HRMS calcd for  $C_{27}H_{42}N_5O_5$  ( $MH^+$ ) 516.3186, found 516.3173.

**N-Acetyl-(S)-alanyl-(S)-alanyl-(2*S*,5*R*)-5-*tert*-butylprolyl-(S)-phenylalanine methyl ester (14a).** The peptide was cleaved from the resin (240 mg) according to the procedure described above to afford 18.7 mg of product. Purification of 18.7 mg of the peptide by RP-HPLC and collection of the pure fractions afforded 4.0 mg (10% overall yield) of product shown to be of >96% purity by RP-HPLC ( $t_R = 21.2$ ); LRMS calcd for  $C_{27}H_{41}N_4O_6$  ( $MH^+$ ) 517.3 found 517.3.

**N-Acetyl-(S)-alanyl-(S)-leucyl-(2*S*,5*R*)-5-*tert*-butylprolyl-(S)-leucine *N*'-methylamide (13d).** The peptide was cleaved from the resin (454 mg) according to the procedure described above to afford 77 mg of product. Purification of 40 mg of the peptide by RP-HPLC and collection of the pure fractions afforded 19.1 mg (48% overall yield) of product shown to be of >95% purity by RP-HPLC ( $t_R = 28.5$ ); LRMS calcd for  $C_{27}H_{50}N_5O_5$  ( $MH^+$ ) 524.0 found 524.3; HRMS calcd for  $C_{27}H_{50}N_5O_5$  ( $MH^+$ ) 524.3812, found 524.3802.

**N-Acetyl-(S)-alanyl-(S)-leucyl-(2*S*,5*R*)-5-*tert*-butylprolyl-(S)-phenylalanine *N*'-methylamide (13e).** The peptide was cleaved from the resin (543 mg) according to the procedure described above to afford 95 mg of product. Purification of 36 mg of the peptide by RP-HPLC and collection of the pure fractions afforded 21.8 mg (61% overall yield) of product shown to be of >95% purity by RP-HPLC ( $t_R = 26.2$ ); LRMS calcd for  $C_{30}H_{48}N_5O_5$  ( $MH^+$ ) 558.0 found 558.2; HRMS calcd for  $C_{30}H_{48}N_5O_5$  ( $MH^+$ ) 558.3655, found 558.3665.

**N-Acetyl-(S)-alanyl-(S)-phenylalanine-(2*S*,5*R*)-5-*tert*-butylprolyl-(S)-phenylalanine *N*'-methylamide (13f).** The peptide was cleaved from the resin (608 mg) according to the procedure described above to afford 110 mg of product. Purification of 45 mg of the peptide by RP-HPLC and collection of the pure fractions

afforded 19.6 mg (44% overall yield) of product shown to be of >95% purity by RP-HPLC ( $t_R = 30.1$ ); LRMS calcd for  $C_{33}H_{46}N_5O_5$  ( $MH^+$ ) 592.0 found 592.1; HRMS calcd for  $C_{33}H_{46}N_5O_5$  ( $MH^+$ ) 592.3499, found 592.3483.

**N-Acetyl-(S)-alanyl-(S)-phenylalanyl-(2*S,5R*)-5-*tert*-butylprolyl-(S)-leucine N-methylamide (13g).** The peptide was cleaved from the resin (459 mg) according to the procedure described above to afford 78 mg of product. Purification of 49 mg of the peptide by RP-HPLC and collection of the pure fractions afforded 21.5 mg (44% overall yield) of product shown to be of >95% purity by RP-HPLC ( $t_R = 29.2$ ); LRMS calcd for  $C_{30}H_{48}N_5O_5$  ( $MH^+$ ) 558.0 found 558.4; HRMS calcd for  $C_{30}H_{48}N_5O_5$  ( $MH^+$ ) 558.3655, found 558.3665.

**N-Acetyl-(S)-alanyl-(S)-phenylalanyl-(2*S,5R*)-5-*tert*-butylprolyl-(S)-valine N-methylamide (13h).** The peptide was cleaved from the resin (174 mg) according to the procedure described above to afford 45 mg of product. Purification of 45 mg of the peptide by RP-HPLC and collection of the pure fractions afforded 28.2 mg (54% overall yield) of product shown to be of >95% purity by RP-HPLC ( $t_R = 18.4$ ); LRMS calcd for  $C_{29}H_{46}N_5O_5$  ( $MH^+$ ) 544.3 found 544.3.

**N-Acetyl-(S)-alanyl-(S)-phenylalanyl-(2*S,5R*)-5-*tert*-butylprolyl-(S)-valine methyl ester (14b).** The peptide was cleaved from the resin (171 mg) according to the procedure described above to afford 16.7 mg of product. Purification of 16.7 mg of the peptide by RP-HPLC and collection of the pure fractions afforded 3.6 mg (8% overall yield) of product shown to be of >95% purity by RP-HPLC ( $t_R = 21.8$ ); LRMS calcd for  $C_{29}H_{45}N_4O_6$  ( $MH^+$ ) 545.3 found 545.3.

**N-Acetyl-(S)-alanyl-(S)-phenylalanyl-(2*S*,5*R*)-5-*tert*-butylprolyl-(S)-lysine methyl ester (14c).** *N*-Acetyl-(S)-alanyl-(S)-phenylalanyl-(2*S*,5*R*)-5-*tert*-butylprolyl-(S)-*N*-(Cbz)lysine methyl ester was cleaved from the resin (174 mg) according to the procedure described above to afford 14.1 mg of product. Purification of 14 mg of the peptide by RP-HPLC and collection of the pure fractions afforded 2.5 mg (4% overall yield) of product shown to be of >99% purity by RP-HPLC ( $t_R$  = 23.2); LRMS calcd for  $C_{38}H_{54}N_5O_8$  ( $MH^+$ ) 708.0 found 708.4. The peptide was then dissolved in 9:1 MeOH:H<sub>2</sub>O (0.5 mL), treated with HCl (4.2  $\mu$ L, 150 mol%) and Pd black (2.8 mg) under 1 atm of H<sub>2</sub> and stirred for 18 h at room temperature. The solution was filtered onto Celite, washed with MeOH and the filtrate was evaporated to afford 23; RP-HPLC ( $t_R$  = 14.6), LRMS calcd for  $C_{30}H_{48}N_5O_6$  ( $MH^+$ ) 574.0 found 574.3.

**N-Acetyl-(S)-alanyl-(S)-phenylalanyl-(2*S*,5*R*)-5-*tert*-butylprolyl-(S)-alanine *N*'-methylamide (13i).** The peptide was cleaved from the resin (416 mg) according to the procedure described above to afford 52 mg of product. Purification of 44 mg of the peptide by RP-HPLC and collection of the pure fractions afforded 22.9 mg (52% overall yield) of product shown to be of >95% purity by RP-HPLC ( $t_R$  = 25.6); LRMS calcd for  $C_{27}H_{42}N_5O_5$  ( $MH^+$ ) 516.0 found 516.2; HRMS calcd for  $C_{27}H_{42}N_5O_5$  ( $MH^+$ ) 516.3186, found 516.3173.

**N-Acetyl-(S)-alanyl-(S)-phenylalanyl-(2*S*,5*R*)-5-*tert*-butylprolyl-(S)-alanine methyl ester (14d).** The peptide was cleaved from the resin (268 mg) according to the procedure described above to afford 53 mg of product. Purification of 53 mg of the peptide by RP-HPLC and collection of the pure fractions afforded 16.5 mg (30% overall yield) of product shown to be of >95% purity by RP-HPLC ( $t_R$  = 18.2); LRMS calcd for  $C_{27}H_{41}N_4O_6$  ( $MH^+$ ) 517.3 found 517.3.

**N-Acetyl-(S)-seryl-(S)-phenylalanyl-(2*S*,5*R*)-5-*tert*-butylprolyl-(S)-alanine N'-methylamide (13j).** The peptide *N*-Acetyl-*O*-benzyl-(S)-seryl-(S)-phenylalanyl-(2*S*,5*R*)-5-*tert*-butylprolyl-(S)-alanine *N'*-methylamide was cleaved from the resin (146 mg) according to the procedure described above to afford 5.5 mg of product. Purification of 5.5 mg of the peptide by RP-HPLC and collection of the pure fractions afforded 1.4 mg (3% overall yield) of product shown to be of >90% purity by RP-HPLC ( $t_R = 19.9$ ). The peptide was than treated in the hydrogenation conditions described above to afford 13j.

**N-Acetyl-(S)-seryl-(S)-phenylalanyl-(2*S*,5*R*)-5-*tert*-butylprolyl-(S)-alanine methyl ester (14e).** The peptide *N*-Acetyl-*O*-benzyl-(S)-seryl-(S)-phenylalanyl-(2*S*,5*R*)-5-*tert*-butylprolyl-(S)-alanine methyl ester was cleaved from the resin (152 mg) according to the procedure described above to afford 5.3 mg of product. Purification of 5.3 mg of the peptide by RP-HPLC and collection of the pure fractions afforded 1.7 mg (4% overall yield) of product shown to be of >90% purity by RP-HPLC ( $t_R = 20.7$ ). The peptide was than treated in the hydrogenation conditions described above to afford 14e.

**N-Acetyl-(S)-valyl-(S)-phenylalanyl-(2*S*,5*R*)-5-*tert*-butylprolyl-(S)-alanine methyl ester (14f).** The peptide was cleaved from the resin (173 mg) according to the procedure described above to afford 16.2 mg of product. Purification of 15.0 mg of the peptide by RP-HPLC and collection of the pure fractions afforded 2.8 mg (5% overall yield) of product shown to be of >97% purity by RP-HPLC ( $t_R = 21.6$ ); LRMS calcd for  $C_{29}H_{45}N_4O_6$  ( $MH^+$ ) 545.0 found 545.4.

**N-Acetyl-(S)-alanyl-(S)-phenylalanyl-(S)-prolyl-(S)-alanine N'-methylamide (15).** The peptide was cleaved from the resin (288 mg) according to the procedure

described above to afford 42 mg of product. Purification of 42 mg of the peptide by RP-HPLC and collection of the pure fractions afforded 8.4 mg (15% overall yield) of product shown to be of >95% purity by RP-HPLC ( $t_R = 22.3$ ); LRMS calcd for  $C_{23}H_{34}N_5O_5$  ( $MH^+$ ) 460.2 found 460.2.

**N-Acetyl-(S)-alanyl-(S)-phenylalanyl-(S)-prolyl-(S)-alanine methyl ester (16).**

The peptide was cleaved from the resin (280 mg) according to the procedure described above to afford 23.8 mg of product. Purification of x mg of the peptide by RP-HPLC and collection of the pure fractions afforded 21.4 mg (28% overall yield) of product shown to be of >94% purity by RP-HPLC ( $t_R = 21.2$ ).

**Acknowledgment:** This research was supported in part by the Natural Sciences and Engineering Research Council of Canada and the Ministère de l'Éducation du Québec. We thank Sylvie Bilodeau and Dr. M. T. Phan Viet of the Regional High-Field NMR Laboratory for their assistance.

### 3.12. References

1. (a) Wilmot, C.M.; Thornton, J.M. *J. Mol. Biol.* **1988**, *203*, 221. (b) Rose, G.D.; Giersch, L.M.; Smith, J.A. *Adv. Protein Chem.* **1985**, *37*, 1.
2. Reviewed in: (a) Dobson, C.M. *Curr. Opin. Struct. Biol.* **1993**, *3*, 57. (b) Fersht, A.R.; Dill, K.A. *Curr. Opin. Struct. Biol.* **1994**, *4*, 67.
3. Grathwohl, C.; Wüthrich, K. *Biopolymers* **1981**, *20*, 2623 and Refs 7-14 therein.
4. Müller, G.; Gurrath, M.; Kurz, M.; Kessler, H. *Proteins: Struct., Funct. Genet.* **1993**, *15*, 235.
5. Reviewed in: (a) Fischer, G. *Angew. Chem. Int. Ed. Engl.* **1994**, *33*, 1415. (b) Liu, J.; Chen, C.-M.; Walsh, C. T. *Biochemistry* **1991**, *30*, 2306.

6. (a) Fischer, S.; Michnick, S.; Karplus, M. *Biochemistry* **1993**, *32*, 13830. (b) Kallen, J.; Walkinshaw, M. D. *FEBS Lett.* **1992**, *300*, 286.
7. Johnson, M. E.; Lin, Z.; Padmanabhan, K.; Tulinsky, A.; Kahn, M. *FEBS Lett.* **1994**, *337*, 4.
8. Reviewed in: MacArthur, M.W.; Thornton, J.M. *J. Mol. Biol.* **1991**, *218*, 397.
9. (a) Yaron, A.; Naider, F. *CRC Biochemistry and Molecular Biology* **1993**, *28*, 31. (b) Williams, K.A.; Deber, C.M. *Biochemistry* **1991**, *30*, 8919. (c) Brandl, C.J.; Deber, C.M. *Proc. Natl. Acad. Sci. USA* **1986**, *83*, 917. (d) Markley, J.L.; Hinck, A.P.; Loh, S.N.; Prehoda, K.; Truckses, D.; Walkenhorst, W.F.; Wang, J. *Pure & Appl. Chem.* **1994**, *66*, 65. (e) Richards, N.G.; Hinds, M.G.; Brennand, D.M.; Glennie, M.J.; Welsh, J.M.; Robinson, J.A.; *Biochem. Pharm.* **1990**, *40*, 119. (f) Lin, L.-N.; Brandts, J.F. *Biochemistry* **1979**, *18*, 43.
10. Reviewed in: Etzkorn, F.A.; Travins, J.M.; Hart, S.A. *Adv. Amino Acid Peptidomim.* **1999**, *2*, 125.
11. (a) Brady, S. F.; Paleveda, W. J. Jr.; Arison, B. H.; Saperstein, R.; Brady, E. J.; Raynor, K.; Reisine, T.; Veber, D. F.; Freidinger, R. M. *Tetrahedron* **1993**, *49*, 3449. (b) Cumberbatch, S.; North, M.; Zagotto, G. *Tetrahedron* **1993**, *49*, 9049. (c) Cumberbatch, S.; North, M.; Zagotto, G. *J. Chem. Soc., Chem. Commun.* **1993**, 641. (d) Horne, A.; North, M.; Parkinson, J. A.; Sadler, I. H. *Tetrahedron* **1993**, *49*, 5891.
12. Ösapay, G.; Zhu, Q.; Shao, H.; Chadha, R. K.; Goodman, M. *Int. J. Peptide Protein Res.* **1995**, *46*, 290.
13. (a) Zabrocki, J.; Dunbar, J. B.; Marshall, K. W.; Toth, M. V.; Marshall, G. R. *J. Org. Chem.* **1992**, *57*, 202. (b) Garofolo, A.; Tarnus, C.; Remy, J.-M.; Leppik, R.; Piriou, F.; Harris, B.; Pelton, J. T. In *Peptides: Chemistry, Structure and Biology*, J.E. Rivier and G.R. Marshall, Editors; ESCOM

- Science Publishers B.V.: Leiden, The Netherlands, 1990, 833-834. (c) Beusen, D. D.; Zabrocki, J.; Slomczynska, U.; Head, R. D.; Kao, J. L.-F.; Marshall, G. R. *Biopolymers* **1995**, *36*, 181. (d) Abell, A. D.; Foulds, G. J. *J. Chem. Soc., Perkin Trans. 1* **1997**, 2475.
14. (a) Dumas, J.-P.; Germanas, J. P. *Tetrahedron Lett.* **1994**, *35*, 1493. (b) Kim, K.; Dumas, J.-P.; Germanas, J. P. *J. Org. Chem.* **1996**, *61*, 3138. (c) Kim, K.; Germanas, J. P. *J. Org. Chem.* **1997**, *62*, 2847. (d) Kim, K.; Germanas, J. P. *J. Org. Chem.* **1997**, *62*, 2853. (e) Gramberg, D.; Robinson, J. A. *Tetrahedron Lett.* **1994**, *35*, 861. (f) Gramberg, D.; Weber, C.; Beeli, R.; Inglis, J.; Bruns, C.; Robinson, J. A. *Helv. Chim. Acta* **1995**, *78*, 1588.
15. (a) Didierjean, C.; Del Duca, V.; Benedetti, E.; Aubry, A.; Zouikri, M.; Marraud, M.; Boussard, G. *J. Peptide Res.* **1997**, *50*, 451. (b) Zouikri, M.; Vicherat, A.; Aubry, A.; Marraud, M.; Boussard, G. *J. Peptide Res.* **1998**, *52*, 19.
16. (a) Curran, T. P.; McEnaney, P. M. *Tetrahedron Lett.* **1995**, *36*, 191. (b) Lenman, M. M.; Ingham, S. L.; Gani, D. *Chem. Commun.* **1996**, 85.
17. (a) Magaard, V. W.; Sanchez, R. M.; Bean, J. W.; Moore, M. L. *Tetrahedron Lett.* **1993**, *34*, 381. (b) An, S. S. A.; Lester, C. C.; Peng, J.-L.; Li, Y.-J.; Rothwarf, D. M.; Welker, E.; Thannhauser, T. W.; Zhang, L. S.; Tam, J. P.; Scheraga, H. A. *J. Am. Chem. Soc.* **1999**, *121*, 11558.
18. Keller, M.; Sager, C.; Dumy, P.; Schutkowski, M.; Fischer, G. S.; Mutter, M. *J. Am. Chem. Soc.* **1998**, *120*, 2714.
19. (a) Hart, S. A.; Sabat, M.; Etzkorn, F. A. *J. Org. Chem.* **1998**, *63*, 7580. (b) Andres, C. J.; Macdonald, T. L.; Ocain, T. D.; Longhi, D. *J. Org. Chem.* **1993**, *58*, 6609.
20. Hart, S. A.; Etzkorn, F. A. *J. Org. Chem.* **1998**, *64*, 2998.

21. (a) Beausoleil, E.; L'Archevêque, B.; Bélec, L.; Atfani, M.; Lubell, W. D. *J. Org. Chem.* **1996**, *61*, 9447. (b) Beausoleil, E.; Lubell, W.D. *J. Am. Chem. Soc.* **1996**, *118*, 12902. (c) Beausoleil, E.; Lubell, W.D. *Biopolymers* **2000**, *53*, 249.
22. (a) Halab, L.; Lubell, W.D. *J. Org. Chem.* **1999**, *64*, 3312. (b) Halab, L.; Lubell, W.D. *J. Peptide Sci.* **2001**, *7*, 92. (c) Halab, L.; Lubell, W.D. In *Peptides 2000, Proc. Eur. Pept. Symp.*, *26th* (Martinez, J. & Fehrentz, J.-A., Eds) Montpellier, France, pp.815.
23. Bélec, L.; Slaninova, J.; Lubell, W. D. *J. Med. Chem.* **2000**, *43*, 1448.
24. (a) Hetzel, R.; Wüthrich, K. *Biopolymers* **1979**, *18*, 2589. (b) Grathwohl, C.; Wüthrich, K. *Biopolymers* **1976**, *15*, 2025.
25. (a) Yao, J.; Brüschiweiler, R.; Dyson, H. J.; Wright, P. E. *J. Am. Chem. Soc.* **1994**, *116*, 12051. (b) Yao, J.; Dyson, H. J.; Wright, P. E. *J. Mol. Biol.* **1994**, *243*, 754. (c) Yao, J.; Feher, V.A.; Espejo, B.F.; Reymond, M.T.; Wright, P. E.; Dyson, H. J. *J. Mol. Biol.* **1994**, *243*, 736. (d) Dyson, H. J., Rance, M., Houghten, R. A., Lerner, R. A.; Wright, P. E. *J. Mol. Biol.* **1988**, *201*, 161.
26. Wu, W.-J.; Raleigh, D. P. *Biopolymers* **1998**, *45*, 381.
27. (a) DeGrado, W.F.; Kaiser, E.T. *J. Org. Chem.* **1982**, *47*, 3258. (b) Voyer, N.; Lavoie, A.; Pinette, M.; Bernier, J. *Tetrahedron Lett.* **1994**, *35*, 355.
28. Moraes, C.M.; Bemquerer, M.P.; Miranda, M.T.M. *J. Peptide Res.* **2000**, *55*, 279.
29. (a) Valdeavella, C. V.; Blatt, H. D.; Pettitt, B. M. *Int. J. Peptide Protein Res.* **1995**, *46*, 372. (b) Wang, Y.; Scott, P. G.; Sejbal, J.; Kotovych, G. *Can. J. Chem.* **1996**, *74*, 389.
30. Oka, M.; Montelione, G. T.; Scheraga, H. A. *J. Am. Chem. Soc.* **1984**, *106*, 7959.

31. Woody, R. W. (1974) In *Peptides, Polypeptides and Proteins* (Blout, E. R., Bovey, F. A., Goodman, M. & Lotan, N., Eds). John Wiley, Inc., New York, pp. 338.
32. (a) Kawai, M.; Nagai, U. *Biopolymers* **1978**, *17*, 1549. (b) Bush, C.A.; Sarkar, S.K.; Kopple, K.D. *Biochemistry* **1978**, *17*, 4951.
33. The structure of **1c** was solved at l'Université de Montréal X-ray facility using direct methods (SHELXS96) and refined with NRCVAX and SHELXL96: C<sub>42</sub>H<sub>64</sub>N<sub>6</sub>O<sub>9</sub>; M<sub>r</sub> = 796.992; orthorhombic, colorless crystal; space group P2<sub>1</sub>2<sub>1</sub>2<sub>1</sub>; unit cell dimensions (Å) a = 9.294 (2), b = 12.895 (3), c = 36.837 (7); volume of unit cell (Å<sup>3</sup>) 4415.12 (16); Z = 4; R<sub>1</sub> = 0.0614 for I>2 sigma(I), wR<sub>2</sub> = 0.1569 for all data; GOF = 1.054. The author has deposited the atomic coordinates for the structure of **1c** with the Cambridge Crystallographic Data Center. The coordinates can be obtained, on request, from the Cambridge Crystallographic Data Center, 12 Union Road, Cambridge, CB2 1EZ, UK.
34. (a) Burley, S.K.; Petsko, G.A. *FEBS* **1986**, *203*, 139. (b) Dougherty, D.A. In *Peptides 1999 Proc. Am. Pept. Symp., 16th* (Fields, G. B. & Barany, G., eds.).
35. (a) Kartha, G.; Bhandary, K.K.; Kopple, K.D.; Go, A.; Zhu, P.-P. *J. Am. Chem. Soc.* **1984**, *106*, 3844. (b) Chiang, C.C.; Karle, I.L. *Int. J. Peptide Protein Res.* **1982**, *20*, 133.
36. (a) Poznański, J.; Ejchart, A.; Wierzchowski, K.L.; Ciurak, M. *Biopolymers* **1993**, *33*, 781. (b) Juy, M.; Lam-Thanh, H.; Lintner, K.; Fermandjian, S. *Int. J. Peptide Protein Res.* **1983**, *22*, 437. (c) Stimson, E.R.; Montelione, G.T.; Meinwald, Y.C.; Rudolph, R.K.E.; Scheraga, H.A. *Biochemistry* **1982**, *21*, 5252.
37. (a) Frömmel, C.; Preissner, R. *FEBS* **1990**, *277*, 159. (b) Stewart, D.E.; Sarkar, A.; Wampler, J.E. *J. Mol. Biol.* **1990**, *214*, 253.

38. Wüthrich, K. *NMR of Proteins and Nucleic Acids*; John Wiley & Sons, 1986; pp 162.
39. Reviewed in: Kessler, H. *Angew Chem. Int. Ed. Engl.* **1982**, *21*, 512.
40. (a) Imperiali, B.; Shannon, K.L.; Rickert, K.W. *J. Am. Chem. Soc.* **1992**, *114*, 7942. (b) Abbadi, A.; Mcharfi, M.; Aubry, A.; Prémilat, S.; Boussard, G.; Marraud, M. *J. Am. Chem. Soc.* **1991**, *113*, 2729.
41. (a) Fischer, S.; Dunbrack, Jr. R. L.; Karplus, M. *J. Am. Chem. Soc.* **1994**, *116*, 11931. (b) Cox, C.; Young, Jr. V. G.; Lectka, T. *J. Am. Chem. Soc.* **1997**, *119*, 2307. (c) Beausoleil, E.; Sharma, R.; Michnick, S.; Lubell, W. D. *J. Org. Chem.* **1998**, *63*, 6572. (d) Cox, C.; Lectka, T. *J. Am. Chem. Soc.* **1998**, *120*, 10660.
42. (a) Haque, T. S., Little, J. C. & Gellman, S. H. *J. Am. Chem. Soc.* **1996**, *118*, 6975. (b) Haque, T. S., Little, J. C. & Gellman, S. H. *J. Am. Chem. Soc.* **1994**, *116*, 4105. (c) Aubry, A.; Marraud, M. *Biopolymers* **1989**, *28*, 109. (d) Boussard, G.; Marraud, M. Neel, J.; Maigret, M.; Aubry, A. *Biopolymers* **1977**, *16*, 1033.
43. (a) Sibanda, B.L.; Thorton, J.M. *Nature* **1985**, *316*, 170. (b) Sibanda, B.L.; Thorton, J.M. *J. Mol. Biol.* **1993**, *229*, 428.
44. Dobson, C.M.; Šali, A.; Karplus, M. *Angew. Chem. Int. Ed.* **1998**, *37*, 868.

## **CHAPITRE 4**

**Incorporation des acides aminés  
azacycloalcanes dans des ligands peptidiques  
pour étudier le récepteur ORL1.**

#### 4.1. ORL1 et ses ligands

Ce chapitre décrit l'utilisation des acides aminés azacycloalcanes dans un peptide d'intérêt biologique. Nous avons incorporé ces acides aminés dans des structures peptidiques par synthèse peptidique sur support solide afin d'étudier l'interaction avec le récepteur "opioid receptor like" (ORL1).

Le clonage des récepteurs opiacés a amené la découverte en 1994 d'un nouveau membre de cette famille, le récepteur ORL1.<sup>1</sup> Bien que la séquence de ce récepteur possède une grande ressemblance avec les récepteurs opiacés connus,  $\mu$ ,  $\kappa$  et  $\delta$ , le récepteur ORL1 ne lie pas les ligands opiacés avec une grande affinité.<sup>1a,2</sup> Peu après, le ligand endogénique, un heptadecapeptide, a été identifié par deux groupes simultanément et indépendamment.<sup>3</sup> Le peptide a été nommé orphanin FQ par Reinscheid *et al.* pour désigner un ligand endogénique pour un récepteur orphelin et les lettres FQ représentent le premier et dernier acide aminé du peptide, soit phenylalanine et glutamine.<sup>3a</sup> Meunier *et al.* l'ont nommé nociceptin pour indiquer son activité *in vivo*.<sup>3b</sup> Ainsi, le ligand est reconnu aujourd'hui sous le nom nociceptin/orphanin FQ (NC).

Le récepteur ORL1 et son ligand NC sont distribués largement dans le système nerveux central.<sup>4</sup> Des études du système NC-ORL1 ont démontré des rôles importants dans la régulation du douleur, de la mémoire, de l'anxiété et du système cardiovasculaire.<sup>5</sup> Cependant, contrairement aux récepteurs opiacés  $\mu$ ,  $\kappa$  et  $\delta$ , les propriétés pharmacologiques et les rôles physiologiques du récepteur ORL1 sont mal connus en raison de l'absence de ligand sélectif pour ce récepteur.

NC	H-Phe-Gly-Gly-Phe-Thr-Gly-Ala-Arg-Lys-Ser-Ala-Arg-Lys-Leu-Ala-Asn-Gln-OH
NC(1-13)-NH <sub>2</sub>	H-Phe-Gly-Gly-Phe-Thr-Gly-Ala-Arg-Lys-Ser-Ala-Arg-Lys-NH <sub>2</sub>
[Nphe <sup>1</sup> ]NC(1-13)-NH <sub>2</sub>	H-Nphe-Gly-Gly-Phe-Thr-Gly-Ala-Arg-Lys-Ser-Ala-Arg-Lys-NH <sub>2</sub>

Figure 1. Structures de NC et de ses dérivés.

Afin de développer des ligands puissants et sélectifs pour le récepteur ORL1, des dérivés de NC ont été rapportés (Figure 1). Le peptide NC(1-13)-NH<sub>2</sub> est le plus

petit fragment de NC qui maintient l'activité et l'efficacité du peptide naturel.<sup>6</sup> Un analogue de NC, [Nphe<sup>1</sup>]NC(1-13)-NH<sub>2</sub>, a démontré une faible sélectivité et activité antagoniste pour ORL1.<sup>7</sup>

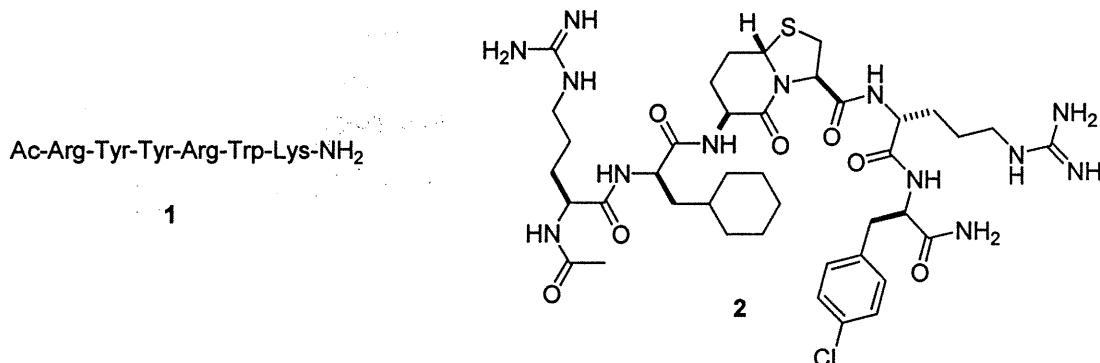


**Figure 2. Structures de ligands peptidiques du récepteur ORL1.**

Une série d'hexapeptides non reliés structuralement à NC a été synthétisée en utilisant les techniques de chimie combinatoire et le hexapeptide **1** a été identifié comme un agoniste partiel de ORL1 (Figure 2).<sup>8</sup> Récemment, une bibliothèque combinatoire de peptides incorporant des mimétiques de repliement  $\beta$  a été testée pour le récepteur ORL1.<sup>9</sup> Le peptide **2** incorporant le bicyclic thiaindolizidinone a été identifié comme un faible antagoniste au ORL1.<sup>9-10</sup>

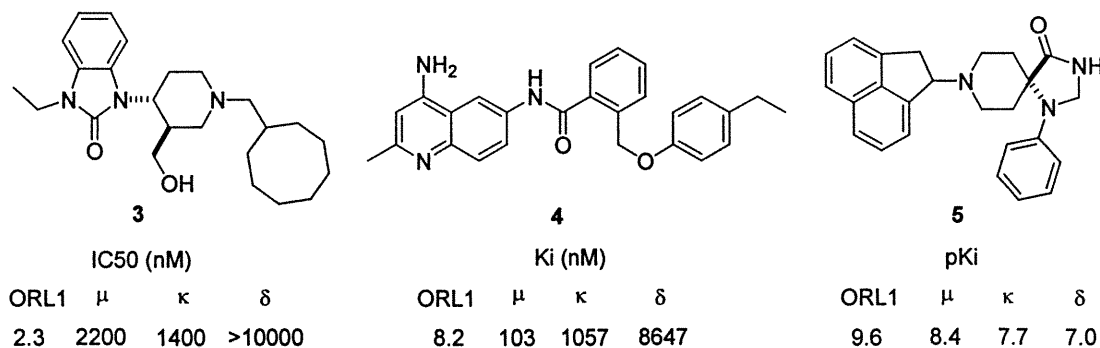


**Figure 3. Structures de ligands non peptidiques du récepteur ORL1.**

Les molécules organiques non peptidiques **3-5** ont été examinées aussi pour leur sélectivité et activité au récepteur ORL1 (Figure 3). Les molécules **3-5** ont montré une grande sélectivité pour le récepteur ORL1 par rapport aux autres récepteurs opiacés.<sup>11-13</sup> Les molécules **3** et **4** ont démontré des activités

antagonistes<sup>11,12</sup> et la molécule **5** possède une activité agoniste<sup>13</sup> au récepteur ORL1. De plus, la molécule **4** est en cours d'évaluation en test clinique comme un nouveau type d'analgésique.<sup>12</sup>

Par conséquent, il serait important de développer un ligand sélectif du récepteur ORL1 avec une activité puissante. De plus, il serait intéressant d'étudier l'interaction des ligands au récepteur ORL1 pour comprendre la relation entre la conformation et l'activité. Dans l'article qui suit, nous présentons la synthèse sur support solide de peptides incorporant des acides aminés azacycloalcanes, l'étude conformationnelle par spectroscopie RMN et dichroïsme circulaire et une étude de l'activité biologique. Ainsi, nous avons obtenu un antagoniste puissant qui exhibe une grande sélectivité au récepteur ORL1. Ces travaux ont démontré que la sélectivité aux récepteurs opiacés est affectée par la structure de l'acide aminé azacycloalcane et le type de conformation de repliement  $\beta$ .

#### **4.2. Références**

1. (a) Bunzow, J.R.; Saez, C.; Mortrud, M.; Bouvier, C.; Williams, J.T.; Low, M.; Grandy, D.K. *FEBS Lett.* **1994**, *347*, 284. (b) Fukuda, K.; Kato, S.; Mori, K.; Nishi, M.; Takeshima, H.; Iwabe, N.; Miyata, T.; Houtani, T.; Sugimoto, T. *FEBS Lett.* **1994**, *343*, 42. (c) Mollereau, C.; Paementier, M.; Mailleux, P.; Butour, J.L.; Moisand, C.; Chalon, P.; Caput, D.; Vassart, G.; Meunier, J.C. *FEBS Lett.* **1994**, *341*, 33. (d) Nishi, M.; Takeshima, H.; Mori, M.; Nakagawara, K.; Takeuchi, T. *Biochem. Biophys. Res. Commun.* **1994**, *205*, 1353.
2. Chen, Y.; Fan, Y.; Liu, J.; Mestek, A.; Tian, M.; Kozak, C.A.; Yu, L. *FEBS Lett.* **1994**, *347*, 279.
3. (a) Reinscheid, R.K.; Nothacker, H.-P.; Bourson, A.; Ardati, A.; Henningssen, R.A.; Bunzow, J.R.; Grandy, H.; Langen, D.K.; Monsma, F.J., Jr.; Civelli, O. *Science* **1995**, *270*, 792. (b) Meunier, J.C.; Mollereau, C.; Toll, L.; Suaudeau, C.; Moisand, C.; Alvinerie, P.; Butour, J.L.; Guillemot, J.C.; Ferrara, P.; Monserrat,

- B.; Mazarguil, H.; Vassart, G.; Parmentier, M.; Costentin, J. *Nature* **1995**, 377, 532.
4. (a) Anton, B.; Fein, J.; To, T.; Li, X.; Silberstein, L.; Evans, C.J. *J. Comp. Neurol.* **1996**, 368, 229. (b) Darland, T.; Heinricher, M.M.; Grandy, D.K. *Trends Neurosci.* **1998**, 21, 215. (c) Ikeda, K.; Watanabe, M.; Ichikawa, T.; Kobayashi, T.; Yano, R.; Kumanishi, T. *J. Comp. Neurol.* **1998**, 399, 139. (d) Monteillet-Agius, G.; Fein, J.; Anton, B.; Evans, C.J. *J. Comp. Neurol.* **1998**, 399, 373. (e) Neal, C.R., Jr.; Mansour, A.; Reinscheid, R.K.; Nothacker, H.-P.; Civelli, O.; Watson, S.J., Jr. *J. Comp. Neurol.* **1999**, 406, 503.
  5. Voir la revue: Calo', G.; Guerrini, R.; Rizzi, A.; Salvadori, S.; Regoli, D. *Br. J. Pharmacol.* **2000**, 129, 1261.
  6. (a) Calo', G.; Rizzi, A.; Bogoni, G.; Neugebauer, W.; Salvadori, S.; Guerrini, R.; Bianchi, C.; Regoli, D. *Eur. J. Pharmacol.* **1996**, 311, R3. (b) Dooley, C.T.; Houghten, R.A. *Life Sci.* **1996**, 59, 23.
  7. Calo', G.; Guerrini, R.; Bigoni, R.; Rizzi, A.; Marzola, G.; Okawa, H.; Bianchi, C.; Lambert, D.G.; Salvadori, S.; Regoli, D. *Br. J. Pharmacol.* **2000**, 129, 1183.
  8. Dooley, C.T.; Spaeth, C.G.; Berzetei-Gurske, I.P.; Craymer, K.; Adapa, I.D.; Brandt, S.R.; Houghten, R.A.; Toll, L. *J. Pharmacol. Exp. Ther.* **1997**, 283, 735.
  9. Becker, J.A.; Wallace, A.; Garzon, A.; Ingallinella, P.; Bianchi, E.; Cortese, R.; Simonin, F.; Kieffer, B.L.; Pessi, A. *J. Biol. Chem.* **1999**, 274, 27513.
  10. Bigoni, R.; Rizzi, A.; Rizzi, D.; Becker, J.A.; Kieffer, B.L.; Simonin, F.; Regoli, D.; Calo', G. *Life Sci.* **2000**, 68, 233.
  11. (a) Kawamoto, H.; Nakashima, H.; Kato, T.; Arai, S.; Kamata, K.; Iwasawa, Y. *Tetrahedron* **2001**, 57, 981-986. (b) Kawamoto, H.; Ozaki, S.; Itoh, Y.; Miyaji, M.; Arai, S.; Nakashima, H.; Kato, T.; Ohta, H.; Iwasawa, Y. *J. Med. Chem.* **1999**, 42, 5061.

12. Shinkai, H.; Ito, T.; Iida, T.; Kitao, Y.; Yamada, H.; Uchida, I. *J. Med. Chem.* **2000**, *43*, 4667.
13. (a) Röver, S.; Wichmann, J.; Jenck, F.; Adam, G.; Cesura, A.M. *Bioorg. Med. Chem. Lett.* **2000**, *10*, 831-834. (b) Wichmann, J.; Adam, G.; Röver, S.; Cesura, A.M.; Dautzenberg, F.M.; Jenck, F. *Bioorg. Med. Chem. Lett.* **1999**, *9*, 2343.

**Article 8**

**Halab, L.; Darula Z.; Tourwé D.; Becker, J.A.J.; Keiffer, B.L.; Simonin, F. and Lubell, W.D.** "Probing Opioid Receptor Interactions with Azacycloalkane Amino Acids. Synthesis of a Potent and Selective ORL1 Antagonist. Soumis à *The Journal of Biological Chemistry* 2001.

## Probing opioid receptor interactions with azacycloalkane amino acids.

### Synthesis of a potent and selective ORL1 antagonist.

**Liliane Halab, Zsuzsanna Darula<sup>§</sup>, Dirk Tourwé<sup>§</sup>, Jérôme A. J. Becker<sup>†</sup>, Brigitte L. Keiffer<sup>†</sup>, Frédéric Simonin<sup>†</sup> and William D. Lubell\***

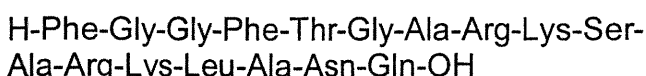
*Département de chimie, Université de Montréal, C. P. 6128, Succursale Centre Ville, Montréal, Québec, Canada H3C 3J7. <sup>§</sup>Eenheid Organische Chemie, Vrije Universiteit Brussel, 2, Pleinlaan, Brussels, B-1050, Belgium. <sup>†</sup>Ecole supérieure de Biotechnologie de Strasbourg, 67400 Illkirch, France.*

### **4.3. Abstract**

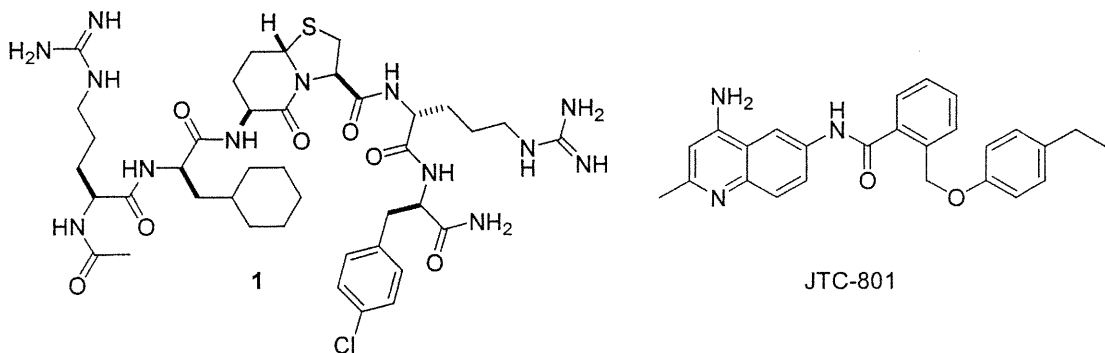
Azacycloalkane turn mimics **6-9** were used to explore the relationship between conformation and biological activity of peptide ligands to the opioid receptor like (ORL1) receptor. Three azabicyclo[X.Y.0]alkane amino acids and a 5-*t*BuPro type VI β-turn mimic were introduced into peptides **15-18** by solid-phase synthesis on MBHA resin. Biological examination of peptides **15-18** showed two new potent antagonists (**15** and **17**) exhibiting increased selectivity for the ORL1 receptor. Conformational analysis using NMR and CD spectroscopy illustrated that the 6,6-bicyclic lactam of the active peptide **17** was situated in an open β-turn conformation possessing no intramolecular hydrogen bond in water.

### **4.4 Introduction**

The opioid receptor like (ORL1) was identified through cloning experiments and shown to have high homology (~60%) with known opioid receptors ( $\mu$ ,  $\kappa$  and  $\delta$ ) without having high affinity for the common opioid ligands (1-4). The heptadecapeptide nociceptin/orphanin FQ (NC) was soon shown to be the endogenous ligand of the ORL1 receptor (Figure 1) (5-6). The shorter C-terminal fragment of NC, NC<sub>1-13</sub>NH<sub>2</sub> was found to be a selective agonist, and the analogue [Nphe<sup>1</sup>]NC<sub>1-13</sub>NH<sub>2</sub> was identified to be an antagonist (7-9).



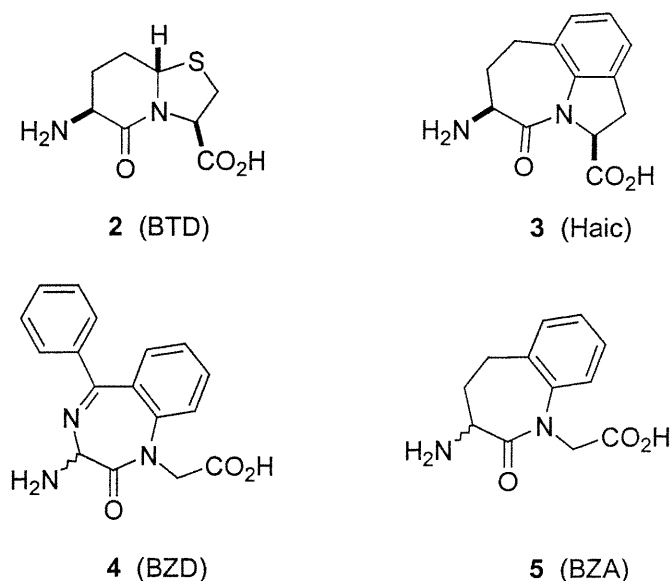
**Figure 1. Structure of nociceptin/orphanin FQ.**



**Figure 2. Structures of peptide III-BTD (1) and JTC-801.**

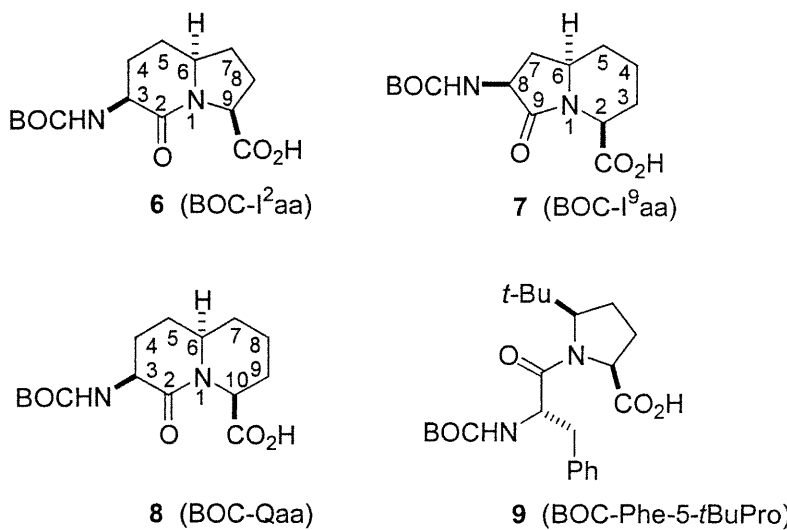
Hexapeptide and non-peptide ligands were later synthesized and shown to bind to ORL1 receptor with high affinity (10-13). Among the small peptide analogues, from a positional scanning library of  $2 \times 10^7$   $\beta$ -turn-constrained peptides, the thiaindolizidinone analogue III-BTD (**1**) was recently selected because it displayed good affinity and a modest selectivity for the ORL1 receptor (1:5:22:6  $K_i$  ratio of hORL1 / hMOR / hDOR / hKOR) with competitive ORL1 receptor antagonist activity and agonist activity at the other opioid receptors at higher concentrations (Figure 2) (14-15).

The development of new ORL1 ligands with high selectivity and bioavailability remains an important challenge for the elucidation and control of the physiological role of the ORL1 receptor. A broad spectrum of potential therapeutic applications have been reported for the ORL1 receptor system (16). For example, ORL1 agonists have been identified as anxiolytics, stimulants of food-intake, analgesics, suppressants of drug abuse, anti-epileptics and for the management of hyponatremic and water-retaining syndromes (16). Furthermore, ORL1 receptor antagonists have been evaluated as anorectics, analgesics as well as nootropic agents (16). The non-peptide antagonist JTC-801, which exhibits high affinity and selectivity to the ORL1 receptor, is currently undergoing evaluation in clinical trials as a novel analgesic (Figure 2) (12). Selective ligands for the ORL1 receptor possessing agonist and antagonist activity are thus desired as tools for characterizing the physiology of ORL1.



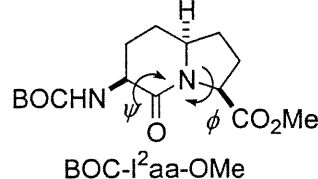
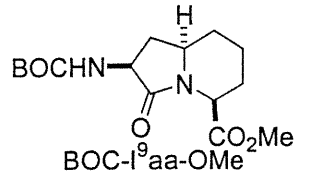
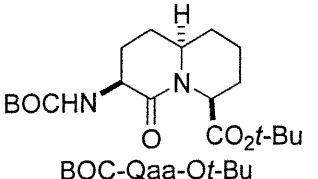
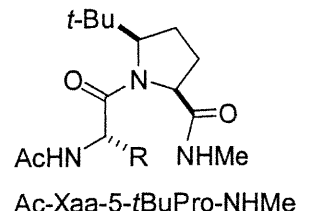
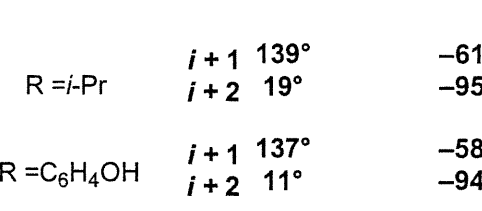
**Figure 3. Structures of alternative turn mimics incorporated at residues 3 and 4 of hexapeptide ligands.**

The exploration of opioid peptides with azabicycloalkane amino acids has improved understanding of the conformational requirements at the opioid receptors (14, 17-19). For example, in a combinatorial approach to study the ORL1 receptor, peptide **1** possessing the thiaindolizidinone amino acid **2** demonstrated greater selectivity for hORL1 relative to related analogues incorporating the turn mimics **3-5** which showed higher affinities for hKOR (Figure 3) (14). Because a deeper understanding of the conformational requirements for receptor interaction may arrive through a systematic examination of the turn region of NC analogues, a series of related scaffolds have now been used to study structure-activity relationships at the ORL1 (Figure 4). Three different azabicycloalkane amino acids (**6-8**), (3*S*,6*S*,9*S*)-indolizidin-2-one, (2*S*,6*R*,8*S*)-indolizidin-9-one, and (2*S*,6*R*,8*S*)-quiolizidinone amino acids (I<sup>2</sup>aa, I<sup>9</sup>aa and Qaa respectively), as well as the phenylalanyl-(2*S*,5*R*)-5-*tert*-butylproline (Phe-5-*t*BuPro, **9**) dipeptide, all were employed in complementary strategies featuring the use of structural links and steric interactions for inducing turn conformations.



**Figure 4. Structures of dipeptide mimics used in the present study of the ORL1 receptor.**

Comparison of the X-ray crystal structures of esters of azabicycloalkane amino acids has demonstrated that the heterocycle ring size influenced significantly the preferred geometry of the internal  $\psi$  and  $\phi$  dihedral angle values of the peptide backbone contained within the bicyclic system (Figure 5) (20-23). The I<sup>2</sup>aa and I<sup>9</sup>aa systems, for example, mimic different features of the central residues in an ideal type II'  $\beta$ -turn (Figure 5, 21-22). X-ray analysis of Ac-L-Leu-5-*t*BuPro-NHMe and Ac-L-Tyr-5-*t*BuPro-NHMe have shown that the steric interactions of the 5-*t*BuPro residue induced the backbone to adopt dihedral angles characteristic of the central *i* + 1 and *i* + 2 residues of an ideal type VIa  $\beta$ -turn (Figure 5) (24-25). Employing dipeptide mimics to study the relationships between dihedral angle geometry, conformation and activity, we have maintained the potency and improved the selectivity of the parent peptide **1**. Two new potent antagonists have been synthesized that exhibit increased selectivity for the ORL1 receptor. Conformational analysis of peptides **15-18** has provided new insight concerning the backbone geometry of the ORL1 ligands when exhibiting their activity and selectivity.

	$\psi$	$\phi$
BOC-I <sup>2</sup> aa-OMe	-176°	-78°
	-161°	-69°
BOC-BTD-OH		
	-141°	-34°
BOC-I <sup>9</sup> aa-OMe		
	-163°	48°
BOC-Qaa-Ot-Bu		
<b>Ideal Type II' <math>\beta</math>-turn <math>i + 1</math> and <math>i + 2</math> Residues</b>	-120°	-80°
<b>Inverse <math>\gamma</math>-turn <math>i + 2</math> Residue</b>		-80°
<b>Ideal Type VIa <math>\beta</math>-turn <math>i + 1</math> and <math>i + 2</math> Residues</b>	$i + 1$ 120° $i + 2$ 0°	-60° -90°
	$i + 1$ 139° $i + 2$ 19°	-61° -95°
R = <i>i</i> -Pr		
	$i + 1$ 137° $i + 2$ 11°	-58° -94°
R = C <sub>6</sub> H <sub>4</sub> OH		

**Figure 5.** Dihedral angle values from X-ray data of turn mimics and ideal peptide turns.<sup>20-25</sup>

#### 4.5. Experimental Section

**Peptide Synthesis.** The synthesis of the peptides was carried out on a semi-automatic peptide synthesizer using 4-methyl-benzhydrylamine resin (MBHA) 1.10

mmol/g. Solvents and reagents were purified as previously described (24). Arginine was introduced as BOC-L- and D-Arg(Tos)-OH (Tos, toluene-4-sulfonyl) derivative. Couplings were performed with BOC-protected amino acids (200 mol%), TBTU (200 mol%) and DIEA (400 mol%) in DMF for 90 min. Coupling reactions were monitored by Kaiser ninhydrin test (26). In cases of incomplete couplings, the resin was resubmitted to the same coupling conditions. Deprotections were performed with a cocktail of TFA:CH<sub>2</sub>Cl<sub>2</sub>:anisole 49:49:2 (2 x 30 min) and the resin was free-based with 20% DIEA in CH<sub>2</sub>Cl<sub>2</sub> (2 x 5 min). N-Terminal acetylation of the peptides was accomplished by treating the resin with Ac<sub>2</sub>O (1000 mol%) and DIEA (1000 mol%) in CH<sub>2</sub>Cl<sub>2</sub> for 1 h. The peptides were cleaved from the solid support by treating the resin with liquid HF and anisole at 0°C for 90 min (*caution: HF is a highly toxic, corrosive gas that must be handled in a well ventilated hood*). The reaction mixture was treated with diethyl ether (2 x 10 mL) to precipitate the peptide and filtered. The peptide was separated from the resin by washing with acetic acid (2 x 25 mL) to afford a solution that was lyophilized. The crude material was purified by semi-preparative RP-HPLC (Higgins C18 column, 20 x 250 mm, particle size 5 µm) with solvent A, H<sub>2</sub>O (0.05% TFA) and solvent B, 75% CH<sub>3</sub>CN/H<sub>2</sub>O (0.05% TFA). Analytical RP-HPLC was performed on a Higgins C18 (4.6 x 250 mm, particle size 5 µm) using a gradient of 0-90% eluant B in A over 30 min with a flow rate of 1.5 mL/min and the detector centered at 214 nm: B (CH<sub>3</sub>CN containing 0.003% TFA) in A (H<sub>2</sub>O containing 0.03% TFA) and retention times (*t<sub>R</sub>*) are reported in minutes. Mass spectral data for peptides and intermediates, LRMS and HRMS (EI and FAB), were obtained by the Université de Montréal Mass Spectroscopy facility.

**N-Acetyl-(S)-arginyl-(R)-cyclohexylalanyl-(3S,6S,9S)-I<sup>2</sup>aa-(R)-arginyl-(R)-p-chloro-phenylalanyl amide (15).** The peptide was cleaved from the resin (580 mg) according to the procedure described above to afford 185.8 mg of product that was shown to be of 70% purity by RP-HPLC. Purification of 30.6 mg of the peptide by RP-HPLC and collection of the purest fractions afforded 21.5 mg (54% overall yield from the resin loading) of product shown to be of >99% purity by analytical RP-HPLC (*t<sub>R</sub>* = 13.61); LRMS calcd for C<sub>41</sub>H<sub>65</sub>N<sub>13</sub>O<sub>7</sub>Cl (MH<sup>+</sup>) 886.5 found 886.5; <sup>1</sup>H

NMR  $\delta$  0.83 (m, 1 H), 0.92 (m, 1 H), 1.02-1.34 (m, 6 H), 1.50-1.76 (m, 16 H), 1.94 (s, 3 H), 1.98 (m, 1 H), 2.09-2.23 (m, 4 H), 2.91 (dd, 1 H,  $J$  = 11.2, 14.0), 3.02 (m, 2 H), 3.16 (m, 2 H), 3.27 (dd, 1 H,  $J$  = 4.7, 14.0), 3.73 (m, 1 H), 4.11 (q, 1 H,  $J$  = 6.5, 12.8), 4.23 (q, 1 H,  $J$  = 7.0, 13.7), 4.35 (q, 1 H,  $J$  = 7.7, 15.4), 4.41 (d, 1 H,  $J$  = 8.4), 4.46 (q, 1 H,  $J$  = 7.6, 15.1), 4.58 (m, 1 H), 6.61 (br s, 7 H), 7.02 (br s, 1 H), 7.17 (br s, 1 H), 7.22 (br s, 1 H), 7.25 (d, 2 H,  $J$  = 8.4), 7.33 (d, 2 H,  $J$  = 8.5), 8.10 (d, 1 H,  $J$  = 8.4), 8.13 (d, 1 H,  $J$  = 6.4), 8.22 (d, 1 H,  $J$  = 8.1), 8.38 (d, 1 H,  $J$  = 7.8), 8.65 (d, 1 H,  $J$  = 5.9).

***N*-Acetyl-(*S*)-arginyl-(*R*)-cyclohexylalanyl-(2*S*,6*R*,8*S*)-I<sup>9</sup>aa-(*R*)-arginyl-(*R*)-*p*-chlorophenylalanyl amide (16).** The peptide was cleaved from the resin (910 mg) according to the procedure described above to afford 390 mg of product that was shown to be of 71% purity by RP-HPLC. Purification of 140 mg of the peptide by analytical RP-HPLC and collection of the purest fractions afforded 88.3 mg (44% overall yield from the resin loading) of product shown to be of 97% purity by RP-HPLC ( $t_R$  = 14.17); LRMS calcd for C<sub>41</sub>H<sub>65</sub>N<sub>13</sub>O<sub>7</sub>Cl (MH<sup>+</sup>) 886.5 found 886.4; <sup>1</sup>H NMR  $\delta$  0.86 (m, 1 H), 0.96 (m, 1 H), 1.04-1.28 (m, 5 H), 1.38-1.56 (m, 4 H), 1.57-1.69 (m, 13 H), 1.74 (s, 3 H), 1.97 (m, 1 H), 1.99 (s, 3 H), 2.63 (m, 1 H), 2.92 (dd, 1 H,  $J$  = 10.0, 14.0), 3.11 (m, 2 H), 3.18 (m, 3 H), 3.66 (m, 1 H), 4.20 (m, 2 H), 4.34 (m, 1 H), 4.54 (m, 1 H), 4.62 (m, 1 H), 4.64 (m, 1 H), 6.61 (br s, 6 H), 7.07 (br s, 1 H), 7.10 (t, 1 H,  $J$  = 5.5), 7.20 (t, 1 H,  $J$  = 4.3), 7.23 (d, 2 H,  $J$  = 8.4), 7.33 (d, 2 H,  $J$  = 8.4), 7.57 (br s, 1 H), 8.10 (d, 1 H,  $J$  = 7.0), 8.23 (d, 1 H,  $J$  = 5.9), 8.25 (d, 1 H,  $J$  = 8.2), 8.27 (d, 1 H,  $J$  = 8.4), 8.56 (d, 1 H,  $J$  = 7.6).

***N*-Acetyl-(*S*)-arginyl-(*R*)-cyclohexylalanyl-(2*S*,6*R*,8*S*)-Qaa-(*R*)-arginyl-(*R*)-*p*-chlorophenylalanyl amide (17).** The peptide was cleaved from the resin (340 mg) according to the procedure described above to afford 112 mg of product that was shown to be of 39% purity by RP-HPLC. Purification of 18.8 mg of the peptide by RP-HPLC and collection of the purest fractions afforded 3.5 mg (32% overall yield from the resin loading) of product shown to be a mixture of conformers by analytical RP-HPLC ( $t_R$  = 13.36, 14.08, 14.21, 14.65); LRMS calcd for C<sub>42</sub>H<sub>66</sub>N<sub>13</sub>O<sub>7</sub>Cl (MH<sup>+</sup>)

900.5 found 900.4;  $^1\text{H}$  NMR for the major conformation  $\delta$  1.00-1.33 (m, 4.8 H), 1.38-1.69 (m, 11 H), 1.70-1.80 (m, 4 H), 1.90-2.11 (m, 7.4 H), 2.88 (dd, 0.8 H,  $J$  = 10.0, 14.3), 3.12 (m, 1.6 H), 3.16 (m, 0.8 H), 3.18 (m, 1.6 H), 3.72 (m, 0.8 H), 4.14 (m, 0.8 H), 4.15 (m, 0.8 H), 4.21 (m, 0.8 H), 4.24 (m, 0.8 H), 4.31 (m, 0.8 H), 4.62 (m, 0.8 H), 5.15 (m, 0.8 H), 6.62 (br s, 4.8 H), 7.07 (s, 0.8 H), 7.15 (s, 0.8 H), 7.19 (s, 0.8 H), 7.22 (d, 1.6 H,  $J$  = 8.4), 7.33 (d, 1.6 H,  $J$  = 8.4), 7.46 (br s, 0.8 H), 8.07 (d, 0.8 H,  $J$  = 6.4), 8.17 (d, 0.8 H,  $J$  = 8.1), 8.23 (d, 0.8 H,  $J$  = 6.0), 8.27 (d, 0.8 H,  $J$  = 7.5), 8.54 (d, 0.8 H,  $J$  = 7.5).

**N-Acetyl-(S)-arginyl-(R)-cyclohexylalanyl-(S)-phenylalanyl-(2S,5R)-5-tert-butylprolyl-(R)-arginyl-(R)-p-chloro-phenylalanylamide (18).** The peptide was cleaved from the resin (569 mg) according to the procedure described above to afford 168.4 mg of product that was shown to be of 48% purity by RP-HPLC. Purification of 31 mg of the peptide by RP-HPLC and collection of the purest fractions afforded 15 mg (52% overall yield from the resin loading) of product shown to be of 99% purity by analytical RP-HPLC ( $t_{\text{R}} = 16.87$ ); LRMS calcd for  $\text{C}_{50}\text{H}_{76}\text{N}_{13}\text{O}_7\text{Cl} (\text{MH}^+)$  1006.5, found 1006.6;  $^1\text{H}$  NMR  $\delta$  [0.64 (s, 3.6 H)] 0.89 (s, 5.4 H), 0.77 (m, 1 H), 0.84 (m, 1 H), 1.00-1.16 (m, 5 H), 1.22-1.76 (m, 16 H), 1.95 (s, 1.8 H) [1.98(s, 1.2 H)], 1.99 (m, 1 H), 2.20 (m, 1 H), [2.84 (dd, 0.4 H,  $J$  = 10.0, 14.1)] 2.97 (m, 1.2 H) [3.26 (dd, 0.4 H,  $J$  = 4.8, 14.0)], 3.08 (m, 3 H), 3.15 (m, 2 H), 3.66 (t, 1 H,  $J$  = 8.2), [4.06 (dd, 0.4 H,  $J$  = 1.8, 8.7)] 4.11 (d, 0.6 H,  $J$  = 8.4), 4.12 (m, 1 H), 4.16 (q, 0.6 H,  $J$  = 7.0, 14.2) [4.20 (m, 0.4 H)], 4.21 (m, 0.6 H) [4.30 (m, 0.4 H)], [4.38 (m, 0.4 H)] 4.43 (m, 0.6 H), [4.45 (m, 0.4 H)] 4.55 (m, 0.6 H), 6.61 (br s, 6 H), 7.04 (br s, 1 H), 7.16-7.38 (m, 9 H), 7.60 (br s, 1 H), [7.97 (d, 0.4 H,  $J$  = 5.2)] 8.34 (d, 0.6 H,  $J$  = 3.8), 7.98 (d, 0.6 H,  $J$  = 7.1) [8.36 (br s, 0.4 H)], 8.11 (d, 0.6 H,  $J$  = 6.4), [8.18 (d, 0.4 H,  $J$  = 6.3)], 8.12 (d, 0.6 H,  $J$  = 7.2) [8.36 (br s, 0.4 H)], [8.22 (d, 0.4 H,  $J$  = 7.6)] 8.26 (d, 0.6 H,  $J$  = 8.4).

**NMR Measurements.**  $^1\text{H}$  NMR experiments were performed on a Bruker DMX600. The chemical shifts are reported in ppm ( $\delta$  units) downfield of the internal tetramethylsilane ((CH<sub>3</sub>)<sub>4</sub>Si). Coupling constants are in Hz. The chemical shifts for

the carbons and the protons of the minor isomers are respectively reported in parentheses and in brackets. COSY, NOESY and ROESY spectra were obtained with 2048 by 512 data points. A mixing time of 250 ms was used for the NOESY and ROESY spectra. The temperature coefficients of the amide proton chemical shifts in 10% D<sub>2</sub>O/H<sub>2</sub>O were measured for at least five different temperatures in 5 deg intervals varying the temperature between 298-328 K. The value of the temperature coefficient was obtained by a linear least-squares fit of the data.

**Circular Dichroism Measurements.** CD spectra of 0.1 mM solutions in H<sub>2</sub>O were measured on a Jasco J-710 spectropolarimeter using a circular quartz cell with a path length of 1 mm at 23°C. Spectra were run with a band width of 1 nm, a response time of 0.25 s and a scan speed of 100 nm min<sup>-1</sup>. Each measurement was the average result of ten repeated scans in steps of 0.2 nm. Baseline spectra of the solvents were subtracted.

#### Protocols For Biological Testing.

**Materials.** Naloxone, DAMGO, orphanin FQ/nociceptin, GDP and GTPγS were purchased from Sigma (Saint Quentin, France). CI-977 was kindly provided by John Hughes (Parke-Davis Neuroscience Research Centre, Cambridge U.K.). [<sup>3</sup>H]diprenorphine (37 Ci/mmol; 1Ci = 37GBq) and [<sup>3</sup>H]Leucyl-nociceptin (172 Ci/mmol) were obtained from Amersham (Paris, France) and [<sup>35</sup>S]GTPγS (1156 Ci/mmol) from Dupont NEN (Paris, France). The hMOR cDNA was a gift from Lei Yu (Department of Medical and Molecular Genetics, Indianapolis, USA). The carrier plasmid used in the electroporation procedure (pBluescript) was from Stratagene (La Jolla, USA).

**Cell culture.** All cell lines were from ATCC and maintained in the presence of 5% FCS and 5% CO<sub>2</sub>. COS-1 cells were grown in DMEM (Eurobio, Les Ulis, France), CHO cells in DMEN-F'12 (Eurobio). CHO stably transfected with pCDNA3/Neo (Invitrogen, Nu Leek, Netherlands) hORL1 were gifts from Lawrence Toll, (Torrey Pines Institute for Molecular Biology, San Diego, USA).

**Cell transfections.** Cells were electroporated essentially as described (27). Briefly,  $2 \times 10^7$  COS-1 cells were seeded the night before transfection at a density of  $10^7$  cells/140 mm dish. Cells were washed two times with PBS, detached by applying trypsin/EDTA (Eurobio). Cells were collected by centrifugation for 10 min at 400 g, and resuspended at a density of  $10^8$  cells/mL in EP 1X buffer (50 mM K<sub>2</sub>HPO<sub>4</sub>, 20 mM CH<sub>3</sub>CO<sub>3</sub>K, 20 mM KOH, pH 7.4). hMOR, hDOR or hKOR plasmidic DNA, prepared using Nucleobond columns (Macherey Nagel, Düren, Germany) and consisting of variable amount of receptor-encoding plasmid and a carrier plasmid (pBluescript) up to a final 20 µg DNA quantity was diluted into EP 1X buffer to a total volume of 300 µl. The DNA mix was then supplemented with 13 µl 1M MgSO<sub>4</sub> and incubated with 200 µl cell suspension for 20 min at room temperature. The cell/DNA mixture was then transferred to a 0.4 cm cuvette and electroporated using a Gene Pulser apparatus (Biorad, Hercules, USA) at a capacitance setting of 2000 microfarad and voltage setting of 240 volts. Cells were then immediately transferred into 50 ml DMEM with 10% FCS and seeded into two 140 mm dishes. After 72 hours growth the cells were harvested and membranes were then prepared as previously described (27).

**Cell membrane preparations.** Transfected cells (four 140 mm dishes at a 50 to 100% confluency) were washed two times with PBS, scrapped off the plates in PBS, pelleted by centrifugation at 400 g for 10 min at 4°C, frozen at -80°C for at least 30 min and thawed in 30 ml of cold 50 mM Tris HCl at pH 7 when membranes were prepared for ligand binding experiments, and in 30 ml of cold 50 mM Tris HCl at pH 7, containing 2.5 mM EDTA and 0.1 mM PMSF (added extemporaneously) for [<sup>35</sup>S]GTPγS binding experiments. All of the following steps were performed at 4°C. The cell lysate was dounce homogenized and spun at 400 g for 10 min. The pellet was resuspended in 15 ml of buffer, dounce homogenized and spun again at 400 g for 10 min. Both supernatants were pooled and centrifuged at 100,000 g for 30 min. The pellet was then resuspended in 4 ml of 50 mM Tris HCl at pH 7 and the protein concentration was measured using the Bradford assay. Membranes were then aliquoted at a 1 mg protein/ml concentration and stored at -80°C. When membranes

were prepared for [<sup>35</sup>S]GTP $\gamma$ S binding experiments the pellet was resuspended in 25 ml of 50 mM Tris HCl at pH 7, dounce homogenized and spun again at 100,000 g for 30 min. The pellet was then resuspended in 4 ml of 50 mM Tris HCl at pH 7, containing 0.32 M sucrose and the protein concentration was measured as described above.

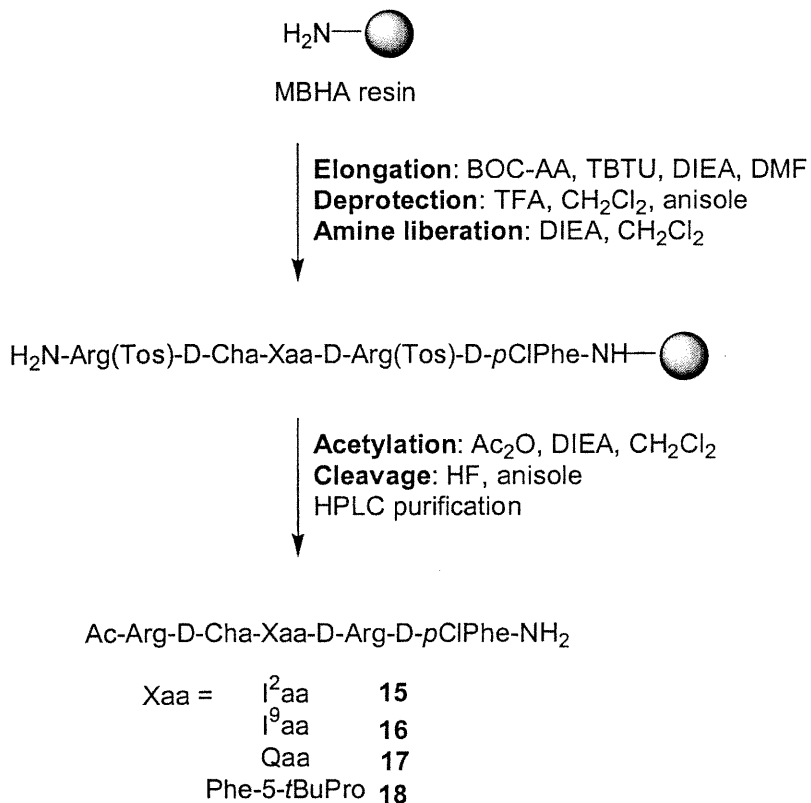
**Receptor Binding assay.** Binding experiments were done as described previously (28). For competition experiments membrane proteins were diluted in 50 mM of Tris HCl at pH 7.4 and incubated with [<sup>3</sup>H]diprenorphine (0.2 nM for hMOR and hDOR, and 0.4 nM for hKOR) or 0.1 nM [Leucyl-<sup>3</sup>H]nociceptin (for hORL1) and variable concentrations of competitor peptide ( $7.8 \times 10^{-11}$  to  $5 \times 10^{-5}$  M) in a total volume of 0.2 ml for one hour at 25°C. Non-specific binding was determined in presence of 1  $\mu$ M naloxone (hMOR, hDOR, hKOR) or 1  $\mu$ M nociceptin/orphanin FQ (hORL1).  $K_i$  values were determined using the EBDA/Ligand program (G. A. McPherson, Biosoft, Cambridge, UK).

**[<sup>35</sup>S]GTP $\gamma$ S binding assay.** For the opioid receptors, 5  $\mu$ g of hMOR, hKOR and hORL1 membrane proteins were incubated for 1 h at 30°C (hMOR and hKOR) or 37°C (hORL1) in 50 mM of Tris at pH 7.4, containing 5 mM MgCl<sub>2</sub>, 1 mM EGTA, 100 mM NaCl, 0.1 % BSA, GDP (30  $\mu$ M for hMOR, 3  $\mu$ M for hKOR and 40  $\mu$ M for hORL1), 0.2 nM [<sup>35</sup>S]GTP $\gamma$ S and ligands ( $1.8 \times 10^{-11}$  to  $1 \times 10^{-5}$  M for the prototypical agonists and  $2.8 \times 10^{-10}$  to  $5 \times 10^{-5}$  M for the competitor peptides). Non specific binding was determined in the presence of 10  $\mu$ M GTP $\gamma$ S. Incubation mixtures were rapidly washed, using a cell harvester (Brandell, Gaithersburg USA), with cold 50 mM Tris HCl at pH 7.5 on H<sub>2</sub>O presoaked GF/B filters. Bound radioactivity was determined by scintillation counting. EC<sub>50</sub> values were determined using the Prism software (GraphPad, San Diego, USA).

## 4.6. Results

### 4.6.1. Synthesis.

Scheme 1. Synthesis of peptides 15-18.



Enantiopure turn-inducing amino acids, *N*-BOC-Xaa, were synthesized according to procedures developed in our laboratory from aspartic and glutamic acids as inexpensive chiral educts as described in the literature (21-24). Azabicyclo[X.Y.0]alkane amino acids, I<sup>2</sup>aa, I<sup>9</sup>aa and Qaa were made by procedures involving reactions of the  $\omega$ -carboxylates of the aminodicarboxylates to provide a linear ketone intermediate, followed by intramolecular reductive amination and lactam cyclization to give the bicycle (21-23). 5-*tert*-Butylproline was synthesized from glutamic acid via our acylation/decarboxylation/reductive amination sequence and converted to the dipeptide by coupling BOC-Phe to 5-*t*BuPro benzyl ester in solution (24, 29). The set of peptides **15-18** incorporating I<sup>2</sup>aa, I<sup>9</sup>aa, Qaa and Phe-5-*t*BuPro were synthesized using the solid-phase strategy of Merrifield on MBHA resin (30). Sequential elongation of the peptides involved couplings of *N*-BOC-protected

amino acids using TBTU as coupling reagent in DMF followed by deprotections using TFA in  $\text{CH}_2\text{Cl}_2$ . The peptides were cleaved and the tosyl groups of the arginyl residues were deprotected by treatment of the resin with anhydrous liquid HF in the presence of anisole. The crude peptides were purified by reverse-phase HPLC and lyophilized. The purity of the peptides was assessed by analytical HPLC and the composition was determined by fast atom bombardment mass spectrometry (FAB-MS). The conformation of the peptides was examined using NMR and CD spectroscopy in water.

#### **4.6.2. Conformational analysis by NMR spectroscopy.**

The  $^1\text{H}$  NMR spectra of the peptides were studied in 9:1  $\text{H}_2\text{O}/\text{D}_2\text{O}$  and the signals were assigned using COSY, TOCSY and ROESY experiments. Peptides **15** and **16** containing  $\text{I}^2\text{aa}$  and  $\text{I}^9\text{aa}$  residues respectively showed a single set of proton signals, whereas, peptides **17** and **18** with Qaa and Phe-5-*t*BuPro residues displayed multiple sets of proton signals in the  $^1\text{H}$  NMR spectra. In peptide **18**, a prolyl amide isomer equilibrium was observed about the Phe-5-*t*BuPro bond. The relative population of the *cis*- and *trans*-isomers were measured by integration of the isomeric *tert*-butyl singlets at 0.64 and 0.89 ppm in the proton NMR spectra. The cross-peak in the ROESY spectra arising from the nuclear Overhauser effect between the  $\delta$ -hydrogen of proline and the  $\alpha$ -hydrogen of the phenylalanine residue confirmed the assignment of the major conformation as the *trans*-isomer. A 60:40 ratio of *trans:cis* prolyl amide isomer populations was observed in peptide **18** in water. Peptide **17** possessing the Qaa residue existed in multiple low energy conformers as observed in its NMR spectrum. The  $^1\text{H}$  NMR spectrum indicated three sets of signals in a ratio of 11 : 2 : 1 as measured by integration of the D-*p*-ClPhe amide protons respectively at 8.17, 8.64 and 8.12 ppm. The structural assignment of the protons for the major isomer of **17** was accomplished using the TOCSY spectrum. Sequential  $\text{H}\alpha\text{N}(i, i+1)$  NOEs were observed for all expected residues in the four peptides **15-18**. In the spectra of peptide **15** with the  $\text{I}^2\text{aa}$  residue, an additional  $\text{NN}(i, i+1)$  NOE was observed between the D-arginine and D-*p*-chlorophenylalanine residues. In addition, long-range NOE cross-peaks were observed between the guanidine NH of L-arginine

and the  $\alpha$ - and amide protons of D-*p*-chlorophenylalanine in the ROESY spectrum of **15**. No long-range NOEs were observed in the spectra of peptides **16-18**.

Coupling constant values ( $^3J_{\text{NH-C}\alpha\text{H}}$ ) can provide information on the peptide conformation. However, for flexible peptides, the coupling constant may be less significant because the value may be averaged due to conformational equilibria (31-32). The spin-spin coupling constant for the  $i + 1$  and  $i + 2$  residues of a turn structure have been used to assign peptide backbone geometry (33). The coupling constant value obtained for the NHXaa-C $\alpha$ H (where Xaa = I<sup>2</sup>aa, I<sup>9</sup>aa and Qaa) were in the range of 7.5-8.4 Hz for all three peptides **15-17** (Table 1). Values of this kind suggest that the bicyclic residues may be situated at the  $i + 1$  and  $i + 2$  positions of turn structures in the peptides because  $^3J_{\text{NH-C}\alpha\text{H}}$  values of 7 Hz have been reported for the  $i + 1$  residue of type I' and II'  $\beta$ -turns (34). For extended peptide conformations, coupling constant values of >9 Hz have been reported (34). A small coupling constant value of 3.8 Hz was observed for the major *trans*-isomer of the Phe-5-*t*BuPro residue in peptide **18**. Values of  $^3J_{\text{NH-C}\alpha\text{H}}$  coupling constant below 4 Hz arise from  $\phi$  dihedral angles in the ranges of 0° to -60° and correspond to the  $i + 1$  residue of type I or type II  $\beta$ -turn conformations (34). A coupling constant of 5.2 Hz was measured for the Phe-5-*t*BuPro residue of the minor *cis*-isomer of peptide **18** which corresponded well with a  $\phi$  dihedral angle of -60° for the  $i + 1$  residue in a type VIa  $\beta$ -turn conformation (24).

**Table 1.** Chemical shift (ppm) assignments of selected proton resonances and coupling constant values ( $^3J_{NH}$ ) for amide protons within peptides 15-18 in 10% D<sub>2</sub>O/H<sub>2</sub>O.

	L-Arg	D-Cha	Xaa	D-Arg	D-pClPhe	Acetyl	D-pClPhe	Arg	D-Arg
	NH ( $^3J_{NH}$ )	H $\alpha$ ( $^3J_{NH}$ )	NH ( $^3J_{NH}$ )	H $\alpha$ ( $^3J_{NH}$ )	NH ( $^3J_{NH}$ )	H $\alpha^1$ ( $^3J_{NH}$ )	H $\alpha^2$ ( $^3J_{NH}$ )	NH ( $^3J_{NH}$ )	H $\alpha$ ( $^3J_{NH}$ )
<b>15</b>	7.16	4.23	8.38	4.35	8.22	4.46	4.41	8.65	4.11
	(6.4)		(7.8)		(8.1)			(5.9)	(8.4)
<b>16</b>	8.23	4.20	8.56	4.34	8.26	4.54	4.64	8.10	4.21
	(5.9)		(7.6)		(8.4)			(7.0)	(8.2)
<b>17<sup>a</sup></b>	8.23	4.21	8.53	4.31	8.27	4.14	5.15	8.06	4.14
	(6.0)		(7.5)		(7.5)			(6.4)	(8.1)
<b>18 trans</b>	8.11	4.17	8.13	4.12	8.35	5.22	4.44	7.98	4.21
	(6.4)		(7.2)		(3.8)			(7.1)	(8.4)
<i>cis</i>	8.18	4.20	8.35	4.38	7.97	4.33	4.37	8.35	4.30
									(5.2)

<sup>a</sup> Chemical shifts are for the major conformer.

**Table 2. Temperature coefficient  $\Delta\delta/\Delta T$  (–ppb/K) values of peptides **15–18** in 10% D<sub>2</sub>O/H<sub>2</sub>O and DMSO.**

Peptides	$\Delta\delta/\Delta T$ (–ppb/K) in water [DMSO]				
	NHArg	NHD-Cha	NHXaa	NHD-Arg	NHD- <i>p</i> ClPhe
<b>15</b>	6.7	8.3 [4.3]	8.3 [4.1]	9.2	4.6 [5.5]
<b>16</b>	7.7	10.0 [5.7]	5.5 [4.3]	7.9	8.5 [2.5]
<b>17<sup>a</sup></b>	7.8	10.6	5.4	5.8	7.8
<b>18<sup>a</sup></b>	6.8	7.5 [7.3]	7.1 [6.0]	4.6	5.2 [2.5]

<sup>a</sup> Values are for the major conformer.

The temperature coefficient values ( $\Delta\delta/\Delta T$ ) were measured for the amide protons in peptides **15–18** in 10% D<sub>2</sub>O/H<sub>2</sub>O as well as DMSO (Table 2). A low temperature coefficient value in DMSO ( $\Delta\delta/\Delta T < -3$  ppb/K) for the amide proton has been shown to be indicative of intramolecular hydrogen bonds in peptides (31). In DMSO, the temperature coefficient values for the amide protons of D-*p*ClPhe residue in peptide **15** and the major conformer of **18** were –2.5 ppb/K, indicative of intramolecular hydrogen bonds. In 10% D<sub>2</sub>O/H<sub>2</sub>O, the amide protons of D-*p*ClPhe residue in peptide **15** and of D-Arg residue of peptide **18** exhibited the lowest observed temperature coefficient values (–4.6 ppb/K) which may indicate their participation in intramolecular hydrogen bonds. The chemical shift variation with temperature for the other amide protons in water and DMSO for all four peptides were respectively in the range of –5.2 to –10.6 ppb/K and –4.1 to –7.5 ppb/K indicative of solvent exposed amide protons (31).

#### **4.6.3. Conformational analysis by circular dichroism spectroscopy.**

Circular dichroism (CD) spectra of peptides **15–18** were measured in water to examine if the peptides existed in a folded conformation in solution. The CD spectra of peptides **16**, **17** and **18** showed a minima at  $225 \pm 5$  nm, a maxima at  $190 \pm 5$  nm and a minima at <180 nm (Figure 6).

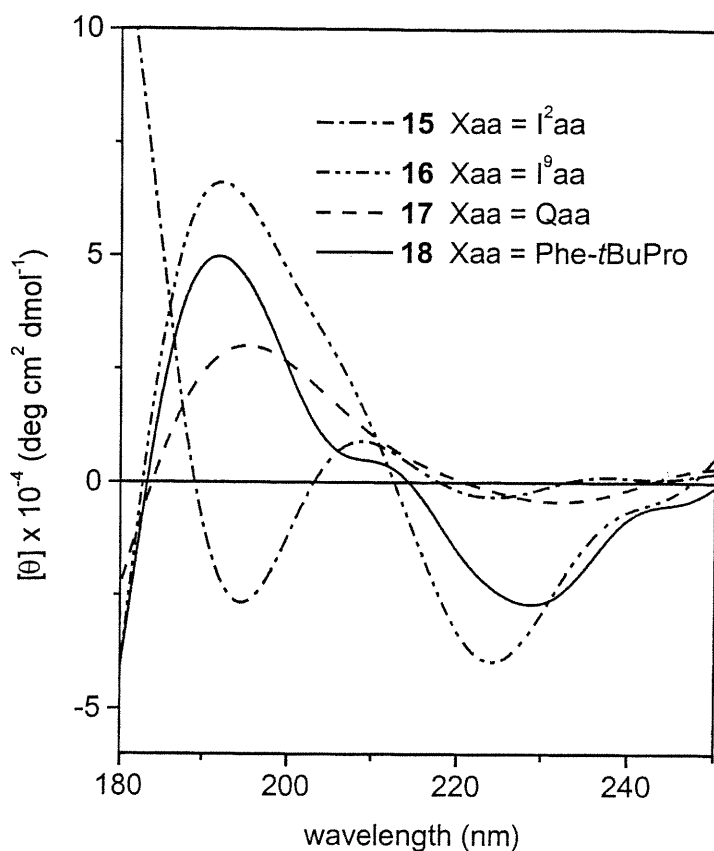


**Figure 6. Circular dichroism spectra of Ac-Arg-D-Cha-Xaa-D-Arg-D-p-ClPhe-NH<sub>2</sub> in water at 0.1mM.**

The relative intensities of the maxima and minima varied with each peptide, however their general curve shape could be classified as a type B spectrum (35). The CD spectrum of peptide **15** exhibited a minimum at 223 nm, a maximum at 210 nm, a minimum at 195 nm and a maximum at <180 nm, which corresponded to a class D spectrum (35). Both class B and D spectra have been previously assigned to  $\beta$ -turn conformations (35-37). For example, a class B spectrum has been assigned to 5-*tert*-butylprolyl dipeptides that were shown to adopt type VIa  $\beta$ -turn conformations in water and acetonitrile (24). Moreover, a Leu-enkephalin analogue in which I<sup>9</sup>aa replaced the Gly<sup>2</sup>-Gly<sup>3</sup> residues of the parent peptide was previously shown to have a type B CD spectrum and suggested to adopt a  $\beta$ -turn conformation (19).

#### 4.6.4. Biological Activity

**Binding characterization.**

**Table 3. Binding affinities for hKOR, hMOR, hDOR and hORL1 of peptides 15-18.**

Ligands	Ac-Arg-D-Cha-Xaa-D-Arg-D-pClPhe-NH <sub>2</sub>	<i>Ki</i> (nM) <sup>a</sup>			
		hKOR	hMOR	hDOR	hORL
<b>1</b>	BTD	78 ± 14	53 ± 20	222 ± 44	34 ± 8
<b>15</b>	I <sup>2</sup> aa	190 ± 1	75 ± 21	5200 ± 50	44 ± 2
<b>16</b>	I <sup>9</sup> aa	1085 ± 5	2700 ± 20	10900 ± 370	2130 ± 10
<b>17</b>	Qaa	441 ± 85	496 ± 89	7050 ± 850	35 ± 10
<b>18</b>	Phe-5-tBuPro	282 ± 81	368 ± 80	2340 ± 260	1700 ± 300

<sup>a</sup> *Ki* values were determined using [<sup>3</sup>H]Diprenorphine for hKOR, hMOR, hDOR and [<sup>3</sup>H]Leucyl-nociceptin. Experiments were conducted on hKOR, hMOR, hDOR transiently transfected into COS-1 cells and hORL1 stably expressed into CHO cells. Values are means ± s.e.m. from three or more separated experiments, performed in duplicate.

The *Ki* values of peptides incorporating I<sup>2</sup>aa (**15**), I<sup>9</sup>aa (**16**), Qaa (**17**) and Phe-5-tBuPro (**18**) were determined on membrane homogenates of COS-1 or CHO cells expressing recombinant human  $\mu$ -,  $\delta$ - and  $\kappa$ -opioid receptors (hMOR, hDOR and hKOR) and the human opioid receptor like (hORL1), and compared to the *Ki* values of the original peptide, peptide III-BTD (**1**, Table 3). Peptides **16** and **18** did not exhibit any improvement in affinity nor of selectivity relative to peptide **1**. Peptides **15** and **17**, like peptide **1**, showed high affinity for hORL1 (44 and 35 nM, respectively). Peptide **15** displayed an improved selectivity for hORL1 versus hDOR (1: 1.7 : 118 : 4 *Ki* ratio of hORL1 / hMOR / hDOR / hKOR) relative to that previously observed with peptide **1** (1: 1.5 : 6.5 : 2 *Ki* ratio of hORL1 / hMOR / hDOR / hKOR). A greater improvement in selectivity for hORL1 over the other

opioid receptors was exhibited by peptide 17 (1: 14: 201: 13 Ki ratio of hORL / hMOR / hDOR / hKOR).

#### [<sup>35</sup>S]GTPγS Binding Assay.

We further characterized the peptides having I<sup>2</sup>aa (15) and Qaa (17) residues in a functional assay consisting in agonist promoted stimulation of [<sup>35</sup>S]GTPγS binding to hORL1, hKOR and hMOR cell membranes (14), because they exhibited submicromolar affinities for these receptors. Figure 7 shows the results obtained with CHO-hORL1 membranes. In this experiment, orphanin FQ/nociceptin, a potent agonist of hORL1, stimulated the [<sup>35</sup>S]GTPγS binding with an EC<sub>50</sub> value of  $24 \pm 2$  nM and a maximal activity corresponding to  $733 \pm 23$  % that of the basal level of [<sup>35</sup>S]GTPγS binding.

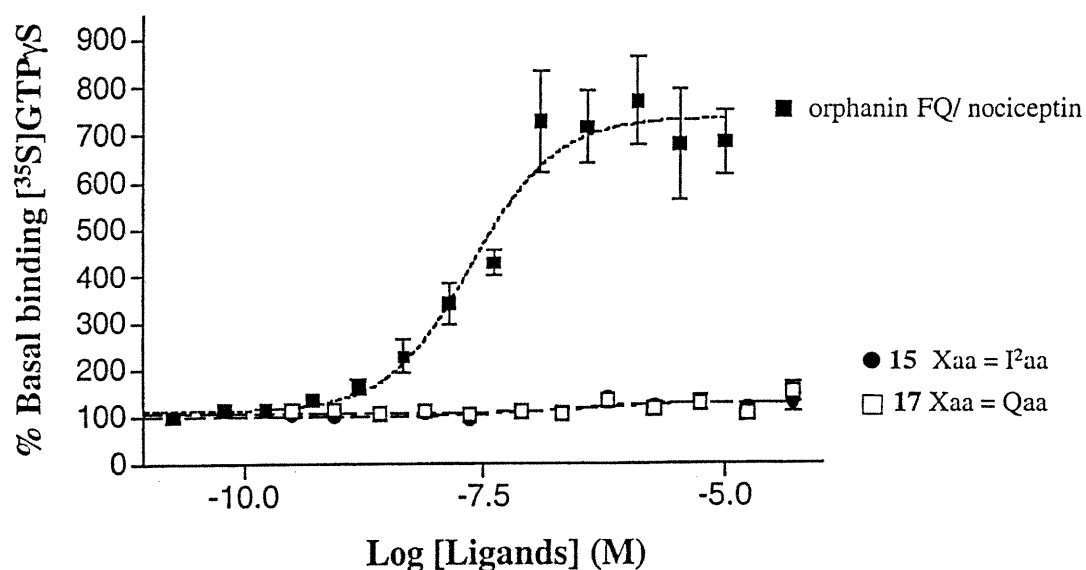


**Figure 7. Stimulation of [<sup>35</sup>S]GTPγS binding to hORL1 by orphanin FQ/nociceptin and peptides 15 and 17.**

CHO-hORL1 membranes (5 µg proteins) were incubated one hour at 37°C with [<sup>35</sup>S]GTPγS (0.2 nM) and GDP (40 µM), with increasing concentrations of ligands: nociceptin/orphanin FQ (■), peptide 15 (●), peptide 17 (□). Data are expressed as percentage of basal [<sup>35</sup>S]GTPγS binding and represent mean ± s.e.m. from at least two separated experiments.

Peptides **15** and **17**, neither increased nor decreased significantly the [<sup>35</sup>S]GTP $\gamma$ S binding at low concentration. To further confirm the antagonist activity of the two latter peptides, we performed concentration-effect curves of orphelin FQ/nociceptin in presence of 100 Ki of each competitor peptide (Fig. 8). Peptide **15** (4.5  $\mu$ M) and peptide **17** (3.5  $\mu$ M) shifted the concentration – effect curve of orphelin FQ/nociceptin to the right by about 15- and 16-fold, respectively. Peptides **15** and **17** were thus demonstrated to act like peptide **1** and exhibited potent antagonist activity toward hORL1.

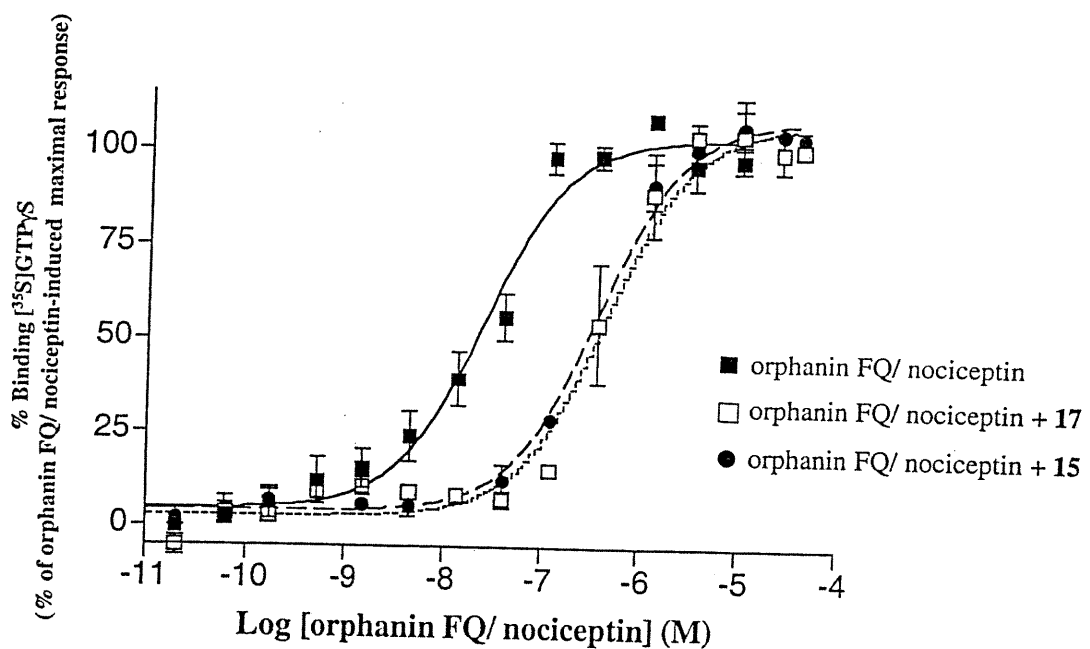


**Figure 8. Stimulation of [<sup>35</sup>S]GTP $\gamma$ S binding by nociceptin/orphanin FQ on hORL1 in presence of putative antagonist peptides.**

CHO-hORL1 membranes (5  $\mu$ g proteins) were incubated one hour at 37°C with [<sup>35</sup>S]GTP $\gamma$ S (0.2 nM) and GDP (40  $\mu$ M), with increasing concentrations of nociceptin/orphanin FQ (■) and 4.4  $\mu$ M of peptide **15** (●) and 3.5  $\mu$ M of peptide **17** (□). Peptides **15** and **17** shifted the concentration effect-curve of nociceptin/orphanin FQ to the right by 15-16-fold. Data are expressed as percentage nociceptin/orphanin FQ-induced maximal [<sup>35</sup>S]GTP $\gamma$ S binding and represent mean  $\pm$  s.e.m. from at least two separated experiments.

The activity of peptides **15** and **17** was also assessed in the [<sup>35</sup>S]GTP $\gamma$ S binding assay using COS-hKOR membranes. Under our conditions, CI-977 stimulated the [<sup>35</sup>S]GTP $\gamma$ S binding with an EC<sub>50</sub> value of  $3.9 \pm 0.7$  nM and a maximal activity corresponding to  $190 \pm 3\%$  that of the basal level of [<sup>35</sup>S]GTP $\gamma$ S binding. Peptides **15** and **17** stimulated the [<sup>35</sup>S]GTP $\gamma$ S binding to COS-hKOR membranes with EC<sub>50</sub> values  $> 1$   $\mu$ M and maximal activity of about 115% that of the basal level of [<sup>35</sup>S]GTP $\gamma$ S binding (Fig. 9), indicative of their partial agonist activity at hKOR.

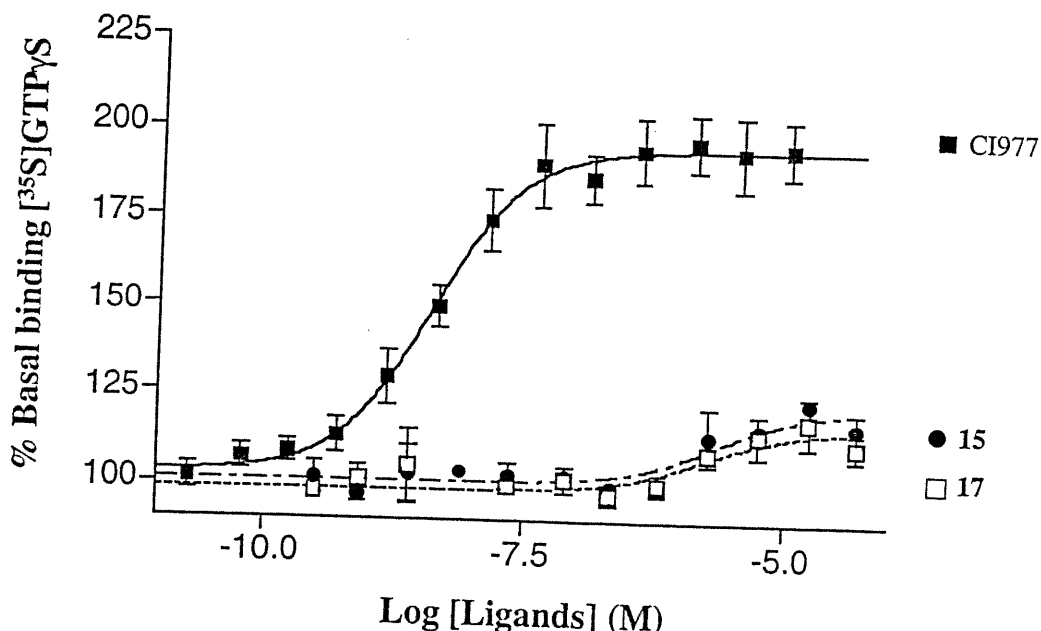


**Figure 9. Stimulation of [<sup>35</sup>S]GTP $\gamma$ S binding to hKOR by CI-977 and peptides **15** and **17**.**

COS-hKOR membranes (5  $\mu$ g proteins) were incubated one hour at 30°C with [<sup>35</sup>S]GTP $\gamma$ S (0.2 nM) and GDP (3  $\mu$ M), with increasing concentrations of ligands: CI-977 (■), peptide **15** (●), peptide **17** (□). Data are expressed as percentage of basal [<sup>35</sup>S]GTP $\gamma$ S binding and represent mean  $\pm$  s.e.m. from at least two separated experiments.

The two peptides with I<sup>2</sup>aa (**15**) and Qaa (**17**) residues also displayed submicromolar affinities for hMOR. We therefore tested their activity at this receptor in the [<sup>35</sup>S]GTP $\gamma$ S binding assay (Fig. 10). Peptides **15** and **17** stimulated the [<sup>35</sup>S]GTP $\gamma$ S binding to COS-hMOR membranes with EC<sub>50</sub> values of  $1.4 \pm 0.7$   $\mu$ M

and  $2.8 \pm 0.5 \mu\text{M}$  respectively. Maximal activation values obtained with peptide **15** (207 %) and peptide **17** (140 %) on COS-hMOR membranes were lower than that obtained with DAMGO (239 %), a classical peptidic MOR-agonist, indicative of their partial agonist activity at hMOR.

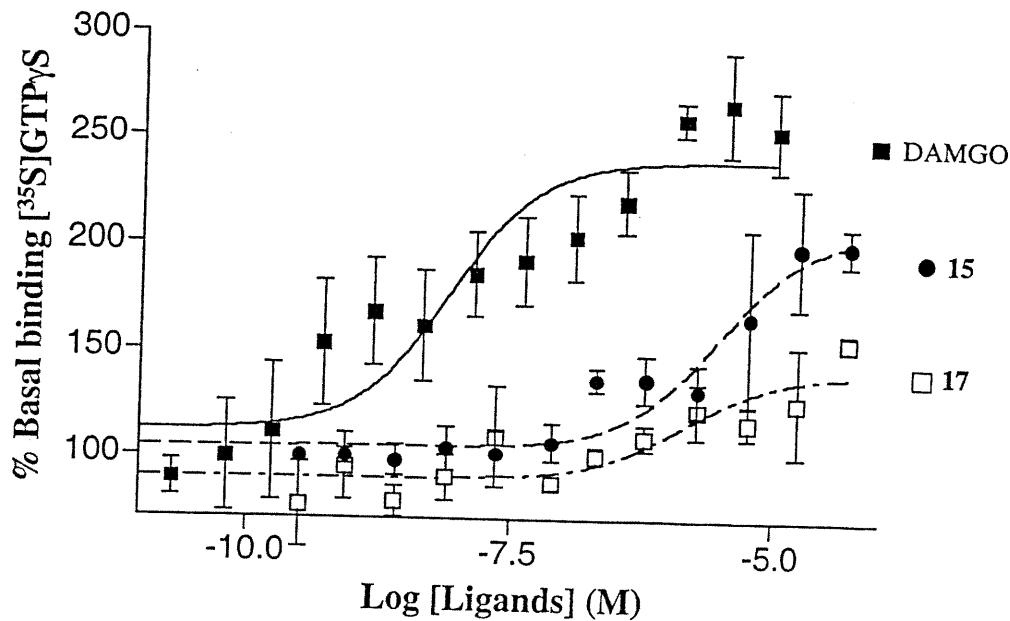


**Figure 10. Stimulation of  $[^{35}\text{S}]GTP\gamma\text{S}$  binding to hMOR by DAMGO and peptides **15** and **17**.**

COS-hMOR membranes (5  $\mu\text{g}$  proteins) were incubated one hour at 30°C with  $[^{35}\text{S}]GTP\gamma\text{S}$  (0.2 nM) and GDP (30  $\mu\text{M}$ ), with increasing concentrations of ligands: DAMGO (■), peptide **15** (●), peptide **17** (□). Data are expressed as percentage of basal  $[^{35}\text{S}]GTP\gamma\text{S}$  binding and represent mean  $\pm$  s.e.m. from at least two separated experiments.

#### 4.7. Discussion

Conformationally constrained mimics can be incorporated into biologically active peptides to identify turn regions, to stabilize active conformations and to increase metabolic stability (38-43). Cyclic analogues with varying ring sizes have been used to explore structure-activity relationships of bioactive peptides (44-46). In a pioneering study of opioid receptor ligands, a series of lactams possessing different ring sizes was used to constrain the Gly<sup>2</sup> residue of Met-enkephalin (44). The (*R*)- $\delta$ -lactam was the most active relative to  $\gamma$ - and  $\epsilon$ -lactam counterparts and possessed 2-

10% of the activity of the parent peptide (44). Furthermore, a series of potent dual inhibitors of angiotensin-converting enzyme (ACE) and neutral endopeptidase (NEP) were generated by using thiaquinolizidinone, and pyrrolo- and pyrido-azepinone amino acids to restrict the conformation of mercaptoacyl dipeptides (45). Because the 7,6-fused pyrido-thiazepinone analogue exhibited increased potency, it was selected for advancement into clinical development (45). Recently, indolizidin-2-one and pyrroloazepinone amino acids were used to study integrin receptors ligands (46). Potent and selective integrin antagonists were obtained from constraining cyclic RGD pentapeptides using the bicyclic lactams (46).

The conformation of peptides **15-18** were studied in water because of its biological relevance. Caution must be taken, however, when studying linear peptides such as **15-18** because they may adopt multiple conformers in rapid equilibrium in solution (47). Although the aqueous structure of such peptides may not necessarily reflect their conformation when finally bound to the receptor, they may illustrate the solvated form of the peptides that first encounters the receptor (47). In light of the limitations of alternative systems, water represents a good first candidate for studying peptide conformation.

Conformational analysis of peptides **15**, **16**, **17** and **18** by NMR and CD spectroscopy demonstrated that these peptides may adopt folded conformations in water. In the ROESY spectra of peptide **15**, a NOE was observed between the guanidine NH side-chain of L-arginine and the  $\alpha$ - and amide protons of D-*p*-chlorophenylalanine, which suggested a close proximity between the *N*- and *C*-termini of this peptide. The CD spectrum of peptide **15** was different from that of peptides **16-18** yet still characteristic of a  $\beta$ -turn conformation. The NMR and CD data suggested that peptide **15** may adopt an open  $\beta$ -turn conformation with the I<sup>2</sup>aa residue situated at the *i* and *i* + 1 position of a  $\beta$ -turn that does not possess an intramolecular hydrogen bond as shown by the temperature coefficient study. This hypothesis is in accordance with protein X-ray data, which show that proline is more favored at the *i* + 1 rather than the *i* + 2 position of a  $\beta$ -turn (48). Moreover,

dipeptides and cyclic peptides possessing Pro-D-Xaa residues adopt preferably  $\beta$ -turn conformations with proline at the  $i + 1$  position as indicated by NMR spectroscopy, X-ray analysis and computational study (49-51). In a cyclic hexapeptide mimic of tendamistat, the BTD residue was also found at the  $i$  and  $i + 1$  positions of a turn by NMR spectroscopy in a mixture of water and DMSO (52).

In peptide **16**, the coupling constant value for the I<sup>9</sup>aa residue was compatible with its situation at the  $i + 1$  and  $i + 2$  position of a turn conformation in water. The CD curve of peptide **16** was indicative of a  $\beta$ -turn conformation. However, in DMSO, the I<sup>9</sup>aa residue may have shifted to the  $i$  and  $i + 1$  positions of a turn possessing an intramolecular hydrogen bond between the carbonyl oxygen of the I<sup>9</sup>aa and the amide proton of D-*p*-chlorophenylalanine which exhibited a notably low temperature coefficient value (-2.5 ppb/K).

Peptide **17** exhibited conformational equilibria in water that may be related to the pseudo-boat/chair forms of the quinolizidinone ring system. The CD spectra of peptide **17** exhibited a curve shape indicative of a  $\beta$ -turn conformation. The major conformation of peptide **17** exhibited a coupling constant value for the  $i + 1$  residue that was indicative of a turn structure positioning the Qaa residue at the  $i + 1$  and  $i + 2$  position. The temperature coefficient study revealed that peptide **17** possessed no intramolecular hydrogen bond in water.

The coupling constant and the temperature coefficient values for the major *trans*-isomer of peptide **18** in water suggested that the proline residue sits at the  $i + 2$  position of a  $\beta$ -turn with a possible intramolecular hydrogen bond between the carbonyl oxygen of the D-cyclohexylalanine and the amide proton of D-*p*-chlorophenylalanine. This  $\beta$ -turn conformation was supported by the CD curve shape of peptide **18**. In DMSO, the 5-*t*BuPro residue may shift to the  $i + 1$  position of a  $\beta$ -turn that possessed an intramolecular hydrogen bond between the carbonyl oxygen of the phenylalanine and the amide proton of D-*p*-chlorophenylalanine which exhibited a low temperature coefficient value (-2.5 ppb/K). In the minor *cis*-conformer of

peptide **18**, the low coupling constant value for the phenylalanine residue suggested a type VI  $\beta$ -turn conformation in water.

The spectrum of biological activity exhibited by peptides **15-18** suggested that the ring size of the bicyclic system and the steric interactions of the 5-*t*BuPro residue caused significant modification of the peptide conformation. Peptides **16** and **18** exhibited significantly reduced affinity and selectivity at the ORL1 receptor relative to peptide **1** which demonstrated that replacement of the BTD residue by I<sup>9</sup>aa and Phe-5-*t*BuPro caused structural modifications that decreased the activity. Potent antagonist activity at the ORL1 receptor was maintained and ORL1 versus DOR selectivity was enhanced on replacement of the thiaindolizidinone BTD by I<sup>2</sup>aa which introduced a methylene for sulfur and flipped the ring fusion stereochemistry. Peptide **17** incorporating the Qaa residue revealed the importance of a 6,6-bicyclic system for selectivity at the ORL1 receptor. Conversion of the sulfur in BTD to an ethylene group and flipping the ring fusion stereochemistry in Qaa produced a peptide that exhibited similarly potent antagonist activity and enhanced selectivity for the ORL1 receptor. Replacement of the BTD residue by azabicycloalkane amino acids **6-8** demonstrated that ligands with 6,5- and 5,6-bicyclic lactams manifested less selectivity for the ORL1 receptor than the 6,6-bicycle. The 7,5-bicyclic lactam **3** was previously incorporated into peptide **1** and exhibited decreased selectivity for the ORL1 receptor (14). X-ray analysis of analogues of azabicycloalkane amino acids has revealed that the dihedral angle  $\psi$  was similar ( $-141 \pm 35^\circ$ ) for all three residues, however the  $\phi$  torsion angle for the Qaa residue was significantly different (Fig. 5). Thus,  $\psi$  and  $\phi$  dihedral angles of  $-163^\circ$  and  $48^\circ$  may be important for the peptide conformation to exhibit activity and specificity at the ORL1 receptor.

In conclusion, we have employed structurally related and complementary turn inducing amino acids to provide information on the relationship between conformation and activity at the ORL1 receptor. We have synthesized two new potent antagonists for the ORL1 receptor, peptide **15** exhibited improved ORL1/DOR selectivity relative to the parent BTD ligand and peptide **17** showed a increased

overall selectivity relative to ligand 1. This methodology has enhanced the pharmacological profile of the parent ligand and advanced the understanding of the conformational requirements for ORL1 receptor affinity. This methodology may be similarly applied to study on other peptide ligands that possess turn conformation. The quinolizidinone amino acid is presently serving as a scaffold to provide potent and selective antagonists for the ORL1 receptor possessing improved bioavailability.

**Acknowledgment:** This research was supported in part by the Natural Sciences and Engineering Research Council of Canada, the Ministère de l'Éducation du Québec, the AW1 grant BIL from Belgium, the institutional grants from CNRS of France and by specific grants from Association pour la Recherche sur le Cancer of France. We thank Sylvie Bilodeau and Dr. M. T. Phan Viet of the Regional High-Field NMR Laboratory for their assistance. We are grateful for the support of P. Chambon.

#### **Abbreviations:**

BTD, (3S,6S,9R)-2-oxo-3-amino-7-thia-1-aza-bicyclo[4.3.0]nonane-9-carboxylic acid; Haic, 5-amino-1,2,4,5,6,7-tetrahydroazepino[3,2,1-hi]indole-4-one-2-carboxylate; BZA, 3-amino-1-carboxymethyl-2,3,4,5-tetrahydro-1H-[1]-benzazepine-2-one; BZD, 3-amino-N-1-carboxymethyl-2-oxo-5-phenyl-1,4-benzodiazepine; I<sup>2</sup>AA, (3S,6R,10S)-3-amino indolizidin-2-one-9-carboxylate; I<sup>9</sup>AA, (2S,6R,8S)-8-amino indolizidin-9-one-2-carboxylate; QAA, (3S,6R,10S)-3-amino quinolizidin-2-one-10-carboxylate; 5-*t*BuPro, (2S,5R)-5-*tert*-butylproline; CI-977, [5R-(5 $\alpha$ ,7 $\alpha$ ,8 $\beta$ )-N-methyl-N-[7-(1-pyrrolidinyl)-1-oxaspiro[4.5]dec-8-yl]benzo[b]furan-4-acetamide; DAMGO, [D-Ala<sup>2</sup>,N-Me-Phe<sup>4</sup>,Gly-ol<sup>5</sup>]enkephalin; hDOR, human  $\delta$ -opioid receptor; hKOR, human  $\kappa$ -opioid receptor; hMOR, human  $\mu$ -opioid receptor; hORL1, human opioid receptor like.

#### **4.8. References:**

1. Bunzow, J.R., Saez, C., Mortrud, M., Bouvier, C., Williams, J.T., Low, M., and Grandy, D.K. (1994) *FEBS Lett.* **347**, 284-288

2. Fukuda, K., Kato, S., Mori, K., Nishi, M., Takeshima, H., Iwabe, N., Miyata, T., Houtani, T., and Sugimoto, T. (1994) *FEBS Lett.* **343**, 42-46
3. Mollereau, C., Paementier, M., Mailleux, P., Butour, J.L., Moisand, C., Chalon, P., Caput, D., Vassart, G., and Meunier, J.C. (1994) *FEBS Lett.* **341**, 33-38
4. Nishi, M., Takeshima, H., Mori, M., Nakagawara, K., and Takeuchi, T. (1994) *Biochem. Biophys. Res. Commun.* **205**, 1353-1357
5. Meunier, J.C., Mollereau, C., Toll, L., Suaudeau, C., Moisand, C., Alvinerie, P., Butour, J.L., Guillemot, J.C., Ferrara, P., Monserrat, B., Mazarguil, H., Vassart, G., Parmentier, M. and Costentin, J. (1995) *Nature* **377**, 532-535
6. Reinscheid, R.K., Nothacker, H.-P., Bourson, A., Ardati, A., Henningse, R.A., Bunzow, J.R., Grandy, H., Langen, D.K., Monsma, F.J., Jr., and Civelli, O. (1995) *Science* **270**, 792-794
7. Calo', G., Rizzi, A., Bogoni, G., Neugebauer, W., Salvadori, S., Guerrini, R., Bianchi, C., and Regoli, D. (1996) *Eur. J. Pharmacol.* **311**, R3-R5
8. Dooley, C.T., and Houghten, R.A. (1996) *Life Sci.* **59**, 23-29
9. Calo', G., Guerrini, R., Bigoni, R., Rizzi, A., Marzola, G., Okawa, H., Bianchi, C., Lambert, D.G., Salvadori, S., and Regoli, D. (2000) *Br. J. Pharmacol.* **129**, 1183-1193
10. Dooley, C.T., Spaeth, C.G., Berzetei-Gurske, I.P., Craymer, K., Adapa, I.D., Brandt, S.R., Houghten, R.A., and Toll, L. (1997) *J. Pharmacol. Exp. Ther.* **283**, 735-741
11. Wichmann, J., Adam, G., Röver, S., Cesura, A.M., Dautzenberg, F.M., and Jenck, F. (1999) *Bioorg. Med. Chem. Lett.* **9**, 2343-2348
12. Shinkai, H., Ito, T., Iida, T., Kitao, Y., Yamada, H., and Uchida, I. (2000) *J. Med. Chem.* **43**, 4667-4677
13. Kawamoto, H., Nakashima, H., Kato, T., Arai, S., Kamata, K., and Iwasawa, Y. (2001) *Tetrahedron* **57**, 981-986
14. Becker, J.A., Wallace, A., Garzon, A., Ingallinella, P., Bianchi, E., Cortese, R., Simonin, F., Kieffer, B.L., and Pessi, A. (1999) *J. Biol. Chem.* **274**, 27513-27522

15. Bigoni, R., Rizzi, A., Rizzi, D., Becker, J.A., Kieffer, B.L., Simonin, F., Regoli, D., and Calo', G. (2000) *Life Sci.* **68**, 233-239
16. Calo', G., Guerrini, R., Rizzi, A., Salvadori, S., and Regoli, D. (2000) *Br. J. Pharmacol.* **129**, 1261-1283
17. Nagai, U., Sato, K., Makamura, R., and Kato, R. (1993) *Tetrahedron* **49**, 3577-3592
18. Claridge, T.D.W., Hulme, C., Kelly, R.J., Lee, V., Nash, I.A., and Schofield, C.J. (1996) *Bioorg. Med. Chem. Lett.* **6**, 485-490
19. Gosselin, F., Tourwé, D., Ceusters, M., Meert, T., Heylen, L., Jurzak, M., and Lubell, W.D. (2000) *J. Peptide Res.* **57**, 337-344
20. Halab, L., Gosselin, F., and Lubell, W.D. (2000) *Biopolymers (Peptide Science)* **55**, 101-122
21. Lombart, H.-G., and Lubell, W.D. (1996) *J. Org. Chem.* **61**, 9437-9446
22. Gosselin, F., and Lubell, W.D. (1998) *J. Org. Chem.* **63**, 7463-7471
23. Gosselin, F., and Lubell, W.D. (2000) *J. Org. Chem.* **65**, 2163-2171
24. Halab, L., and Lubell, W.D. (1999) *J. Org. Chem.* **64**, 3312-3321
25. Halab, L., and Lubell, W.D. (2001) *manuscript in preparation.*
26. Kaiser, E., Colescott, R.L., Bossinger, C.D., and Cook, P.L. (1970) *Anal. Biochem.* **34**, 595-598.
27. Befort, K., Tabbara, L., and Kieffer, B. L. (1996) *Neurochem. Res.* **21**, 1301-1307
28. Simonin, F., Gavériaux-Ruff, C., Befort, K., Matthes, H. W. D., Lannes, B., Micheletti, G., Mattei, M.-G., Charron, G., Bloch, B., and Kieffer, B. (1995) *Proc. Natl. Acad. Sci. USA* **92**, 7006-7010
29. Beausoleil, E., L'Archevêque, B., Bélec, L., Atfani, M., and Lubell, W.D. (1996) *J. Org. Chem.* **61**, 9447-9454
30. Merrifield, R.B. (1963) *J. Am. Chem. Soc.* **85**, 2149-2154.
31. Kessler, H. (1982) *Angew. Chem. Int. Ed. Engl.* **21**, 512-523
32. Dyson, H.J., and Wright, P.E. (1991) *Annu. Rev. Biophys. Chem.* **20**, 519-538
33. Bystrov, V.F., Ivanov, V.T., Portnova, S.L., Balashova, T.A., and Ovchinnikov, Y.A. (1973) *Tetrahedron* **29**, 813-877

34. Wüthrich, K. (1986) in *NMR of Proteins and Nucleic Acids* pp. 162-175, John Wiley & Sons, USA
35. Woody, R.W. (1974) in *Peptides, Polypeptides and Proteins* (Blout E.R., Bovey, F.A., Goodman, M., and Lotan, N., eds) pp. 338-348, Wiley: New York
36. Bush, C.A., Sarkar, S.K., and Kopple, K.D. (1978) *Biochemistry* **17**, 4951-4954
37. Park, C., and Burgess, K. (2001) *J. Comb. Chem.* **3**, 257-266
38. Hirschmann, R. (1991) *Angew. Chem. Int. Ed. Engl.* **30**, 1278-1301
39. Giannis, A., and Kolter, T. (1993) *Angew. Chem. Int. Ed. Engl.* **32**, 1244-1267
40. Gante, J. *Angew. Chem. Int. Ed. Engl.* **33**, 1699-1720
41. Gillespie, P., Cicariello, J., and Olson, G.L. (1997) *Biopolymers (Peptide Science)* **43**, 191-217
42. Hanessian, S., McNaughton-Smith, G., Lombart, H.-G., and Lubell, W.D. (1997) *Tetrahedron* **53**, 12789-12854
43. Etzkorn, F.A., Travis, J.M., and Hart, S.A. (1999) *Adv. Amino Acid Mimetics Peptidomim.* **2**, 125-163
44. Freidinger, R.M. (1981) in *Peptides: Synthesis, Structure, Function. Proceedings of the 7<sup>th</sup> Am. Chem. Symp.* (Rich, D.H., and Gross, E., eds) pp. 673-683, Pierce Chemical Co., Rockford, Il.
45. Robl, J.A., Sun, C.-Q., Stevenson, J., Ryono, D.E., Simpkins, L.M., Cimarusti, M.P., Dejneka, T., Slusarchyk, W.A., Chao, S., Stratton, L., Misra, R.N., Bednarz, M.S., Asaad, M.M., Cheung, H.S., Abboa-Offei, B.E., Smith, P.L., Mathers, P.D., Fox, M., Shaeffer, T.R., Seymour, A.A., and Trippodo, N.C. (1997) *J. Med. Chem.* **40**, 1570-1577
46. Belvisi, L., Bernardi, A., Checchia, A., Manzoni, L., Potenza, D., Scolastico, C., Castorina, M., Cupelli, A., Giannini, G., Carminati, P., and Pisano, C. (2001) *Org. Lett.* **3**, 1001-1004
47. Pellegrini, M., and Mierke, D.F. (1999) *Biopolymers (Peptide Science)* **51**, 208-220
48. Wilmot, C.M., and Thornton, J.M. (1988) *J. Mol. Biol.* **203**, 221-232

49. Giersch, L.M., Deber, C.M., Madison, V., Niu, C.-H., and Blout, E.R. (1981) *Biochemistry* **20**, 4730-4738
50. Aubry, A., and Marraud, M. (1989) *Biopolymers* **28**, 109-122
51. Chiang, C.C., and Karle, I.L. (1982) *Int. J. Peptide Protein Res.* **20**, 133-138
52. Etzkorn, F.A., Guo, T., Lipton, M.A., Goldberg, S.D., and Bartlett, P.A. (1994) *J. Am. Chem. Soc.* **116**, 10412-10425

# **CHAPITRE 5**

## **Conclusion**

Les peptides linéaires sont des molécules flexibles qui existent en équilibre conformationnel en solution. Des contraintes conformationnelles peuvent être utilisées pour restreindre la flexibilité des peptides. Un type de contrainte est l'utilisation des interactions stériques qui peuvent être employées afin d'induire ou de défavoriser certaines conformations. Nous avons utilisé les interactions stériques de la 5-*tert*-butylproline pour étudier l'équilibre conformationnel du lien prolyl amide et le mimétisme d'une structure secondaire définie.

Il a été montré que la (2*S*,5*S*)-5-*tert*-butylproline *N*-acétyle *N*<sup>t</sup>-méthylamide favorise une plus grande population d'isomère *cis* par rapport à l'analogue possédant la (2*S*,5*R*)-5-*tert*-butylproline. De plus, la barrière d'isomérisation n'est pas influencée par la (2*S*,5*S*)-5-*tert*-butylproline en comparaison avec la proline. Une synthèse efficace de la (2*S*,5*R*)-*N*-BOC-5-*tert*-butylproline a déjà été rapportée dans la littérature, cependant, une synthèse énantiopure était requise pour la (2*S*,5*S*)-5-*tert*-butylproline afin de l'incorporer dans des peptides et permettre une étude conformationnelle. En utilisant le même produit de départ que pour la synthèse du (2*S*,5*R*)-5-*tert*-butylproline, nous avons développé une synthèse énantiopure de la (2*S*,5*S*)-*N*-BOC-5-*tert*-butylproline via la réduction stéréosélective de l'imine du *tert*-butylprolinol. Cette voie a produit la (2*S*,5*S*)-*N*-BOC-5-*tert*-butylproline avec un rendement global de 39% et une pureté énantiomérique de >96%. Cet acide aminé pourra ainsi être incorporé dans des peptides afin d'étudier l'effet de la stéréochimie du groupement *tert*-butyle sur l'équilibre conformationnel et la stabilisation d'une structure secondaire de repliement.

Par ailleurs, nous avons incorporé la (2*S*,5*R*)-5-*tert*-butylproline dans une série de dipeptides *N*-acétyles *N*<sup>t</sup>-méthylamides pour mimer et reproduire la conformation de repliement  $\beta$  de type VI. Nous avons développé une méthodologie versatile pour générer les dipeptides *N*-acétyles *N*<sup>t</sup>-méthylamides. Les interactions stériques du groupement *tert*-butyle ont augmenté considérablement la population d'isomère *cis* dans les dipeptides *N*-acétyles *N*<sup>t</sup>-méthylamides. Nous avons démontré par une analyse conformationnelle (RMN, DC et rayons-X) que la conformation de

ces dipeptides dépendait de la stéréochimie de l'acide aminé *N*-terminal de la 5-*tert*-butylproline. Ainsi, nous avons obtenu les conformations en repliement  $\beta$  de type VIa et VIb en utilisant respectivement les acides aminés de configuration L et D. Par conséquent, nous sommes capable de reproduire et de mimer les deux types de conformation de repliement  $\beta$  de type VI en utilisant les interactions stériques de la 5-*tert*-butylproline.

Une étude détaillée de la séquence d'acide aminé *N*-terminal de la proline et de la 5-*tert*-butylproline dans les dipeptides *N*-acétyles *N'*-méthylamides a été réalisée afin de comprendre l'importance des chaînes latérales de ces acides aminés sur la conformation du peptide. Une augmentation de la population *cis* a été observée lorsque la chaîne latérale de l'acide aminé était modifiée d'un groupement pouvant former des ponts d'hydrogène, à un substituent alkyle, à un groupement aromatique. Nous avons démontré que la population d'isomère *cis* élevée dans les dipeptides avec des résidues aromatiques résultait d'une interaction entre le cycle de la proline et le système  $\pi$  aromatique du résidu *N*-terminal de la proline.

Pour étudier les facteurs qui contrôlent l'isomérisation *cis-trans* du prolyle amide ainsi que l'induction d'une épingle  $\beta$  par un repliement  $\beta$  de type VIa, une série de tétrapeptides incorporant la (2*S*,5*R*)-5-*tert*-butylproline a été synthétisée. Une étude systématique de la séquence des tétrapeptides a démontré une augmentation de l'isomère *cis* pour les tétrapeptides *N*-acétyles méthylesters possèdant un résidu aromatique *N*-terminal de la 5-*tert*-butylproline. Une conformation de repliement  $\beta$  de type VIa a été stabilisée dans ces tétrapeptides, cependant, des peptides de séquences plus longues sont nécessaires pour observer la géométrie d'épingle  $\beta$ . Par conséquent, il serait intéressant de synthétiser des peptides de plus longues séquences incorporant la (2*S*,5*R*)-5-*tert*-butylproline pour induire une épingle  $\beta$  et ainsi une conformation de feuillets  $\beta$ .

Finalement, nous avons exploré la relation entre la conformation et l'activité biologique de ligands peptidiques pour le récepteur opioid "opioid receptor like"

(ORL1). Nous avons employé des contraintes d'interactions stériques ainsi que des mimétiques de dipeptides pour étudier la relation entre structure-activité. Des acides aminés azabicycloalcanes ( $I^2aa$ ,  $I^9aa$  et  $Qaa$ ) et un mimétique de repliement  $\beta$  de type VIa avec la  $(2S,5R)$ -5-*tert*-butylproline (Phe-5-*t*BuPro) ont été introduits dans des peptides d'intérêt biologique en utilisant la synthèse sur support solide. Les tests biologiques de ces quatre peptides ont démontré deux nouveaux antagonists puissants qui font preuve d'une sélectivité accrue pour le récepteur ORL1. L'analyse conformationnelle de ces peptides a indiqué que la dimension des hétérocycles modifient la conformation adoptée par chaque peptide. Ainsi, nous avons démontré que la dimension et les angles dièdres de l'hétérocycle  $Qaa$  sont importantes pour stabiliser la conformation bioactive au récepteur ORL1.

Les travaux présentés dans cette thèse contribuent à l'avancement des recherches dans le domaine du mimétisme peptidique. Plus spécifiquement, nous espérons que nos résultats ont amené une plus ample compréhension des facteurs impliqués dans les repliements peptidiques.

## **ANNEXE**

### **Article 9**

**Halab, L.; Gosselin, F.; Lubell, W.D. "Design, Synthesis and Conformational Analysis of Azacycloalkane Amino Acids as Conformationally Constrained Probes for Mimicry of Peptide Secondary Structures." Publié dans *Biopolymers (Peptide Science)* 2000, 55, 101-122.**

the introduction of strategies for peptide mimicry,<sup>1-6</sup> many innovative approaches have been used to accelerate the process from peptide to biologically active small molecule.<sup>7-24</sup> Kindly asked to review our own work on the synthesis and analysis of new scaffolds for peptide mimicry, we are pleased to write about two strategies that we have pursued for generating peptide mimics. The first employs structural links to constrain a dipeptide unit. The second uses the steric interactions of bulky ring substituents to influence the geometry and conformation of peptide amide bonds in order to enhance or diminish the population of particular conformations. Key to the success of these two strategies has been the effective use of  $\alpha$ -amino acids as inexpensive chiral educts for synthesizing the desired azacycloalkane and azabicycloalkane amino acids, as new tools for crafting mimics of peptide structure.

### Synthesis of Azabicyclo[X.Y.0]alkane Amino Acids

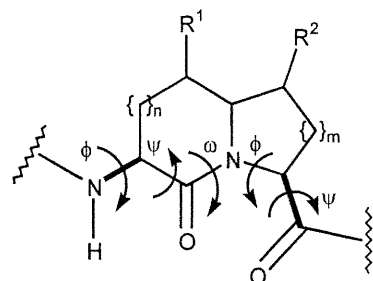


**FIGURE 1** General structure illustrating the five dihedral angles constrained by an azabicyclo[X.Y.0] alkane amino acid in a peptide.

Azabicycloalkane amino acids are constrained dipeptide surrogates that embody the peptide backbone within a bicyclic framework.<sup>23\*</sup> Three contiguous  $\phi$ ,  $\psi$ - and  $\omega$ -dihedral angles are restricted by the structural constraints of the heterocycle. In addition, because the outer two  $\psi$ - and  $\phi$ -dihedral angles are restricted by gauche interactions with the ring system, the azabicycloalkane amino acid offers the capacity for restricting five backbone bonds in a row within the peptide (Figure 1).

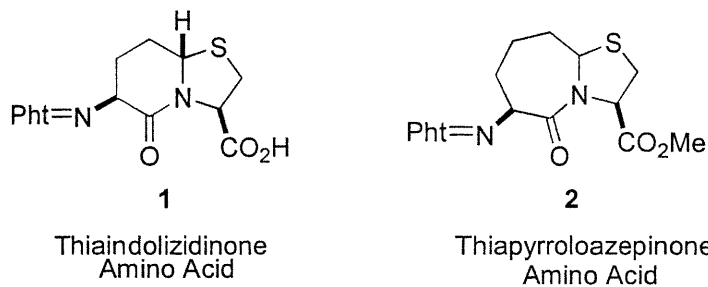


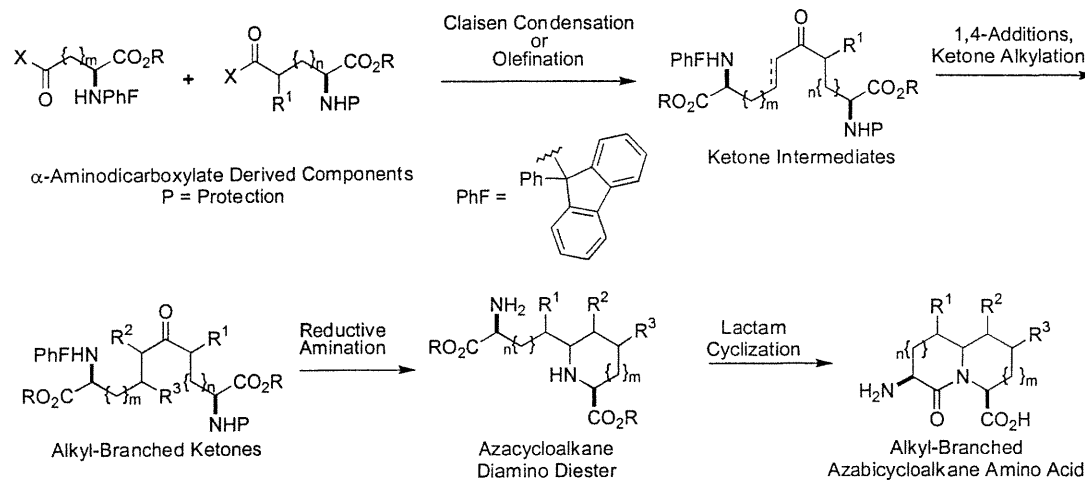
**FIGURE 2 Representative thiazabicycloalkane amino acids.**

Since their inception<sup>†</sup> with the first syntheses of the thiaindolizidinone amino acid **1** (BTD)<sup>26</sup> and the related thiapyrroloazepinone amino acid **2**<sup>27,28</sup> (Figure 2), these scaffolds have been applied as secondary structure replacements and spatially defined platforms for pharmacophore display.<sup>23</sup> Inherent in their synthesis is three important challenges: stereocontrol, side-chain attachment and ring-size (the three S's, Stereochemistry, Side-chains and Size). Because configuration influences conformation, stereochemistry should be introduced with control at the chiral backbone carbons, ring fusion center and attachment sites of the side-chain appendages. The addition of various functional groups at different points along the azabicycloalkane heterocycle is desired for mimicry of the nature and the spatial orientation of a spectrum of amino acid side-chains. Finally, the approach should give rise to a variety of azabicycloalkane ring systems through employment of starting materials of different chain length, because the size of the heterocycle will likely bias the peptide conformation.

Our strategy for synthesizing azabicyclo[X.Y.0]alkane amino acid tries to address the criteria raised above by joining together the  $\omega$ -carboxylates of two  $\alpha$ -aminodicarboxylates to provide a linear ketone intermediate (Scheme 1).<sup>29-36</sup> Side-chains may then be introduced by conjugate additions and alkylations of the ketone. The first heterocycle ring is closed by intramolecular reductive amination or methanesulfonate displacement. The bicycle is finally assembled by a lactam cyclization. Employing both the L- and D-enantiomers of aspartic acid and glutamic acid in this approach has given stereocontrolled entry to four

azabicyclo[X.Y.0]alkane amino acids: indolizidin-2-one, indolizidin-9-one, quinolizidinone and pyrroloazepinone amino acids. Protecting group shuffling has provided both their BOC- and Fmoc-amino acid derivatives suitable for solid-phase synthesis of peptide mimic libraries.

**SCHEME 1. General Strategy for Azabicyclo[X.Y.0]alkane Amino Acid Synthesis**



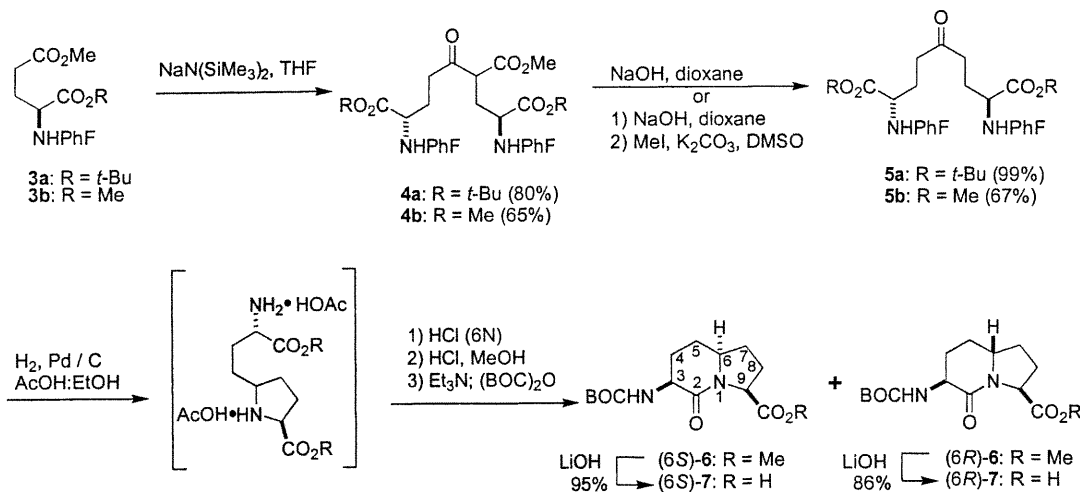
**Stereocontrolled Synthesis of Indolizidin-2-one Amino Acid (I<sup>2</sup>AA)**

The employment of the L- and D-enantiomers of aspartate, glutamate and  $\alpha$ -amino adipate as chiral building blocks in diastereoselective transformations has led to the syntheses of many heterocycles and amino acids.<sup>37</sup> The principal issue to address in this approach is achieving reasonable selectivity with capacity for isomer separation without racemization. To insure configurational stability, we have employed the 9-(9-phenylfluorenyl) (PhF) amine-protecting group that was initially introduced by Christie and Rapoport for amino acid protection in indole alkaloid synthesis.<sup>38</sup> This group creates a steric environment that shields the  $\alpha$ -proton from deprotonation under alkaline conditions.<sup>39</sup> In addition, X-ray structural data show that the  $\alpha$ -proton and  $\alpha$ -carbonyl of N-(PhF)- $\alpha$ -amino carbonyl compounds adopt a coplanar geometry that is stereoelectronically less favored for  $\alpha$ -deprotonation than an orthogonal geometry.<sup>40,41</sup> Like a trityl group,<sup>42</sup> the PhF protection has a

lipophilic character that facilitates manipulation of polar amino acid derivatives; however, the PhF group is much more inert to acid conditions.<sup>§</sup> Prepared conveniently on mole scale from inexpensive starting materials,<sup>44</sup> the PhF group can also be effectively recovered after its removal and recycled.<sup>45</sup>

Our initial synthesis of indolizidin-2-one amino acid **7** illustrated the effective use of the PhF group for protection of glutamic acid in the stereoselective construction of azabicyclo[X.Y.0]alkane amino acid.<sup>29-31††</sup> A Claisen condensation between the  $\omega$ -methyl esters of L-*N*-(PhF)glutamate diesters **3** was achieved using sodium bis(trimethylsilyl)amide as base in THF to provide  $\beta$ -keto ester **4** that was hydrolyzed and decarboxylated to give C2-symmetric  $\delta$ -keto  $\alpha,\omega$ -diaminoazelate **5**. Good yields of azelates **5a** and **5b** were attained from employment of  $\omega$ -methyl L- and D-*N*-(PhF)glutamates **3** with better yields in the case of the  $\alpha$ -*tert*-butyl (**3b**) relative to the  $\alpha$ -methyl ester (**3a**, Scheme 2).

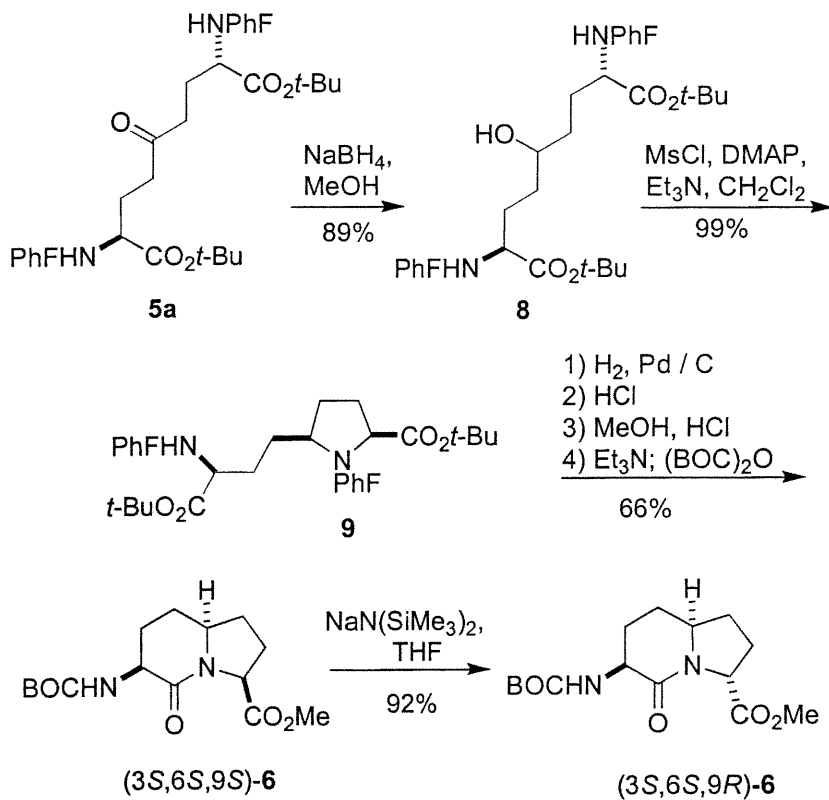
**SCHEME 2. Synthesis of *N*-(BOC)Amino Indolizidin-2-one Acid via Claisen Condensation / Reductive Amination / Lactam Cyclization Sequence**



Indolizidin-2-one amino acid was then prepared from  $\delta$ -keto  $\alpha,\omega$ -diaminoazelate **5** using two different routes. In the first, hydrogenation of azelate **5** with palladium-on-carbon as catalyst in 9:1 EtOH:AcOH proceeded by cleavage of

the phenylfluorenyl groups, intramolecular imine formation, protonation, and hydrogen addition to the iminium ion intermediate (Scheme 2). Increasing the hydrogen pressure from 1 to 11 atm augmented the reaction diastereoselectivity in favor of the *cis*-isomer from 2:1 to 49:1. *N*-(BOC)Amino indolizidin-2-one methyl ester **6** was then produced from conversion of the *tert*-butyl esters to methyl esters, lactam cyclization and BOC protection. Hydrolysis of the methyl esters without concomitant epimerization could be accomplished under carefully controlled conditions using lithium hydroxide as base. Enantiopure indolizidin-2-one amino acid **7** was obtained in 7 steps and 61% yield from glutamate **3a**.

**SCHEME 3.** Synthesis of *N*-(BOC)Amino Indolizidin-2-one Methyl Ester **6** via Methanesulfonate Displacement.



In a different route,<sup>31</sup> hydride reduction of azelate **5a**, methanesulfonate displacement and lactam cyclization gave indolizidin-2-one amino ester **6** as a single diastereomer (Scheme 3). This outcome required the attack of each of the two

amines fifty percent of the time in an S<sub>N</sub>2 displacement of the symmetrical methanesulfonate. A significant difference in the energy of the transition states appeared to favor the *cis*- over the *trans*-5-alkylproline diastereomer and furnished the concave indolizidin-2-one amino ester (3*S*, 6*S*, 9*S*)-6.

Treatment of indolizidin-2-one amino methyl ester (3*S*, 6*S*, 9*S*)-6 using sodium bis(trimethylsilyl)amide in THF gave access to the C-9 epimer (3*S*, 6*S*, 9*R*)-6. The employment of both L- and D-glutamate provided thus a convenient and practical means for synthesizing all stereoisomers of the indolizidin-2-one amino acid (I<sup>2</sup>AA).

### Side-Chain Attachment to the 5- and 7-positions of I<sup>2</sup>AA

The introduction of functional groups that mimic the side chains of the natural amino acids was initially investigated by alkylation of symmetric ketone **5a**. This strategy proved effective for synthesizing enantiopure 5-benzyl-, 7-benzyl- and 5,7-dibenzyl indolizidinone amino acids by a sequence featuring alkylation of di-*tert*-butyl  $\alpha,\omega$ -di-[*N*-(PhF)amino]azelate  $\delta$ -ketone **5a**, cyclization to an alkylproline, and subsequent lactam formation.<sup>32</sup> To compliment this strategy for introduction of aliphatic and aromatic side-chains, we later developed a route for preparing indolizidinone amino acids possessing heteroatomic side-chains that used  $\beta$ -keto ester **4a** as starting material.<sup>33</sup>

In the former approach, alkylation of  $\delta$ -keto  $\alpha,\omega$ -diaminoazelate **5a** was accomplished after enolization with KN(SiMe<sub>3</sub>)<sub>2</sub> in THF at -78°C followed by treatment with DMPU and an alkyl halide for 1-2 h before aqueous work-up (Scheme 4). Under these conditions ketone **5a** behaved normally giving good conversion to alkylated material (63-95%) with reactive electrophiles and lower conversion (28%) with *iso*-propyl iodide. Diastereoselectivity was typically low (1:1 - 7:1) using these conditions. Higher diastereoselectivities (up to 20:1) and better conversions have been obtained on larger scale in the absence of DMPU by allowing the reaction

**Design, Synthesis and Conformational Analysis of  
Azacycloalkane Amino Acids as Conformationally Constrained Probes  
for Mimicry of Peptide Secondary Structures**

**Liliane Halab, Francis Gosselin and William D. Lubell\***

*Département de chimie, Université de Montréal*

*C. P. 6128, Succursale Centre Ville, Montréal, Québec, Canada H3C 3J7*

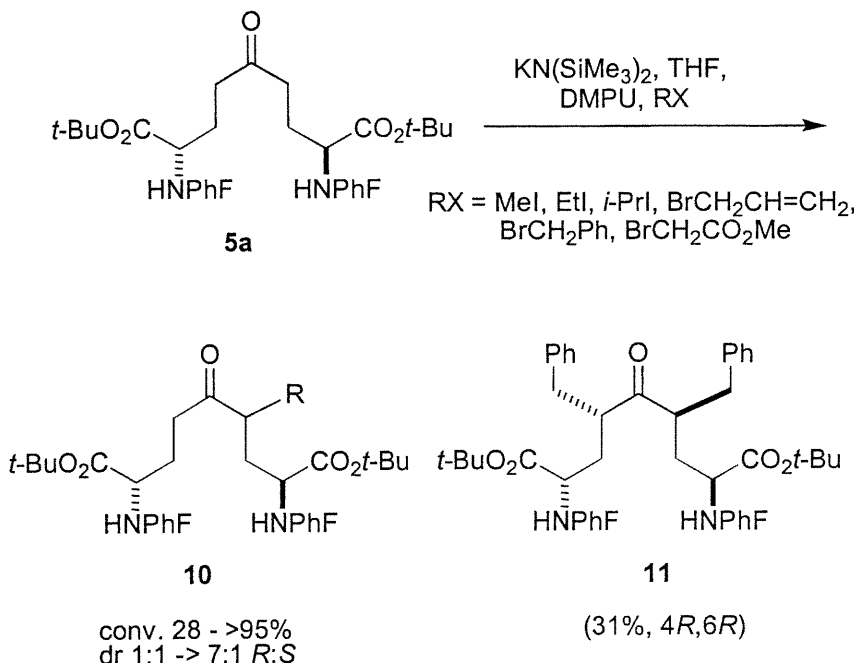
**Abstract**

Conformationally constrained amino acid and dipeptide units can serve in mimics of specific secondary structures for studying relationships between peptide conformation and biological activity. A variety of mimics are required to study systematically the structure-activity relationships in biologically relevant peptides. We present our efforts on the design, synthesis and conformational analysis of a series of rigid surrogates of amino acid and dipeptide units for application within constrained peptide analogs and for employment as inputs for combinatorial science. Conceived to be general and versatile, our methodology has delivered a variety of azacycloalkane and azabicycloalkane amino acids in enantiomerically pure form, via practical methods, from readily available and inexpensive starting materials.

**Introduction**

The art of peptide mimicry has necessitated development of new tools for transforming peptide lead compounds into drugs and biomaterials. Conversion of a peptide into a mimic requires diagnostic means for dissecting the native peptide to furnish information for recreating the elements required for receptor recognition and signal transduction. To enhance metabolic stability and biological availability relative to the native peptide, additional characteristics may later be built into the design of the mimic, after initial understanding has been established of the spatial requirements for recognition. Multiple strategies are necessary for accomplishing this task effectively, because of the diverse spectrum of conformations that peptides can adopt by variations of the orientations of side-chain and back-bone atoms. Since

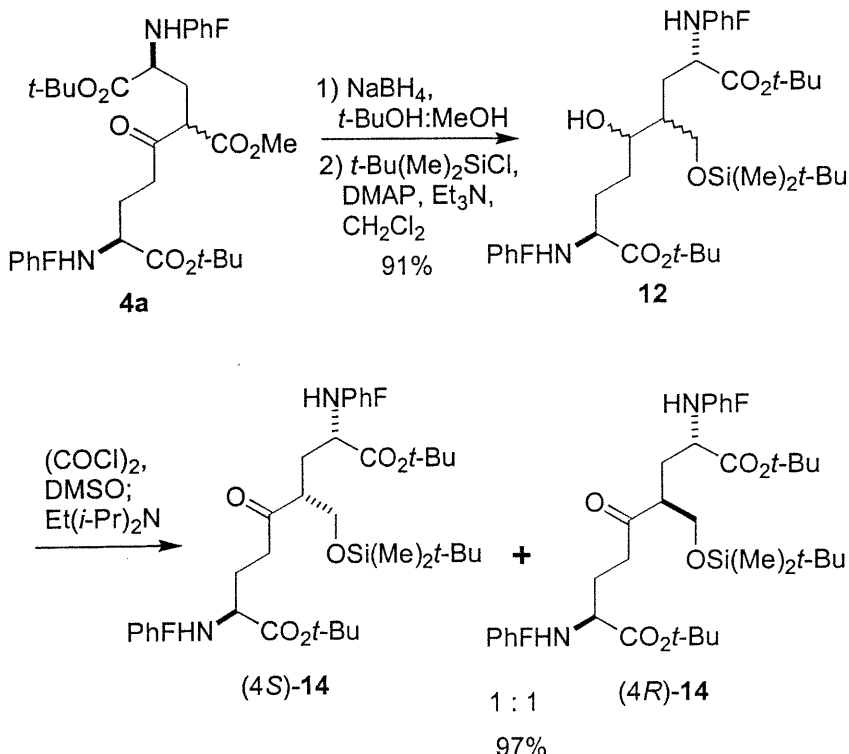
**SCHEME 4. Alkylation of 5-Keto 2,8-Diaminoazelate Di-*tert*-Butyl Ester **5a****



mixture to warm from  $-78^\circ\text{C}$  up to  $-10^\circ\text{C}$  after the addition of the alkyl halide. In the alkylation with benzyl bromide, we found that varying the stoichiometry of base influenced the ratio of mono- and dialkylated product.

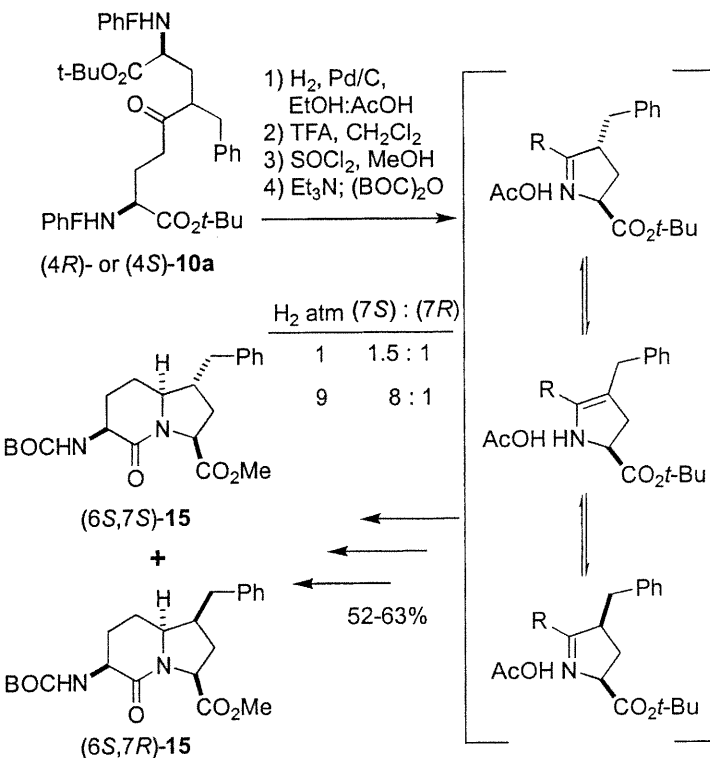
In the later approach,<sup>33</sup> reduction of  $\beta$ -keto ester **4a** with  $\text{NaBH}_4$  in alcoholic solvent gave the diol as a mixture of diastereomers in 88% yield (Scheme 5). Selective protection of the primary alcohol with chloro *tert*-butyldimethylsilane,  $\text{Et}_3\text{N}$  and DMAP in dichloromethane provided silyloxymethyl ketone **12** in 97% yield. Finally, oxidation of the secondary alcohol of **12** with oxalyl chloride and DMSO in dichloromethane gave a separable mixture of diastereomeric ketones **14** in 97% yield.

**SCHEME 5. Synthesis of Protected 4-Hydroxymethyl 5-Keto 2,8-Diaminoazelate 14**



With 4-benzyl, 4-silyloxymethyl and 4,6-dibenzyl ketones **10a**, **14** and **11** in hand, we have studied both the reductive amination and methanesulfonate displacement sequences to respectively furnish benzyl, hydroxymethyl and dibenzyl indolizidinone amino acids (Schemes 6-9).<sup>32,33</sup> In the reductive amination sequence with 4-benzyl ketone **10a** (Scheme 6), we observed that the stereochemistry of the 4-position substituent had no influence on the final stereochemistry of the 7-benzyl indolizidinone amino ester **15**. Epimerization of the alkyl branched chiral center occurred via iminium ion–enaminium ion tautomerization during hydrogenation. Tautomerization was also encountered in the reductive amination sequence with 4-silyloxymethyl ketone **14** to form 7-hydroxymethyl indolizidinone amino ester **16**; however, formation of the enaminium ion was accompanied by  $\beta$ -elimination of the silyloxy substituent such that 7-methyl indolizidinone amino ester **17** was isolated as a major side-product (Scheme 7).<sup>49</sup> Application of the reductive amination / lactam cyclization procedure with (4*R*, 6*R*)-dibenzyl ketone **11** and hydrogenation at 9 atm

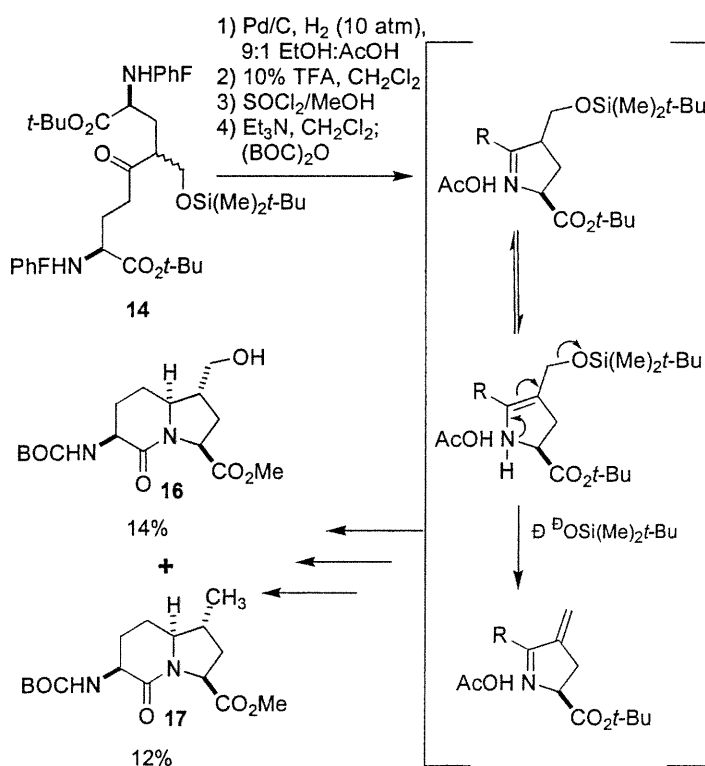
**SCHEME 6. Synthesis of 7-Benzyl Indolizidin-2-one 15 via Reductive Amination of 10a**



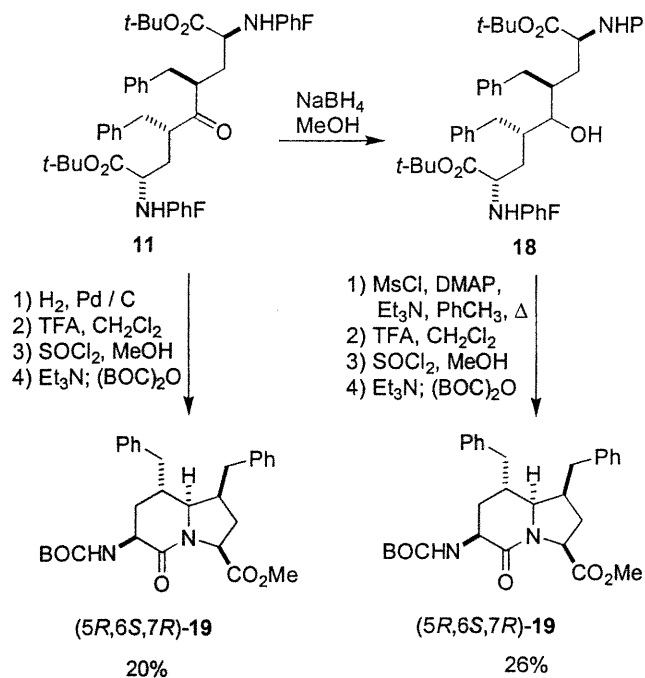
with palladium-on-carbon gave (*5R, 6S, 7R*)-5,7-dibenzylindolizidinone isomer **19** as the only isolated product in 20% overall yield (Scheme 8).<sup>32</sup>

In the strategy involving methanesulfonylation and displacement by the phenylfluorenylamine, we have found that this cyclization step was influenced by both the stereochemistry of the methanesulfonate and alkyl-branch carbons as well as the steric bulk of the 4-position substituent. The promotion of ring formation by steric interactions<sup>50</sup> from the alkyl substituent was observed to cooperate and

**SCHEME 7. Reductive Amination of Protected 4-Hydroxymethyl 5-Keto 2,8-Diaminoazelate 14**

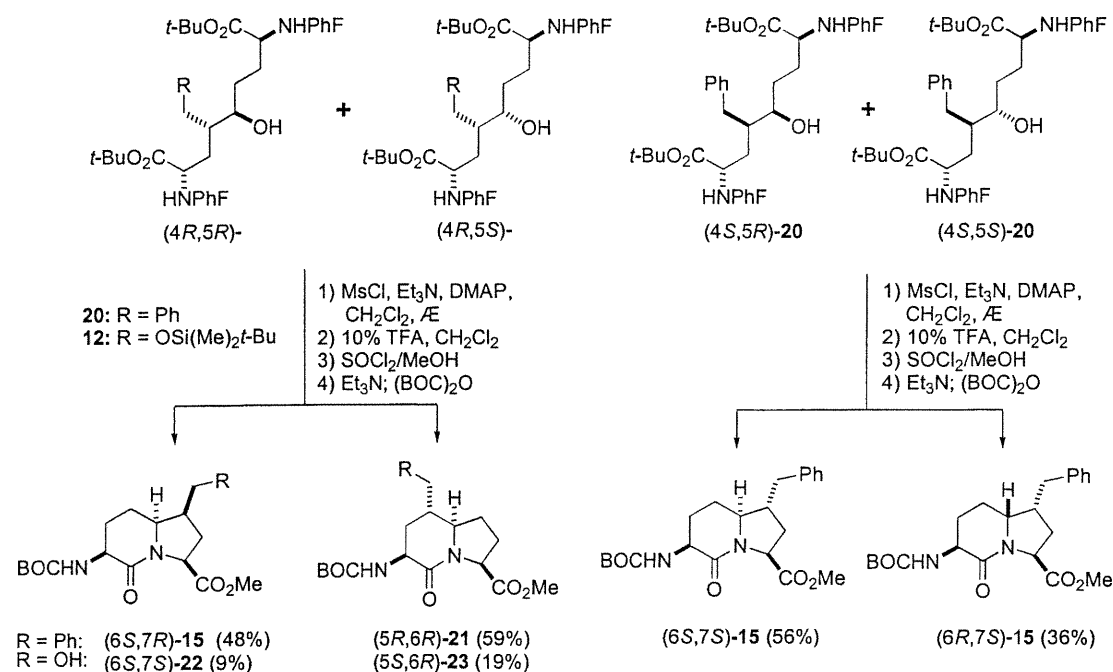


**SCHEME 8. Synthesis of 5,7-Dibenzyl Indolizidin-2-one Amino Ester 19**



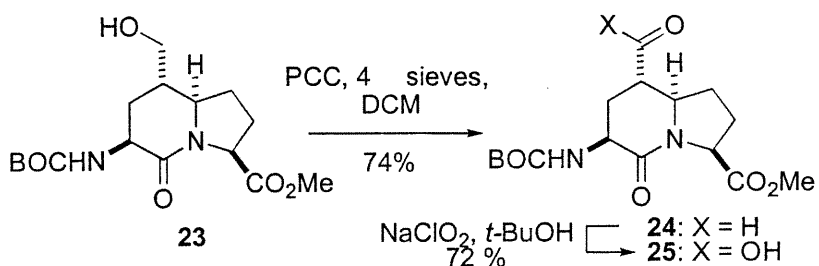
compete with the factors that favored the *cis*- over the *trans*-5-alkylproline diastereomer in the cyclization of simple  $\delta$ -hydroxy  $\alpha,\omega$ -diaminoazelate **20** (Scheme 9). These factors worked cooperatively to furnish the concave isomer of the 7-alkyl indolizidinone amino esters (*6S, 7R*)- and (*6S, 7S*)-**15** as well as (*6S, 7S*)-**22**.

**SCHEME 9. 5- and 7-Alkylindolizidinone Amino Esters via Methanesulfonate Displacements**



The convex isomer of the 7-alkyl indolizidinone amino ester **15** was produced from the sequence with (4*S*, 5*S*)-**20** and indicated that the steric effects from the 4*S*-benzyl group were significant enough to promote a transition state providing the *trans*- rather than the *cis*-5-alkylproline diastereomer. On the other hand, the concave isomer of the 5-alkyl indolizidinone amino ester **21** was obtained from the sequence with (4*R*, 5*S*)-**20** and illustrated that the steric effects from the 4*R*-benzyl group did not perturb the transition state favoring the *cis*-5-alkylproline diastereomer. Although intramolecular cyclization of (4*R*, 5*S*)-**12** gave similarly a predominance of 5-hydroxymethyl indolizidinone (5*S*, 6*R*)-**23**, a small amount of (6*R*, 7*S*)-**22** (3% not shown) was also formed as a result of the greater steric compression caused by the *tert*-butyldimethylsilyloxyethylene group.<sup>33</sup>

**SCHEME 10. Synthesis of *N*-(BOC)Amino Indolizidin-2-one Dicarboxylate 25**

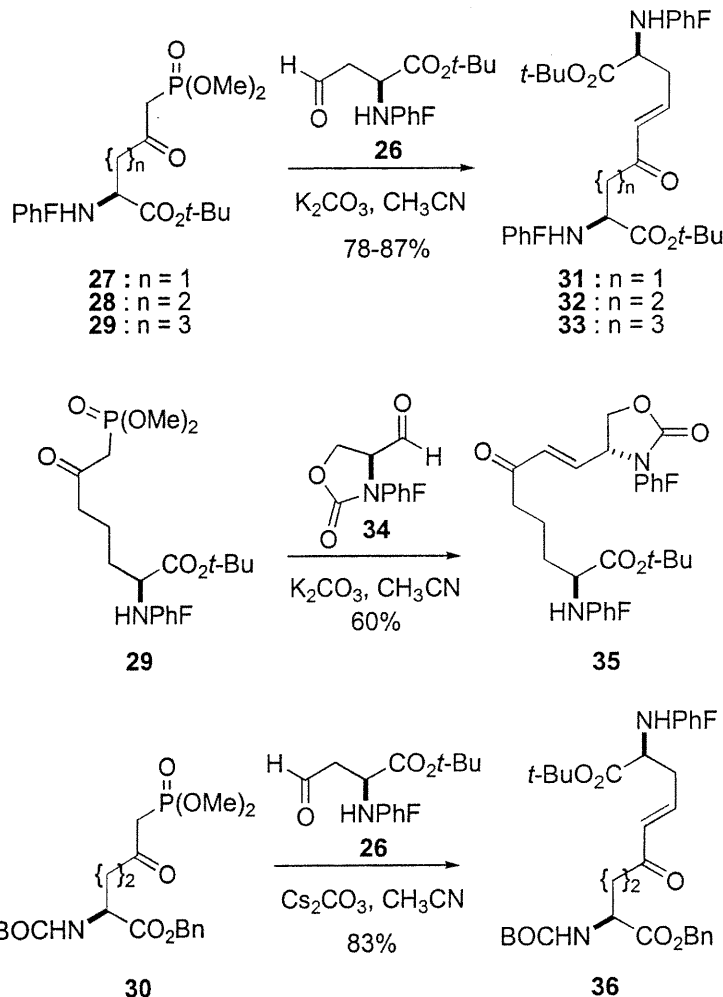


The potential for the hydroxymethyl substituent to serve in the synthesis of indolizidinone amino acids possessing different heteroatomic side-chains was illustrated by the synthesis of orthogonally-protected constrained Glu-Pro surrogate **25** (Scheme 10).<sup>33</sup> A two step oxidation of 5-hydroxymethyl indolizidinone *N*-(BOC)amino ester (*5S*)-**23** proceeded via aldehyde **24** to provide carboxylate **25** in 53% overall yield. Alcohol **23**, aldehyde **24** and acid **25**, all offer potential for further modifications to install other heteroatomic functions for mimicry of a full spectrum of amino acid side-chains.<sup>49</sup>

**Size Matters: Synthesis of Indolizidin-9-one, Quinolizidinone and Pyrroloazepinone Amino Acids**

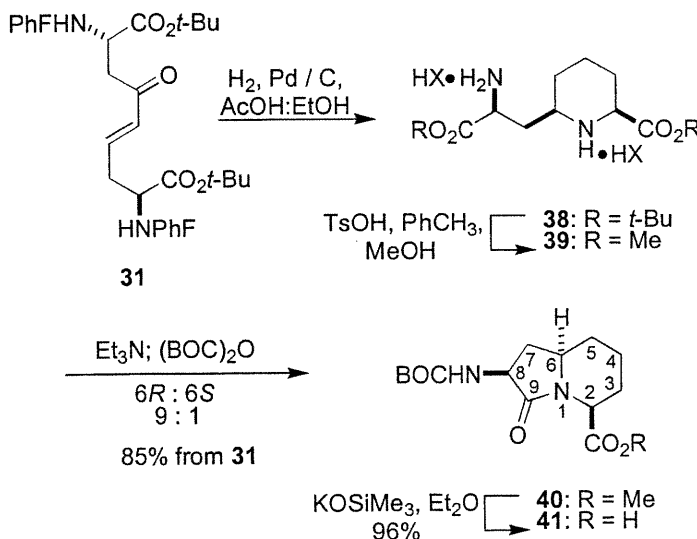
Azabicycloalkane amino acids of different ring sizes are attractive probes for mimicry of a variety of peptide conformations, because ring size can influence the  $\psi$  and  $\phi$  dihedral angles constrained within the heterocycle. The construction of different chain-length  $\alpha,\omega$ -diaminodicarboxylate precursors and selective cyclization of their amino and carboxylate functions were the two major issues that needed to be addressed to extend our approach to other ring systems. Because the self condensation of *N*-(PhF)glutamate produced efficiently the linear precursor for making indolizidin-2-one amino acid,<sup>31</sup> we tried and were disappointed to find that Claisen condensations with *N*-(PhF)aspartate and *N*-(PhF)amino adipate diesters failed to furnish  $\alpha,\omega$ -diaminodicarboxylate intermediates of different lengths.<sup>34</sup>

**SCHEME 11. Synthesis of Diaminodicarboxylates by Olefination of Amino Aldehydes with Aminodicarboxylate-derived  $\beta$ -Ketophosphonates**



Switching to a Horner-Wadsworth-Emmons olefination approach for joining amino acid-derived aldehydes and  $\beta$ -ketophosphonates proved effective for synthesizing linear precursors suitable for elaboration into azabicycloalkane amino acid.<sup>34-36</sup> To date, we have effectively synthesized  $\alpha,\omega$ -diaminodicarboxylates of nine to eleven carbon chain lengths using the olefination sequence<sup>34</sup> by reacting both  $\alpha$ -*tert*-butyl *N*-(PhF)aspartate  $\beta$ -aldehyde **26** and serine-derived  $\alpha$ -amino aldehyde **34**<sup>51</sup> with  $\beta$ -keto-phosphonates **27-30** (Scheme 11).

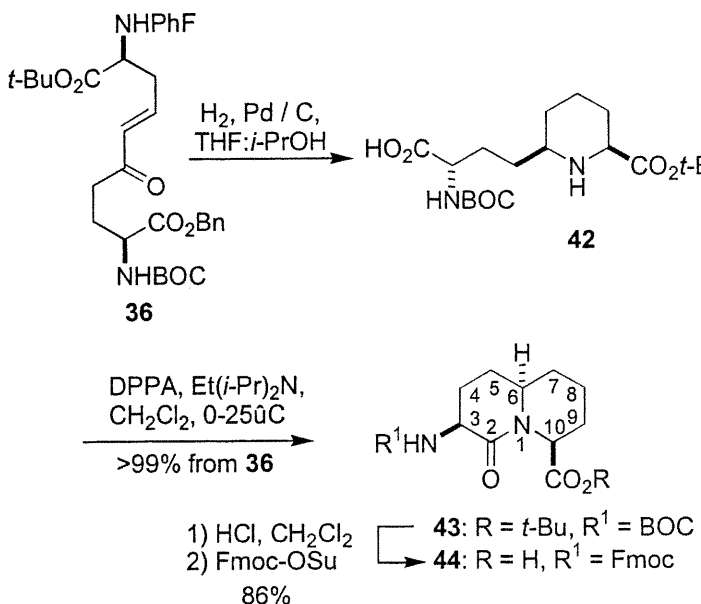
**SCHEME 12. Synthesis of *N*-(BOC)Amino Indolizidin-9-one Acid 41**



Indolizidin-9-one amino acid **41** was selectively synthesized in enantiopure form by the reductive amination / lactam cyclization strategy on aspartate-derived  $\gamma$ -keto- $\alpha,\omega$ -diaminoazelate **31** (Scheme 12).<sup>34,35</sup> Hydrogenation of azelate **31** with palladium-on-carbon as catalyst in 9:1 EtOH:AcOH at 6 atm of hydrogen proceeded by olefin reduction, cleavage of the phenylfluorenyl groups, intramolecular imine formation, protonation, and hydrogen addition to the iminium ion intermediate. Preferred formation of the 6-member piperidine rather than the 4-member azetidine ring gave only 6-alkylpipecolate **38** as a 9:1 mixture of diastereomers, that were converted to indolizidin-9-one amino ester by a one-pot three-step reaction sequence. Subsequent amine protection provided *N*-(BOC)amino indolizidin-9-one ester **40** in 85% overall yield from ketone **31**. Methyl ester **40** was then hydrolyzed with KOSiMe<sub>3</sub> in ether<sup>52</sup> to furnish *N*-(BOC)amino indolizidin-9-one acid **41** in 96% yield.

Quinolizidin-2-one amino acid **44** and pyrroloazepin-2-one amino acid **49**, both were recently synthesized from the same linear precursor,  $\delta$ -keto  $\alpha,\omega$ -diaminosebacate **36**.<sup>36</sup> Ring closure could be directed using a combination of judicious employment of protecting groups and the (*E*)-double bond geometry to

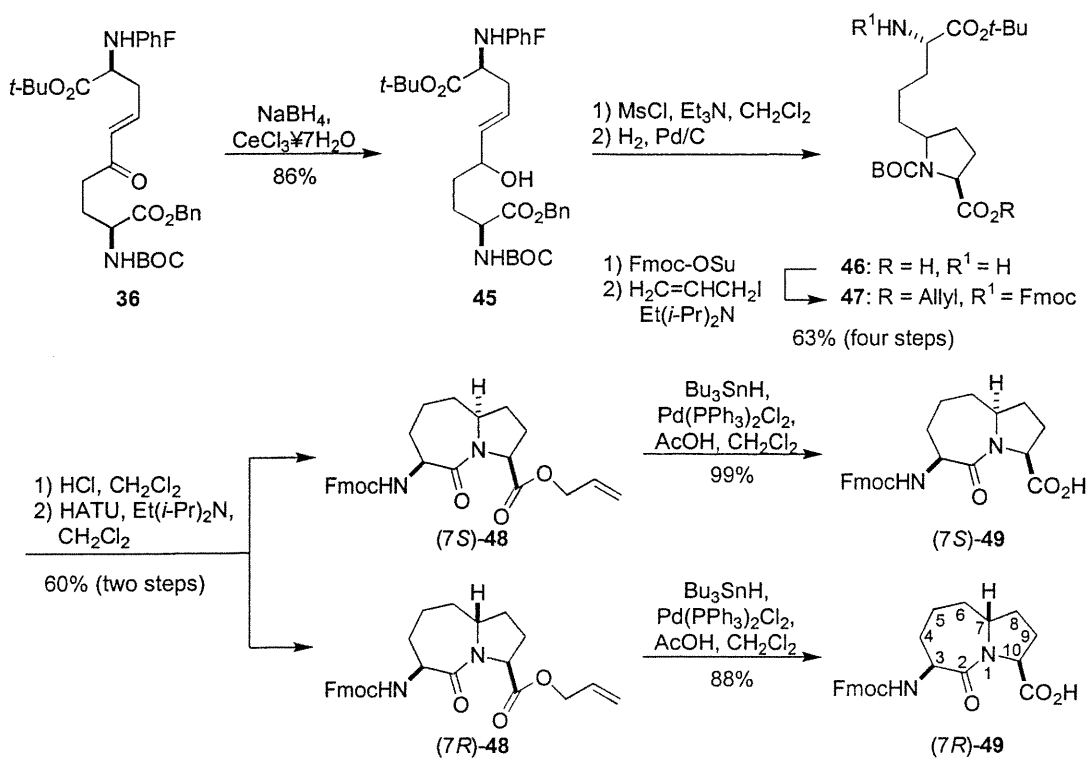
**SCHEME 13. Synthesis of Quinolizidin-2-one Amino Acid**



control cyclization. Selective removal of the PhF and benzyl groups from sebacate 36 by hydrogenolysis during the reductive amination sequence led specifically to the formation of 6-alkylpipecolate 42 as a single diastereomer that was treated with diphenylphosphoryl azide<sup>53</sup> in CH<sub>2</sub>Cl<sub>2</sub> in the presence of DIEA to furnish crystalline quinolizidin-2-one N-(BOC)amino ester 43 in >99% yield from ketone 36 after chromatography (Scheme 13). The Fmoc derivative was then prepared by simultaneous removal of the BOC and *tert*-butyl groups with HCl gas in CH<sub>2</sub>Cl<sub>2</sub> followed by acylation with 9-fluorenylmethyloxycarbonyl hydroxysuccinimide. Quinolizidinone N-(Fmoc)amino acid 44 was thus synthesized in enantiopure form in 7 steps and 40% overall yield from pyroglutamic acid.

Pyrroloazepin-2-one amino acid was synthesized using the methanesulfonate displacement route from sebacate 36 (Scheme 14).<sup>36§§</sup> Hydride reduction of ketone 36 in the presence of cerium trichloride provided a 1:1 mixture of diastereomeric allylic alcohols 45 that were activated with methanesulfonyl chloride and triethylamine in CH<sub>2</sub>Cl<sub>2</sub> to afford 5-alkylproline 46. The (*E*)-olefin geometry prevented the attack of the N-(PhF)amine onto the methanesulfonate such that

**SCHEME 14. Synthesis of Pyrroloazepin-2-one Amino Acid**



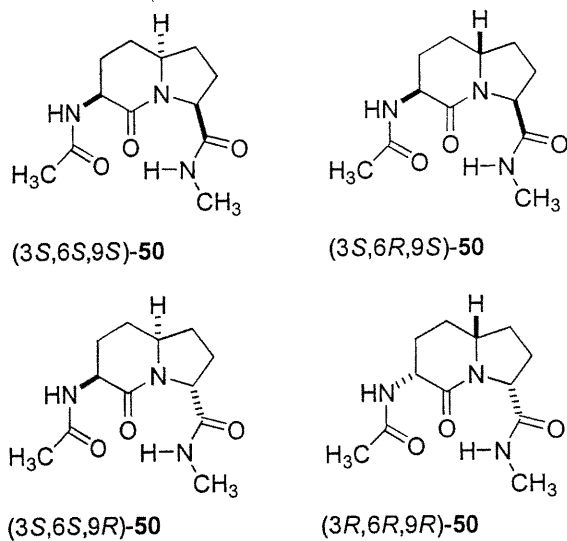
exclusive cyclization of the *N*-(BOC)amine occurred. Furthermore, 5-alkylprolines **46** were obtained as a 2:1 mixture of *5R*:*5S* diastereomers. This enhancement of the stereochemical ratio relative to starting allylic alcohol **45** was ascribed to  $S_N1$ -like cyclization, presumably due to ionization of the methanesulfonates under the reaction conditions.<sup>56</sup> A shuffling of protecting groups followed by lactam cyclization using azabenzotriazolyl-1,1,3,3-tetramethylaminium hexafluorophosphate (HATU)<sup>57</sup> gave pyrroloazepin-2-one *N*-(Fmoc)amino ester **48** as a 2:1 mixture of diastereomers that were easily separated by chromatography on silica gel. Pyrroloazepin-2-one *N*-(Fmoc)amino acids **(7S)-49** and **(7R)-49** were synthesized by Pd-catalyzed allyl ester cleavage in the last step of a route consisting of 11 steps giving 13% overall yield from pyroglutamic acid.

## Conformational Analysis of Peptide Models Containing Azabicycloalkane Amino Acids

The conformational preferences of azabicycloalkane amino acid analogs has been studied using computational analysis as well as spectroscopic and crystallographic methods. Information with respect to the favored conformers of different azabicyclo[X.Y.0]alkane amino acid isomers has been obtained primarily through study of indolizidin-2-one amino acid derivatives. Data concerning the influences of side-chain substituents and ring-size on conformation has come from X-ray crystallographic analyses. We present some of our preliminary investigations of the conformations of these rigid dipeptide surrogates in order to guide their use in future investigations of peptide structure.

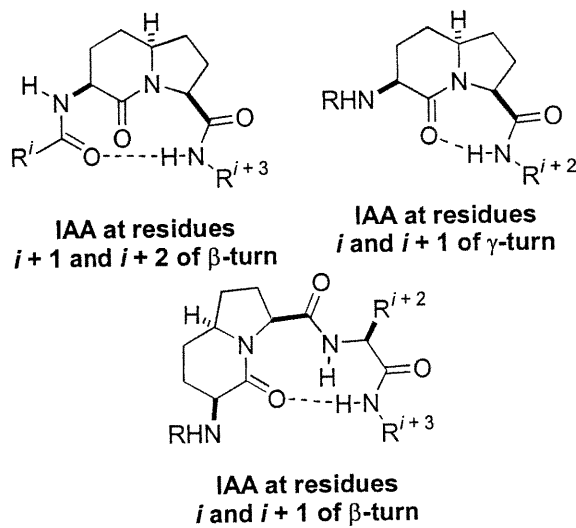
### Computational Analyses of I<sup>2</sup>AA Analogs

**FIGURE 3** *N*-Acetamido indolizidin-2-one *N'*-methylamides.



To model the influence of the different indolizidin-2-one amino acid isomers on peptide conformation, the energy minima for *N*-acetyl-I<sup>2</sup>AA-*N'*-methylamides (Figure 3) were calculated<sup>58</sup> using the MacroModel 3.5× program, the AMBER force field and the GB/SA solvent models for water and chloroform.<sup>59,60</sup> In both solvent models, amides (3S, 6S, 9S)-50 and (3S, 6R, 9S)-50 were shown to adopt  $\gamma$ - and  $\beta$ -

**FIGURE 4 Representations of possible turn conformations adopted by peptides containing (3*S*,6*S*,9*S*)-indolizidin-2-one amino acid.**

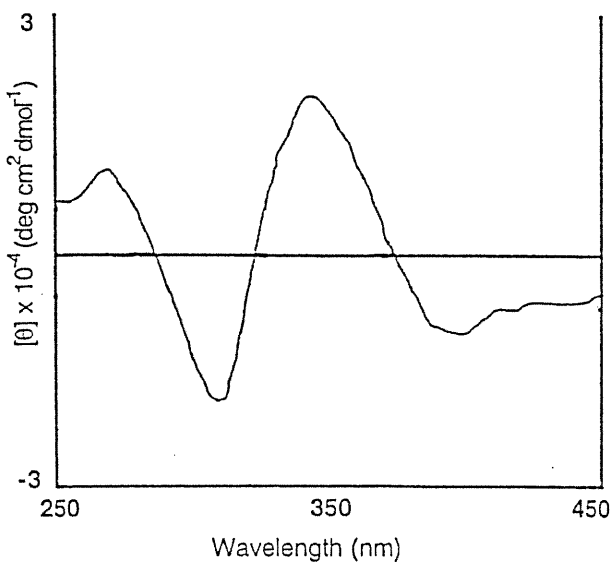


turn conformations (Figure 4). Among the minima conformations, a larger number of  $\gamma$ -turn conformations were found (60-70%) relative to  $\beta$ -turn conformations (20-30%) in the solvent model for chloroform. Comparing their low energy conformations, the *N*-acetyl *N'*-methylamide (3*S*, 6*S*, 9*S*)-**50** was found to be more likely to adopt a  $\beta$ -turn than its diastereomer (3*S*, 6*R*, 9*S*)-**50**. The dihedral angles  $\psi$  and  $\phi$  of the minima were characteristic of an inverse  $\gamma$ -turn and a type II'  $\beta$ -turn for (3*S*, 6*S*, 9*S*)- and (3*S*, 6*R*, 9*S*)-**50** and of a normal  $\gamma$ -turn and type II  $\beta$ -turn for their respective (3*R*, 6*R*, 9*R*)- and (3*R*, 6*S*, 9*R*)-enantiomers. A conformation without an intramolecular hydrogen bond was predicted as the lowest energy minimum in the solvent model for water. Although similar in energy, the  $\gamma$ -turn conformer was calculated to be of lower energy than its  $\beta$ -turn counterpart in both solvent systems.<sup>¶</sup>

### Spectroscopic Analyses of Model Peptides Containing I<sup>2</sup>AA Residues

Circular dichroism (CD) spectroscopy of *N*-(2,4-dinitrophenyl)tetrapeptide *N*-*p*-nitroanilides has been developed as an effective means for examining peptide conformation.<sup>62-64</sup> For example, Dnp-Gly-D-Phe-Pro-*p*NA (Dnp: 2,4-dinitrophenyl; *p*-NA: *p*-nitroaniline) was shown by CD and NMR spectral analysis to adopt a type II'  $\beta$ -turn conformation with the D-Phe-Pro residue situated at the central

**FIGURE 5 Circular dichroism spectra of Dnp-Gly-I<sup>2</sup>AA-Gly-pNA 51 at 0.1 mM in MeOH.**

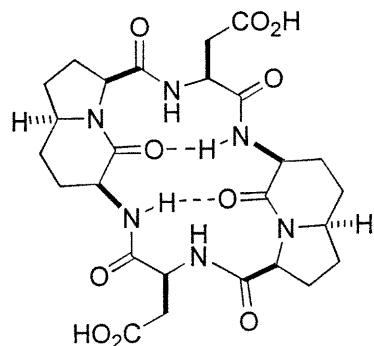


*i* + 1 and *i* + 2 positions.<sup>62,63</sup> Furthermore, application of this CD technique demonstrated that a peptide containing the convex thiaindolizidinone amino acid **1** can adopt a type II' β-turn secondary structure in methanol.<sup>26</sup> To study the conformational preferences of concave I<sup>2</sup>AA in peptides, we introduced (3*S*, 6*S*, 9*S*)-I<sup>2</sup>AA into Dnp-Gly-I<sup>2</sup>AA-Gly-*p*NA (**51**) and measured its CD spectrum in methanol.<sup>65</sup> The CD spectrum of **51** resembled closely the CD curve of the tetrapeptide possessing its related convex thiaindolizidinone counterpart and exhibited a strong positive band at 350 nm and a negative band at 310 nm (Figure 5). From the result of this CD spectral analysis, we may conclude that the concave indolizidinone amino acid can also adopt the *i* + 1 and *i* + 2 residues of a type II' β-turn conformation.

Two (3*S*, 6*S*, 9*S*)-I<sup>2</sup>AA residues were incorporated into a novel cyclic peptide, *cyclo*-[I<sup>2</sup>AA-Asp-I<sup>2</sup>AA-Asp]<sup>66</sup> as the first step towards mimicry of the active site of an aspartate protease.<sup>67,68</sup> Like in cyclic hexapeptide models that have used natural

proline as a turn inducing element,<sup>69</sup> the azabicycloalkane amino acid was employed to restrain the conformation of this cyclic peptide with the design of placing the  $\omega$ -carboxylate groups of the aspartic acids in close proximity. Unlike proline, the I<sup>2</sup>AA bicycles fix the X-Pro amide bond in a *trans*-geometry by locking it in a 6-member lactam, thus making isomerization of the prolyl amide bond impossible.

**FIGURE 6. cyclo-[I<sup>2</sup>AA-Asp-I<sup>2</sup>AA-Asp] 52.**

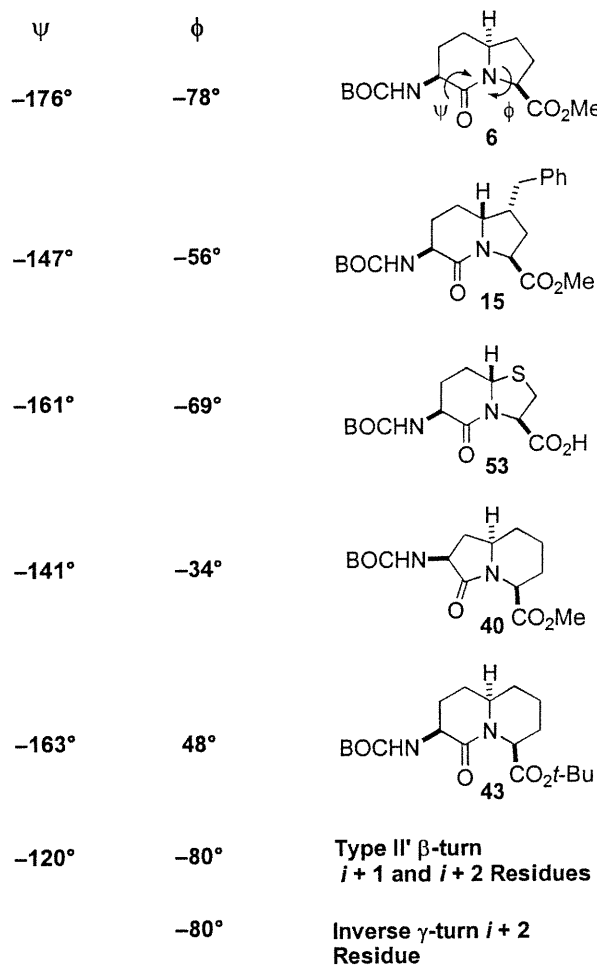


Cyclic peptide **52** has been synthesized using solution-phase techniques and more recently on solid phase.<sup>66,70</sup> Its conformation was studied by <sup>1</sup>H NMR experiments. For example, in its <sup>1</sup>H NMR spectrum in H<sub>2</sub>O : acetone-d<sub>6</sub> (9:1), the presence of only two amide signals characterized peptide **52** in a C2 symmetry. The assignment of the conformation was based in part on the cross-peak arising from the nuclear Overhauser effect (nOe) between the different amide protons in the NOESY spectra. The amide protons of the I<sup>2</sup>AA residues were implicated in an intramolecular hydrogen bond as demonstrated by measurement of their temperature coefficients in DMSO-d<sub>6</sub>.<sup>71</sup> The amide signal of the I<sup>2</sup>AA residue exhibited a temperature coefficient ( $\Delta\delta / \Delta T$ ) value of 0 ppb / K that was indicative of a solvent-shielded amide proton engaged in an intramolecular hydrogen bond. The amide signal of the aspartate residues possessed a temperature coefficient that was -4 ppb / K, a value suggesting a solvent-exposed amide proton. Cyclic peptide **52** appeared to adopt a conformation where the I<sup>2</sup>AA residues were situated at the *i* and *i* + 1 positions of a  $\beta$ -turn having an intramolecular hydrogen bond between the amide

hydrogen of the I<sup>2</sup>AA residue and the carbonyl oxygen of the aspartate residue (Figure 6).

### X-ray Crystallographic Analyses of I<sup>2</sup>AA, I<sup>9</sup>AA and QAA Analogs

**FIGURE 7 Dihedral angle values from azabicycloalkane *N*-(BOC)amino carboxylate X-ray data and ideal peptide turns.**



The dihedral angles of *N*-(BOC)amino esters of indolizidin-2-one, indolizidin-9-one and quinolizidin-2-one were examined in the solid state by X-ray crystallography.<sup>31,32,34,36</sup> Crystal packing forces and the solvent of crystallization may influence the geometry of the azabicycloalkane heterocycle and more profoundly its appendages. Taking this precaution into consideration, the influences of

stereochemistry, side-chains and size on conformation may be examined by comparing the internal  $\phi$  and  $\psi$  dihedral angle values from our X-ray data with those reported for thiaindolizidinone amino acid **53**<sup>72</sup> and with values for ideal turn conformations<sup>10,73</sup> (Figure 7). For example, because indolizidin-2-one, indolizidin-9-one and quinolizidin-2-one *N*-(BOC)amino esters **6**, **40** and **43**, all possess the same relative stereochemistry, significant differences in the internal  $\psi$  and  $\phi$  dihedral angles from their X-ray data indicate that ring-size has a profound effect on conformation. The influences on conformation brought about by changes of ring fusion stereochemistry and the addition of a side-chain substituent were also noticeable yet more moderate in comparison to the influence of ring-size. Modification of the back-bone stereochemistry would of course be the same as changing an L- to a D-amino acid within a peptide which is expected to have a significant influence on conformation.

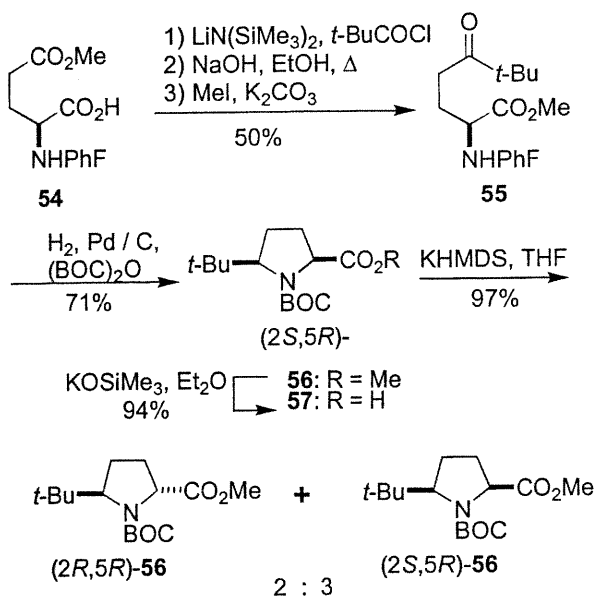
In summary, study of *N*-acetyl-I<sup>2</sup>AA-*N'*-methylamide **50**, Dnp-Gly-I<sup>2</sup>AA-Gly-*p*-NA **51** and *cyclo*-[Asp-I<sup>2</sup>AA-Asp-I<sup>2</sup>AA] **52** using computational and spectroscopic techniques<sup>58,65,66</sup> as well as the X-ray structure of I<sup>2</sup>AA *N*-(BOC)amino methyl ester,<sup>31</sup> all have indicated that I<sup>2</sup>AA may adopt the *i* and *i* + 1 positions as well as the *i* + 1 and *i* + 2 positions of a  $\beta$ -turn and the *i* and *i* + 1 positions of a  $\gamma$ -turn (Figure 4). The thiaindolizidinone amino acid **1** (Figure 2) has exhibited similar conformational preferences for the *i* and *i* + 1 positions and the *i* + 1 and *i* + 2 positions of  $\beta$ -turn conformations when introduced respectively into cyclic hexapeptide mimics of tendamistat<sup>74</sup> and in the antibiotic cyclic peptide gramicidin S.<sup>75,76</sup> Addition of a ring substituent can have a subtle influence on the back-bone dihedral angles of the I<sup>2</sup>AA residue.<sup>32</sup> Moreover, variation of the size of the azabicycloalkane influenced significantly the conformation of the dipeptide moiety embodied within the bicyclic heterocycle.<sup>34,36</sup>

## Azacycloalkane Amino Acid Synthesis

Isomerization about the amide bond *N*-terminal to prolyl residues can produce multiple conformers in biologically active peptides that can complicate their characterization. Because the rational design of therapeutics based on peptide lead structures requires a detailed knowledge of their spatial requirements for activity, conformationally rigid prolyl amide surrogates have emerged as important tools for probing the relationship between amide geometry and peptide bioactivity. Through the synthesis and analysis of a series of 3- and 5-alkylprolines, as well as 6-alkyl and 5,6-dialkylpipecolates, we have been exploring the influence of steric bulk on the conformations of the amides at the *N*- and *C*-termini of proline and pipecolate residues.

## 5-Alkylprolines

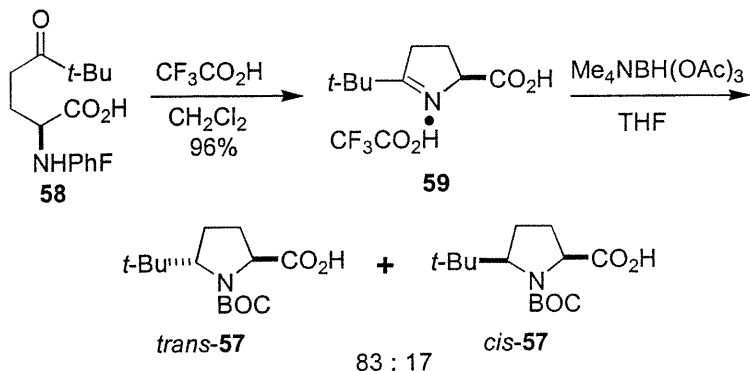
**SCHEME 15.** Synthesis of *cis*- and *trans*-5-*tert*-Butylproline



Enantiopure 5-alkylprolines were synthesized by sequences featuring acylation of  $\gamma$ -ester enolates of *N*-(PhF)glutamate derivatives followed by ester hydrolysis, decarboxylation and reductive amination.<sup>77-79</sup> For example, in the synthesis of (2*S*, 5*R*)-5-*tert*-butylproline,<sup>79</sup> deprotonation of the  $\alpha$ -carboxylate and regioselective enolization of the  $\gamma$ -ester of  $\gamma$ -methyl *N*-(PhF)glutamic acid **54** with lithium bis(trimethylsilyl)amide followed by acylation with pivaloyl chloride gave  $\beta$ -

keto ester that was hydrolyzed, decarboxylated and esterified to provide  $\delta$ -keto ester (*2S*)-**55** in 50% yield (Scheme 15). Catalytic hydrogenation of (*2S*)-**55** in methanol with di-*tert*-butyldicarbonate gave (*2S, 5R*)-*N*-BOC-5-*tert*-butylproline methyl ester **56** with high diastereoselectivity in favor of the *cis*-isomer.

### SCHEME 16. Synthesis of *trans*-5-*tert*-Butylproline



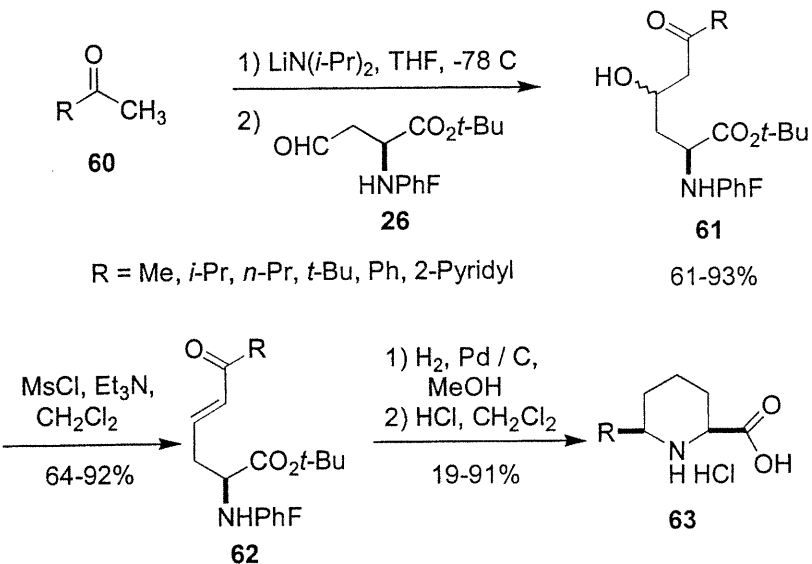
The *trans*-diastereomer of 5-*tert*-butylproline was synthesized with good diastereoselectivity from **58** by solvolysis of the PhF group in trifluoroacetic acid and subsequent reduction of 5-*tert*-butyl- $\Delta^5$ -dehydroproline **59** with tetramethylammonium triacetoxyborohydride; however, imino acid **59** was found to be configurationally labile and racemized under acidic conditions (Scheme 16). Enantiopure *trans*-diastereomer, (*2R, 5R*)-methyl *N*-BOC-5-*tert*-butylproline **56** was prepared by epimerization of (*2S, 5R*)-**56** (Scheme 15). Methyl ester hydrolysis with potassium trimethylsilanolate in ether provided *N*-BOC-5-*tert*-butylproline **57**. This synthetic methodology provided access to all four enantiopure 5-*tert*-butylproline isomers from inexpensive L- and D-glutamate as chiral educts.<sup>79</sup>

### 6-Alkyl and 5,6-Dialkylpipecolates

Concurrent with our research employing 5-alkylprolines in peptide mimicry, we became interested in the effects of azacycloalkane amino acids of larger ring-size. 6-Alkylpipecolates were synthesized to study the influence of the 6-position substituent on the pipecolyl amide equilibrium. We modeled our synthesis approach after the diaminopimelate pathway for L-lysine biosynthesis, which features the

enzyme catalyzed aldol condensation between pyruvate and aspartate  $\beta$ -aldehyde with subsequent cyclization to provide L-dihydropicolinic acid.<sup>80</sup> Our route has employed *N*-(PhF)aspartate  $\beta$ -aldehyde **26** in aldol condensations followed by reductive aminations which have furnished enantiopure 6-alkyl as well as 5,6-dialkylpipecolic acids.<sup>45,81,82</sup>

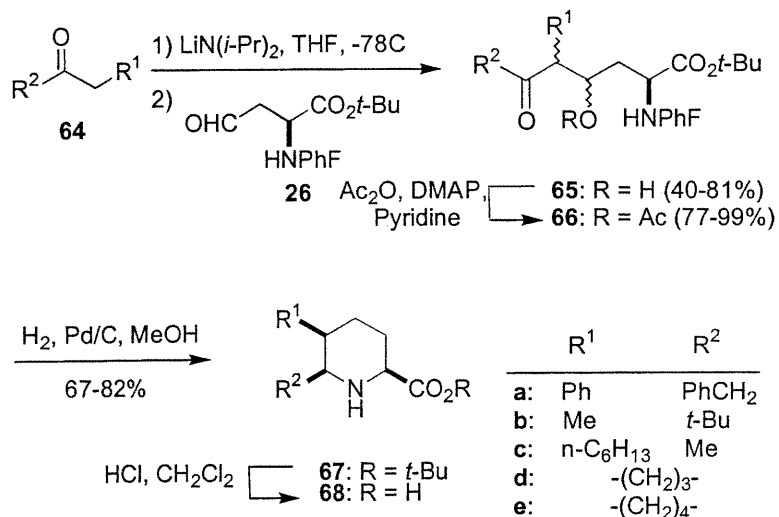
**SCHEME 17. Synthesis of 6-alkylpipecolates**



Aldol condensations with *N*-(PhF)aspartate  $\beta$ -aldehyde **26** and the lithium enolates of a variety of methyl ketones gave diastereomeric mixtures of  $\beta$ -hydroxy ketones **61** that were dehydrated to give enones **62**. The 6-alkylpipecolate *cis*-diastereomers **63** were obtained stereospecifically from catalytic hydrogenation of enones **62** and isolated as their hydrochloride salts after acidolysis of the *tert*-butyl ester. Enantiopure pipecolates possessing primary, secondary and tertiary alkyl as well as aryl 6-position substituents, all were prepared by this 5 step route from  $\alpha$ -*tert*-butyl  $\beta$ -methyl *N*-(PhF)aspartate in overall yields ranging from 15-59% (Scheme 17).

5,6-Dialkylpipecolates were synthesized by a similar sequence featuring homologation of  $\alpha$ -*tert*-butyl *N*-(PhF)aspartate  $\beta$ -aldehyde **26** (Scheme 18).<sup>82</sup> In the aldol condensation, lithium enolates reacted with aldehyde **26** to furnish the

**SCHEME 18. Synthesis of 5,6-Dialkylpipecolic Acids**

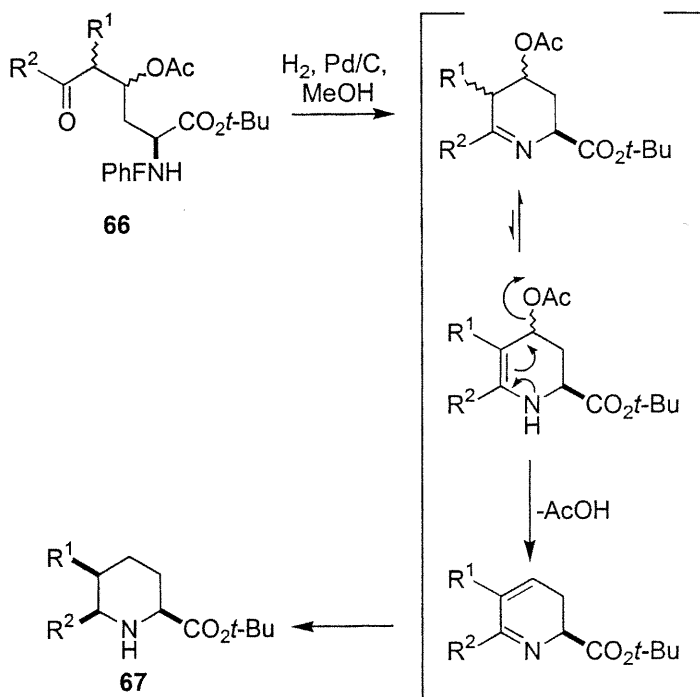


corresponding  $\epsilon$ -oxo  $\gamma$ -hydroxy  $\alpha$ -N-(PhF)amino esters **65** as mixtures of up to four diastereomers in total yields ranging from 40-81%. Although dehydration was retarded by the greater steric encumbrance about the dialkyl substituted hydroxy ketone **65**, 5,6-dialkylpipecolates **67** were directly synthesized by *O*-acetylation of the diastereomeric alcohols followed by hydrogenation with 10% palladium-on-carbon as catalyst in methanol under 3 atm of hydrogen.

Iminium ion tautomerization occurred during hydrogenation of  $\beta$ -acetoxy ketones **66** as in the reductive aminations in the syntheses of alkyl-branched indolizidinone amino esters **15** and **16** (Figure 8). Enaminium ion formation accompanied  $\beta$ -elimination of acetate to form a 1-azadiene intermediate. Hydrogen delivery to the face of the azadiene opposite to the bulky *tert*-butyl ester accounts for the selective formation of the all *cis*-diastereomer of 5,6-dialkylpipecolate **67**. In the hydrogenation of acetate **66c**, azadiene reduction may have competed with imine-to-enamine tautomerization such that the predominant all *cis*-diastereomer was accompanied by its minor C-5 epimer. Exposure of esters **67** to gaseous HCl in dichloromethane furnished the 5,6-dialkylpipecolic acid hydrochlorides **68** in quantitative yields. Five dialkylpipecolic acids **68** have been synthesized by this

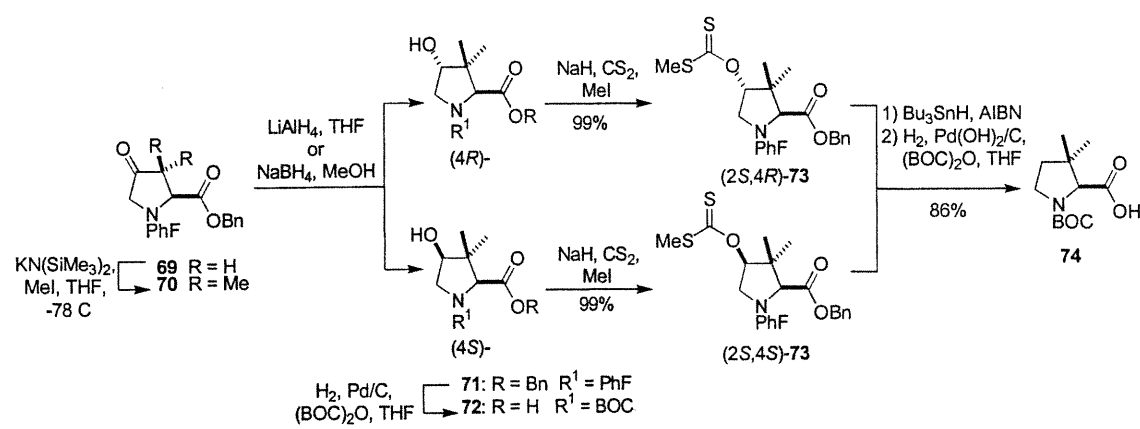
effective process for selective and stereocontrolled introduction of alkyl substituents at two of the ring carbons.

**FIGURE 8** Proposed mechanism for reductive amination to form 5,6-dialkylpipecolates 67.



### 3-Alkylprolines

**SCHEME 19.** Synthesis of 3,3-Dimethylproline and 3,3-Dimethyl-4-hydroxyprolines



Proline residues possessing 3-alkyl substituents can influence the geometry of their  $\psi$ -dihedral angle and C-terminal amide.<sup>83-87</sup> Furthermore, attachment of side-chain functions to the 3-position of the pyrrolidine ring can provide a proline-amino acid chimera for exploring geometric relations of side-chain groups to the peptide back-bone.<sup>88</sup> Enantiopure proline-valine and hydroxyproline-valine chimeras were synthesized from L-*trans*-hydroxyproline by a route featuring regioselective enolization of 4-oxo-*N*-(PhF)proline benzyl ester **69** (Scheme 19).<sup>88</sup> Alkylation of the enolate of **69** with different electrophiles has provided a series of 3-alkyl-4-oxo-*N*-(PhF)prolines. Excellent yields of 3,3-dimethyl-4-oxo-*N*-(PhF)proline **70** were obtained when iodomethane was used in excess as the electrophile. Hydride reduction using either NaBH<sub>4</sub> in MeOH at rt or LiAlH<sub>4</sub> in THF at -78°C gave the separable alcohols **71** with opposite albeit low selectivity. The alcohol function was removed by conversion to a xanthate followed by radical initiated deoxygenation. Shuffling of the protecting groups provided enantiopure 3,3-dimethyl *N*-(BOC)proline **74** and hydroxyprolines **72**.

### **Conformational Analysis of Peptide Models Containing Azacycloalkane Amino Acids**

#### **Steric Interactions on Amide Isomer Equilibrium**

The populations of the *cis*- and *trans*-amide isomers and the energy barrier for amide isomerization of proline and pipecolate *N*-acetyl *N*-methylamides were examined by NMR spectroscopy. Our studies of the steric influences of alkyl substituents on amide geometry were performed in water because of its physiological importance and for comparison with literature examples.<sup>89,90</sup> The rate of amide isomerization *N*-terminal to proline also proceeds more slowly in water than in nonprotic and nonpolar solvents because of stabilization of the polar amide ground states relative to the less-polar transition state.<sup>91</sup>

Prolyl amide isomer geometry was assigned based on the <sup>13</sup>C NMR chemical shift values for the  $\alpha$ - and  $\delta$ -carbon signals:<sup>92</sup> the  $\alpha$ -carbon signal of the *trans*-

isomer appearing upfield to that of the *cis*-isomer and the  $\delta$ -carbon signal of the *trans*-isomer appearing downfield from that of the *cis*-isomer in the  $^{13}\text{C}$  NMR spectra. Pipocolinamide isomer geometry was assigned based on observation of a nuclear Overhauser effect between the *N*-acetyl methyl group and the  $\alpha$ -hydrogen for the *cis*-amide isomer in the NOESY and ROESY spectra.<sup>45</sup> The ratio of amide isomers of the proline and pipcolate analogs were then measured by integration of the isomeric  $\alpha$ - and *N*-acetyl proton signals in the  $^1\text{H}$  NMR spectra.<sup>45,89</sup>

Steric interactions of a single methyl substituent at the proline 5-position were previously shown to augment the population of the X-Pro *cis*-amide isomer by 5% without affecting the energy barrier for isomerization of *N*-acetyl *trans*-5-methylproline *N*-methylamide.<sup>90</sup> In *N*-acetyl *cis*-5-methylproline *N*'-methylamide, no change from the natural prolyl amide isomer equilibrium was observed; however, the barrier for amide isomerization was reduced by 1.2 kcal/mol. The combined effect of two methyl substituents at the proline 5-position was first studied in *N*-BOC-phenylalanyl-5,5-dimethylproline methyl ester which existed as a 9:1 mix of amide *cis:trans* isomers.<sup>93</sup>

In our studies with the bulkier *tert*-butyl substituent at the 5-position of proline and at the 6-position of pipcolate, steric interactions significantly disfavored the *trans*-isomer causing a notable increase in the *cis*-amide population of their respective *N*-acetyl *N*'-methylamides (Table 1).<sup>45,89</sup> The *cis*-amide isomer population predominated (66%) in *N*-acetyl *trans*-5-*tert*-butylproline *N*'-methylamide 77. In addition, *trans*-5-*tert*-butylprolyl amide 77 did not adopt a  $\gamma$ -turn conformation in  $\text{CHCl}_3$  and exhibited only a single amide N-H stretch band at  $3454\text{ cm}^{-1}$  in the FT-IR spectra.<sup>89</sup> The absence of a seven-member intramolecular hydrogen-bond in the spectrum for 77 was in contrast to the spectra for its proline and *cis*-5-*tert*-butyl counterparts in which the stronger intensity of the hydrogen-bonded amide N-H stretch band at around  $3320\text{ cm}^{-1}$  indicated a preferred  $\gamma$ -turn geometry.

**TABLE 1. Amide Isomer Equilibrium of Proline and Pipecolate *N*-Acetyl *N*<sup>1</sup>-Methylamides in Water.**

		<i>trans</i> -isomer		<i>cis</i> -isomer	
entry	n	R	R <sup>1</sup>	% <i>cis</i> -isomer ± 3%	Tc(°C) ΔG‡±0.3 kcal/mol
75	0	H	H	27	>85 20.4
76	0	<i>t</i> -Bu	H	49	45 16.5
77	0	H	<i>t</i> -Bu	66	>85 20.2
78	1	H	H	28	80 17.8
79	1	<i>t</i> -Bu	H	43	70 17.0

The energy barriers for amide isomerization were determined by <sup>1</sup>H NMR coalescence and magnetization transfer experiments (Table 1). A remarkable steric effect has been the reduction of the barrier for prolyl amide isomerization by 3.9 kcal/mol in the *cis*-5-*tert*-butylproline amide relative to its proline and *trans*-5-*tert*-butylproline counterparts, which have similarly high energy barriers for isomerization.<sup>89</sup> Relative to the proline amide, the *N*-acetyl *N*<sup>1</sup>-methylpipecolinamide had a 2.6 kcal/mol lower barrier for isomerization. The steric impact of the bulky *tert*-butyl substituent was less pronounced on the acetamide geometry and the isomerization barrier in the pipecolate series relative to the proline amides.<sup>45</sup>

The steric interactions of two methyl substituents at the 3-positions of proline and hydroxyprolines were found to have little effect on the amide isomer populations; however, their presence diminished the rate of prolyl amide isomerization (Table 2).<sup>83,84</sup> For example, *cis*-to-*trans* isomerization of *N*-acetyl 3,3-dimethylproline *N*<sup>1</sup>-methylamide was nearly 7-fold slower than that of the proline amide counterpart.

**TABLE 2. Amide Isomer Equilibrium and Isomerization Rates for Proline and 3,3-Dimethylproline *N*-Acetyl *N'*-Methylamides in Water.**

entry	<i>R</i> <sup>1</sup>	<i>R</i> <sup>2</sup>	<i>R</i> <sup>3</sup>	<i>R</i> <sup>4</sup>	%cis-isomer		<i>k</i> <sub>ct</sub> (s <sup>-1</sup> )	<i>k</i> <sub>tc</sub> (s <sup>-1</sup> )
					±3% <sup>a</sup>	%cis-isomer		
80	H	H	H	H	28 (29)	28 (29)	2.01	0.82
81	OH	H	H	H	21 (24)	21 (24)	1.46	0.47
82	H	OH	H	H	21 (29)	21 (29)	2.05	0.82
83	H	H	CH <sub>3</sub>	CH <sub>3</sub>	30 (30)	30 (30)	0.32	0.12
84	OH	H	CH <sub>3</sub>	CH <sub>3</sub>	28 (25)	28 (25)	0.81	0.27
85	H	OH	CH <sub>3</sub>	CH <sub>3</sub>	21 (25)	21 (25)	0.39	0.47

<sup>a</sup> Determined by 300 MHz NMR at 25 °C (60 °C)

The slower rate for isomerization of the 3,3-dimethyl analogs may arise from steric interactions that restrict the  $\psi$ -dihedral angle to values around 150° and away from values of  $\psi \approx 0^\circ$ . At the 150°  $\psi$ -dihedral angle, the C-terminal carbonyl oxygen is placed in a position that can disfavor amide pyramidalization by Coulomb interactions.<sup>94</sup> The FT-IR data for dimethylproline **83** in CHCl<sub>3</sub> and the X-ray data for dimethylhydroxyproline **85**, both demonstrated that the 3,3-dimethyl substituents restricted the proline  $\psi$ -dihedral angle in a way that prevented a  $\gamma$ -turn conformation.<sup>83</sup>

### Influences of 5-*tert*-Butylproline on Peptide Turn Conformation

In light of the significant augmentation of the *cis*-amide isomer caused by the *tert*-butyl group in the simple *N*-acetyl *N'*-methyl amides **76** and **77**, the steric interactions of 5-*tert*-butylproline were next employed for inducing peptide turn geometry.<sup>95-97</sup> The type VI  $\beta$ -turn is a unique secondary structure that features an

amide *cis*-isomer *N*-terminal to a prolyl residue situated at the *i* + 2 position of the peptide bend.<sup>24,98</sup> Towards a general route for synthesizing mimics of type VI  $\beta$ -turn conformation, (*2S, 5R*)-5-*tert*-butylproline was incorporated at the *C*-terminal of a series of *N*-(acetyl)dipeptide *N'*-methylamides of the general structure Ac-Xaa-5-*t*-BuPro-NHMe.<sup>96</sup>

**TABLE 3. Influence of Solvent on the Amide Isomer Equilibrium of *N*-(Acetyl)dipeptide *N'*-Methylamides**

entry	Xaa (D-Xaa)	$R^1$	% <i>cis</i> -isomer $\pm$ 3%		
			H <sub>2</sub> O	; DMSO	CDCl <sub>3</sub>
86	Ala (D-Ala)	<i>t</i> -Bu	79 (68)	79 (91)	83 (71)
87	Met	<i>t</i> -Bu	74	72	73
88	Leu (D-Leu)	<i>t</i> -Bu	81 (78)	67 (93)	85 (60)
89	Val	<i>t</i> -Bu	81	73	89
90	Phe (D-Phe)	<i>t</i> -Bu	90 (58)	79 (73)	89 (82)
91	Ala	H	14	30	19
92	Leu	H	19	17	20

The relative populations of the amide *cis*- and *trans*-isomers *N*-terminal to the 5-*tert*-butylprolyl residue were measured by integration of the isomeric *tert*-butyl singlets and *N'*-methyl doublets in the <sup>1</sup>H NMR spectra in CHCl<sub>3</sub>, DMSO and water. The *cis*-amide isomer exhibited a cross-peak arising from a nuclear Overhauser effect between the *N*-terminal amino acid and proline  $\alpha$ -hydrogens in the NOESY and ROESY spectra. Although the *trans*-amide isomer was favored in prolyl peptides that were synthesized as controls, the Xaa-5-*t*-BuPro peptide bond adopted preferably

the *cis*-amide isomer for all of the 5-*tert*-butylprolyl peptides (Table 3). Only 55% *cis*-amide isomer was measured for Ac-Gly-5-*t*-BuPro-NHMe in water, similar to the amount of *cis*-isomer observed for *N*-acetyl-*cis*-5-*tert*-butylproline *N*-methylamide (48%).<sup>89</sup> Replacement of glycine for L- and D-alanine residues augmented respectively the *cis*-isomer population of Ac-Ala-5-*t*-BuPro-NHMe in water to 79% and 68%.<sup>96,97</sup> As previously noted in prolyl peptides,<sup>99-101</sup> the presence of an aromatic amino acid *N*-terminal to 5-*tert*-butylproline gave higher amounts of *cis*-amide isomer in all three solvents. In addition, we observed >90% *cis*-isomer population in DMSO-d<sub>6</sub> when D-amino acids with aliphatic side-chains were introduced *N*-terminal to 5-*tert*-butylproline.<sup>97</sup>

The influences of solvent composition and temperature on the chemical shift of the amide proton signals were examined to identify intramolecular hydrogen bonds.<sup>96,97</sup> The signal for the *N*-methylamide proton was observed downfield relative to the signal for the acetamide proton of the major conformer of Ac-Xaa-5-*t*-BuPro-NHMe dipeptides in all three solvents. Switching solvents from CHCl<sub>3</sub> to DMSO-d<sub>6</sub> and from CHCl<sub>3</sub> to water had little influence on the *N*-methylamide proton signal of the major conformer of Ac-Xaa-5-*t*-BuPro-NHMe (0.12-0.71 ppm downfield). On the other hand, the signal for the acetamide proton was shifted 1.71-2.53 ppm downfield. Solvent exposed protons were observed for all of the amide signals of the *cis*- and *trans*-conformers of Ac-Xaa-Pro-NHMe (Xaa = L-Ala, L-Leu), which exhibited chemical shift temperature coefficient values less than -4 ppb/K in DMSO-d<sub>6</sub>.<sup>71</sup> Similarly, the amide protons of the *trans*-isomer and the acetamide proton of the *cis*-isomer of 5-*tert*-butylprolyl peptides possessed values in the solvent exposed range. Only the *N*-methylamide protons of the major conformer of Ac-Xaa-5-*t*-BuPro-NHMe exhibited temperature coefficient values greater than -4 ppb/K indicative of solvent shielding.<sup>71</sup> The sum of the NMR experiments indicated that the *N*-methylamide of Ac-Xaa-5-*t*-BuPro-NHMe was engaged in an intramolecular hydrogen bond in a type VI β-turn conformation.

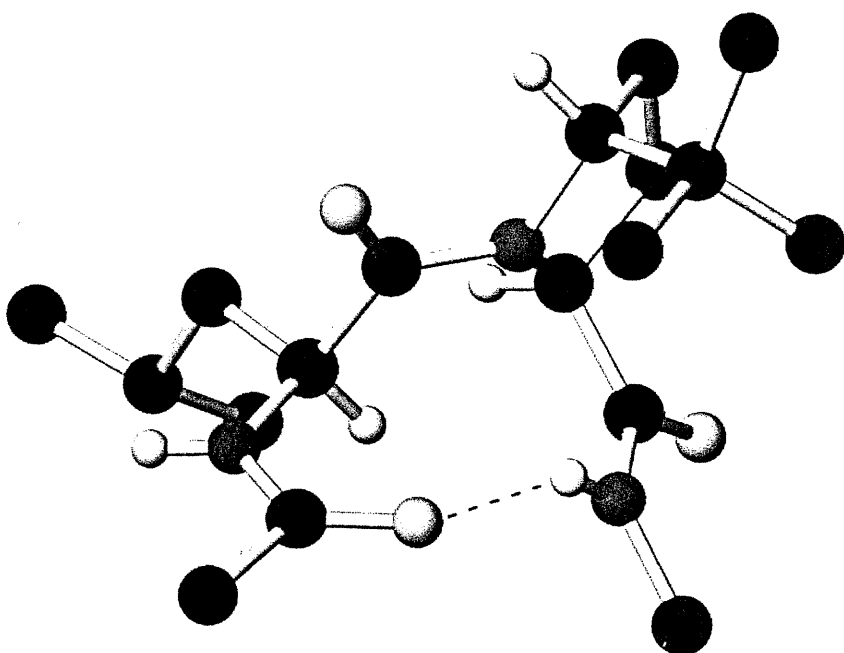


**FIGURE 9** Structure of Ac-L-Leu-*t*-BuPro-NHMe 88 from X-ray crystallography. Hydrogens are only shown on nitrogens and chiral carbons (C, black; N, dark gray; O, light gray; H, white).

Further evidence for a type VI structure came from X-ray crystallographic analysis of Ac-L-Leu-*t*-BuPro-NHMe which exhibited the dihedral angles characteristic of the central  $i+1$  and  $i+2$  residues of an ideal type VIa  $\beta$ -turn (Figure 9).<sup>96</sup> An intramolecular hydrogen bond between the  $N'$ -methylamide nitrogen and the acetamide carbonyl oxygen could be inferred by their interatomic distance of 2.13 Å.

The type of CD curve previously assigned to  $\beta$ -turn conformations<sup>102</sup> was observed in the CD spectra of Ac-L-Leu-*t*-BuPro-NHMe which exhibited a strong negative band at 188 nm, a positive band at 209 nm and a weak negative band at 227 nm in acetonitrile (Figure 10). Furthermore, the shape of its CD curve remained constant as the solvent was changed from acetonitrile to water. The type VI  $\beta$ -turn conformation adopted by the 5-*tert*-butylprolyl peptide was thus shown to be independent of solvent composition.<sup>#</sup>

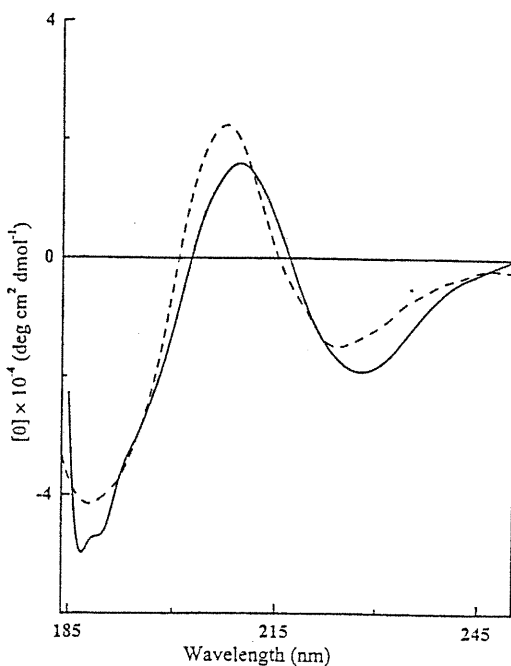


**FIGURE 10 Circular dichroism spectra of *N*-(acetyl)-L-leucyl-5-*tert*-butylproline *N'*-methylamide in water (---) and acetonitrile (—).**

#### Effects of 5-*tert*-Butylproline on Polyproline Helicity

Polyproline adopts two helical conformations: type I polyproline, a right handed helix with an axial translation of 190 pm and all *cis*-amide isomers, and type II polyproline, a left handed helix with an axial translation of 320 pm with all *trans*-amide bonds.<sup>104,105</sup> The influence of steric effects on the helical geometry and the interconversion of type II to type I polyproline was examined by NMR and CD spectroscopy of oligo-proline dimers and hexamers possessing (2*S*, 5*R*)-5-*tert*-butylproline.<sup>106,107</sup>

The local influence of the 5-*tert*-butyl group on the Pro-Pro amide bond geometry was initially examined by comparing Ac-Pro-Pro-NH<sub>2</sub> (93) with Ac-Pro-5-*t*-BuPro-NH<sub>2</sub> (94). In the prolyl dipeptides, a strong nOe between the  $\alpha$ -proton of the N-terminal residue and the  $\delta$ -protons of the C-terminal proline signals demonstrated that the amide bond between the prolyl residues of Ac-Pro-Pro-NH<sub>2</sub> existed predominantly in the *trans*-isomer in D<sub>2</sub>O. However, Ac-Pro-5-*t*-BuPro-NH<sub>2</sub> exhibited 63% *cis*-amide isomer and a strong nOe between the proline  $\alpha$ -proton and

the  $\delta$ -proton of 5-*tert*-butylproline in the *trans*-isomer and between the proline and 5-*tert*-butylproline  $\alpha$ -protons in the *cis*-isomer in the NOESY spectra.

The global effects of the 5-*tert*-butyl group on the helical conformation were examined next by placing one to three (2*S*, 5*R*)-5-*tert*-butylprolines into proline hexamers. In the hexapeptide Ac-(Pro)<sub>6</sub>-NH<sub>2</sub> (**95**), the all *trans*-amide type II polyproline conformation was adopted as demonstrated by a strong nOe between the  $\alpha$ - and  $\delta$ -protons of proline signals in the NOESY spectrum, the <sup>13</sup>C NMR chemical shift values, as well as the strong negative band at 204 nm and weak positive band at 226 nm in its CD spectrum.<sup>106-108</sup> Using NOESY spectroscopy on Ac-(Pro)<sub>5</sub>-5-*t*-BuPro-NH<sub>2</sub> (**96**), we detected 61% amide *cis*-isomer about the Pro-5-*t*-BuPro bond; however, the other prolyl amide bonds adopted *trans*-amide geometry. Although the NMR spectra of Ac-(Pro-Pro-5-*t*-BuPro)<sub>2</sub>-NH<sub>2</sub> (**97**) and Ac-(Pro-5-*t*-BuPro)<sub>3</sub>-NH<sub>2</sub> (**98**) could not be interpreted due to multiple conformers, CD spectroscopy could be used to analyze the influence of the 5-*tert*-butyl groups on the conformation of proline hexamers **95-98** in water at 5°C. As mentioned, the CD spectrum of Ac-(Pro)<sub>6</sub>-NH<sub>2</sub> was assigned to a type II poly-L-proline conformation. The curves of the CD spectra of the hexamers containing 5-*tert*-butylproline deviated from that of Ac-(Pro)<sub>6</sub>-NH<sub>2</sub> and indicated a perturbation of the type II helical conformation. Introduction of more 5-*tert*-butylproline residues into Ac-(Pro)<sub>6</sub>-NH<sub>2</sub> [Ac-(Pro)<sub>5</sub>-5-*t*-BuPro-NH<sub>2</sub>, Ac-(Pro-Pro-5-*t*-BuPro)<sub>2</sub>-NH<sub>2</sub> and Ac-(Pro-5-*t*-BuPro)<sub>3</sub>-NH<sub>2</sub>] caused a lowering of the intensity of the negative band at 207 nm which shifted to higher wavelength, as well as a fading of the positive band at 229 nm. The CD spectrum of Ac-(Pro-5-*t*-BuPro)<sub>3</sub>-NH<sub>2</sub> exhibited a weak positive band at 195 nm and a negative band at 221 nm. The CD curve for a type I poly-L-proline CD spectrum is characterized by a medium intensity band at 199 nm, a strong positive band at 215 nm and a weak negative band at 232 nm.<sup>109</sup> Thus, although the 5-*tert*-butylproline residues destabilized the polyproline type II conformation, they failed to interconvert the type II helix to a type I helical geometry in water. The 5-*tert*-butylproline

hexamers may thus mimic transitional intermediates proposed to form during helical interconversion.<sup>110-112</sup>

### Concluding Remarks

The wealth of peptide structures that exhibit remarkable biology has traditionally inspired the Peptide Scientist to devise tools for deciphering the spatial requirements for their activity. Endeavoring to understand the relationships between conformation and peptide biology, the chemistry of peptide mimicry has produced various strategies for replicating different secondary structures.<sup>1-24</sup> With the advent of combinatorial science,<sup>113-115</sup> new templates have recently emerged that possess different attributes as tools for building libraries of small molecules that may serve as peptide mimics. Often such strategies and tools have been conceived within the contexts of programs either specifically focused on the exploration of a particular biologically active peptide or oriented towards the rapid production of arrays of structurally diverse and readily accessible candidates for screening against a variety of receptor subtypes. In this respect, our approach differs because we have sought to develop practical methods for constructing a spectrum of related and complementary tools for systematically replicating the various orientations of the side-chain and back-bone atoms within any generic peptide.\*\* Conformational analyses of these tools in model peptide systems has already demonstrated their capacity to replicate the backbone dihedral angle geometry found in type II and type VI  $\beta$ -turn as well as  $\gamma$ -turn conformations. Furthermore, the consequences of their stereochemistry, side-chains and ring size on peptide conformation has begun to be elucidated by studying the conformational preferences of different azacyclo- and azabicycloalkane amino acids and suggests their potential to act as surrogates of alternative structural motifs such as extended  $\beta$ -sheet conformations. In this review, we have cited references where experimental details and characterization data can be obtained to facilitate the construction of these tools. Furthermore, we have resumed our conformational analyses to characterize their potential for replicating particular conformations in model peptides. In this way, we hope to encourage the future employment of these

tools as conformationally constrained probes for mimicry of peptide secondary structures.

### Acknowledgments

We are particularly grateful for our colleagues and collaborators whose contributions have advanced this research program in a productive and enjoyable manner. We thank Sylvie Bilodeau and Dr. M. T. Phan Viet of the Regional High-Field NMR Laboratory and Francine Bélanger-Gariépy at l'Université de Montréal X-ray facility for their invaluable assistance. This research has been supported in part by the Natural Sciences and Engineering Research Council of Canada, the Ministère de l'Éducation du Québec, and the Medical Research Council of Canada.

- \* We have adopted the nomenclature and ring system numbering used in reference 23 in order to maintain clarity and consistency when comparing these different heterocyclic systems.
- † Because penicillin and related  $\beta$ -lactams mimic the acyl-D-Ala-D-Ala residues in peptidoglycans, they can be argued to be the first members of the azabicyclo[X.Y.0]alkane amino acid family. The interested reader should see reference 25 for a lead article as well as reference 29 in reference 23 for reviews.
- § In solvolysis studies PhFCI was 6000 times less reactive than trityl chloride.<sup>43</sup>
- †† Alternative approaches to indolizidin-2-one amino acids are reported in references 46-48.
- §§ The concave (*7S*)-isomer of pyrroloazepinone amino acid had been previously synthesized in references 54 and 55.
- ¶ In a comparative analysis, (*3S*, *6S*, *9S*)-indolizidinone amino acid **7** was found to be "more effective as a reverse turn than other  $\beta$ -turn mimetics" yet the geometry of the turn induced by the indolizidinone residue "differs significantly from that of an ideal  $\beta$ -turn".<sup>61</sup>
- # During the preparation of this review, 5,5-dimethylproline (dmP) was shown by computational analysis and NMR spectroscopy in water to induce a type VI  $\beta$ -turn conformation in the tripeptides Ac-Tyr-dmP-Asn and Ac-Asn-dmP-Tyr.<sup>103</sup>

\*\* For a systematic use of lactams of different ring sizes and stereochemistry in the constraint of Leu-enkephalin see reference 116.

### References

1. Rudinger, J. In Drug Design; Ariëns E.J., Ed.; Academic: New York, 1971; Vol II, 319-419.
2. Friedinger, R. M.; Veber, D. F.; Perlow, D. S.; Brooks, J. R.; Saperstein, R. Science 1980, 210, 656-658.
3. Farmer, P.S. In Drug Design; Ariëns E.J., Ed.; Academic: New York, 1980; Vol X, 119.
4. Veber, D. F.; Freidinger, R. M.; Perlow, D. S.; Paleveda, W. J. Jr.; Holly, F. W.; Strachan, R. G.; Nutt, R. F.; Arison, B. H.; Homnick, C.; Randall, W. C.; Glitzer, M. S.; Saperstein, R.; Hirschmann, R. Nature 1981, 292, 55-58.
5. Spatola, A. F. In Chemistry and Biochemistry of Amino Acids, Peptides, and Proteins; Weinstein, B., Ed.; Marcel Dekker: New York, 1983, 267.
6. Bélanger, P. C.; Dufresne, C. Can J Chem 1986, 64, 1514-1520.
7. Hruby, V. J. Life Science 1982, 31, 189-199.
8. Veber, D. F.; Freidinger, R. M. TINS, 1985, 392-396.
9. Morgan, B. A.; Gainor, J. A. Ann Rep Med Chem 1989, 243-252.
10. Ball, J. B.; Alewood, P. F. J Mol Recogn 1990, 3, 55-64.
11. Kemp, D. S. TIBTECH 1990, 8, 249-255.
12. Hirschmann, R. Angew Chem Int Ed Engl 1991, 30, 1278-1301.
13. Hölzemann, G. Kontakte (Darmstadt) 1991, 3-12.
14. Kahn, M. Synlett 1993, 821.
15. Marshall G.R., Tetrahedron 1993, 49, 3547-3558.
16. "Peptide Secondary Structure Mimetics" Tetrahedron, Symposia-in-print # 50, M. Kahn, Ed.; 1993, 49, 3433-3689.
17. Olson, G. L.; Bolin, D. R.; Bonner, M. P.; Bös, M.; Cook, C. M.; Fry, D. C.; Graves, B. J.; Hatada, M.; Hill, D. E.; Kahn, M.; Madison, V. S.; Rusiecki, V. K.; Sarabu, R.; Sepinwall, J.; Vincent, G. R.; Voss, M. E. J Med Chem 1993, 36, 3039-3049.

18. Giannis, A.; Kolter, T. *Angew Chem Int Ed Engl* 1993, 32, 1244-1267.
19. Liskamp, R. M. *J Recl Trav Chim Pays-Bas* 1994, 113, 1-19.
20. Adang, A. E. P.; Hermkens, P. H. H.; Linders, J. T. M.; Ottenheijm, H. C. J.; van Staveren, C. *J Recl Trav Chim Pays-Bas* 1994, 113, 63-78.
21. Gante, J. *Angew Chem Int Ed Engl* 1994, 33, 1699-1720.
22. Gillespie, P.; Cicariello, J.; Olson, G. L. *Biopolymers, Peptide Science* 1997, 43, 191-217.
23. Hanessian, S.; McNaughton-Smith, G.; Lombart, H.-G.; Lubell, W. D. *Tetrahedron* 1997, 53, 12789-12854.
24. Etzkorn, F. A.; Travis, J. M.; Hart, S. A. *Advances in Amino Acid Mimetics and Peptidomimetics* 1999, 2, 125-163.
25. Du Vigneaud, V.; Carpenter, F. H. In *The Chemistry of Penicillin*; Clarke, H. T. Johnson, J. R., Robinson, R., Eds; Princeton University Press, Princeton, N.J., 1949, 1004-1017.
26. Nagai, U.; Sato, K. *Tetrahedron Lett* 1985, 26, 647-650.
27. Wyvratt, M. J.; Tischler, M. H.; Ikeler, T. J.; Springer, J. P.; Tristram, E. W.; Patchett, A. A. In *Peptides: Peptide, Structure and Function (Proceedings of the 8th Am Peptide Symp)* Hruby, V. J. and Rich, D. H., Eds; Pierce Chem Company, Rockford, Ill, 1983, 551.
28. Thorsett, E. D. *Actual Chim Thér 13e série*, 1986, 257-268.
29. Lombart, H.-G.; Lubell, W. D. *J Org Chem* 1994, 59, 6147-6149.
30. Lombart, H.-G.; Lubell, W. D. In *Peptides 1994 (Proceedings of the 23rd European Peptide Symposium)*, H. L. S. Maia, Ed.; ESCOM, Leiden, The Netherlands, 1995, 696-697.
31. Lombart, H.-G.; Lubell, W. D. *J Org Chem* 1996, 61, 9437-9446.
32. Polyak, F.; Lubell, W. D. *J Org Chem* 1998, 63, 5937-5949.
33. Polyak, F.; Lubell, W. D. In *Peptides: Chemistry, Structure and Biology*, G. Fields and G. Barany, Eds; ESCOM, Leiden, The Netherlands, 2000, In Press.
34. Gosselin, F.; Lubell, W. D. *J Org Chem* 1998, 63, 7463-7471.

35. Gosselin, F.; Lubell, W. D. In Peptides 1998 (Proceedings of the 25th European Peptide Symposium), S. Bajusz & F. Hudecz, Eds; Akadémia Kiadó: Budapest, Hungary, 1998, 660-661.
36. Gosselin, F.; Lubell, W. D. *J Org Chem* 2000, 65, in press.
37. Sardina, F. J.; Rapoport, H. *Chem Rev* 1996, 96, 1825-1872.
38. Christie, B. D.; Rapoport, H. *J Org Chem* 1985, 50, 1239-1246.
39. Lubell, W. D.; Rapoport, H. *J Am Chem Soc* 1987, 109, 236-239.
40. Humphrey, J. M.; Bridges, R. J.; Hart, J. A.; Chamberlin, A. R. *J Org Chem* 1994, 59, 2467-2472.
41. Atfani, M.; Lubell, W. D. *J Org Chem* 1995, 60, 3184-3188.
42. Barlos, K.; Papaioannou, D.; Theodoropoulos, D. *J Org Chem* 1982, 47, 1321-1326.
43. Bolton, R.; Chapman, N. B.; Shorter, J. *J Chem Soc* 1964, 1895-1906.
44. Jamison, T. F.; Lubell, W. D.; Dener, J. M.; Krisché, M. J.; Rapoport, H. *Org Synth* 1992, 71, 220-225.
45. Swarbrick, M. E.; Gosselin, F.; Lubell, W. D. *J Org Chem* 1999, 64, 1993-2002.
46. Mueller, R.; Revesz, L. *Tetrahedron Lett* 1994, 35, 4091-4092.
47. Hanessian, S.; Ronan, B.; Laoui, A. *Bioorg Med Chem Lett* 1994, 4, 1397-1400.
48. Kim, H.-Ok; Kahn, M. *Tetrahedron Lett* 1997, 38, 6483-6484.
49. Polyak, F.; Lubell, W. D. manuscript in preparation.
50. Sammes, P. G.; Weller, D. *J. Synthesis* 1995, 1205-1222.
51. Lubell, W. D.; Rapoport, H. *J Org Chem* 1989, 54, 3824-3831.
52. Laganis, E. D.; Chenard, B. L. *Tetrahedron Lett* 1984, 25, 5831-5834.
53. Shioiri, T.; Ninomiya, K.; Yamada, S. *J Am Chem Soc* 1972, 94, 6203-6205.
54. Robl, J. A. *Tetrahedron Lett* 1994, 35, 393.
55. Colombo, L.; Di Giacomo, M.; Belvisi, L.; Manzoni, L.; Scolastico, C.; Salimbeni, A. *Gazz Chim Ital* 1996, 126, 543.
56. Ohta, T.; Hosoi, A.; Kimura, T.; Nozoe, S. *Chem Lett* 1987, 2091-2094.
57. Carpino, L. A. *J Am Chem Soc* 1993, 115, 4397-4398.

58. Lombart, H.-G.; Lubell, W. D. In peptides: Chemistry, Structure and Biology. P.T.P. Kaumaya and R.S. Hodges, Eds.; ESCOM, Leiden, The Netherlands, 1996, 695-696.
59. Still, W. C.; Tempczyk, A.; Hawley, R. C.; Hendrickson, T. J Am Chem Soc 1990, 112, 6127-6129.
60. McDonald, D. Q.; Still, W. C. J Org Chem 1996, 61, 1385-1391.
61. Takeuchi, Y.; Marshall, G. R. J Am Chem Soc 1998, 120, 5363-5372.
62. Sato, K.; Kawai, K.; Nagai, U. Biopolymers 1981, 20, 1921-1927.
63. Higashijima, T.; Sato, K.; Nagai, U. Bull Chem Soc Jpn 1983, 56, 3323-3328.
64. Baldwin, J. E.; Claridge, T. D. W.; Hulme, C.; Rodger, A.; Schofield, C. Int J Pept Protein Res 1994, 43, 180-183.
65. Lombart, H.-G. Développement d'un nouveau acide aminé indolizidinone et applications en mimétique peptidique. Thèse de doctorat, Université de Montréal, 1997.
66. Thouin, E. Nouveau mimétisme du site actif des protéases aspartiques: conception, synthèse et caractérisation du cyclo[IAA-Asp-IAA-Asp]. Mémoire de maîtrise, Université de Montréal, 1997.
67. Somayaji, V.; Keillor, J.; Brown, R. S. J Am Chem Soc 1988, 110, 2625-2629.
68. Kemp, D. S.; Petrakis, K. S. J Org Chem 1981, 46, 5140-5143.
69. Giersch, L. M.; Deber, C. M.; Madison, V.; Niu, C.-H.; Blout, E. R. Biochemistry 1981, 20, 4730-4738.
70. Dairi, K.; Lubell, W. D. unpublished results.
71. Kessler, H. Angew Chem Int Ed Engl 1982, 21, 512-523.
72. Nagai, U.; Sato, K.; Nakamura, R.; Kato, R. Tetrahedron 1993, 49, 3577-3592.
73. Madison, V.; Kopple, K. D. J Am Chem Soc 1980, 102, 4855-4863.
74. Etzkorn, F. A.; Guo, T.; Lipton, M. A.; Goldberg, S. D.; Bartlett, P. A. J Am Chem Soc 1994, 116, 10412-10425.
75. Bach, II, A. C.; Markwalder, J. A.; Ripka, W. C. Int J Peptide Protein Res 1991, 38, 314-323.
76. Sato, K.; Nagai, U. J Chem Soc Perkin Trans I 1986, 1231-1234.
77. Ibrahim, H.H.; Lubell, W. D. J Org Chem 1993, 58, 6438-6441.

78. Ibrahim, H. H.; Beausoleil, E.; Atfani, M.; Lubell, W. D. In Peptides: Chemistry, Structure and Biology, R.S. Hodges and J.A. Smith, Eds.; ESCOM Science Publishers B.V.: Leiden, The Netherlands, 1994, 307-309.
79. Beausoleil, E.; L'Archevêque, B.; Bélec, L.; Atfani, M.; Lubell, W. D. *J Org Chem* 1996, 61, 9447-9454.
80. Cox, R. J. *Nat Prod Rep* 1996, 13, 29-43.
81. Gosselin, F.; Swarbrick, M. E.; Lubell, W. D. In Peptides 1998 (Proceedings of the 25th European Peptide Symposium), S. Bajusz & F. Hudecz, Eds; Akadémia Kiadó: Budapest, Hungary, 1999, 678-679.
82. Swarbrick, M. E.; Lubell, W. D. *Chirality* 2000, 12, in press.
83. Beausoleil, E.; Sharma, R.; Michnick, S.; Lubell, W. D. *J Org Chem* 1998, 63, 6572-6578.
84. Beausoleil, E.; Sharma, R.; Michnick, S.; Lubell, W. D. In Peptides 1996 (Proceedings of the 24th European Peptide Symposium), R. Ramage and R. Epton, Eds; ESCOM, Leiden, The Netherlands, 1997, 241-242.
85. Delaney, N. G.; Madison, V. *J Am Chem Soc* 1982, 104, 6635-6641.
86. Baures, P. W.; Ojala, W. H.; Gleason, W. B.; Johnson, R. L. *J Peptide Res* 1997, 50, 1-13.
87. Samanen, J.; Zuber, G.; Bean, J.; Eggleston, D.; Romoff, T.; Kopple, K.; Saunders, M.; Regoli, D. *Int J Peptide Protein Res* 1990, 35, 501-509.
88. Sharma, R.; Lubell, W.D. *J Org Chem* 1996, 61, 202-209 and refs 1-6 therein.
89. Beausoleil, E.; Lubell, W. D. *J Am Chem Soc* 1996, 118, 12902-12908.
90. Delaney, N. G.; Madison, V. *Int J Peptide Protein Res* 1982, 19, 543-548.
91. Stein, R. L. *Adv Protein Chem* 1993, 44 , 1-24.
92. Deslauriers, R.; Smith, I.C.P. In Biological Magnetic Resonance, L. J. Berliner and J. Reuben Eds.; Plenum Press, NY, 1980, vol. 2, 275-280.
93. Magaard, V. W.; Sanchez, R. M.; Bean, J. W.; Moore, M. L. *Tetrahedron Lett* 1993, 34, 381-384.
94. Fischer, S.; Dunbrack Jr., R. L.; Karplus, M. *J Am Chem Soc* 1994, 116, 11931-11937.

95. Halab, L.; Lubell, W. D. In Peptides 1998 (Proceedings of the 25th European Peptide Symposium), S. Bajusz and F. Hudecz, Eds; Akadémia Kiadó, Budapest, Hungary, 1999, 356-357.
96. Halab, L.; Lubell, W. D. *J Org Chem* 1999, 64, 3312-3321.
97. Halab, L.; Lubell, W. D. In Peptides: Chemistry, Structure and Biology, G. Fields and G. Barany, Eds; ESCOM, Leiden, The Netherlands, 2000, In Press.
98. Müller, G.; Gurrath, M.; Kurz, M.; Kessler, H. *Proteins: Structure, Function and Genetics* 1993, 15, 235-251.
99. Dyson, H. J.; Rance, M.; Houghten, R. A.; Lerner, R. A.; Wright, P. E. *J Mol Biol* 1988, 201, 161-200.
100. Oka, M.; Montelione, G. T.; Scheraga, H. A. *J Am Chem Soc* 1984, 106, 7959-7969.
101. Wu, W.-J.; Raleigh, D. P. *Biopolymers* 1998, 45, 381-394.
102. Brahms, S.; Brahms, J. *J Mol Biol* 1980, 138, 149-178.
103. An, S. S. A.; Lester, C. C.; Peng, J.-L.; Li, Y.-J.; Rothwarf, D. M.; Welker, E.; Thannhauser, T. W.; Zhang, L. S.; Tam, J. P.; Scheraga, H. A. *J Am Chem Soc* 1999, 121, 11558-11566.
104. Traub, W.; Shmueli, U. *Nature* 1963, 198, 1165-1166.
105. Cowan, P. M.; McGavin, S. *Nature* 1955, 176, 501-503.
106. Beausoleil, E.; Lubell, W. D. *Biopolymers* 2000, 53, 249-256.
107. Beausoleil, E.; Lubell, W. D. In Peptides: Frontiers of Peptide Science, J.P.Tam and P.T.P. Kaumaya, Eds; Kluwer, The Netherlands, 1999, 150-151.
108. McCafferty, D. G.; Slate, C. A.; Nahkle, B. M.; Graham Jr., H. D.; Austell, T. L.; Vachet, R. W.; Mullis, B. H.; Erickson, B. W. *Tetrahedron* 1995, 51, 9859-9872.
109. Rabanal, F.; Ludevid, M. D.; Pons, M.; Giralt, E. *Biopolymers* 1993, 33, 1019-1028.
110. Harrington, W. F.; Sela, M. *Biochem Biophys Acta* 1958, 27, 24-41.
111. Steinberg, I. Z.; Harrington, W. F.; Berger, A.; Sela, M.; Katchalski, E. *J Am Chem Soc* 1960, 82, 5263-5279.
112. Dukor, R. K.; Keiderling, T. A. *Biospectroscopy* 1996, 2, 83.

113. Wilson, S.R.; Czarnik, A.W. Combinatorial Chemistry, Wiley:New York, 1997.
114. Gordon, E.M.; Kerwin, J. F. Jr Combinatorial Chemistry and Molecular Diversity in Drug Discovery, Wiley: New York, 1998.
115. Jung, G. Combinatorial Peptide and Nonpeptide Libraries, VCH: New York, 1996.
116. Friedinger, R. M.; In Peptides: Synthesis, Structure, Function. (Proceedings of the 7th American Peptide Symposium), Rich, D. H. and Gross, E.; Eds; Pierce Chemical Co: Rockford, 1981, 673-683.